Delineating the Alteration Zone at the Big Easy Prospect using Geophysical Methods

by

© Adam Wall

A Thesis submitted to the School of Graduate Studies
in partial fulfillment of the requirements
for the degree of

Master of Science
Department of Earth Science (Geophysics)

Memorial University of Newfoundland
May 2017
St. John’s, Newfoundland and Labrador

Abstract

The Big Easy Prospect is a low-sulphidation (LS) style epithermal system located along the northern extension of the Burin Peninsula High Sulphidation Belt in Newfoundland. It is believed to have formed during an extensional magmatic episode during the rifting of Avalonia from Gondwana in the late Neoproterozoic era. Despite its age, the Big Easy is well preserved which is likely due to rapid burial shortly after it was formed. Overlying sediments have since been eroded exposing what is believed to be the paleosurface of the Big Easy LS system. However, the property is covered extensively with overburden, forests, bogs, and ponds resulting in limited outcrop exposure. Therefore, delineating the alteration zone has proved to be challenging. The alteration zone associated with the auriferous mineralization should be detectable through the use of various geophysical methods. Several surveys were conducted over the property, including magnetics, gravity, and ground penetrating radar (GPR) in an attempt to gain a better understanding of the lateral and vertical extent of the alteration zone. These surveys were followed by two-dimensional forward and inverse modelling. Results of the magnetic survey mainly revealed features caused by mafic dykes. Since mafic dykes are noted to be spatially related to faulting in the area, a new potential boundary for the eastern extent of the epithermal alteration is identified. Bathymetry profiles of the bogs and lakes were created using data collected from the GPR survey. This allowed for proper corrections in the gravity data as well as more accurate modelling of the near subsurface. The gravity survey was the most effective for estimating the depth of the alteration zone since the altered material was slightly less dense than the surrounding units but further drilling is required to confirm this conclusion.

Acknowledgements

I would like to express my gratitude toward my supervisors Dr. Alison Leitch and Dr. Colin Farquharson for their support and guidance throughout this project. Thanks are also due to committee member Greg Sparkes for passing on his geological understanding of the property, providing input, and guiding several trips into the field.

I would like to acknowledge the contribution of my field assistants; Jonathan Codner, Linden Ernst, Jamal Alsafwani, Jianguang Chen, and Drew Jones. I also appreciate the staff of Lakeside at Thorburn for providing field equipment and their wonderful hospitality.

I would also like to thank Hibernia Project Geophysics Support Fund and the School of Graduate Studies for providing financial support which made this study possible.

Table of Contents

List of Figures

Chapter 1 Introduction

1.1 Purpose and Scope

The Big Easy Prospect is a low-sulphidation (LS) epithermal system located along the northern extension of the Burin Peninsula High Sulphidation Belt (Sparkes & Dunning, 2014; Figure 1.1). A localized auriferous alteration zone has been identified on the property, however the exact extent of the alteration zone is unknown due to significant overburden and lack of outcrop.

LS systems are known to host localized zones of high-grade gold that usually require significant amounts of drilling to define. Since very little bedrock is exposed in the area, it is difficult to establish drill targets with a high level of confidence. The purpose of this project is to map the extent of the epithermal alteration zone, both in width and along strike at surface, as well as at depth by a means of new geophysical surveys including gravity, magnetics, and ground-penetrating radar (GPR), followed by 2D forward and inversion modelling of the collected data.

1.2 Location and Access

The Big Easy prospect is located approximately 16 km NW of the town of Clarenville in Eastern Newfoundland on map sheets NTS 2D/8 and 2D/1. The property is 3.2 km off the Trans-Canada Highway and is easily accessible through a network of regularly maintained gravel roads around Thorburn Lake (Figure 1.2). A small ATV path enables easy mobility as it runs nearly the entire length of the prospect. Thorburn Lake is also accessible via floatplane as it accommodates the main seaplane base for the area. In the winter, the property can be accessed through the same series of trails or shorter alternative trails utilizing ponds and bogs when frozen. The property is covered extensively by wetland areas with intermittent bodies of water, and thick forested areas. Ownership of the property has recently reverted back to the prospector who originally staked the area, which is made up of 21 claims covering 5.25 km^2. The most recent depiction of the alteration zone (AZ-2012) is about 0.3 km wide and has an estimated strike length of about 1.7 km (Silver Spruce Resources Inc., 2012; Figure 1.2).The bulk of this study will focus on the area directly over the alteration zone and the immediate surrounding area.

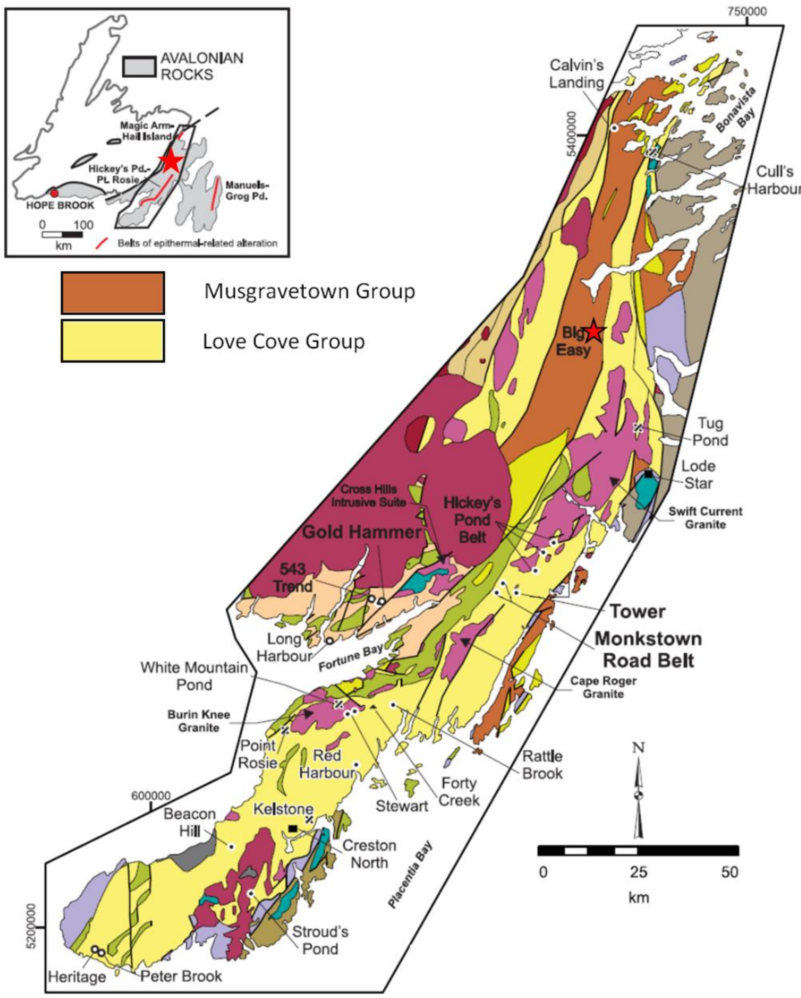

Figure 1.1: Map of the Burin Peninsula High Sulphidation Belt (BPHSB) and associated occurences, including the Big Easy as annotated by the red star (Modified from Sparkes & Dunning (2014)).

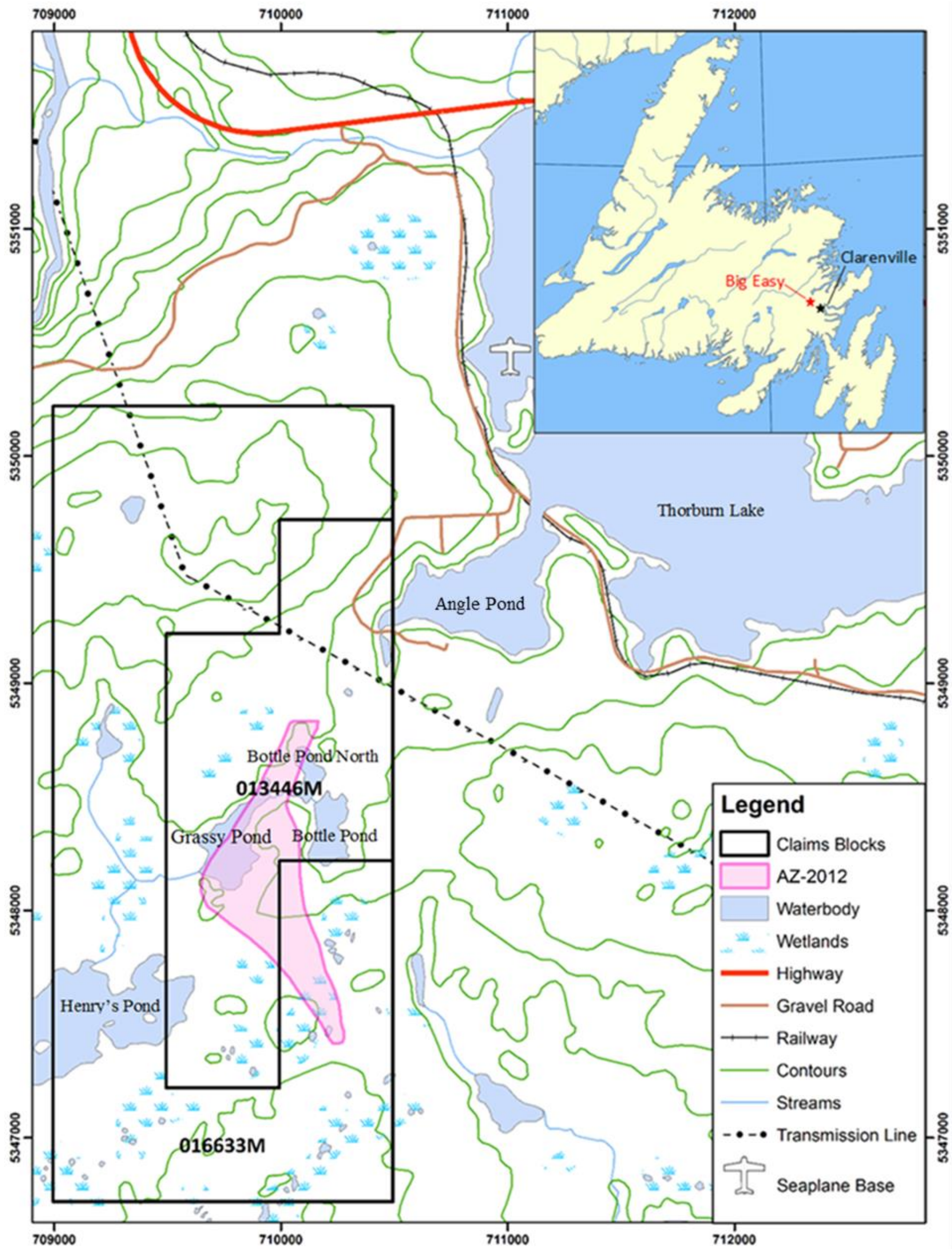

Figure 1.2: Location of the Big Easy Prospect as well as surrounding claim boundaries

1.3 Previous Work

Until the property was acquired by Silver Spruce Resources in 2010, there were very limited academic or government studies done over the prospect. Regional mapping of the area was completed by the Geological Survey of Canada in 1963 (Jenness, 1963) and more detailed mapping was done by the Newfoundland Geological Survey Branch in 1986. Mapping carried out as a part of a M.Sc. thesis study (Hussey, 1979), which was largely focused on the area to the north of the Big Easy prospect, covers a portion of the prospect in the southwestern corner of the thesis map area. In 1988, regional lake sediment sampling was conducted by the Newfoundland Government, and a gold anomaly of 10 ppb was discovered in Grassy Pond (Figure 1.2) (Davenport, 1988). This anomalous gold value generated interest in the property and claims surrounding Grassy Pond were eventually staked by GT Exploration. Grass roots exploration including mapping and prospecting was conducted over the property during 1994 and 1995. Several gold anomalies from grab samples were discovered containing up to 196 ppb Au (Saunders, 1996). Anomalous gold values were observed as far north as the southern edge of Angle Pond, Point 13283 in Figure 1.3, and as far south as Point HP-08 which suggested a potential strike length, at surface, of approximately 1.3 km. Saunders proposed that the alteration zone pinches out toward the north but has no traceable boundary to the south, leaving it open along strike.

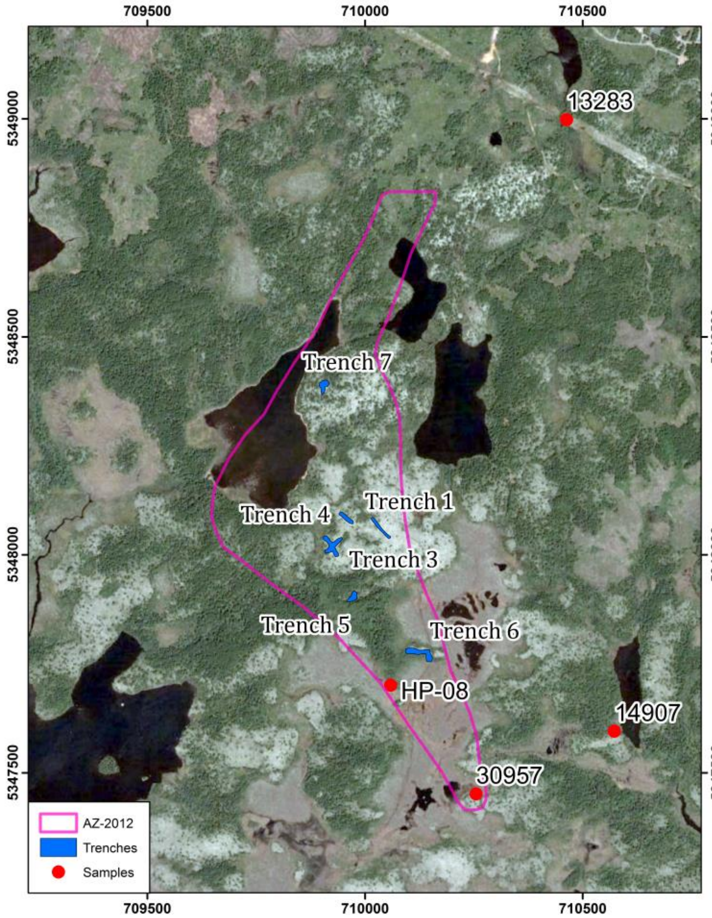

Figure 1.3: Location of trenches as well as significant grab samples taken over the Big Easy Prospect. Trench 2 has been infilled and therefore not shown in this map. Data obtained from Dyke (2008) and Dimmel (2013).

In the same year, a grab sample was submitted to Dr. Derek Wilton of Memorial University. A thin section was prepared and he conducted a petrographic evaluation of the specimen. Wilton interpreted the sample as being a volcanic sediment that was likely deposited near the surface and noted that the pyrite content suggested potential for high-level mineralization that would be associated with an epithermal system (Wilton, 1996).

A brief field program was carried out over the area in 2008 by new owners, Cornerstone Resources. This program included several man days of prospecting and an overall property assessment. A total of 43 rock samples including outcrop, subcrop and float within and surrounding the claim block were collected and assayed. Six of the samples returned assays over 100 ppb Au, the greatest of which was 0.4 g/t Au; in addition 19 of the samples returned assays over 1000 ppb Ag, the greatest of which was 4.6 g/t Ag. The depiction of the alteration zone was extended slightly further south after Sample 30957 (Figure 1.3) ran 154 ppb Au and 1.2 g/t Ag (Dyke, 2008). Although the majority of samples taken reside within the main body of the alteration zone, there were some samples collected at the outer extremities of the claim that contained above background values of Au. Sample 14907 lies several hundred metres to the west of AZ-2012 (Figure 1.3) and was described as frost-heaved subcrop exhibiting pervasive silica alteration (Dyke, 2008).

Silver Spruce purchased the property in 2010 and actively worked towards a better geological understanding of the potential deposit. Between 2010 and 2014 there was continued prospecting over the property as well as a trenching program where 7 trenches were excavated (Figure 1.3) to expose the underlying altered bedrock (Dimmell, 2013). 121 channel samples were taken with lengths varying between 0.5 and 2 metres. As reported in 2010 the assays confirmed that the alteration zone was anomalous in gold and silver with average values of 0.72 g/t and 3.5 g/t, respectively (Silver Spruce Resources Inc., 2010). Mapping of trenches gave progressive structural insight into the host rock and mineralized veining. It was apparent that sediment beds trend roughly S-SW and dip approximately 45 degrees westward. Steeply north-dipping, E-W trending shears were also observed in trenches 3 and 4 whereas SE-trending shears were observed in other areas of Trench 3. A significant discovery of chalcedony in Trench 6 is indicative of sinterlike deposits, which strongly suggests that the currently exposed surface represents or is very near to the paleosurface.

Seven holes were drilled in 2011 (Figure 1.4) and provided 1,577 m of drill core, which gave some insight into the extent of the system and consultation with Caracle Creek Consulting Inc. provided further information regarding the structure of the system. Bedding measurements agreed with Silver Spruce’s findings during the trenching program. However it was noted that veining was oriented perpendicular to bedding while secondary silica flooding was present parallel to bedding. Since the drilling in the 2011 program was oriented at an azimuth of 090 degrees, mineralized zones were intersected sub-parallel to the core axis as reported by Wetherup in the 2012 exploration report (Dimmell, 2012). Generally, intersecting structures perpendicular to the dip direction will provide more useful and reliable information and will increase the likelihood of intersecting mineralization. As a result, future drilling was oriented with an azimuth of 270 degrees such that both bedding and veining could be intersected at moderate angles to the core axis. Wetherup also noted that faults/shears run sub-parallel to the core axis (eastward) and through regional interpretation it was proposed that faulting trends approximately northeast. In highly tectonized zones, mafic dykes commonly occur, and may be concurrent with faulting.

Other highlights from the 2011 drilling program include a better defined north-western extent of the alteration zone. This boundary was defined by drill holes BE-11-05, and BE-11-06, as these drill holes commenced into unaltered red/purple sediments and almost immediately encountered silicified material. Further south, the location of BE-11-03 loosely represents the western extent of the alteration however, there is still potential further west since it collared into altered material.

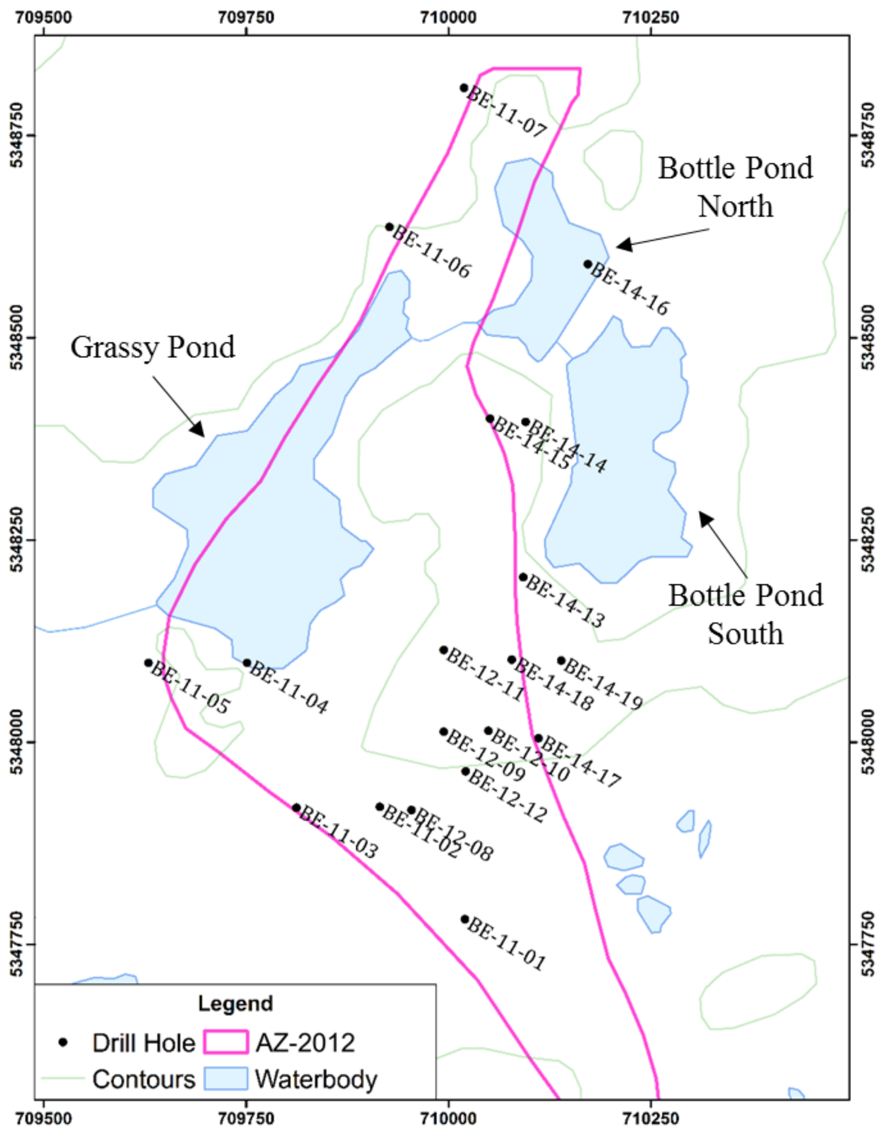

Figure 1.4: Map of all drill hole locations over the Big Easy Property. AZ-2012 depicts the alteration zone at surface as it was understood in 2012.

Orientation of the vein system was confirmed during the drill program in 2012 when veins were intersected at higher angles to the core axis than in previous drilling (Dimmell, 2013). This program included 5 drill holes (Figure 1.4) where 1,080 m were drilled. Another drill program was completed in the fall of 2014 where 1,391.4 m were drilled (Silver Spruce Resources, 2015).

Several drill holes from the 2014 drill program help define the eastern extent of silicification in some areas. For example, BE-14-19 collars into unaltered red/purple sediments but encounters silicified sediments at a depth of approximately 16 metres with a mafic dyke separating the two units. The alteration extends as far east as drill holes BE-14-17, 18, and 14 as all of these commenced in silicified material. However, a region that was previously presumed to be a part of the alteration zone, near BE-14-16, is mainly composed of unaltered red/purple sediments. BE-14-16 commenced in unaltered red and purple sediments and remained in that unit until it terminated in a mafic dyke at a depth of 130 m (for detailed drill logs, refer to Appendix A). This may suggest that a very sharp contact also exists along the eastern margin of the alteration zone.

A mineralogical study was conducted in 2013 on behalf of Memorial University by B.Sc Honours student, Matthew Clarke, under the supervision of Dr. Graham Lane. The main goal of Clarke's study was to gain a better understanding of the precious metal mineralogy and how it relates to the different styles and generations of veining found in the drill core. During the study, Clarke identified bladed textures and adularia, both of which are typical of boiling. The presence of these textures is significant because mineralization in these types of shallow deposits often occurs through boiling-related precipitation (Clarke, 2013). Since the mafic dykes crosscut mineralization, Clarke was able to date the mafic unit to obtain a minimum age on the mineralization of 566 ± 2 Ma.

1.4 Local Geology

The Big Easy is interpreted as a clastic sediment-hosted, LS style epithermal prospect located within the Musgravetown Group near the western margin of the Avalon Zone (Clarke, 2013). The prospect lies along strike with several other epithermal occurrences of similar age and some with similar metallogeny. These related deposits extend as far south as Southern Carolina and as far north as Eastern Newfoundland (Ayuso et al, 2005). The Musgravetown Group consists of the Cannings Cove Formation (CCF), Bull Arm Formation (BAF), Rocky Harbour Formation (RHF), and the Crown Hill Formation (CHF) (Figure 1.5) which are composed mostly of red and green shales along with micaceous sandstones and conglomerates (Reusch & O'Driscoll, 1987), see Figure 1.6. The sedimentary package also contains horizons with a volcanic component including flow-banded rhyolites which are likely associated with its location within an extensional basin, a few km west of a Neoproterozoic volcanic arc (Hedenquist J. W., 2013).

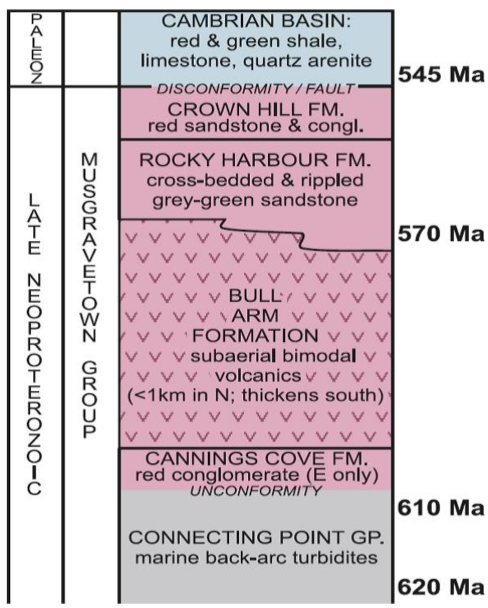

Figure 1.5: Stratigraphic column of the Musgravetown Group and adjacent groups (O'Brien & King, 2002).

1.4.1 Cannings Cove Formation (CCF)

The Cannings Cove formation is the oldest formation within the Musgravetown Group. It consists of sandstones, shales, and red and green conglomerates. The sediments are comprised mostly of felsic volcanic fragments but also include pink granites, cherts, and sediment fragments thought to be derived from the underlying group, the Connecting Point Group (Dal Bello, 1977).

1.4.2 Bull Arm Formation (BAF)

The BAF was first described in 1843 by Jukes and was later added to the Musgravetown Group by Jenness (1963) and is composed mostly of subaerial volcanic rock. The primary facies of the BAF are grey-green vesicular basalt and red to purple felsic flows as well as ash flows. The basalt flows contain abundant hematite, chlorite, epidote, and carbonate. Felsic units of this formation include some porphyritic grey – maroon flows which directly underlie the RHF and are interpreted to be the main contributor of the detrital elements of the RHF conglomerates (O'Brien & King, 2002).

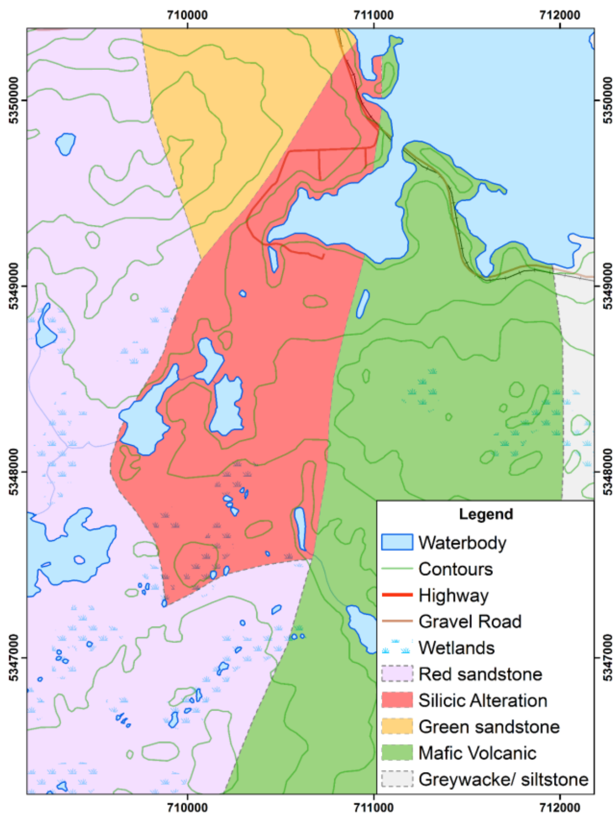

Figure 1.6: Generalized map of the Thorburn Lake area (modified from Sparkes, 2015).

1.4.3 Rocky Harbour Formation (RHF)

The RHF is described by Jenness (1963) as a sequence of crossbedded yellowish-green, lithic sandstones that directly underlie the Crown Hill Formation (CHF). Most sandstones within this formation are poorly sorted and are classified more accurately as greywackes. The poorly sorted, and sub-angular clasts are composed of feldspar and quartz along with fragments of schist and volcanic rock hosted in a matrix of epidote, chlorite and clay materials. The angularity of these clasts implies a short transportation and further evidence (e.g. ripple marks and cross-bedding) supports a shallow marine depositional environment (Jenness, 1967; Normore, 2010). The presence of such high epidote, chlorite, and clay material content relative to quartz suggests that these detrital components originated from an adjacent group, the Love Cove Group (described below), since there are no other rocks exposed in eastern Newfoundland with a similar composition (Jenness, 1963).

1.4.4 Crown Hill Formation (CHF)

The CHF was introduced in 1963 by Jenness and described as a series of red and green pebble conglomerates, sandstones and shales that lie unconformably above the RHF. Its color can be ascribed to the red oxide coating that occurs on the pebbles and smaller particles that make up the units (Jenness, 1963). Sedimentary units within the CHF are well bedded and display sharply defined bedding planes whereas the shales often exhibit a very fissile characteristic. The pebbles within the conglomerate are composed of red, pink, and black rhyolite, red and green sandstone, as well as quartz and on average are approximately 1 – 1 ½ cm wide (Dal Bello, 1977). Dal Bello also believes that a fluvial depositional environment is responsible for the CHF.

1.4.5 Love Cove Group (LCG)

The contact between the Love Cove Group and Musgravetown Group is proposed to run through Thorburn Lake (Figure 1.6) and Jenness (1967) suggests that the contact is likely to be near-vertical. The Love Cove Group is comprised of assorted rock types most of which are sedimentary and volcanic rocks of intermediate and mafic compositions that are interbedded with one another (Reusch and O'Driscoll, 1987; O'Brien, 1987). Dal Bello (1977) proposed that the volcanics within this group are ash-flow as opposed to ash-fall deposits as they are poorly sorted and exhibit no grading. Units of the LCG are dark green in color and are regionally metamorphosed to greenschist facies with the schistosity predominantly oriented north-northeast and steeply dipping (Dal Bello, 1977; Jenness, 1963). Evidence indicates that the LCG is older than the Musgravetown Group as pebbles of the LCG appear within conglomerates of the Musgravetown Group. Evidence also suggests that metamorphism of the LCG occurred before the deposition of the Musgravetown Group (Reusch & O'Driscoll, 1987).

1.5 Depositional Model

LS deposits usually occur in intra-arc or back-arc rifts within continental or island arcs (Robert, et al., 2007). In the Avalon zone, magmatic arc activity ended in the late Neoproterozoic and was followed by extension-related magmatism that was transitional into a Neoproterozoic-Silurian platformal clastic sedimentary sequence (Hibbard, 2007). It is believed that the Big Easy, as well as many other systems within the Avalon Zone, were formed during this extensional magmatic episode. Alteration assemblages typically found in LS epithermal systems are prevalent throughout siliceous hydrothermal breccias within the property. Such assemblages include sericite, illite, adularia, chlorite and epidote (Clarke, 2013).

A schematic diagram of a typical LS depositional model along with the mineral assemblages is shown in Figure 1.7. The study by Clarke in 2013 confirmed several similarities between the characteristics of a classic LS deposit and characteristics observed at surface as well as in drill core at Big Easy. Some characteristics include the presence of chalcedonic silica, adularia, sericite, illite, chlorite and carbonates. The presence of bladed textures along with adularia suggests there was subsurface boiling which implies this process occurred within a few hundred metres of the paleosurface. Ore zones observed to date have occurred primarily within brecciated zones with pervasive silicification as well as adularia and illite precipitation (Clarke, 2013).

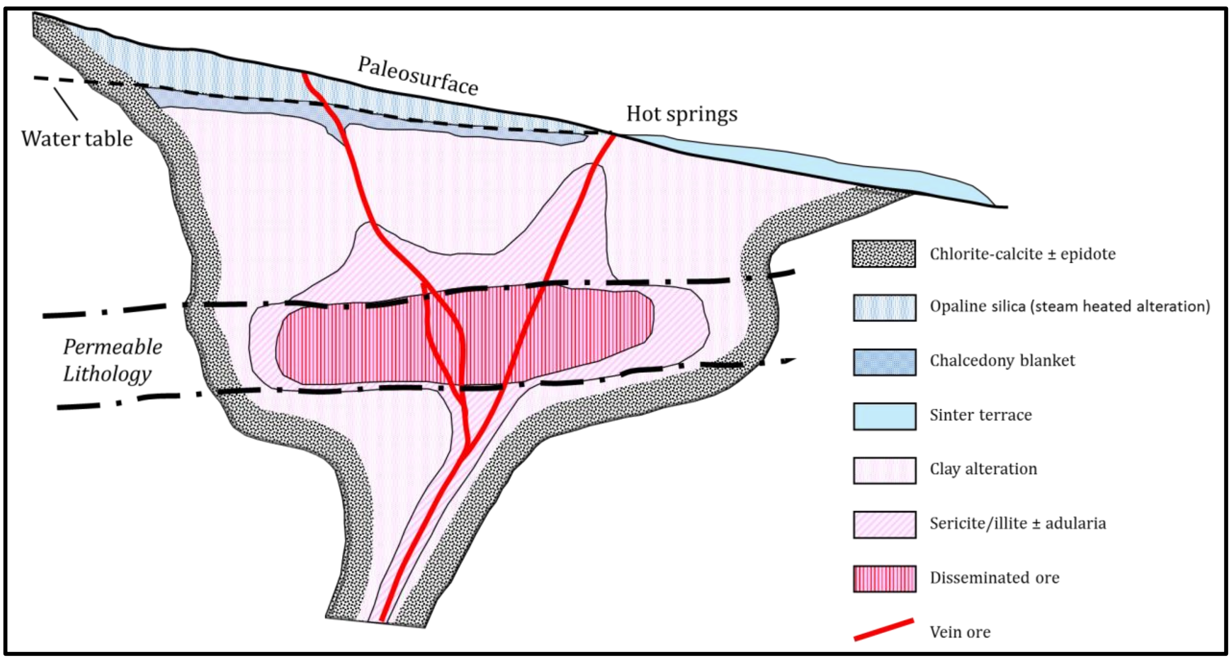

Figure 1.7: Schematic diagram of a typical low-sulphidation style epithermal deposit. Modified from Hedenquist et al (2000).

Chapter 2 Background Theory

2.1 Magnetic Fields and Anomalies

The flow of charge serves as the fundamental source of magnetic fields. Any charge movement, *e.g.* electric current, will have a magnetic field associated with it. A simple example of this would be a current flowing through a wire of infinite length (Figure 2.1). The magnetic field generated forms concentric circles about the wire. The strength of the magnetic field can be found from a form of Amperes Law:

$$\boldsymbol{B} = \frac{\mu_o I}{2\pi r} \tag{2.1}$$

where $\boldsymbol{B}$ is the magnetic field strength, μ_o is the magnetic permeability of free space, I is the current, and r is the distance from the wire.

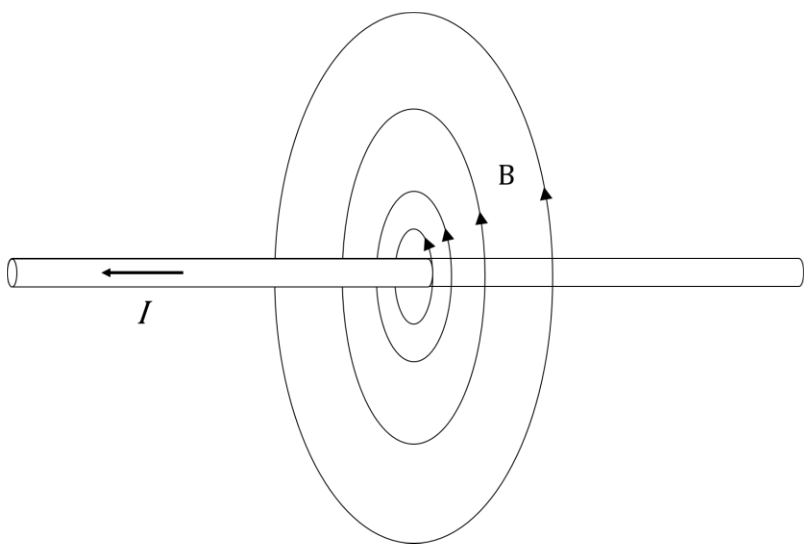

Figure 2.1: Magnetic field (***B***) induced by current (*I*) flowing through a wire of infinite length.

At an atomic level, a magnetic field is generated from the electron and proton spin. The charge on the 'surface' of spinning charged particles is analogous to the current carrying wire with the wire bent into a loop as seen in Figure 2.2. Here, the dot represents the flow of current coming out of the page while the X represents the flow going into the page. Due to the circular nature of the current flow, a dipolar magnetic field will be generated (Telford, 1990).

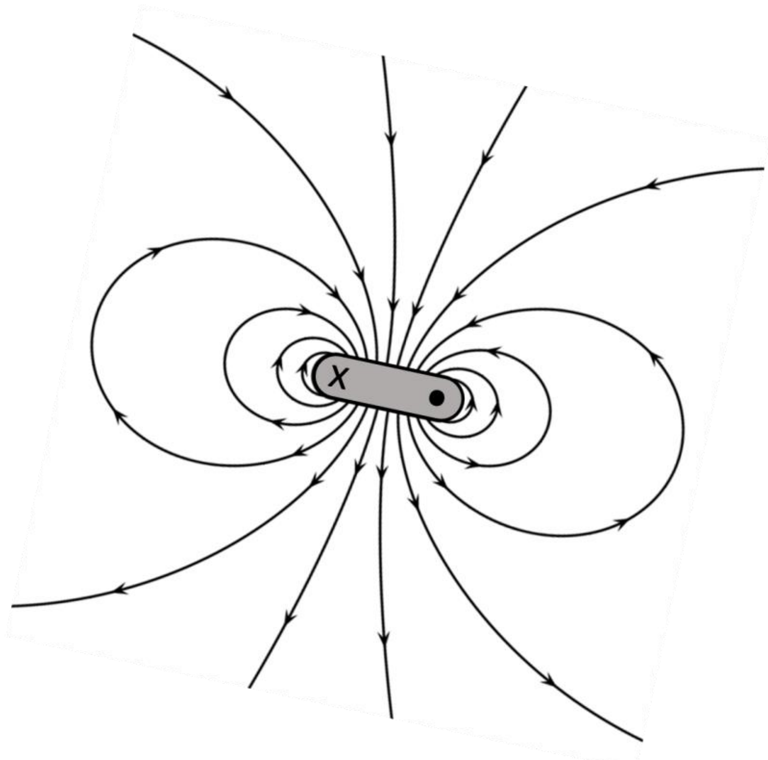

Figure 2.2: Magnetic field about a current carrying loop. Current direction is designated as out of the page at the black dot and into the page at the X (modified from Geek3, (2010)).

This phenomena also occurs on a global scale as currents are generated in the liquid metallic outer core rotating around Earth's solid iron-nickel core. These currents are complex, however at the Earth's surface the magnetic field from the large scale net current, circling counter-clockwise through the outer core, dominates. This net current produces an approximately dipolar field with an axis that is offset by approximately 11° from the Earth's rotational axis and is centred near the centre of Earth (Glatzmaier, 2016). At any point on the Earth's surface, the magnetic field, ***B***, can be entirely defined by three characteristics: the magnitude, the declination, and the inclination (Figure 2.3). The magnitude refers to the total strength of the field. Over the surface of the Earth, this varies between 25 000 nT near the equator and 65 000 nT near the geomagnetic poles. Since the axis of the geomagnetic field is at an angle to the rotational axis, for most points on the Earth's surface there is an angular separation between the direction to geographic north and the direction to magnetic north. This angle is called the declination (positive to the east). The inclination refers to the angle the field makes with the horizontal.

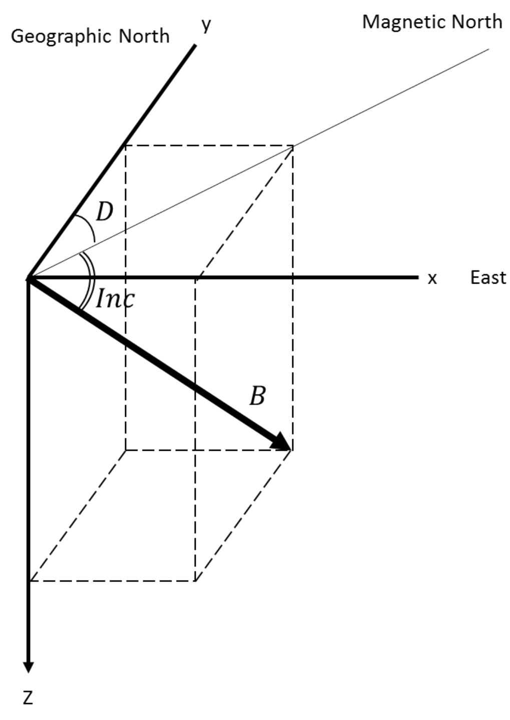

Figure 2.3: Components making up the Earth's magnetic field (modified from Telford et al, 1990). Here, ***B*** is the magnetic field vector, *D* is the declination, *Inc* is the inclination.

If a magnetically susceptible object is in the presence of an external field, this external field can cause the object to acquire an induced magnetization. This phenomenon increases the alignment of the intrinsic magnetic dipoles within the object which generates the magnetization $\boldsymbol{M}$ (Figure 2.4). For most materials, the direction of $\boldsymbol{M}$ is in the same direction as the inducing field, $\boldsymbol{B}$, and the degree to which an object will become magnetized is dependent only on the magnetic susceptibility, k. For simple materials, the magnetic susceptibility is related to the magnetization by

$$\boldsymbol{M} = \frac{k}{1+k}\frac{\boldsymbol{B}}{\mu_0} = \frac{k}{\mu}\boldsymbol{B} = k\boldsymbol{H}. \tag{2.2}$$

Where the magnetic permeability of the material $\mu = \mu_0(1+k)$, and the quantity $\boldsymbol{H}$ also often called 'the magnetic field' in geophysical applications, is related to $\boldsymbol{B}$ by the definition

$$\boldsymbol{H} = \frac{\boldsymbol{B}}{\mu_0} - \boldsymbol{M}$$

Although $\boldsymbol{B}$ and $\boldsymbol{H}$ are conceptually different, often times they are treated as the same entity. This is because they are linearly related by μ which, in air, is constant and equal to the magnetic permeability of free space, μ_0 (Telford et al., 1990). Differentiating between $\boldsymbol{B}$ and $\boldsymbol{H}$ becomes important only when measurements are taken within a magnetisable body. However, for this study, the value being measured will be referred to as the magnetic field, $\boldsymbol{B}$.

Magnetic susceptibility is the fundamental property in magnetic prospecting (Telford et al, 1990). Table 2.1 shows a list of common materials with their associated susceptibilities. The susceptibility of most minerals and rocks are quite small with the exception of the lower portion of the table. Magnetite, being the strongest and most common magnetic material, typically carries the dominate magnetic signature in rocks. Since magnetite is a common accessory mineral in igneous rocks, igneous rocks tend to be more magnetic than, say, sedimentary rocks.

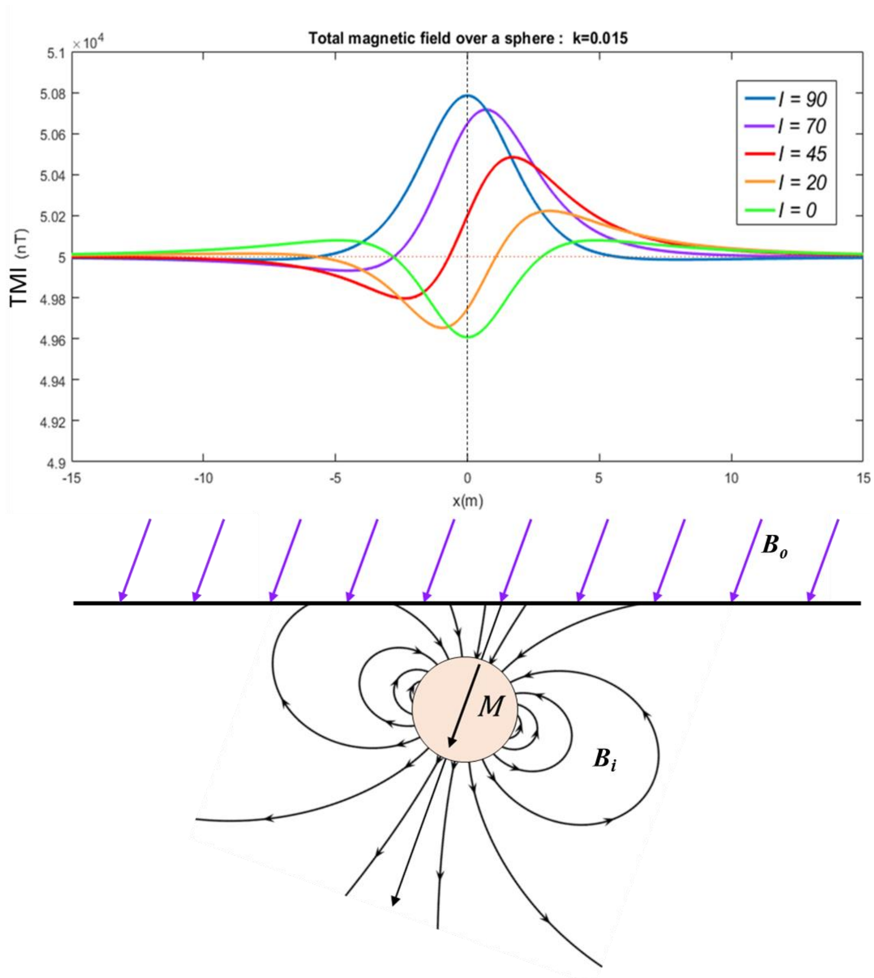

Figure 2.4: Bottom: representation a magnetizable sphere in the presence of the primary field $\mathbf{B}_0$ at an inclination of 70 degrees and the induced magnetization, **M**, the secondary field $\mathbf{B}_i$ generated from the inducing field. Top: Measured total field with varying angles of $\mathbf{B}_0$**.**

One issue often overlooked is that of remnant magnetization. Some materials are known to have a magnetic dipole that is 'frozen' into a position not necessarily in line with $\boldsymbol{B_0}$. Additional precautions must be taken when interpreting magnetic anomalies in areas with known remnant magnetization. However we assume that remnant magnetization is not an issue at the Big Easy.

During a magnetic survey, the measurements being collected reflect the total magnetic field, that is, the sum of the Earth's ambient field, $\boldsymbol{B_0}$, as well as any fields generated via induction,

Table 2.1: Magnetic Susceptibilities of various rock and minerals listed in ascending order of susceptibility (modified from Telford, 1990).

Type	Susceptibility $\times 10^3$ (SI) Range	Average
Sedimentary		
Dolomite	0 - 0.9	0.1
Limestones	0 - 3	0.3
Sandstones	0 - 20	0.4
Shales	0.01 - 15	0.6
Metamorphic		
Amphibolite		0.7
Schist	0.3 - 3	1.4
Phyllite		1.5
Gneiss	0.1- 25	--
Quartzite		4
Serpentine	3 - 17	--
Slate	0 - 35	6
Igneous		
Granite	0 - 50	2.5
Rhyolite	0.2 - 35	--
Dolorite	1 - 35	17
Augite-syenite	30 - 40	--
Olivine-diabase		25
Diabase	1 - 160	55
Porphyry	0.3 - 200	60
Gabbro	1 - 90	70
Basalts	0.2 - 175	70
Diorite	0.6 - 120	85
Pyroxenite		125
Peridotite	90 - 200	150
Andesite		160
Minerals		
Graphite		0.1
Quartz		−0.01
Rock salt		−0.01
Anhydrite, gypsum		−0.01
Calcite	−0.001 - −0.01	--
Coal		0.02
Clays		0.2
Chalcopyrite		0.4
Sphalerite		0.7
Cassiterite		0.9
Siderite	1 - 4	--
Pyrite	0.05 5	1.5
Limonite		2.5
Arsenopyrite		3
Hematite	0.5 - 35	6.5
Chromite	3 - 110	7
Franklinite		430
Pyrrhotite	1 - 6000	1500
Ilmenite	300 - 3500	1800
Magnetite	1200 - 19200	6000

$\boldsymbol{B_i}$. For this study, measurements were collected with the GSM-19 Overhauser magnetometer. This system uses a strong radio frequency current to align the electron spin of the free radicals within a solution encapsulated in the sensor which then couples with the protons via the Overhauser effect (GEM Systems, Inc., 2008). A short pulse is transmitted to deflect the proton magnetization into a direction near perpendicular to the Earth's field. After the pulse, the protons precess around the direction of the Earth's field at a particular frequency. The frequency of this precession is then measured and directly correlates to the strength of the total field.

Unlike gravity anomalies, magnetic anomalies are not necessarily centered about the causative body. Magnetic anomalies also generally have three extrema. A peak (or trough) would only occur centered over the body when both the primary field, $\boldsymbol{B_0}$, and $\boldsymbol{M}$ are vertical. Any other orientation would produce a response with both a positive and negative component. Therefore, the shape of an anomaly depends on the magnetic latitude of survey (*i.e.* the inclination of the inducing field). Figure 2.4 depicts a buried sphere in the presence of a magnetic field, $\boldsymbol{B_0}$. A magnetic dipole moment is created within the sphere and oriented in the direction of the inducing field. This, in turn, generates an additional magnetic field $\boldsymbol{B_i}$. The total field measured over the body is presented in the top panel. Each colored line represents what the anomaly would look like at varying inclinations of the inducing field. If the inducing field is perpendicular to the surface, the anomaly in centered about the body. As the inclination decreases, the anomaly becomes more and more skewed to one side. The asymmetric nature of the magnetic response can make it difficult to interpret the location of the causative source. Since the inclination of magnetic field over the Big Easy is approximately 68° (similar to the purple anomaly) there is only a slight shift in the positive peak of the magnetic response from the centre of the causative body. It is still convenient to apply what is known as a 'Reduction to the Pole' (RTP) mathematical filter to the gridded data. The RTP filter removes the effects of the geomagnetic latitude and produces a map of the data as if it had been collected at the magnetic north pole (*i.e.* I = 90°). All maps in the subsequent sections have had the RTP filter applied.

2.2 Gravitational Fields and Anomalies

The gravitational force was first expressed by Sir Isaac Newton in 1687 as: "The force between two masses is directly proportional to the product of the masses and inversely proportional to the square of the distance between their centres" (Telford et al, 1990):

$$\boldsymbol{F} = \gamma \frac{m_1 m_2}{r^2}\,\hat{\boldsymbol{r}}. \tag{2.3}$$

Here, $\boldsymbol{F}$ is the force exerted on a mass m_2 by another mass, m_1, γ is the universal gravitational constant 6.672×10^{-11} m^3/kg · s^2, r is the distance between centres of m_1 and m_2 and $\hat{\boldsymbol{r}}$ is the unit vector pointing from m_2 to m_1 (Figure 2.5). Newton's second law of motion states that a force is equal to the mass times the acceleration, $\boldsymbol{a}$:

$$\boldsymbol{F} = m\boldsymbol{a}. \tag{2.4}$$

The acceleration of m_2 due to m_1 can be found by dividing $\boldsymbol{F}$ by m_2 in Equation (2.3) to obtain

$$\boldsymbol{a}_g = \gamma \frac{m_1}{r^2}\hat{\boldsymbol{r}}. \tag{2.5}$$

The acceleration $\boldsymbol{a}_g$ is equal to the gravitational force per unit mass (2.4). If m_1 is the mass of the Earth M_e, $\boldsymbol{g}$ becomes the acceleration of gravity which can be expressed as (Telford et al, 1990):

$$\boldsymbol{g} = \gamma \frac{M_e}{r_e^2}\hat{\boldsymbol{r}}. \tag{2.6}$$

Here, r_e is the radius of the Earth and $\hat{\boldsymbol{r}}$ is pointing toward the centre of Earth.

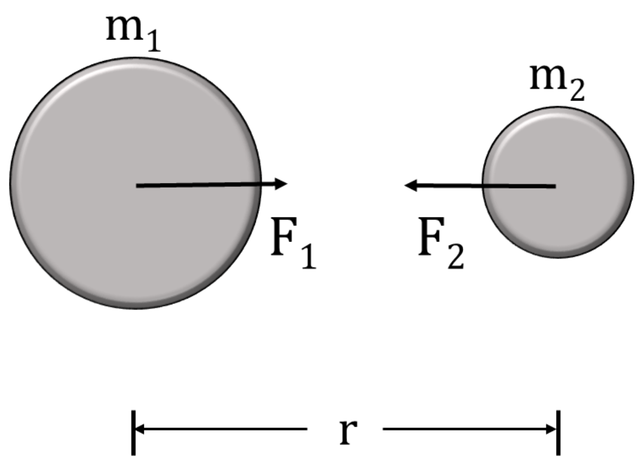

Figure 2.5: Gravitational force between two masses separated by a distance, r.

At any given point on Earth, there are many factors that contribute to the magnitude of gravity including latitude, elevation, surrounding topography, Earth tides, and density variations (Telford et al, 1996). Typically in mineral exploration, the only factor of interest is the density variations in the subsurface. A list of common rocks and minerals with corresponding density values is shown in Table 2.2. We see that igneous rocks, particularly those of mafic composition are on average 2.9 – 3.0 g/cm^3 while sedimentary rocks typically average around 2.5 g/cm^3. Since units are also magnetically different (Table 2.1), one would hope to distinguish between units as well as zones of alterations with a gravity and magnetic survey.

To isolate gravitational signatures due to density variations, several corrections are made to the collected data. These include; latitude correction, free-air correction, simple Bouguer correction, terrain correction, and earth tide corrections (ETC).

The largest variation, in both magnitude and scale, of Earth's gravitational field is due to Earth's approximate ellipsoidal shape and rotation. The latitude correction takes into account the shape of a reference ellipsoid approximating the shape of the surface of the Earth as well as the centrifugal acceleration created by the rotation of Earth. The gravity on the reference ellipsoid varies with latitude λ. There are several variants for the mathematical model representing Earth's gravity; in this study we utilize an approximation similar to the International Gravity Formula from 1980 (IGF 80) which is described by (Moritz, 1980) as

$$\boldsymbol{g}_o = 9.7803267714 \frac{1 + 0.00193185138639 sin^2\lambda}{\sqrt{1 - 0.00669437999013 sin^2\lambda}} \tag{2.7}$$

where $\boldsymbol{g}_o$ is referred to as "theoretical" or "normal" gravity (Blakely, 1996) measured in m/s^2. Equation (2.7) assumes only a vertical variation in density within the Earth's subsurface and neglects any lateral variations.

As can be seen in Equation (2.6), the effect of Earth's gravitation decreases by a factor of $1/r^2$ and therefore any increase in distance above or below the reference ellipsoid will affect any measurements taken. To account for any discrepancies caused by vertical deviations from the ellipsoid, the quantifiable effect of the topography must be removed. If the effect of the elevation is the only factor considered, and not the material that may be between the measurement height and the ellipsoid, this is referred to as the "free-air correction" and is given by:

$$\boldsymbol{g}_{fa} = -0.3086 \times 10^{-5} h \tag{2.8}$$

where $\boldsymbol{g}_{fa}$ is a measure of gravity in mGal and h is the height in metres and is positive above the reference ellipsoid and negative below the ellipsoid (Blakely, 1996). The free-air anomaly is then defined by

$$\delta \boldsymbol{g}_{fa} = \boldsymbol{g}_{obs} - \boldsymbol{g}_{fa} - \boldsymbol{g}_0 \tag{2.9}$$

where $\boldsymbol{g}_{obs}$ is the observed absolute gravity value collected at a given station.

Table 2.2. Densities of various rocks and minerals (modified from Telford et al, 1990)

Rock Type	Range (g/cm^3)	Average (g/cm^3)	Mineral	Range (g/cm^3)	Average (g/cm^3)
Sediments (wet)			*Metallic minerals*		
Overburden		1.92	*Oxides, carbonates*		
Soil	1.20 - 2.40	1.92	Bauxite	2.30 - 2.55	2.45
Clay	1.63 - 2.60	2.21	Limonite	3.50 - 4.00	3.78
Gravel	1.70 - 2.40	2.00	Siderite	3.70 - 3.90	3.83
Sand	1.70 - 2.30	2.00	Rutile	4.18 - 4.30	4.25
Sandstone	1.61 - 2.76	2.35	Manganite	4.20 - 4.40	4.32
Shale	1.77 - 3.20	2.40	Chromite	4.30 - 4.60	4.36
Limestone	1.93 - 2.90	2.55	Ilmenite	4.30 - 5.00	4.67
Dolomite	2.28 - 2.90	2.70	Pyrolusite	4.70 - 5.00	4.82
Sedimentary rocks		2.50	Magnetite	4.90 - 5.20	5.12
Igneous Rocks			Franklinite	5.00 - 5.22	5.12
Rhyolite	2.35 - 2.70	2.52	Hematite	4.90 - 5.30	5.18
Andesite	2.40 - 2.80	2.61	Cuprite	5.70 - 6.15	5.92
Granite	2.50 - 2.81	2.64	Cassiterite	6.80 - 7.10	6.92
Granodiorite	2.67 - 2.79	2.73	Wolframite	7.10 - 7.50	7.32
Porphyry	2.60 - 2.89	2.74	*Sulphides, arsenides*		
Quartz diorite	2.62 - 2.96	2.79	Sphalerite	3.50 - 4.00	3.75
Diorite	2.72 - 2.99	2.85	Malachite	3.90 - 4.03	4.00
Lavas	2.80 - 3.00	2.90	Chalcopyrite	4.10 - 4.30	4.20
Diabase	2.50 - 3.20	2.91	Stannite	4.30 - 4.52	4.40
Basalt	2.70 - 3.30	2.99	Stibnite	4.50 - 4.60	4.60
Gabbro	2.70 - 3.50	3.03	Pyrrhotite	4.50 - 4.80	4.65
Peridotite	2.78 - 3.37	3.15	Molybdenite	4.40 - 4.80	4.70
Acid igneous	2.30 - 3.11	2.61	Marcasite	4.70 - 4.90	4.85
Basic igneous	2.09 - 3.17	2.79	Pyrite	4.90 - 5.20	5.00
Metamorphic rocks			Bornite	4.90 - 5.40	5.10
Quartzite	2.50 - 2.70	2.60	Chalcocite	5.50 - 5.80	5.65
Schists	2.39 - 2.90	2.64	Cobaltite	5.80 - 6.30	6.10
Greywacke	2.60 - 2.70	2.65	Arsenopyrite	5.90 - 6.20	6.10
Marble	2.60 - 2.90	2.75	Bismuththinite	6.50 - 6.70	6.57
Serpentine	2.40 - 3.10	2.78	Galena	7.40 - 7.60	7.50
Slate	2.70 - 2.90	2.79	Cinnabar	8.00 - 8.20	8.10
Gneiss	2.59 - 3.00	2.80	*Non-metallic minerals*		
Amphibolite	2.90 - 3.04	2.96	Petroleum	0.60 - 0.90	--
Eclogite	3.20 - 3.54	3.37	Ice	0.88 - 0.92	--
			Sea Water	1.01 - 1.05	--
			Lignite	1.10 - 1.25	1.19
			Soft coal	1.20 - 1.50	1.32
			Anthracite	1.34 - 1.80	1.50
			Chalk	1.53 - 2.60	2.01
			Graphite	1.90 - 2.30	2.15
			Rock salt	2.10 - 2.60	2.22
			Gypsum	2.20 - 2.60	2.35
			Kaolinite	2.20 - 2.63	2.53
			Orthoclase	2.50 - 2.60	--
			Quartz	2.50 - 2.70	2.65
			Calcite	2.60 - 2.70	--
			Anhydrite	2.29 - 3.00	2.93
			Biotite	2.70 - 3.20	2.92
			Magnesite	2.90 - 3.12	3.03
			Fluorite	3.01 - 3.25	3.14
			Barite	4.30 - 4.70	4.47

As mentioned previously, the free-air correction takes into account only the effect of the elevation and not the attraction of additional mass between the datum and the measurement point. This results in a correlation between free-air gravity and topography which is often useful in marine based surveys but in most cases on land, this effect is wished to be removed.

The simple Bouguer correction approximates mass above the datum using a slab of thickness equal to the observation measurement height h that laterally extends to infinity and has a constant density. The Bouguer correction is given by

$$\begin{aligned}\delta \boldsymbol{g}_B &= 2\pi\gamma\rho h \\ &= 4.191 \times 10^{-10}\rho h.\end{aligned} \tag{2.10}$$

If the average crustal density of $2670\ kg/m^3$ is used, which is generally the case, Equation (2.10) becomes

$$\boldsymbol{g}_B = 0.1119\ \times 10^{-5}\ h. \tag{2.11}$$

The Bouguer anomaly resembles the density contrast as opposed to the total density and is given by:

$$\delta \boldsymbol{g}_B = \boldsymbol{g}_{obs} - \boldsymbol{g}_{fa} - \boldsymbol{g}_B - \boldsymbol{g}_0. \tag{2.12}$$

In cases where measurements are taken over lakes, ponds, or wetlands, using the average crustal density for the Bouguer correction would be inaccurate. Since there is such a large density contrast between crustal rocks and water, for instance, a lower gravity response would be observed over any pond or wetland. The Bouguer anomaly can be calculated more accurately in these cases if more is known about the material immediately below the measurement location. For example, if the thickness of the ice and water were known, both the ice and water column can be included in the calculation. Equation (2.12) would then become:

$$\delta \boldsymbol{g}_B = \boldsymbol{g}_{obs} - \boldsymbol{g}_{fa} - 0.04191[\rho h + (\rho_w - \rho)h_w + (\rho_i - \rho_w)h_i] \tag{2.13}$$

where h_w is the height of the water column (or other material) including ice thickness, h_i.

Since the Bouguer correction uses an infinite slab to estimate the mass, it ignores the shape of the topography adjacent to the measurement location. Hills above the station exert an upward force on the gravimeter while valleys below the station create voids within the slab. Both of these lower the observed gravity and require a terrain correction after the Bouguer correction.

The terrain correction is the most computationally intense correction required for a gravity survey. An in-depth formulation is presented in Appendix C but for the purpose of this study, a simplified explanation is described here. The terrain correction is calculated using a regional scale Digital Elevation Model (DEM) draped over a local scale DEM. The corrections are tabulated based on near zone, intermediate zone, and far zone contributions whereby the near zone has the most influence on the measurement (Geosoft Inc., 2015). Since the far zone contributes less to the overall terrain correction, the regional DEM is sampled more sparsely than the local DEM to save on computational requirements.

Earth-tides created by the positions of the Sun and Moon can have a small but measureable effect on a gravity reading. These values can range up to approximately 0.3 mGal (Telford et al, 1990) and have a sinusoidal pattern. In this study area, and around Newfoundland, the Earth Tide Corrections (ETC) are approximately ± 0.1 mGal. The tidal effect is time dependent as well as latitude-dependent but can be estimated accurately using the Longman's formulas (Longman, 1959) and readily removed. This formula resides both on the CG-5 Gravimeter for immediate removal as well as in the gridding and processing software, Oasis Montaj, for post processing.

2.3 Ground Penetrating Radar

Ground Penetrating Radar (GPR) is a high resolution, electromagnetic technique that allows one to investigate features in the near subsurface up to a few 10s of metres. High frequency pulsed electromagnetic waves, usually between 10 and 1000 MHz, are used to detect boundaries between material with differing electrical properties (permittivity and conductivity). As illustrated in Figure 2.6, an electromagnetic pulse is radiated from a transmitting antenna (Tx) and travels through the medium at a velocity governed by its electrical properties. The wave travels downwards and outwards until it interacts with an object or material with different electrical properties than the surrounding material (*e.g.* a buried pipeline or lake sediments). The wave is then scattered, a portion of the wave's energy continues downward and a portion of the energy reflects back to surface. Some of the waves reflected back to the surface are captured by the receiver antenna (Rx) and are recorded on a digital storage device. The most common way the data is displayed is signal

Table 2.3. Wave velocity in common materials modified from Annan, (2004).

Material	Velocity (m/ns)
Air	0.30
Ice	0.16 - 0.17
Water	0.033
Wet Soil	0.06
Rock	0.12

amplitude vs time and is referred to as a trace (Daniels, 2000). The depths d_i of interfaces can be determined from the travel times of reflected pulses if the velocity of the wave within the material, which for low conductivity materials depends largely on the electrical permittivity, is known. A table of typical wave velocities is shown in Table 2.3. For many materials such as air, water, ice and water, these values are relatively constant. For other substances that have very varying compositions such as soils, the velocity can vary dramatically and is usually heavily dependent on the water content. One way to determine the velocities for unknown materials is to use reflection hyperboles as is discussed in Section 3.2.1.

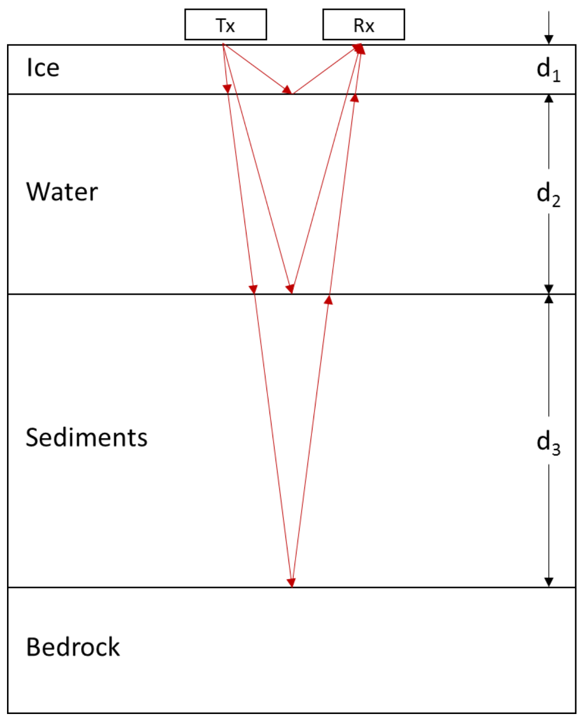

Figure 2.6: Schematic diagram representing the transmitted and reflected waves generated by the transmitter and observed by the receiver of a GPR system.

2.4 Real-Time Kinematic Positioning

Using satellites for positioning and/or navigation has been implemented for decades. A typical stand-alone hand-held global positioning system (GPS) receiver works by receiving pseudorandom noise (PSN) via a carrier wave (panel A in Figure 2.7). This signal is transmitted from the satellite to the receiver and contains a very accurate time stamp of when the signal was sent. The distance between the satellite and receiver can be calculated by comparing the time of the GPR receiver with the time stamp from the satellite. Through trilateration, a single intersection point in 3-dimensional space can be determined when combining signals from at least four satellites. However, this intersection point cannot be located geographically if the position of the satellites are not know. Fortunately, satellites orbits can be predicted quite accurately, but not perfectly. This information is stored in an almanac and used by the GPS to determine its position. A stand-alone receiver is typically able to locate its position with an accuracy of a few metres. For navigational purposes or many geophysical surveys, accuracy of a few metres is likely adequate. However, this is less than ideal when working with gravity surveys since **g** varies strongly with elevation, changing by 0.3086 mGal for every meter (Equation (2.8). For this reason, a real-time kinematic (RTK) system is used.

The RTK system is more complex but can acquire locations with a precision that is orders of magnitude greater than the stand-alone rover (NovAtel, 2016). It uses a base station that collects satellite information over the duration of the survey (typically several hours). Instead of using the information content or matching the phase modulation of the carrier wave, it determines the number of carrier cycles (panel B of Figure 2.7) between the satellite and the base station. Using

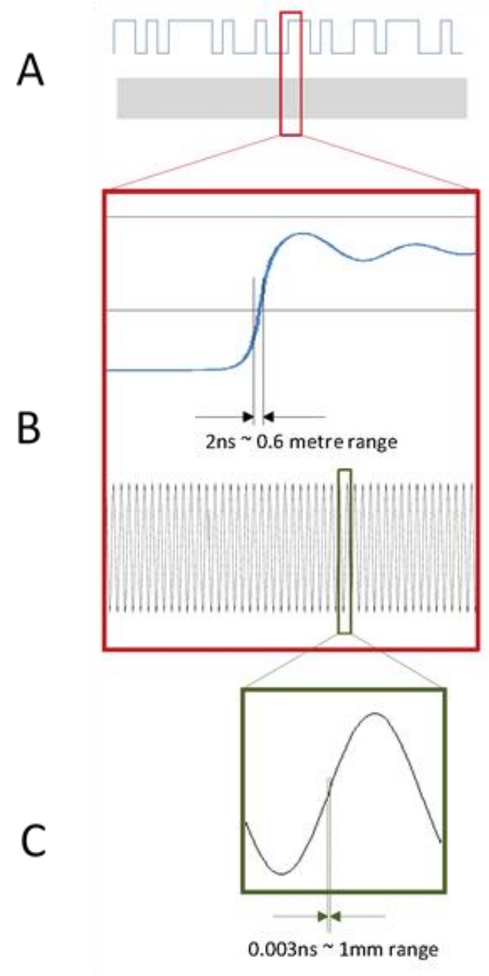

Figure 2.7: Conceptual diagram showing the different scales of phase modulation of a carrier wave (A) and the frequency of the carrier wave (B) and (C) (NovAtel, 2016).

the number of cycles and the wavelength, the distance between the satellite and base can be calculated. The wavelength of the carrier wave is much smaller than the phase modulation of the PSN and hence the greater precision.

Since the RTK system uses a base-receiver pair, errors introduced by ionosphere and atmospheric variability can be corrected as the range fluctuation will be common to both the base station and receiver. In addition to this refinement, post processing can be applied where the base station measurements are processed through Natural Resources Canada (Discussed in Section

3.2.2). In post processing, orbit ephemerides are used to make slight corrections of satellite coordinates and these new positions are used to obtain "absolute" geographical location.

2.5 Computational Modelling

The ultimate goal of this study is to generate a model of the subsurface defined by its physical properties that resembles the observed geophysical data while remaining geologically reasonable. Two methods are used to accomplish this goal: forward modelling and inverse modelling. In geophysics, the term forward modelling refers to the process of generating a response based on the physical properties within a model. Inversion modelling on the other hand, refers to generating a model defined by its physical properties based on the observed data. Forward and inverse modelling have fundamentally different approaches; both are discussed in detail below.

2.5.1 Forward Modelling

For the standard 2D forward modelling used to interpret magnetic and gravity data in this thesis, which is implemented using the software GM-SYS, individual units are typically divided into polygons, as seen in Figure 2.8. Each polygon is prescribed physical properties pertaining to the unit that are uniform throughout that unit. For magnetic and gravity models, the calculated response can be performed readily. The formulation of this procedure is straight forward but tedious and therefore a simplified explanation is presented here. Interested readers are directed to the works of Talwani et al. (1959) and Talwani and Heirtzler (1964) for a more thorough explanation. Essentially, the influence of a body of arbitrary shape can be determined at an observation point by integrating along the periphery of the body. The only information required to determine its influence are the coordinates of the observation point, the coordinates of nodes making up the body, and the body's physical properties. The influence is then calculated for every observation point along the Earth's surface. As mentioned, this process is not computationally demanding and therefore the body geometries can be modified while observing the response change in real time, allowing for quick adaptation of the model.

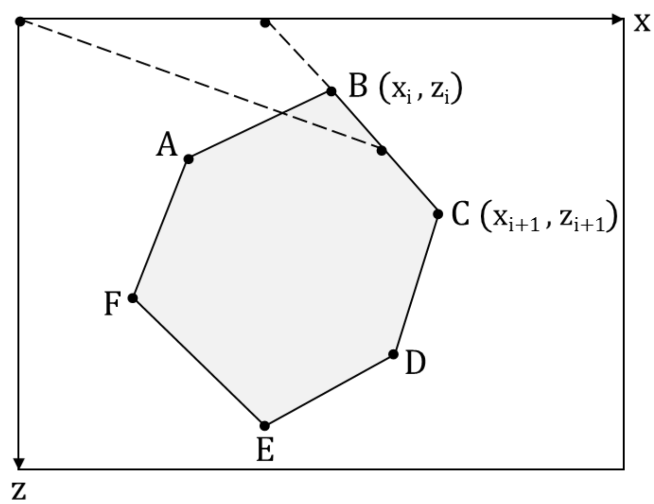

Figure 2.8: Typical approach to forward modelling where the response is generated at a point on the surface due to anomalous body represented by a polygon (modified from Talwani et al., 1959).

2.5.2 Inverse Modelling

Unlike models generated in typical forward modelling programs, inversion models are usually discretized by dividing the model into a series of many small cells where each cell contains one or more physical attributes. The response from the model can then be computed by summing the contribution of each individual cell on each observation point. Traditionally, the Earth model is discretized using a mesh of rectilinear cells (see Figure 2.9a). Using rectilinear cells is an attractive method since the inversion process can be calculated and coded readily. However, real world geology is rarely illustrated accurately when meshed with rectilinear cells and results in a stair-cased representation of interfaces, including the topography. One way to improve a model is by decreasing the cell size such that the model is better resolved (Figure 2.9b). However, decreasing the cell size, and thus increasing the number of cells, will increase the computation requirements. Alternatively, geological features can be represented with a non-uniform or "unstructured" mesh of triangles (Figure 2.9c). This method is particularly advantageous since features such as topography and geologic boundaries can be represented much better while minimizing the number of cells. The downside to representing the Earth model this way is that computing demands are higher due to lack of compression codes (Tycholiz, 2013). This could be very time consuming to compute, particularly for complex 3D models.

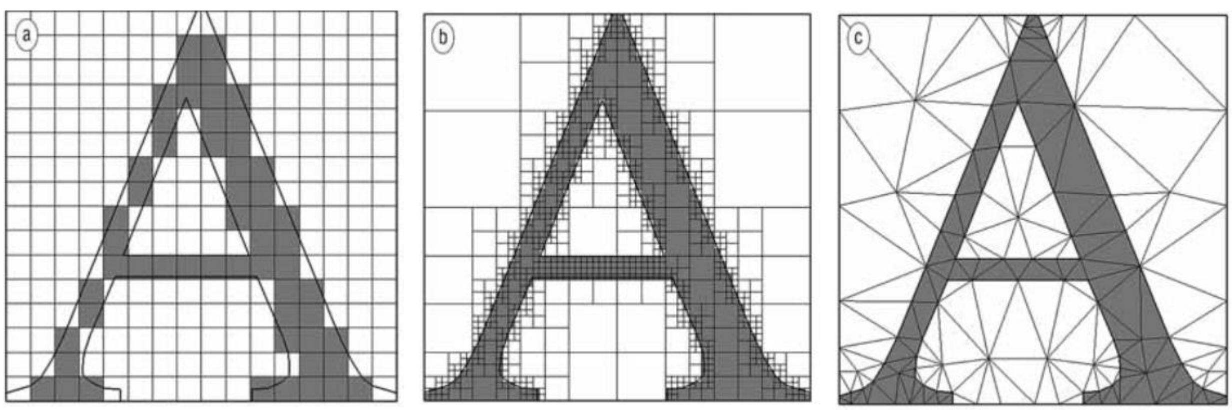

Figure 2.9: An example of discretizing a 2D shape using three types of meshes: (a) rectilinear, (b) quadtree, and (c) unstructured Delaunay triangular. The true shape to be represented (the letter A) is outlined in black while the models attempt is shaded grey. Number of cells are 256, 946, and 183, respectively. (Modified from Lelievre et al., 2012)

In this study, unstructured triangular meshes are generated via the publicly available program, Triangle (Shewchuk, 1996). Triangle's input is a poly file containing a list of nodes and facets referred to as a Planar Straight Line Graph (PSLG). For complex models, the PSLG is generated in FacetModeller, as described in Section 3.4. Triangle will create Delaunay triangulations from the input vertices and will create additional vertices, or Steiner points, along edges until the original facets of the PSLG are represented with facets in the mesh. This will often generate triangles with at least one small angle between its edges which is considered to be of poor quality. This can be overcome by using the –q flag which generates a quality mesh with a user defined minimum angle. Another way of refining the mesh is by triggering the –r flag and specifying the maximum ratio of facet lengths for a given triangle.

Inverse Theory

Calculating a set of physical parameters, m_i, within a model that reproduce measured observations is known as inversion. In this study, two separate inversion models are generated, one for magnetics and one for gravity. It is desired that the calculated response of these models will reproduce observations of the magnetic and gravity fields recorded over the property. To understand the inverse problem, the forward problem must first be discussed. In the forward problem, the physical property distribution is discretized into a volume V using triangles, as mentioned previously. The model is described by the vector $\mathbf{m}$, where $\mathbf{m} = [m_1, m_2, \dots m_N]$ and N is the total number of cells in the model. The expected measurements are calculated along the surface at discrete points and are denoted by the vector $\mathbf{d} = [d_1, d_2, d_3, \dots d_M]$ where M is the total number of data points. For some types of geophysical data, uncluding gravity and magnetic field measurements, the forward problem may be expressed as a linear system of equations:

$$\mathbf{d} = \mathbf{Gm} \tag{2.14}$$

where $\mathbf{G}$ is the forward operator. The solution to the forward problem in simply a vector-matrix product. The issue arises when attempting to move in the opposite direction in order to solve the inverse problem where $\mathbf{m}$ is desired based on a set of observations $\mathbf{d}^{obs}$:

$$\mathbf{m} = \mathbf{G}^{-1}\mathbf{d}^{\mathrm{obs}}. \tag{2.15}$$

In the inverse problem, the physical properties of N cells are sought based on M data points. However, in most cases we are faced with an underdetermined problem where N>M resulting in a non-square matrix **G** which is not invertible. The problem then becomes an optimization problem where a solution that minimizes the difference between the measured and calculated data as well as a numerical measure of the model is desired (Williams, 2008). The solution to the inversion problem can now be formulated as an objective function in the form of:

$$\begin{gathered}\phi(\mathrm{m}) = \phi_d(m) + \beta\phi_m(m), \\ \text{subject to} \quad L_i \le m_i \le U_i.\end{gathered} \tag{2.16}$$

Here, L_i and U_i refer to the upper and lower bounds set on the j$^{\mathrm{th}}$ model cell, the data misfit ϕ_d is a measure of the difference between the observed and calculated data; ϕ_m is some quantified measure of the model attributes, typically how rapidly the model varies spatially, and is known as the model norm; and β is the regularization parameter or Tikhonov parameter. β is essentially a scaling factor that defines the relative importance of the data misfit and model norm. As β approaches zero, more emphasis is placed on the data misfit term thus focusing primarily on fitting the data and not the model parameters. As β gets large, more emphasis is placed on the model norm.

Unlike forward modelling where the solution is unique, inversions tend to be more complex since an infinite number of models can reproduce the observed data equally well. By introducing geologic knowledge, *i.e*. constraints, one can greatly reduce the ambiguity of the results. Some examples of constraints include “compact inversion” where the inversion seeks a model with anomalous densities or susceptibilities in the smallest number of cells (Last & Kubik, 1983), inversions with a known geologic trend, and incorporating drill hole data. In this study, a minimum structure approach, based on Li and Oldenburg (1996), is taken whereby the resultant model is smooth. This minimizes the structural complexity of the resultant model by inhibiting high gradients (*i.e.* differences in physical property values) to exist between adjacent cells. Using the minimum structure approach, the model objective function can be defined by:

$$\Phi_m = \int w_s\left(m - m_{ref}\right)^2 dv + \int w_x (dm/dx)^2\, dv + \int w_y (dm/dy)^2\, dv + \int w_z (dm/dz)^2\, dv \qquad (2.17)$$

If a reference model, m_{ref}, is included in the inversion, the first term is referred to as the closeness term. This term forces the inversion to create a model that best matches the reference model while still maintaining the desired misfit. If a reference model is not included, the starting model is typically filled with zero values. The remaining three terms are the smoothness terms for the three orthogonal directions. As mentioned, the inversion attempts to minimize Φ_m and so, the program generates solutions where the absolute value of the gradients *e.g. dm/dx* are small. However, if a geologic trend is known, the smoothness weights, $w_x, w_{y,}$ and w_z can be adjusted so the resultant model will favour variation, *i.e.* increase the gradient, in a preferred direction while variations remain smooth in the other directions.

Data Misfit

The data misfit term, ϕ_d, measures the difference between the measured data, d_i^{obs}, and the data generated from the model $G[\boldsymbol{m}]_i$. The misfit function is given by Lelièvre et al. (2012) as

$$\phi_d = \sum_{i=1}^{N} \left(\frac{G[\boldsymbol{m}]_i - d_i^{\ obs}}{\sigma_i} \right)^2 . \tag{2.18}$$

The differences are normalized by the estimated uncertainty term, σ_i, which is an estimate of the measurement uncertainty. This term helps determine how well the calculated values should fit the observed data values (Lelièvre et al., 2012).

Depth Weighting

As mentioned previously, the potential field response decays with distance from the source (Section 2.2). This suggests that changing the physical property of a cell closer to the surface will have a greater impact on the calculated response than changing the property of a cell at depth. In order to prevent clustering of anomalous density or susceptibilities near the surface, a depth weighting parameter must be incorporated into the inversion. A method referred to as "sensitivity weighing" is proposed by Li and Oldenburg (2000) where the general form is represented by

$$s_j = \left(\sum_{i=1}^{N} G_{ij}^{\ 2} \right)^{\alpha/4} \tag{2.19}$$

and is subject to $0.5 < \alpha < 1.5$.

Here, s_j is referred to as the rms sensitivity which is a measure of the sensitivity of the whole data set to the j^{th} cell. The rms sensitivity is small when far away from all data points and large when close to one or more data points. The α parameter is chosen by the user to best match the depth decay of the sensitivities depending on the data type.

Chapter 3 Methods and Processing

3.1 Laboratory Methods

3.1.1 Magnetic Susceptibility Measurements

It was hoped that the magnetic susceptibility of the altered material at Big Easy would differ from that of the adjacent unaltered units. To determine whether this was the case and whether it was plausible to map units based on their magnetic signature, a susceptibility study was conducted. In this study, a total of 51 samples were taken by the author from drill core made available by the Department of Natural Resources. Measurements were taken using the KT-10 handheld magnetic susceptibility metre which has a sensitivity of 1×10^{-6} SI units. Since susceptibility can vary throughout a given sample and may be dependent on the orientation, ten measurements were taken along different axes of the specimen. These values were averaged for each sample and are displayed in Figure 3.1. Note the difference in scales within the plot. As the mafic unit has such a high magnetic susceptibility, it should be the most discernable unit in the magnetic data. There are differences between the units, in particular the altered sediments (red and

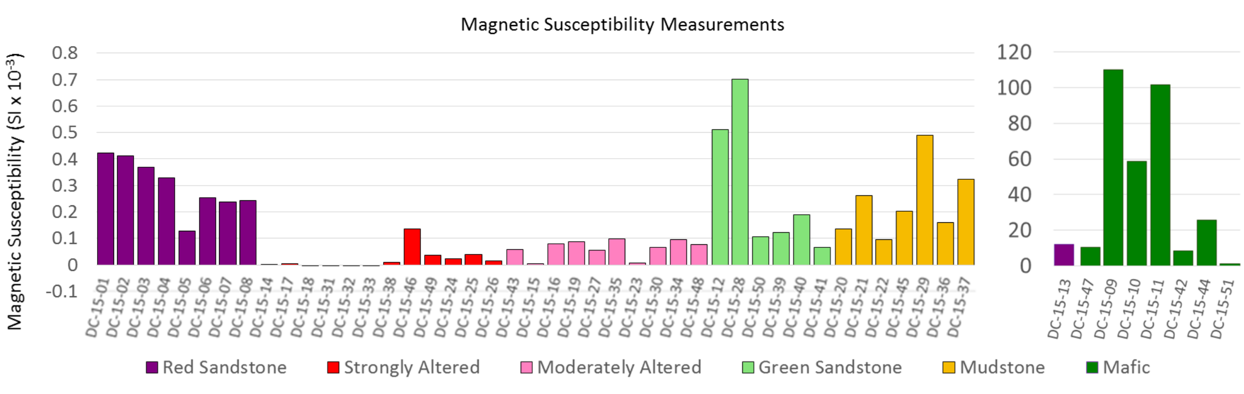

Figure 3.1: Magnetic susceptibility measurements of drill core. Sample numbers are along the x-axis; samples DC-15-14 through DC-15-26 are strongly altered sediments.

pink) have noticeably lower susceptibilities than the unaltered sediments, and almost all of the strongly altered sediments (red) have very low susceptibilities. This is likely due to the replacement of iron oxides of the red sediments with silica. However, the susceptibilities of all the sediments are low ($<10^{-3}$ SI units), especially compared with the mafic igneous rocks, and there is considerable variation of susceptibility within each unit. It is presumed that distinguishing between these units using their magnetic signature alone may not be feasible. Fortunately, as mentioned previously, mafic dykes observed on the property are often spatially associated with faulting thus locating mafic dykes could give insight to structural components of the potential deposit.

3.1.2 Density Measurements

Estimates of rock unit density are essential for two main reasons: determining whether a gravity survey is able to detect different units, and for applying the proper corrections to the collected gravity data. To obtain a better understanding of how the density values vary in the area, density measurements were taken from the same drill core samples mentioned previously.

The density of rock samples was determined using a method based on Archimedes principle which states that the upward buoyant force exerted on an object submerged or partially submerged in water is equal to the weight of water that the object displaces (Heath, 1897). Through simple derivations (not shown in this text), the density can be determined as the ratio of the mass of the sample to the difference of the masses of dry and submerged samples:

$$\rho_R = \frac{m_R}{m_R - m_{WR}} \rho_w \tag{3.1}$$

where: ρ_R is the density of the rock sample,
m_R is the weight of the saturated sample in air,
m_{WR} is the weight of the saturated sample while submerged in water, and
ρ_W is the density of the water.

The density of the water is dependent on several factors including the ambient pressure and the amount of dissolved air, but for the purpose of this thesis, the only relevant variable is the temperature of the water. The formula used to determine the density, as given by the International Committee of Weights and Measurement (CIPM) (MetGen, 2014), of water was:

$$\rho_w = a_5 [1 - \frac{(T + a_1)^2(T + a_2)}{a_3(T + a_4)}] \qquad (3.2)$$

where T is temperature of the water in degrees Celsius and a_1 to a_5 are all coefficients and are listed as:

a_1 = -3.983035 ^oC
a_2 = 301.797 ^oC
a_3 = 522528.9 $^oC^2$
a_4 = 69.34881 ^oC
a_5 = 999.974950 g/cm^3

The device used to determine these weights consisted of a high precision scale, a 5-gallon pail, a digital thermometre, and a harness constructed from lightweight fishing line.

First, the sample was placed in water for 2-3 days. This was done for two reasons: so the sample would not gain mass as the pore spaces fill with water when submerged during the weighing process, and because it is more representative of the rock present below the water table. The sample was then removed from the water in which it was stored, patted dry, and its mass was measured on the scale. The sample was then placed in the harness and suspended from a metal rod placed across the scale. Its mass was again measured while submerged in a pail of water. Density values measured are displayed in Figure 3.2 in order consistent with Figure 3.1. The results of Figure 3.2 show that there is a high variability of rock density values on the Big Easy Prospect. The silica altered rocks generally have a lower density than the surrounding units owing to the dense nature of mafic rocks and unusually high density of the red sedimentary package. As seen in Table 2.2, the average density of sedimentary rocks is approximately 2.50 g/cm^3 whereas the red sedimentary unit at the Big Easy has an average density of about 2.78 g/cm^3. The above-average density is likely due to the iron oxide content which also gives the unit its inherent purple color. The replacement of the dense iron oxides with less-dense silica is likely the reason for the difference in density of the unaltered and altered units.

To determine whether it is plausible to obtain a signature above the noise level of a gravimeter, a rough calculation is made to determine an expected gravity anomaly value. To calculate an expected gravity anomaly, a modified formula of a Bouguer slab is used:

$$g_B = 2\pi\Delta\rho\gamma T$$

Where $\Delta\rho$ is the difference in average densities between the unaltered red sediments and altered sediments, γ is the gravitational constant, 6.672x10^2 Nm/kg^2, and T is the thickness of the alteration zone estimated from drill hole data. Using the values of 2800 kg/m^3 and 2650 kg/m^3 for the unaltered and altered sediments, respectively, and 150 m for alteration zone thickness, it is calculated that the estimated gravity anomaly would be approximately 9.4 x 10^{-6} N/kg, or 0.94 mGal. Observing a gravity anomaly of this size is well above the noise level of a modern gravimeter and therefore it is plausible to detect different units with a gravity survey.

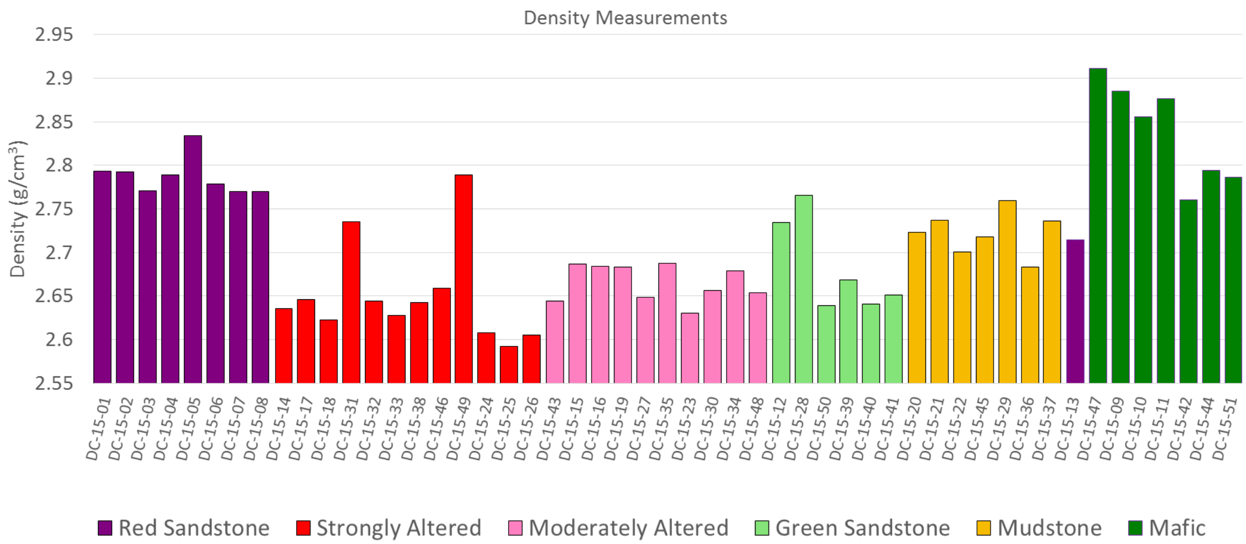

Figure 3.2: Density measurements of drill core. Samples here are presented in the same order as Figure 3.1.

A significant portion of the gravity survey was conducted over wetland areas and since wetlands are much less dense than lithic units, if left uncorrected, large depressions would exist in the gravity data over these regions (*e.g.* lcoation *D* in Figure 4.17). Therefore it was important to obtain accurate density values of the bogs to incorporate into the gravity corrections and modelling.

Three cores were extracted from the large bog area (Figure 3.3) and analysed in the lab. Sites were selected to cover a large portion of the wetland as to gain an average representative density value for the bog. Samples were collected by forcing plastic core liners, approximately 1 m in length and 6.5 cm wide (inside dimensions), into the bog. Inside the tube, a rubber bung was kept in contact with the top of the bog to create a vaccum as the tube was forced into the substrate. With the exception of a layer of grass and roots in the upper 15 cm of core, the bog was mostly a heterogeneous mixture of decaying plant matter with some roots. The density was determined by scanning the whole core with a multi-sensor core logger by Geotek. The core logger uses a method

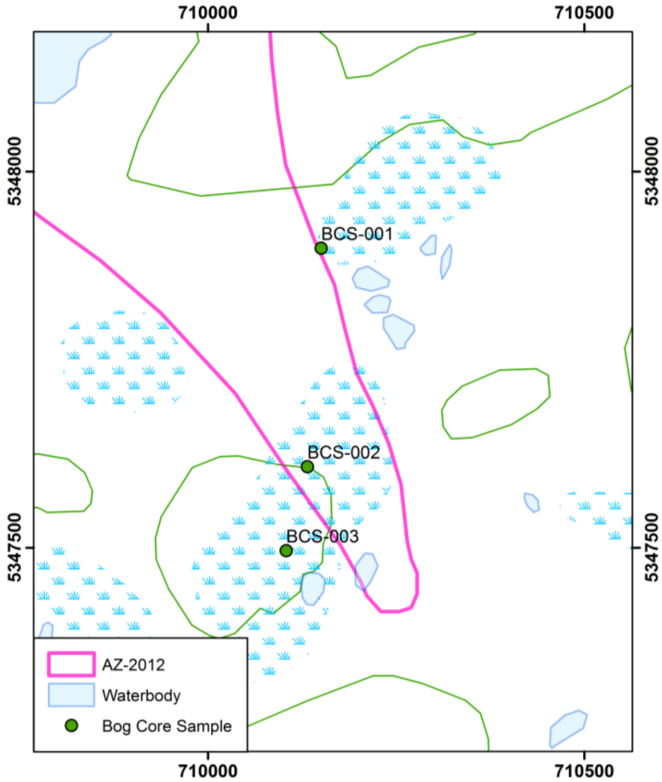

Figure 3.3: Location of bog core samples used for density measurements.

of measuring the density where a thin gamma ray is emitted from a source. Some of the photons are scattered while the rest pass through the core and are detected with a sensor on the other side. The amount of scattering is directly related to the electron density and by measuring this value, the density of the core can be determined (Geotek, 2017). The density was determined to be approximately 1.025 g/cm^3. To confirm this value, a 15 cm wide representative sample was cut from the core. This cut and sealed section was weighed and then the bog material replaced with water and the section weighed again. After subtracting the weight of the empty core section from both weights, the density of the bog material was determined by

$$\rho_b = \frac{m_b}{m_w}\rho_w$$

where m_b is the mass of the bog, and m_w is the mass of the same volume of water.

3.2 Data Collection and Processing

3.2.1 Ground Penetrating Radar

The system used in this study was the pulse_EKKO PRO by Sensors and Software Incorporated. All GPR surveys were conducted during the winter months while the ground was frozen. The system was operated with a 100 MHz transmitter and receiver which obtained information about the subsurface to a depth of approximately 10 m. The transmitter and receiver were housed by wood and fiberglass skis that were towed behind a sled carrying the operator, all of which was pulled by a snowmobile (Figure 3.4). The skis were custom designed and built by Memorial's Technical Services. The RTK roving receiver (discussed later) was mounted in a fixed position in the black sled, a measured distance from the transmitter and receiver to determine the true location of measurements. Survey grids were set up along the three ponds; Grassy Pond, Bottle Pond, and Bottle Pond North as well as a wetland area extending south of AZ-2012 (Figure 3.5). The unit was towed along each grid line at a speed of approximately 7-8 km/h. The data was collected in "free-run" mode which means measurements were taken at specific time intervals as opposed to distance intervals. Therefore the step size between traces is calculated before the survey is initiated by multiplying the known measurement rate by the estimated speed of the snowmobile.

The nature of the subsurface varies throughout the property. Over water bodies there exist a layer of ice, water, soft sediments and bedrock. Over wetland areas there exist a layer of ice, sometimes water, organic material, and bedrock. The data of interest from the GPR survey is the depth of each of these interfaces so they can be accounted for during the gravity corrections discussed in Section 3.2.4.

Figure 3.4: Configuration of GPR survey components including snowmobile, sled for the operator and RTK mount, and skis for housing the transmitter and receiver.

Processing of the GPR data was done using Sensors and Software's EKKO Project, Microsoft Excel, and Oasis Montaj. EKKO Project displays the individual line data in a window so that reflectors can be observed and "interpretations" can be added by the user. Such interpretations include a series of hand-picked points defining the locations of the ice-water, water-sediment, and sediment-bedrock interfaces. Information of the depth of these interfaces can be exported into Excel where corrections to the UTM coordinates of the measurement are made.

The predetermined step size is not necessarily correct since the estimated speed is likely not equal to the true speed of the snowmobile. This difference is most pronounced at the beginning

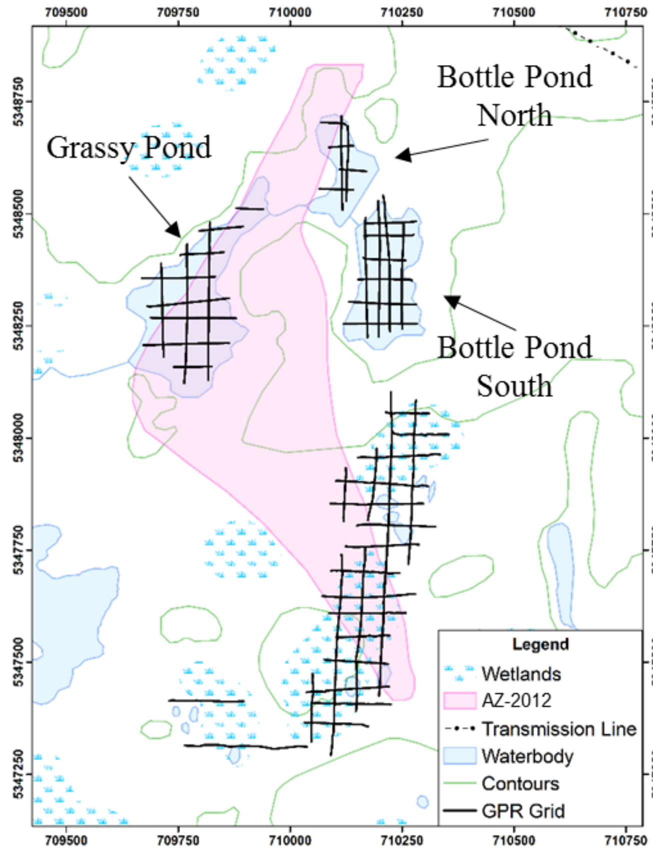

Figure 3.5: Map of GPR coverage over the Big Easy property.

and end of a survey line where the snowmobile was accelerating and decelerating. Therefore, before any analysis or interpretations can be made, the true position of traces must be found. To account for the acceleration and the deceleration, several metres of the data were clipped at the beginning and end of the line to remove these zones. The remaining data was collected with a more stable speed thus has a more uniform step size. The “Reposition using GPS” function is then used to obtain a better estimate of the trace location. This function operates by measuring the distance between every GPS location, summing them together to get the length of the lines, and dividing by the number of traces to get the average step size (Sensors and Software Inc., 2015). Once the horizontal scale is correct, the apparent wave velocity within the subsurface can be obtained as described below.

The apparent wave velocity was determined using a function within EKKO Project that allows one to fit hyperbolas to features within the data (Figure 3.6). These hyperbolic patterns were presumably caused from single reflectors on or near the bedrock surface. It is also assumed that all reflectors lay directly below the survey line. Multiple hyperbolas along several survey lines were analysed and an average value was obtained. The apparent velocity refers to the average velocity of a wave travelling within the subsurface as a whole, but does not provide the propagation velocity within an individual layer (*e.g.*, ice, water, or bog). Such information is required in order to determine the depth of each interface. Since EKKO Project does not provide this sort of processing, determining the velocity of the individual layers becomes laborious and requires the

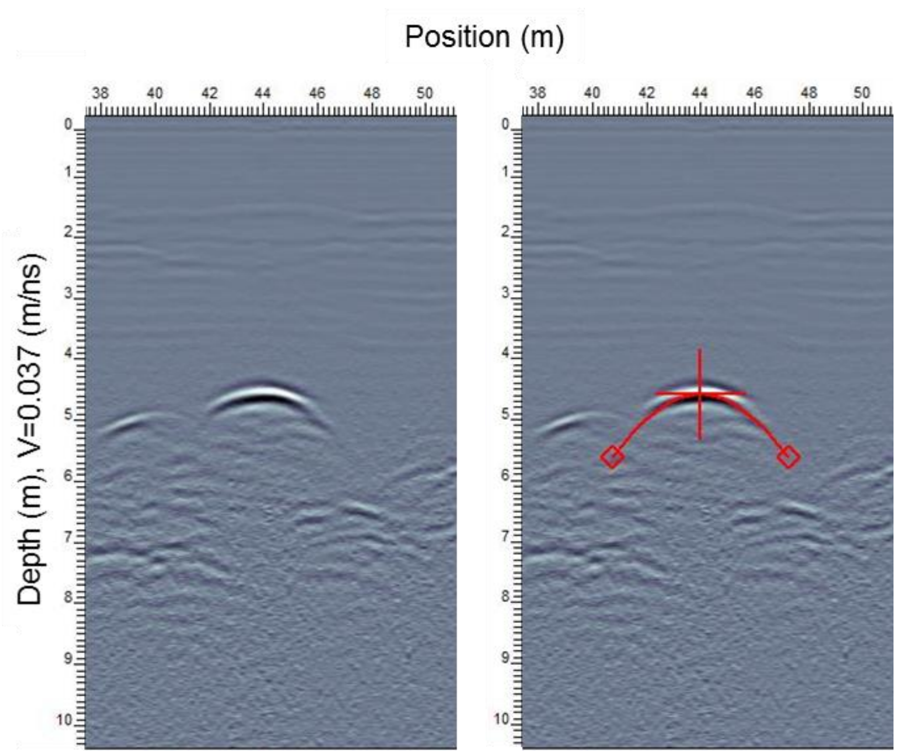

Figure 3.6: Velocity analysis along a GPR profile.

use of additional programs typically used in seismic data processing. Before any additional processing was employed, the effectiveness of using the apparent velocity to determine depth was assessed.

Simple algebra was used to estimate the true depth of each layer but some assumptions of material properties were made. The velocity of an EM wave in ice was chosen to be 0.16 m/ns and in water to be 0.033 m/ns, as they are generally tightly constrained in nature. It is also assumed that the wave traveled straight to the reflector and straight back to the receiver – that is, refraction of the ray was not considered. Since the ice-water interface appears so early in the signal, it is difficult to determine the exact time of the reflection. Fortunately, the ice thickness was measured in several areas on the pond and varied between 38 and 42 cm. For the purpose of the velocity analysis, an average of 40 cm was used for the calculations. The two wave travel time (TWT) of the wave within the ice layer can be determined by:

$$t = \frac{2d}{v} \tag{3.3}$$

since the thickness and velocity in ice is known. Here t is the TWT, d is the thickness of the layer, and v is the velocity of a wave propagating through a medium. A value of 5 ns was determined to be the TWT of the ice layer over the ponds. The time to the bottom of the water layer *i.e.* the top of the sediments is extracted from the GPR profile and the TWT of the wave in water is determined by subtracting the time spent in the ice layer. To determine the thickness of the water layer, Equation (3.3) is used again and solved for d. The TWT of a wave in the mud layer was obtained with the same process as described for the water layer. Determining the thickness of the mud layer is less intuitive since both thickness and velocity are unknown however, the apparent velocity of the combined layers is known. The apparent velocity is defined by:

$$v_{avg} = \frac{2(d_1 + d_2 + d_3)}{t_1 + t_2 + t_3} \tag{3.4}$$

$$d_3 = \frac{v_{avg}\ (t_1 + t_2 + t_3)}{2} - d_1 - d_2 \tag{3.5}$$

where d_1, d_2, and d_3, are the thicknesses of the ice, water, and sediment layer, respectively. The TWT travel time in the ice, water, and sediment layer is represented by t_1, t_2, and t_3, respectively. The only unknown in Equation (3.4) is the sediment layer thickness, d_3, which can be determined by rearranging to get Equation (3.5). Subsequently, the wave velocity in the sediment layer can then be determined by rearranging Equation (3.3) to get:

$$v = \frac{2d}{t}\cdot \tag{3.6}$$

The velocities and depths obtained from this analysis were compared to the results obtained simply using the apparent velocity in EKKO Project to determine the depth of each layer. Several areas were tested with varying depths as well as varying ratios of ice-water-sediments thicknesses to examine the error. It was determined that there is very little difference (typically 2% or less) between the apparent depth and the calculated depth to bedrock.

After the appropriate velocity was chosen, and proper depths were determined, interpretations of the sediment horizon and bedrock horizon could be made. This was accomplished using the polyline interpretation function within EKKO Project and tracing along the boundaries. The points making up the polylines have UTM coordinates and elevation information attached. However, these coordinates are associated with the location of the RTK receiver and do not represent the location of the antennas where the measurement was taken. The UTM coordinates were corrected to the GPR measurement location by shifting the data a fixed distance equal to the offset between the RTK receiver and the midpoint of the GPR transmitter and receiver (see Figure 3.4). To further refine the absolute location of the measurement, the data was again shifted to take into account the shift of the RTK measurement after the correct RTK base station location was obtain from the Precise Point Processing (discussed below). The depths of the nodes, along with their corrected locations were then used to create 2D profiles and incorporated in the modelling process (Section 4.1)

Table 3.1: Table comparing the depth of bedrock at test locations using individual layer velocities versus average velocity. Line column describes the location, Grassy Pond (GP) or Big Bog (BB), oriented either East-West (X) or North-South (Y) as it appears in the GPR file.

Line	Velocity (m/ns)	$Depth_{calc}$	$Depth_{apparent}$	Diff (%)	Diff (m)
GP X Line 04	0.037	4.45	4.48	-0.532	-0.024
GP X Line 02	0.037	4.52	4.55	-0.602	-0.027
GP X Line 03	0.037	4.16	4.18	-0.571	-0.024
GP X Line 03	0.037	4.18	4.20	-0.552	-0.023
GP Y Line 00	0.037	4.53	4.55	-0.532	-0.024
GP Y Line 00	0.037	4.43	4.33	2.154	0.095
GP Y Line 00	0.038	3.62	3.55	2.027	0.073
GP Y Line 02	0.037	4.44	4.47	-0.533	-0.024
BB X Line 00	0.037	4.09	4.12	-0.668	-0.027
BB X Line 00	0.039	2.65	2.80	-5.586	-0.148
BB X Line 01	0.039	4.98	5.02	-0.848	-0.042
BB X Line 01	0.039	4.54	4.58	-0.823	-0.037

3.2.2 Real Time Kinematic Positioning

The RTK system used in this study was TopCon's HiperV and the handheld FC-500. In order to achieve maximum precision, it is recommended that the stationary base receiver take static readings in an open area for a minimum of four hours which, after processing, allows Topcon's base to determine its location with an overall accuracy of ± 4 mm (Topcon Corporation, 2014). The general setup of the RTK base station is shown in Figure 3.7.

Figure 3.7: Setup of the RTK base receiver. System consists of receiver (on top of tripod), external battery (behind yellow case), and the radio which consists of the amplifier (right leg) and antenna (left leg). See Figure 3.4 for roving receiver).

In order to determine the locations of each survey measurement, a portable rover receiver was used (Figure 3.4). The rover has the ability to attain its position via traditional global positioning methods but this level of accuracy, which typically is within a few metres in the x, y, and z direction, is not ideal. Instead, the receiver determines its position relative to the base station.

Since centimetre precision of the base station location can be determined, centimetre accuracy of the receiver can also be determined. The two devices communicate via ultra-high frequency (UHF) waves and a signal booster is used at the base station to extend the range of the UHF waves to several kilometres.

A higher level of accuracy is obtained by processing the static data. Static data refers to the positional information collected by the base station over the period of several hours. This data is input into the Precise Point Positioning (PPP) application accessible through the Natural Resources Canada website (Government of Canada, 2015). In this application, the data undergoes automated processing where it uses the GNSS satellite orbit ephemerides to more accurately determine the base station location. Once the base station location is modified to the 'absolute' location, each point collected from the rover can go through a first order transformation equal to the offset of the new base location and the initial base station. These values now represent the 'absolute' location of each point.

3.2.3 Magnetics

The magnetometer that was used during this project was GEM Systems' GSM-19 Overhauser magnetometer with integrated GPS (Figure 3.8). The GSM-19 is capable of a 5 Hz sampling rate (GEM Systems, Inc., 2008) but to avoid oversampling, the magnetic survey over Big Easy was taken at a 2 Hz sampling rate. Prior to June 2015, a single magnetometer from the Archaeology Department was used for the magnetic survey. The newly acquired system belonging to the Earth Sciences Department had an additional magnetometer to utilize as a base station allowing the measured values to be corrected for diurnal effects.

The magnetic survey followed existing cut lines oriented east-west, near perpendicular to geologic strike, and spaced at approximately 100 metres (Figure 3.9). A base line running perpendicular to the survey lines was used as a tie line. Where possible, extra lines of data were collected in open areas such as bogs and ponds in an attempt to obtain higher resolution. Surveys over these areas were done mainly during the winter months when the surface was frozen.

The GMS-19 magnetometer was used in tandem with a secondary magnetometer base station for removing diurnal effects such as fluctuations in Earth's magnetic field. Before the survey is initiated, the roving unit acquires the Coordinated Universal Time (UTC) from the GPS

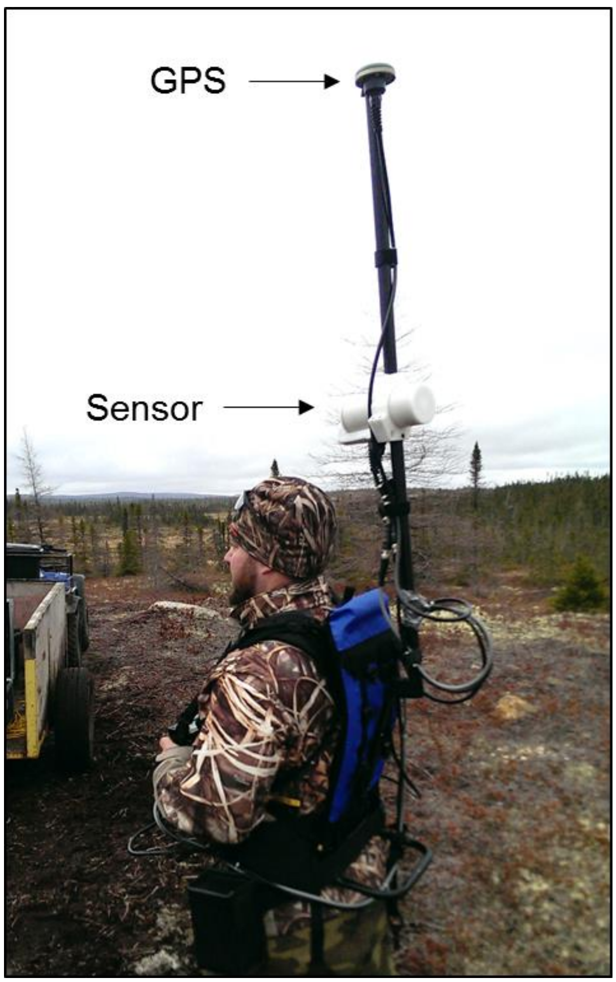

Figure 3.8: Assembled GSM-19 magnetometer with integrated GPS.

system and the time was then transferred to the base station via a synchronization cable. Ensuring the time is synchronized allows diurnal corrections to be made. To reduce the amount of data collected by the base station, a measurement was taken every 4 seconds by the base as opposed to every 0.5 seconds with the rover.

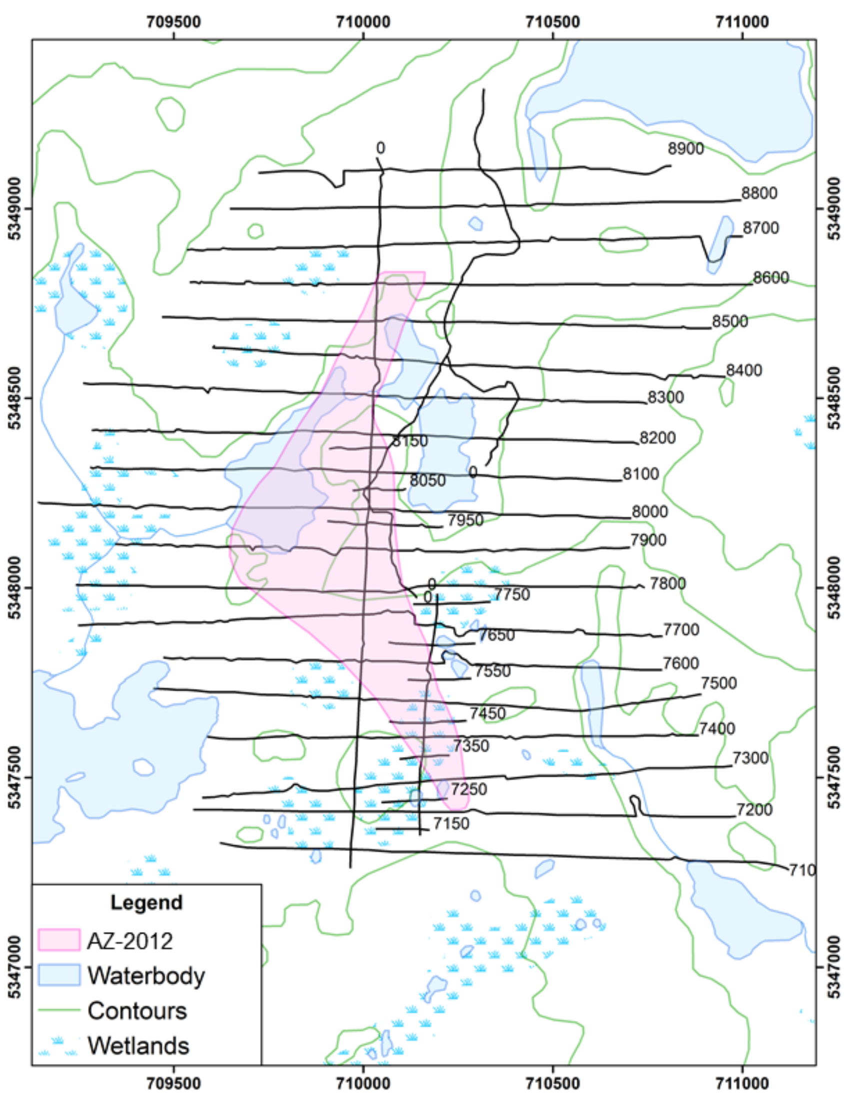

Figure 3.9: Map of magnetic survey coverage.

Diurnal Corrections

The first step in the processing is the diurnal corrections. As discussed earlier, the measurement rate of the rover and base differ and therefore the time stamp of readings taken by the rover may not match that of the base station. To account for this, the value of the base is linearly interpolated to the time of the rover. The true magnetic value, corrected for diurnal effects, was then calculated using:

$$B_D = B_m - B_b + D. \tag{3.7}$$

Here, H_D is the total magnetic intensity corrected for diurnal effects, B_m is the magnetic intensity measured by the mobile unit, B_b is the magnetic intensity measured by the base station (Figure 3.10), and D is the datum which is generally chosen as the average intensity of the survey area (GEM Systems, Inc., 2008) based on the International Geomagnetic Reference Field. For the Big Easy Property, the datum was determined from the IGRF calculator at the National Oceanic and Atmospheric Association to be approximately 51613.8 nT (National Oceanic and Atmospheric Association, 2015).

The magnetic data exported from the GSM-19 module includes the UTM coordinates, B_m, B_D, and number of satellites used to determine the UTM coordinates. The data was sorted by line number in Excel and plotted into 2-D maps using Oasis Montaj. It was observed from the plot of the jittery track that positional uncertainty was greatly increased when fewer than 5 satellites were used to determine the UTM coordinates. All measurements obtained with insufficient satellite counts were removed from the dataset for this reason. Since the magnetic field was so densely sampled, essentially no resolution was lost by removing these data points.

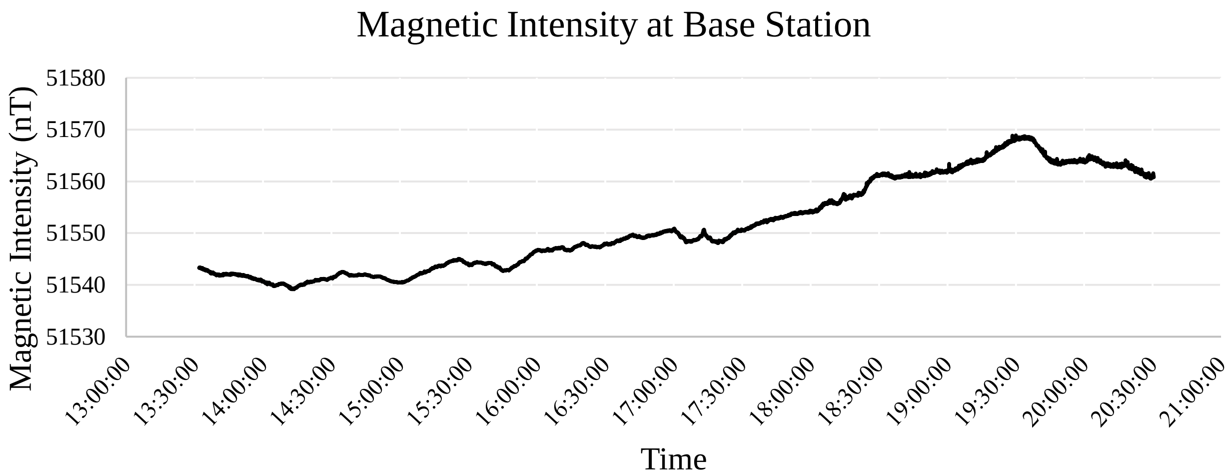

Figure 3.10: Change in the magnetic field intensity during a typical day with time displayed in UTC (2.5 hours ahead of local time). Data collected at the Big Easy during Feb 22, 2016.

There are 19 diamond drill holes on the property which have steel collar casings that mark the top of the hole. These collars are mostly along grid lines and consequently interfere with the magnetic data. Fortunately, the signatures created are easily distinguishable as they show up as large spikes in the data (*e.g.* Figure 3.11). The location of all drill collars were confirmed with geospatial data and their effects were removed by highlighting and deleting affected measurements.

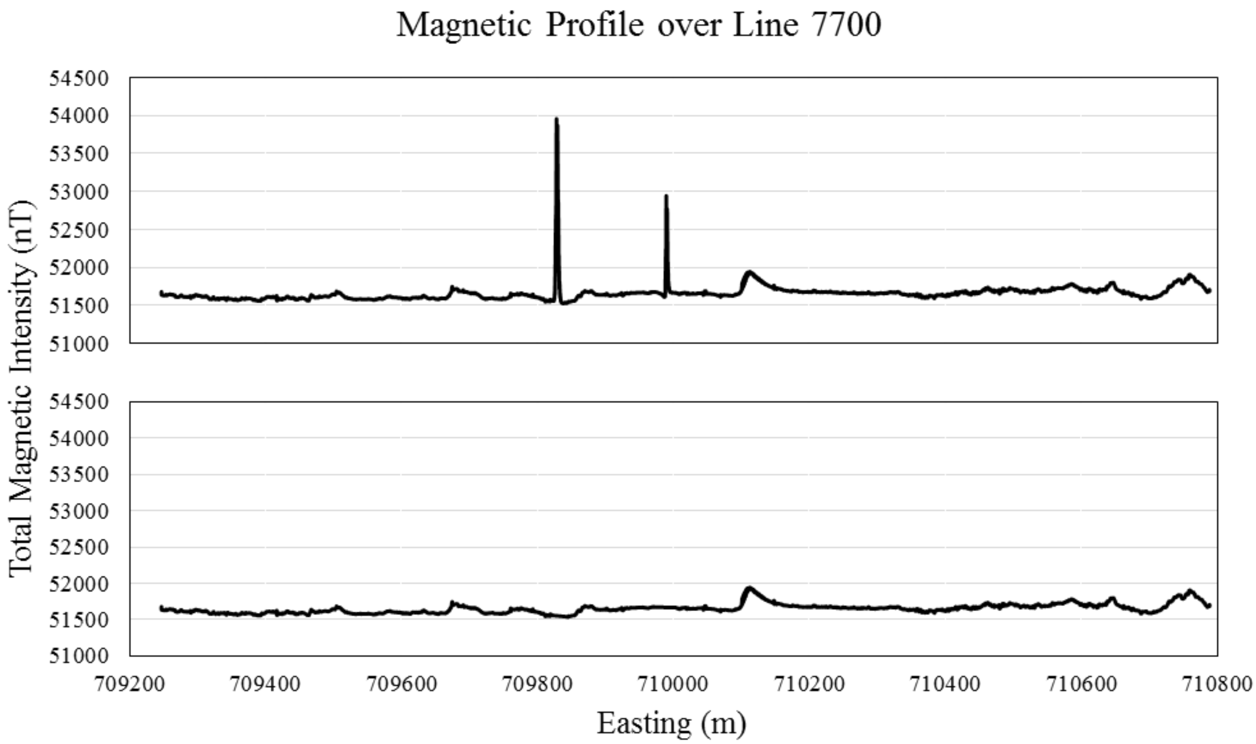

Figure 3.11: Magnetic profile over Line 7700 including the effect of drill collars (top) and with effect of drill collars removed (bottom).

Levelling

The GMS-19 rover and base station pair were not acquired until part way through this study. Before this point, a single GSM-19 rover was used for a portion of the survey. Since only one rover was available, diurnal corrections could not be made. However, it is assumed that variations along a given line are negligible since the time to survey a line was relative short and diurnal effects were very small (see Figure 3.10). However, the diurnal offset must be taken into account when attempting to merge a given line with the rest of the collected data. Since surveys were sometimes months apart, major discrepancies can exist from line to line and to fix this issue, the data must be 'levelled'. The magnetic data was manually levelled using the base line as a reference. This was done using Oasis Montaj which allows one to compare the value of a measurement taken along one survey line and with the measurement taken at the same location while traversing the base line. The magnetic field along the entire survey line is then shifted by the offset value to bring it to the same level as the baseline. This was repeated for all of the data that was collected without using the base station. For other surveys which did not cross the baseline at any point, such as the north-south line traversed toward the south end of the property, the magnetic intensity values were compared with any intersected lines that had already been levelled.

Gridding

Interpolating between data points onto a regularly spaced 'grid' within some coordinate system is referred to as gridding (Geosoft, 2016). To achieve optimal results the grid spacing, or cell size, is chosen to be no less than $1/5^{th}$ of the line spacing. Several methods of gridding exist, each of which is designed to best represent the data based on the collection method, spatial variations, and sampling rate. Choosing a proper gridding technique as well as appropriate parameters is crucial in order to minimize misleading or distracting artifacts in the resulting map. Two methods of gridding are discussed below and results are shown in Section 4.2.

In geologically complex areas where more than one trend is observed, it is beneficial to use the minimum curvature method to avoid focusing on features with a particular trend at the expense of others. The minimum curvature method is analogous to draping a thin sheet through the data points while minimizing the amount of bending (Dressler, 2009). One downside to this method is that, when a geographical coordinate system is used, the rectilinear interpolation grid is oriented N-S and E-W. This can introduce a 'boudinaged' effect when interpolating features that are not oriented in the cardinal directions. Another downside of the minimum curvature method is that amplitudes may not be truly honored. Since it is attempting to create the flattest surface higher amplitude features may be truncated. For these reasons, interpretations were also based on another method of interpolation called bi-directional gridding ("bigrid").

The bigrid method is ideal for data collected along lines where the geological strike of the area is uniform. It is particularly appropriate for data that has been collected much more densely in one direction (along a line) than another direction (across lines) as is the case at the Big Easy property. Figure 3.12 shows the bi-directional gridding process. An E-W survey grid is depicted by Panel A. Firstly, data points are interpolated along each line (blue points in Panel B), ensuring that any point along the grid that overlaps an observed data point matches that value. Note that the tie line is not used during the interpolation since none of the interpolation lines intersect the tie line. A second interpolation occurs at the intersection points, but orthogonal to the initial interpolation. The result is another grid where nodes exist between the survey lines (red points in Panel C). If a general geologic trend is known, the grid can be rotated to the strike direction so the second interpolation is in the direction of strike as seen in *D*. This puts an emphasis on features oriented in this direction. Since the process for bigrid involves two steps, different interpolation methods can be used for down-line and across line. In this case, the Akima spline method was used for both directions as it yielded the best results. Akima is an interpolation method that creates a surface that passes through all the data points while supressing undulations that would typically occur using other spine methods (Akima, 1978). This is particularly useful in gridding magnetic data since higher frequency spikes, such as those generated from mafic dykes, can be accurately displayed without lower amplitude artifacts surrounding the feature. From the minimum curvature attempts, it was clear that many trends exist over the property but one dominant trend of linear features was present. Therefore, the grid was rotated to an orientation of 025 to suit the general trend of what are presumed to be mafic dykes.

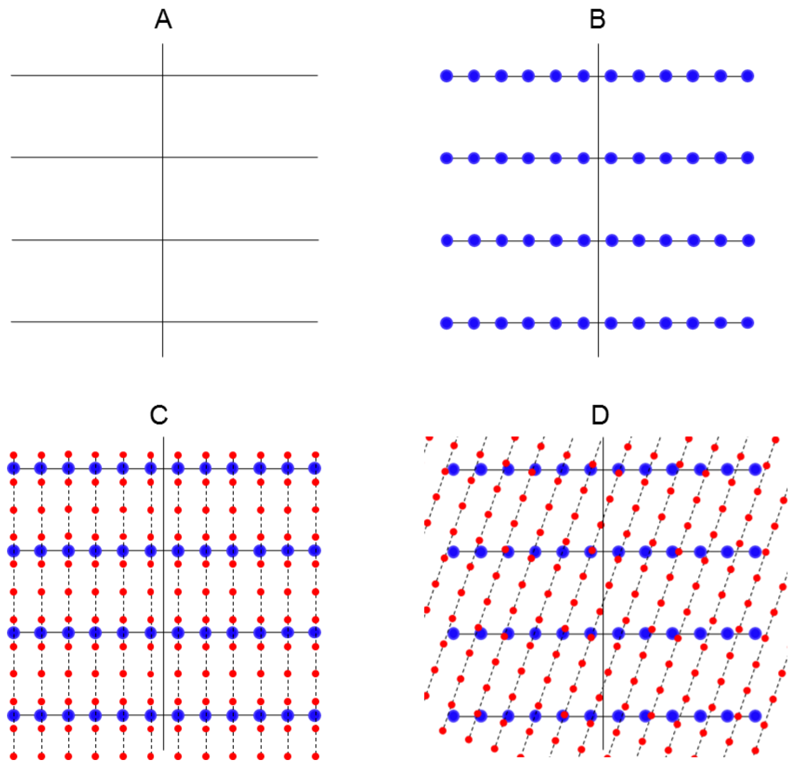

Figure 3.12: Process of bi-directional gridding showing E-W survey lines with N-S tie line (A), interpolation points along grid (B), second interpolation orthogonal to grid (C) and second interpolation at some angle to the grid (D) (modified from Geosoft, 2016).

3.2.4 Gravity

The gravimeter used to collect data was the Scintrex CG-5 Autograv System (Figure 3.13) which is based on a fused quartz elastic system that uses a small electrostatic restoring force on a suspended mass (Scintrex Limited, 2009). The current supplied to create the restoring force is directly proportional to the relative gravity at the measurement site and under ideal conditions is accurate to 0.001 mGal. The CG-5 system includes a leveling tripod that ensures the device is level to within 10 arc-seconds (less than 3 one-thousandths of a degree). It also includes a remote to trigger a reading without physically touching and disrupting the system and a GPS for positioning accurate enough for calculating real-time Earth tide corrections. During the measurement, the tilt of the CG-5 is also recorded for each reading and taken into account. Typically any measurement taken with a tilt greater than 150 arc seconds was discarded and retaken. Measurements were taken over 60 second intervals at a rate of 6Hz and averaged for a single output value. A standard deviation of 0.1 mGal (approximately 10% of anomaly) was used as a threshold to determine quality data. Any recording with a standard deviation greater than the threshold was repeated.

Figure 3.13: CG-5 gravimeter during station measurement.

Since the CG-5 measures relative gravity, and not absolute gravity, it is necessary to have a base station where the absolute gravity is known. If a base station is established, all relative gravity measurements can be determined with respect to the known value at the base station. Essentially, this process establishes a gravity datum for the survey. Two base stations were used as reference stations. One base station, *Murray*, is located in the basement of the Alexander Murray building in St. John’s. Another, labelled *Clarenville,* was located at the former Manpower Centre in the town of Clarenville. *Clarenville* is very close to a station registered under the Canadian Gravity Standardization Network (CGSN). *Murray* is tied into a registered station on the Memorial Campus. Measurements are taken in a specific order called ‘loops’. Loops begin and end with measurements at the same reference station. These loops are used to calculate the amount of drift associated with the instrument as well as any offset associated with transporting the instrument (discussed below). The shorter these loops, the more accurately one can determine the drift. Loops

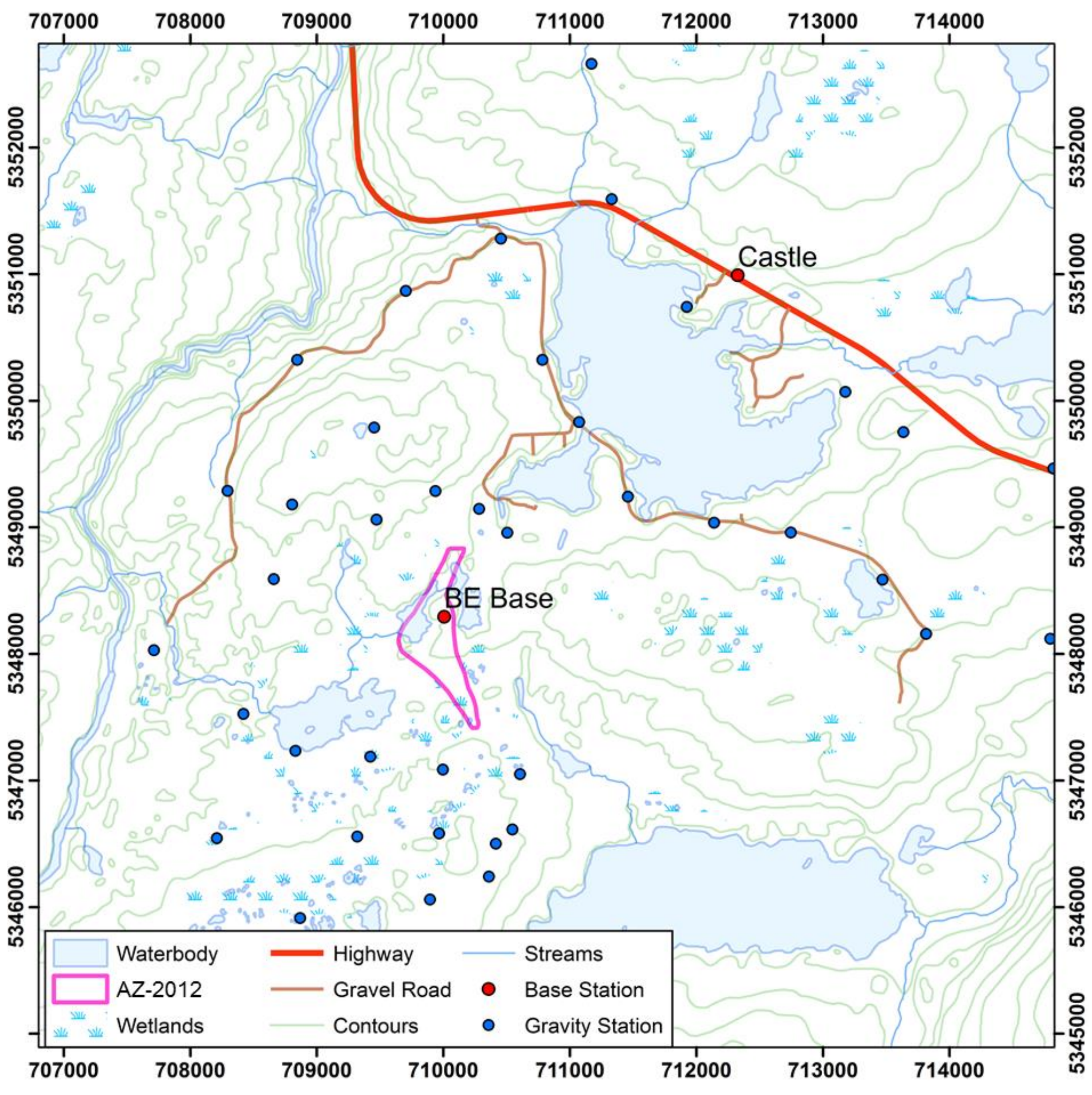

Figure 3.14: Location of regional gravity stations along with base stations used.

can be shortened by either returning to a base station more frequently, or by adding more base stations nearer to the survey area and taking repeat measurements frequently. Since the only registered bases are located in Clarenville and St. John's, additional base stations were defined on and near the property. One was established at *Lakeside at Thorburn*, labelled *Castle*, and another was introduced in the centre of the Big Easy Property and was labelled *BEBase* (Figure 3.14).

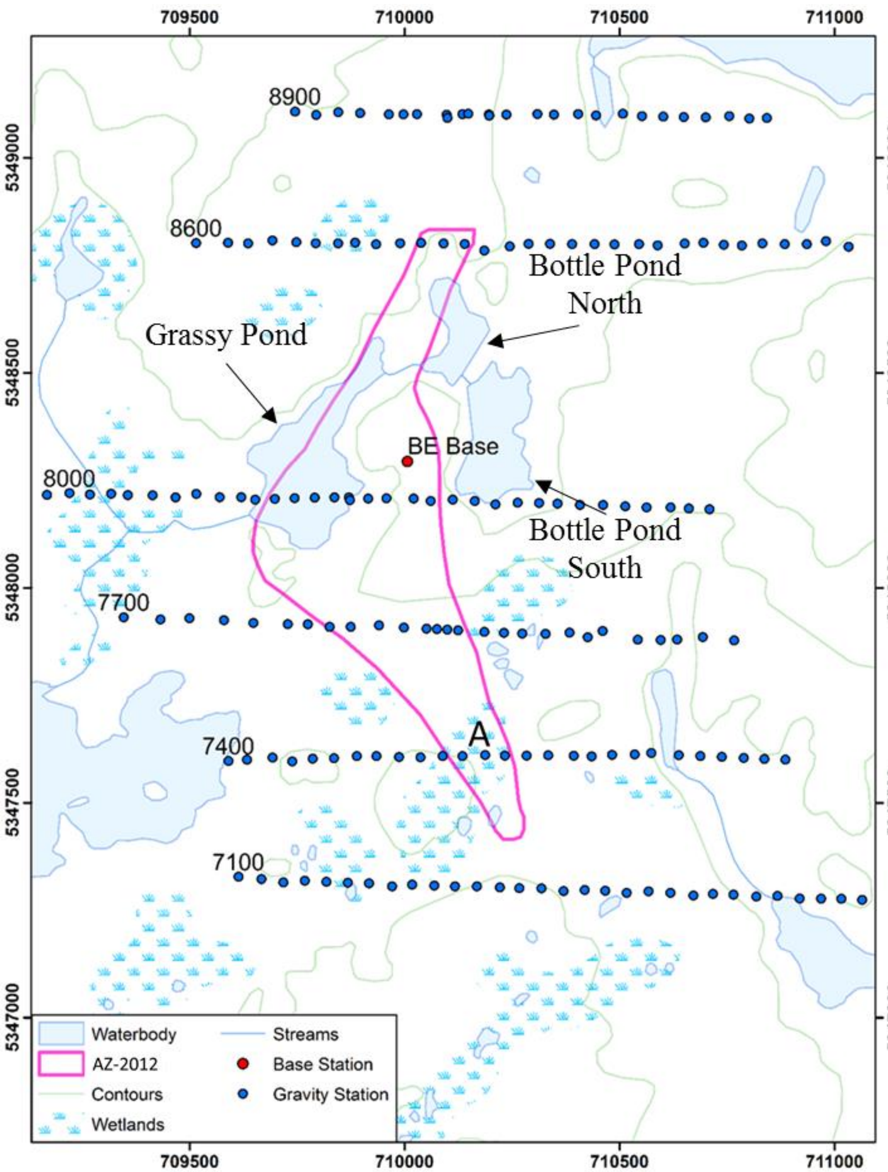

Figure 3.15: Coverage of local scale gravity survey.

Gravity data was collected over the property and surrounding area by the author and consisted of regional and local scale surveys. For the regional scale survey, measurements were taken over an approximate 3 km radius centered about AZ-2012. Measurements were spaced approximately 0.5 – 1.0 km apart. A map of the regional scale survey station locations is shown in Figure 3.14.

The local scale survey was performed over the Big Easy Property along east-west cut lines 7100, 7400, 7700, 8000, 8600 and 8900. Several transects were made over AZ-2012 and extending as far east and west as possible at a spacing of approximately 50 m. A map of the local scale survey locations is shown in Figure 3.15. It should be made clear that the grid line numbers reflect the last four northing digits based on previous surveys in NAD 27 and so offsets exist between line numbers and NAD 83 UTMs presented in this study.

Tidal Corrections

The CG-5 has an attachable GPS for obtaining its position and allows the instrument to determine the tidal effects. The tidal effect is calculated using the Longman formula via onboard software which also requires the time difference from Greenwich Mean Time (GMT). On several occasions, errors were introduced into the data by entering the incorrect time zone resulting in an incorrect tidal correction. Therefore, for consistency, all tidal corrections were removed from the data and tabulated again in Oasis Montaj using the proper time as well as the true latitude and longitude from the RTK data.

Instrument Height

The gravity station locations measured by the RTK system (Section 3.2.2) are measured from the ground below the CG-5. However, the point at which the CG-5 measures the gravitational force is 8.9 cm from the base of the system which sits on an extendable tripod. The tripod adds an additional 16.5 to 20 cm to the height of the instrument. The height at which the tripod is adjusted depends mostly on how level the ground is directly below the instrument but in most cases flat areas were chosen as survey locations. Also, as suggested by the CG-5 operation manual, the left foot screw remained in its lowest position to maintain a constant plateau height. For these reasons, an average height of 27.15 cm was used for the instrument height except for when wooden blocks were used. For the measurements taken on soft, unstable ground wooden blocks were used to add extra stability beneath the tripod legs. Blocks were also used for measurements taken in the winter months when the snow or ice would melt beneath the pointed legs, which would cause the gravimeter to become slanted. It was noted during the survey when these blocks were used and an additional 3.5 cm was added to the total height. Often times, snow was shovelled from a survey location down to ground level where the measurement was taken. In some cases, gravity measurements were taken on top of a layer of snow. When these measurements were taken, elevation measurements were taken from ground level by pushing the base of the RTK staff through the snow. An elevation reading was also taken on top of the snow. The difference of the elevations was used for the instrument height during the gravity reductions in Oasis Montaj and the density of the snow was ignored.

Drift Correction

Instrument drift occurs as the stress on the elastic system within the gravimeter slowly relaxes. In a stable environment, the long term instrument drift can be predicted and removed. The drift of the CG-5 was determined internally before entering the field by running the gravimeter in auto-repeat mode in the same location for approximately 24 hours. A stable environment is crucial for obtaining meaningful results and therefore *Murray* was chosen for measuring the drift value. This is usually done once before each trip and the drift value obtained is utilized for the remainder of the trip. Once the drift constant is established, its effect can be removed from the data. This drift correction takes into account the natural drift of the instrument but does not account for any additional drift introduced due to travel or handling of the instrument. Such drift is generally non-linear but can be corrected by taking repeat measurements several times in the field (Geosoft Incorporated, 2010). This was done by visiting a local base station on the property at the start and end of each day, as well as periodically throughout the day. Oasis Montaj calculates the differences in measurements between base stations and repeat stations and places the drift value in a "Closure" channel in the database which can be removed from the data. The formula for removing the drift is incorporated in the base-tie in Equation (3.8).

Absolute Gravity

Since the instrument used is a relative gravimeter, all gravity readings must be tied into absolute gravity stations. The absolute gravity stations used for this survey were from *Murray* and *Clarenville*. Unfortunately, the original station in Clarenville no longer exists and a new base station had to be defined. The absolute gravity value was determined manually at said station by tying in the gravity reading with the reading taken in *Murray* that was measured immediately before commuting to the field area. The equation used to tie in *Clarenville* station was obtained from the *Oasis Montaj Gravity and Terrain Extension Users Guide* and is expressed as:

$$\boldsymbol{g}_a = \boldsymbol{g}_{b1} + (r_h - r_{b1}) - (t_h - t_{b1})d. \qquad (3.8)$$

where $\mathbf{g}_a$ is the absolute gravity value at the measurement location, $\mathbf{g}_{b1}$ is the known absolute value at the base station used for the tie-in, r, is the measured relative gravity value at the gravity station, t is the time of the reading, d is the instrument drift, and subscripts h and $b1$ refer to the current station and known base station, respectively. To maximize the certainty of the absolute value at *Clarenville*, this calculation was implemented with the values obtained over six visits to the gravity stations while heading into or returning from the field. The absolute gravity value of the Clarenville station was then added to the *Base Station* file used by Oasis Montaj in order to determine the absolute values of the other stations.

The gravity reductions (described in Section 2.2) were also calculated using the *Gravity and Terrain Correction Extension* of Oasis Montaj. A density of 2.67 g/cm^3 was used for the Bouguer corrections except for measurements taken over ponds and bogs. In these areas, the Bouguer anomaly was calculated from Equation (2.13) using a value of 1.0 g/cm^3 for water and 1.025 g/cm^3 for bog. The thickness of the medium was determined from the GPR profile. The gravity maps presented in Section 4.3 represent the gravity data with this refined Bouguer correction applied however the profiles in the 2D modelling represent a simple Bouguer correction where the bogs and ponds were ignored. This was done such that the gravity signature above the bogs and ponds would show up as a negative anomaly. The depths found from the GPR survey could be directly incorporated into the models where the polygons making up the pond of bog would then be assigned the appropriate density.

3.3 Forward Modelling Methods

GM-SYS is a forward modelling program that calculates expected gravity and magnetic anomalies from a specified model of the subsurface. Although the survey dimensions are only approximately 5 km by 5 km, the default models extend from -30 000 km to +30 000 km in the x-direction and 50 km depth to avoid edge effects. Since these are two-dimensional models, it is also assumed that they extend to infinity in the strike direction. The mathematical methods used by GM-SYS are based on those of Talwani et al., (1959) and Talwani & Heirtzle (1964) whereby the response of an arbitrary shape is readily computed. This is convenient since the response is calculated in real time as the model is being manipulated, allowing one to match the calculated response with the observed response. The models can be manipulated to represent real geology by adding, moving, or deleting points that make up the polygons, or blocks. Each block representing a unit of constant density and magnetic susceptibility and assuming remnant magnetization is zero. The influence of these blocks are calculated at the gravity and magnetic stations and plotted with the observed data for comparison.

In this study, the model was generated with the same default spatial dimensions as mentioned above. The density and susceptibility values were assigned to units based on the physical property study provided in Section Chapter 2. Topography was determined from both the gravity and magnetic surveys and the bathymetry of the ponds and bogs were established from the GPR survey (Section 4.1) and imported into GM-SYS. It is very important to specify the magnetic field parameters of the field area so that the appropriate response is generated from the model. Here, the field parameters are based on the International Geomagnetic Reference Field (IGRF) model obtained from Natural Resources Canada. The inclination, declination and field strength around the time of survey were 68.19°, -19.5° and 51613 nT, respectively. To maintain consistency between sections, the DC shift for both the magnetic and gravity response was constant throughout all profiles.

3.4 Inversion Methods

3.4.1 Model Generation

As mentioned in Section 2.5.2, the model used in the inversion was generated first using *FacetModeller* to create the PSLG (Figure 3.16) and then *Triangle* to generate a triangulated mesh (Figure 3.17). Digital Elevation Model (DEM) values, obtained from Natural Resource Canada, along with the RTK measurements of the gravity station elevations were used to create the surface. To avoid edge effects, the model was extended 1200 m on either side of the survey line and to a depth of approximately 1000 m. The model is divided into two regions denoted by the two large dots: bedrock (red) and bog (blue). Doing this allows one to assign different attributes to a given region. For example, in order to maintain as much detail as possible, the bog was created with a maximum triangle area of 5 m^2 while the remainder of the mesh used a coarser maximum triangle area of 500 m^2. Also, different physical attributes can be assigned to each region based on a priori knowledge, described below.

3.4.2 Inversion and Forward Programs

The inversion program, VINV, used in this study was written by Dr. Peter Lelièvre. It is a versatile program that can invert multiple data-types through either independent or joint inversion. The discretization is voxellized on a 2D or 3D rectilinear or unstructured mesh (Lelièvre, 2015). The inversion operates by calling on an input file *vinv.inp* that directly and indirectly contains all files, file locations, and regularization parameters required for the inversion. All files used in the inversion process are included in Appendix D.

3.4.3 Physical Constraints

To minimize the number of solutions, and thus confront the non-uniqueness issue, it is important to impart as much geological knowledge into the inversion as possible. For instance, based on the density measurements discussed in Section 3.1.2, it is evident that the range in density between all bedrock units is approximately 0.35 g/cm^3. Therefore, the lower and upper values obtained from the inversion are set to -0.2 and 0.2 g/cm^3. By restricting the range of values permitted to exist in a cell, the possibility of generating a model with unrealistic densities is eliminated. Since the magnetic susceptibility range is much broader than that for density, more freedom is given to the magnetic inversion and bounds of 0 and 1 SI units are imposed.

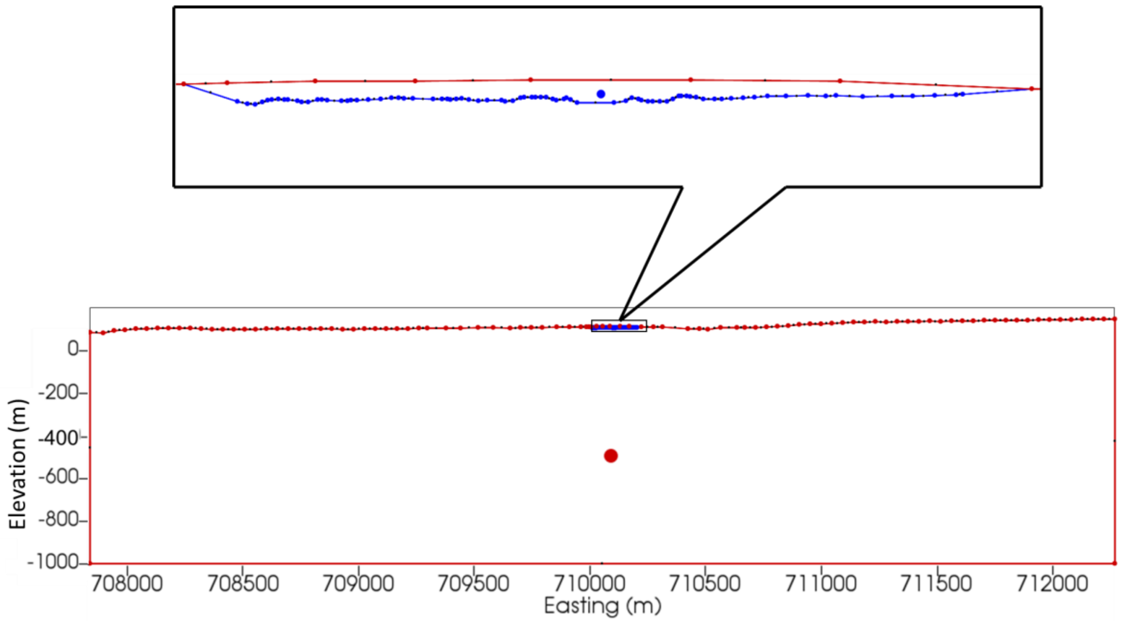

Figure 3.16: Model of Line 7700 generated in FacetModeller using both DEM and GPR data. Bedrock region is represented by the red dot and the bog region is represented by the blue dot. Eastings are in NAD83. Top panel is a 250 m wide zoomed region to show how the bog is modelled.

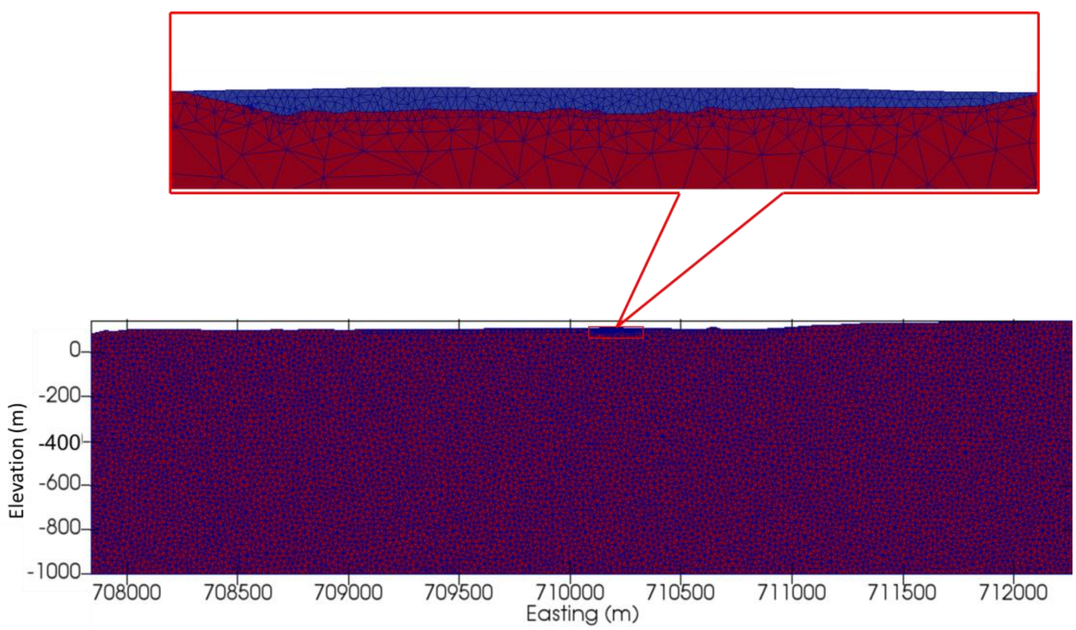

Figure 3.17:Triangulated mesh used for the inversion of data collected over Line 7700. Red region represents bedrock and blue represents the bog. Eastings are in NAD83. Top panel is a 250 m wide zoomed region to show how the bog is modelled.

3.4.4 Trends and Smoothness

In a forthcoming section, it is suggested that the alteration zone may display a particular trend as it follows a fault zone. To enforce a particular trend in the resultant inversions the mesh can be rotated. In doing so, the operator calculates gradients between cell centres and compares the gradients with the preferred direction (Lelièvre, Personal communication, 2016). In essence, this is a form of smoothing where gradients are smaller in the preferred direction and larger elsewhere. The models generated for the inversions in this study have an enforced trend of 55 degrees along the x-z plane to follow the dip of the fault zone.

It was mentioned previously that geologically reasonable models are to be obtained by enforcing smoothly varying models. In general, smooth models are preferred but there are instances where sharp boundaries are known to exist such as those between the bedrock and bog. One way to deal with this issue is to determine the facets that make up a sharp contact and set the smoothness weights very low along those facets. This allows for two cells with strongly contrasting properties to be adjacent to one another in a mesh. Both the trend enforcing method and this method are forms of incorporating smoothness into the model but they are fundamentally different in their approach. The former uses gradients at cell centres while the latter used values along cell edges that have no directional information. Therefore, both methods cannot be used during the same inversion. So, since the bog has a dramatic effect on the gravity response and it must be accounted for, accounting for the bog and enforcing a trend were done in two steps. First, a forward modelling program, fwd, including the bog was used with the mesh described above. This generated a response from the bog with an anomalous density of -1.64 g/cm^3. The expected Bouguer Anomaly from the bog was removed from the Bouguer Anomaly gravity values and the new observed values were fed into the inversion program with a trend of 55 degrees enforced.

Chapter 4 Results

4.1 GPR Maps and Profiles

Near surface features can have a dramatic effect on gravity measurements and as much information as possible should be considered when attempting to model geologic features. Therefore, a GPR survey was conducted over regions of much lower density including a large bog and three ponds. The results are displayed in Figure 4.1 as a bathymetry map showing the depth to bedrock. The deepest measurement, at 10 metres, was observed along the narrow section of Grassy Pond. This coincides with the westernmost extend of the alteration zone and will later be defined as the Grassy Pond Fault.

As mentioned in the previous chapter, for the Bouguer Anomaly maps, the Bouguer slab corrections were calculated using the depth and density of the pond/ bog immediately below each measurement location. However, for the 2D modelling, Bouguer Anomaly profiles were produced in the standard way using Bouguer slab corrections based on a standard density of 2.67 g/cm^3 and individual profiles of the bogs were generated and incorporated into the model. The profiles of the bogs as determined from GPR surveying along Lines 7100, 7400, 7700 and 8000 are shown in Figure 4.2 - Figure 4.5, respectively. Most bogs encountered along these lines are several meters thick and show a sharp contact with the underlying bedrock. In many cases, the boundary has an uneven, bumpy surface indicating there may exist a layer of boulders on top of the bedrock. However, this this boundary is treated as the bog-bedrock interface and the density or susceptibility discrepancies that may exist between bedrock and boulders are ignored.

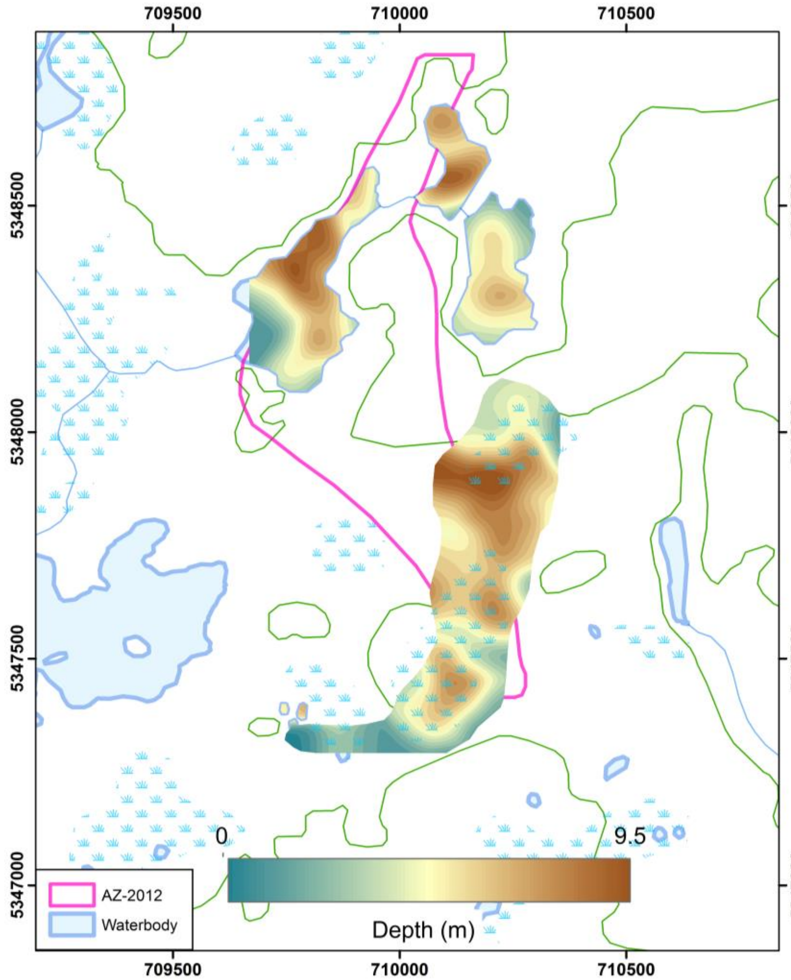

Figure 4.1: Bathymetry of ponds and bogs over Big Easy plotted with a linear scale.

In some cases, the GPR survey did not reach the lateral extent of the bog or pond (Figure 4.3 & Figure 4.4) and so the outer edges were estimated based on vegetation and extrapolating the slope of the bedrock observed in the profiles. In some other cases, the survey did not reach the vertical extent of the bog or pond, as can be seen in Figure 4.5. Here, the boundary was interpolated as seen fit.

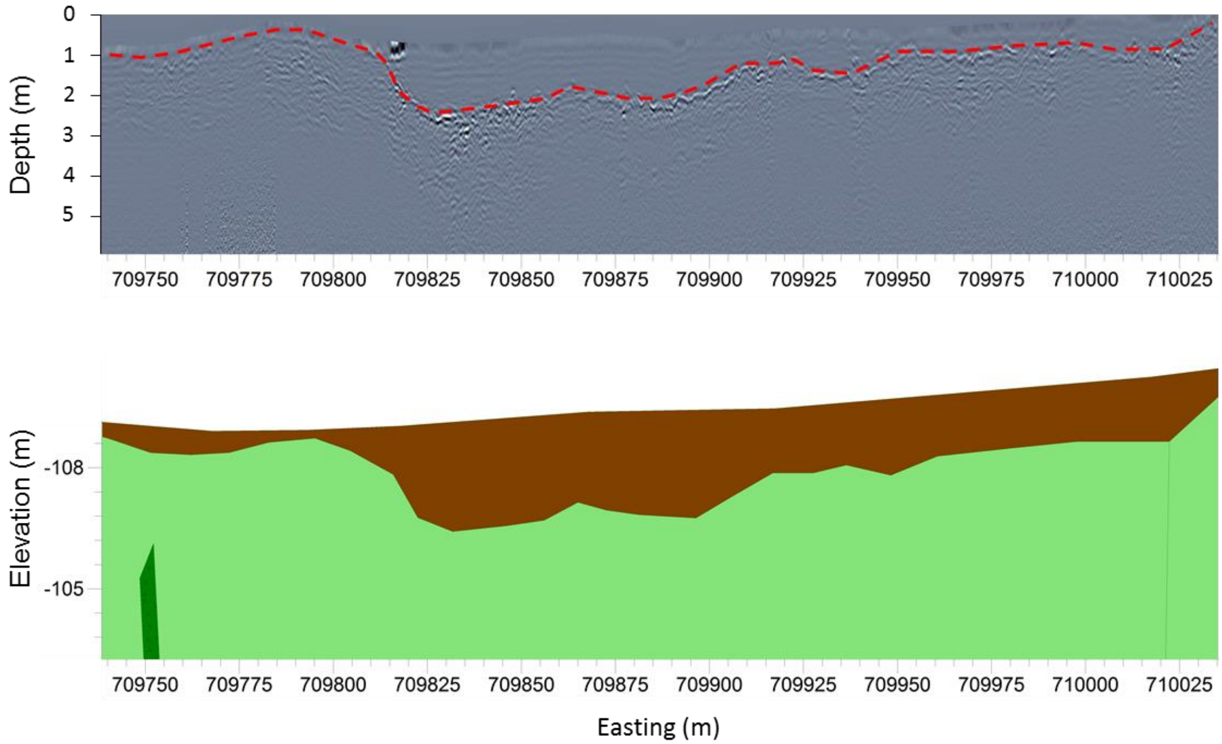

Figure 4.2: Bathymetry profile of bog on Line 7100. Both sections have a vertical exaggeration of 8. The top panel represents the GPR profile with depth measured from the surface. The dashed red line is the interpretation of the bottom of the bog using EKKO Project. Topography has been taken into account when drawing the bottom of the bog. Bottom panel is the zoomed section of the 2-D model generated in GM-SYS with elevation relative to sea level (positive downwards) and Eastings are in NAD83. Color coding follows that given in Figure 4.13.

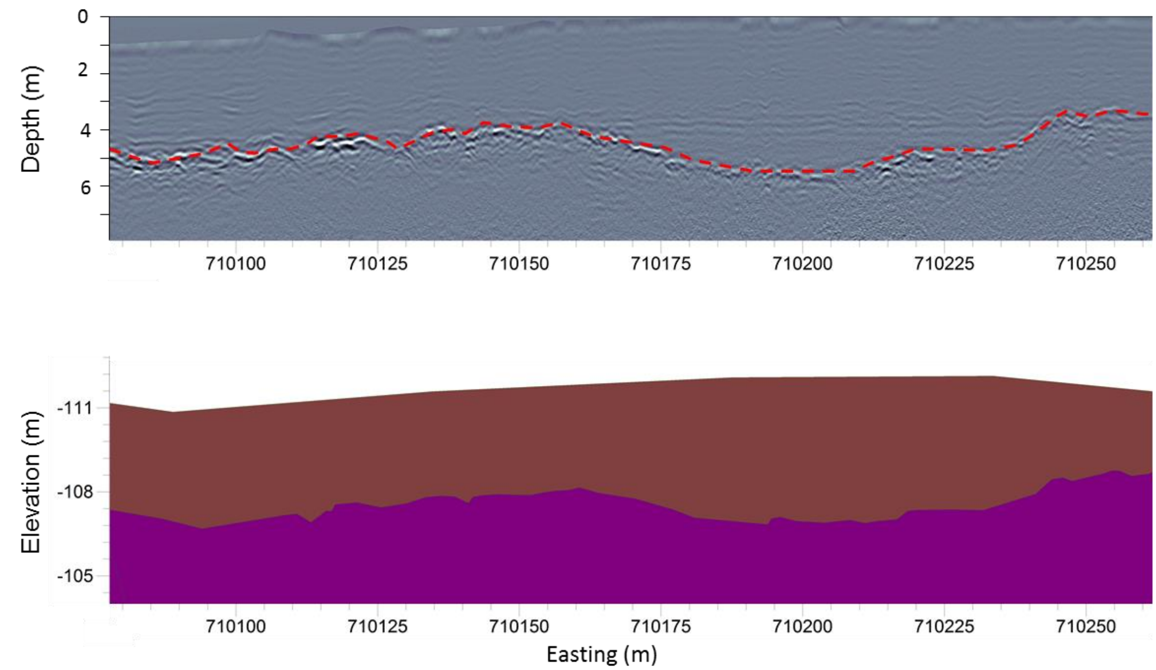

Figure 4.3: Bathymetry profile of bog on Line 7400. Both sections have a vertical exaggeration of 4.94. See caption for Figure 4.2 for more information.

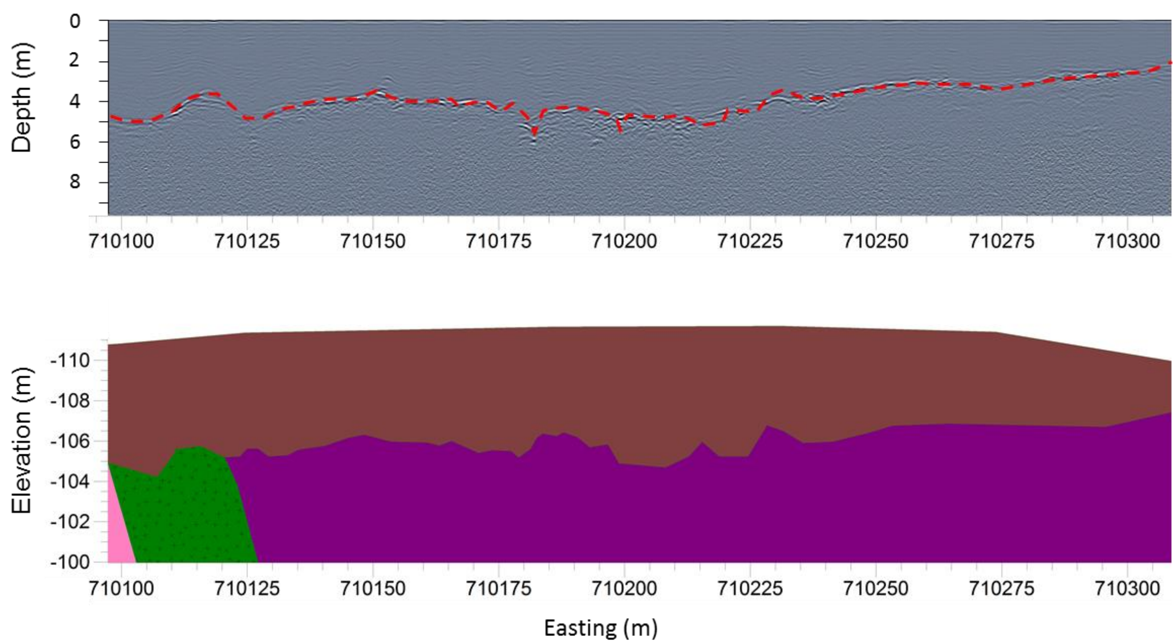

Figure 4.4: Bathymetry profile of bog on Line 7700. Both sections have a vertical exaggeration of 4. See caption for Figure 4.2 for more information

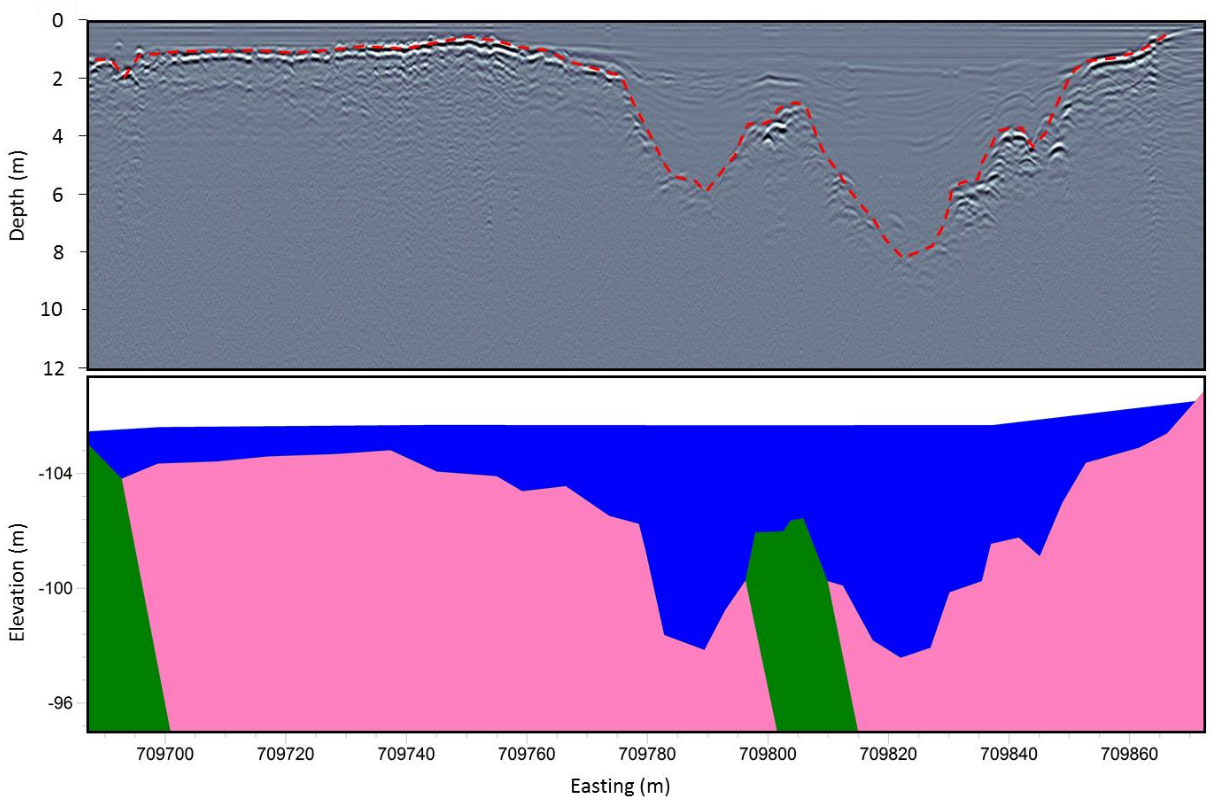

Figure 4.5: Bathymetry profile of Grassy Pond on Line 8000. Both sections have a vertical exaggeration of 4. See caption for Figure 4.2 for more information

4.2 Magnetics Maps

Below are the results of the magnetic survey collected over the Big Easy. The grids were generated using Oasis Montaj and were coloured using the histogram normalization method. Presented first is the levelled, raw data (Figure 4.6). The data has been gridded with the most commonly used gridding method, the minimum curvature method, with a cell size of 25 m and histogram normalization colour method. The first thing to note from the map is that most of the measured responses are of low to moderate amplitude. There are however, some moderate to high amplitude, small scale, mostly linear features. Most of these linear features are oriented N-NE, occasionally exhibit moderate undulations or inflections, and are up to a few hundred nT in amplitude. There also appears to be a slight trend in the data where lower fields are observed to the NW and higher values are observed toward to SE. This is a large-scale trend created by features much larger than the survey area. In an attempt to isolate and emphasize the features of interest, the large scale trend, *i.e*. the regional field, is removed. The first-order trend was removed using the *Trend* filter in Oasis Montaj. The remaining maps presented below have this trend removed and are referred to as magnetic residual maps.

The magnetic residual data reduced to pole and gridded using minimum curvature and bi-directional gridding methods are shown in Figure 4.7 and Figure 4.8, respectively. The surveys encompass at least four major geologic units but it is difficult, and often impossible, to distinguish between the units based on their magnetic signature alone. This is to be expected based on the results of the susceptibility measurements shown in Figure 3.1. However, some units could be tentatively identified: two of the most dominant contacts are highlighted in Figure 4.9 and Figure 4.10. The basalt unit to the west appears as a magnetic high with a trend and amplitude similar to the mafic dykes. This unit has appeared in geology maps in the past and has also been sampled during the most recent field season. Due to the limited extent of the survey, it is not possible to determine how continuous this unit is to the north and south but it likely extends for at least 1.3 km. It is believed that this unit is a part of the Bull Arm Formation (Section 1.4.2) and is not associated with the alteration event. The other prominent contact is in the northeast portion of the map. It is clear that there is a moderate contrast in magnetization however, subcrop and boulders observed in the area suggest there is an abundance of both unaltered red and green sediments in this part of the property. Since the green sediments have a slightly higher magnetic susceptibility then the red sediments (Figure 3.1), the presence of green sediments in this region may be the

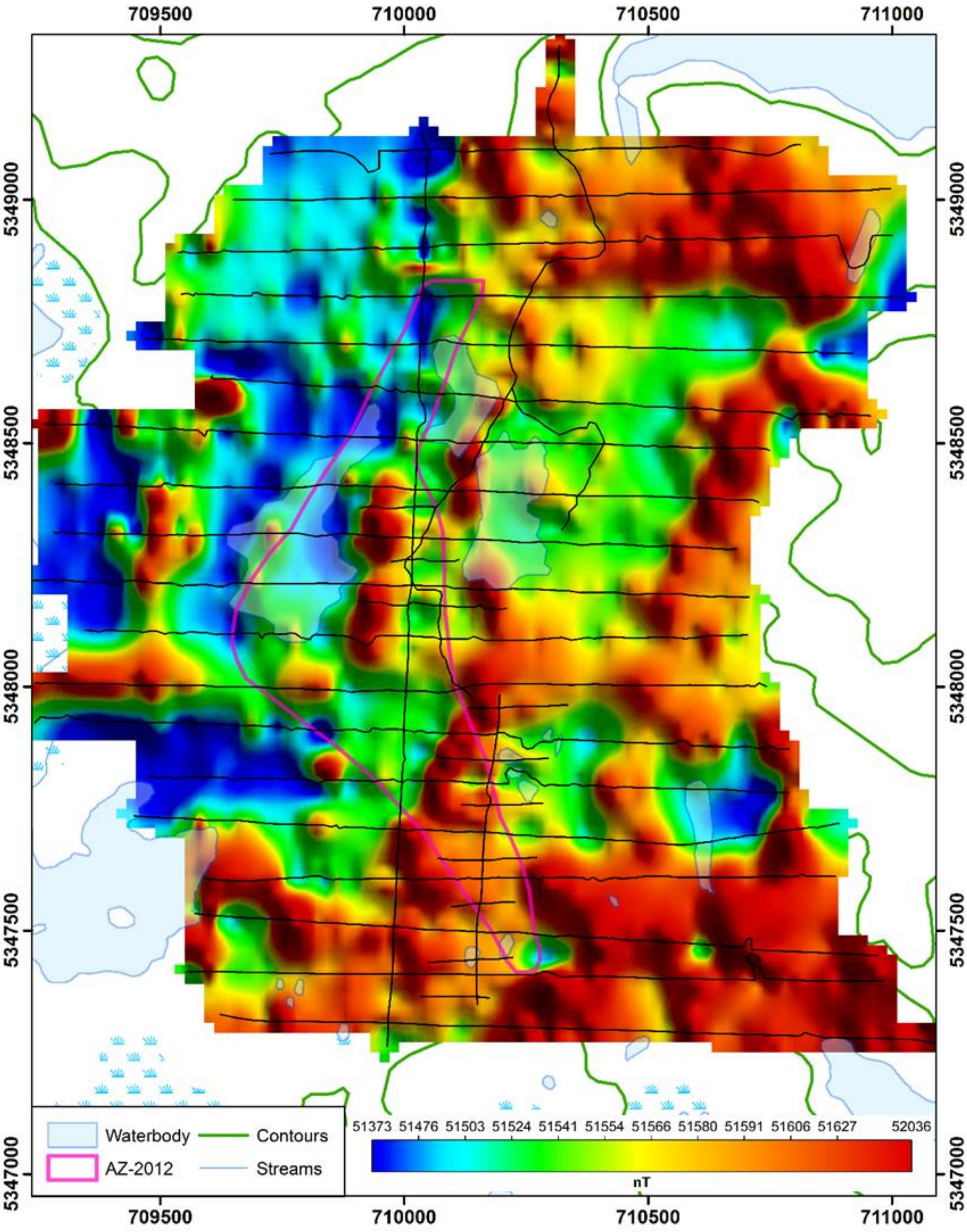

Figure 4.6: Map of raw and levelled total magnetic field using minimum curvature with cell size of 25 m. Black lines indicate where measurements data exists.

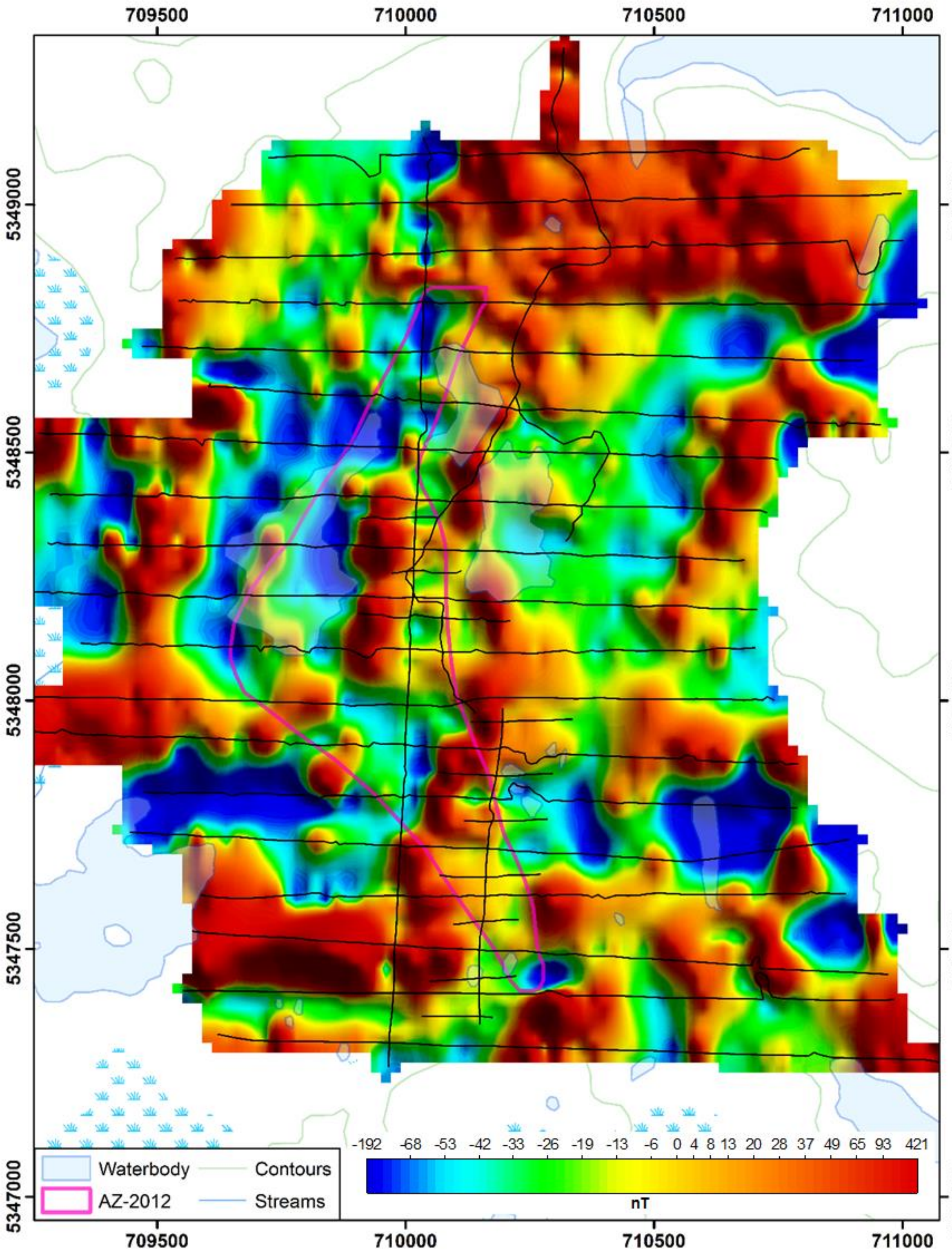

Figure 4.7: Map of magnetic residual, linear trend removed and reduced to pole using minimum curvature gridding with a cell size of 25 m. Black lines indicate where measurement data exists.

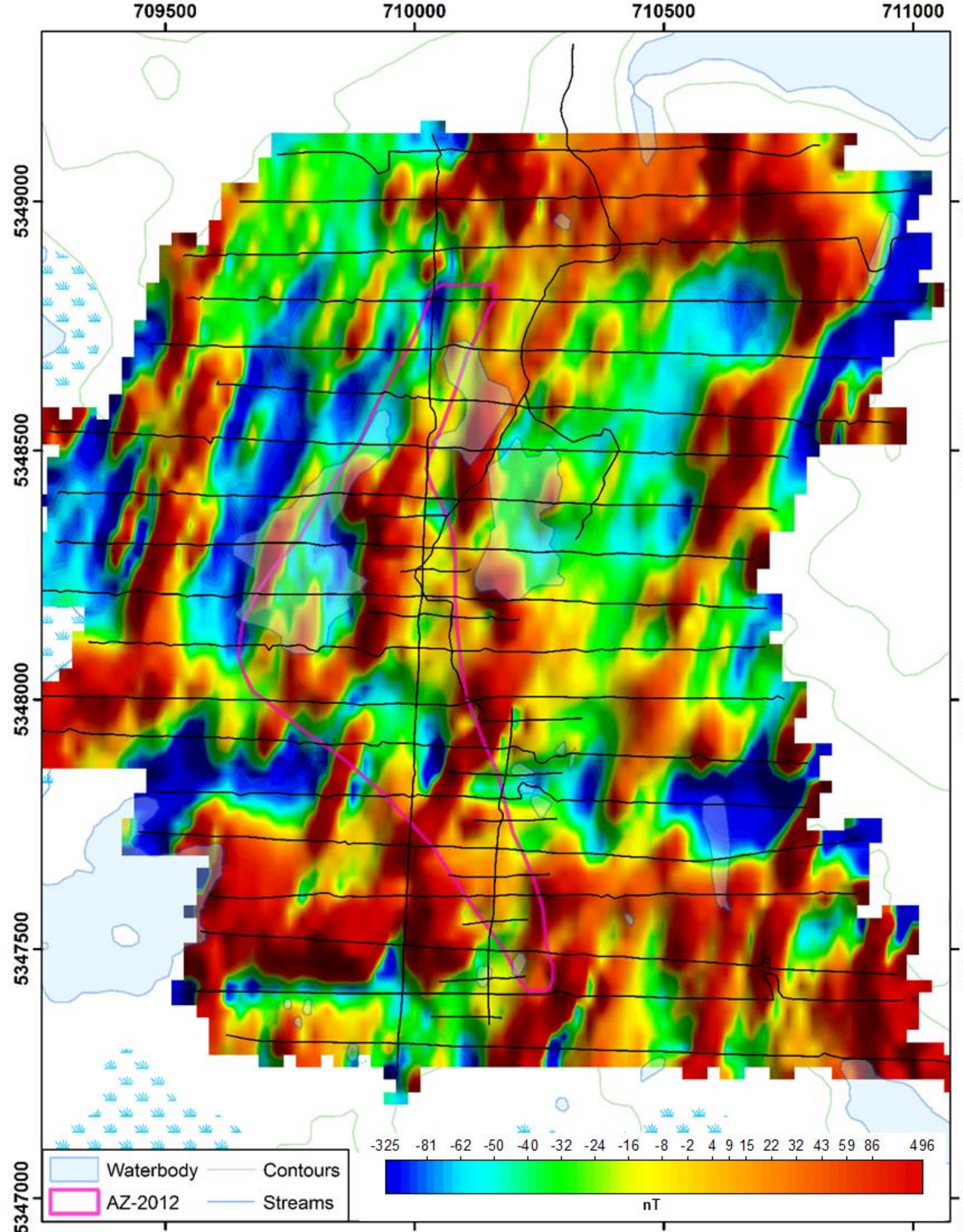

Figure 4.8: Map of magnetic residual, linear trend removed and reduced to pole using bi-directional gridding with a cell size of 25 m and angle of 65 (cw from North). Black lines indicate where measurement data exists.

cause of the slight increase in amplitude.

In the bigrid maps, features oriented approximately 025° or 205° are most prominent. This makes interpreting features oriented in this direction relatively straightforward (Figure 4.10). As is discussed in Section 4.3, mafic dykes can be associated with faulting however, only the major faults have been represented on this map. The most prominent fault running through the centre of the property will be referred to as *The Big Easy Fault (BEF).* This is believed to be a structural limit as minimal alteration is observed east of this feature. Drill hole BE-14-16 (refer to Figure 1.4) is just a few metres to the east of this feature and encounters only unaltered red sediments whereas BE-14-14, BE-14-17, and BE-14-19 are just a few metres west of this feature and commence in altered material. There is an exception however with mineralization present in Trench 6 which lies to the east of the *BEF* (Figure 1.3). A subtle increase in magnetic amplitude is observed to the east of Trench 6 in Figure 4.10. It is possible that this feature could be created from a small splay off the main fault. If the block between the *BEF* and the splay encountered less vertical movement during thrusting, this area may have been preserved from erosion.

The major fault to the west, the *Grassy Pond Fault (GPF),* is believed to be the western limit of the altered zone. The northern half of this fault is assuredly defined by several drill holes: BE-11-05, BE-11-06, and BE-11-07. In Figure 4.8 (and Figure 4.10), this feature can be traced toward the north to the extent of the survey area, but tracing the southern half of the fault is difficult. This is where using multiple gridding techniques becomes useful. The same feature can be seen in the minimum curvature grid (Figure 4.8 and Figure 4.9) and seems to be fairly continuous with an approximately 100° inflection toward the southeast. This southern half of the fault can be traced for several hundred metres to the southeast. Recent interpretations suggested the western extent of AZ-2012 was bounded by two faults, one being the Grassy Pond fault and another northwest-southeast trending fault (MacGillivray et al, 2011). Here, the signature from the fault(s) appear to be cohesive while neither fault seems to extend laterally beyond this inflection. This indicates that there may be some larger scale folding in the area. The Big Easy Fault has several undulations which also supports the idea of some sort of deformation. That being said, there is little evidence to prove any large scale folding since bedding measurements are scarce. To fully determine whether this is the case, either more outcrop would need to be uncovered or drill core would need to be oriented in future drilling.

One other feature that is almost as prominent as the *BEF* is the mafic dyke feature to the east of the *BEF*, indicated with a black star. This mafic feature lacks the deformation present in the Big Easy Fault and hence is presumed to be younger than the altered material and unrelated to its deposition.

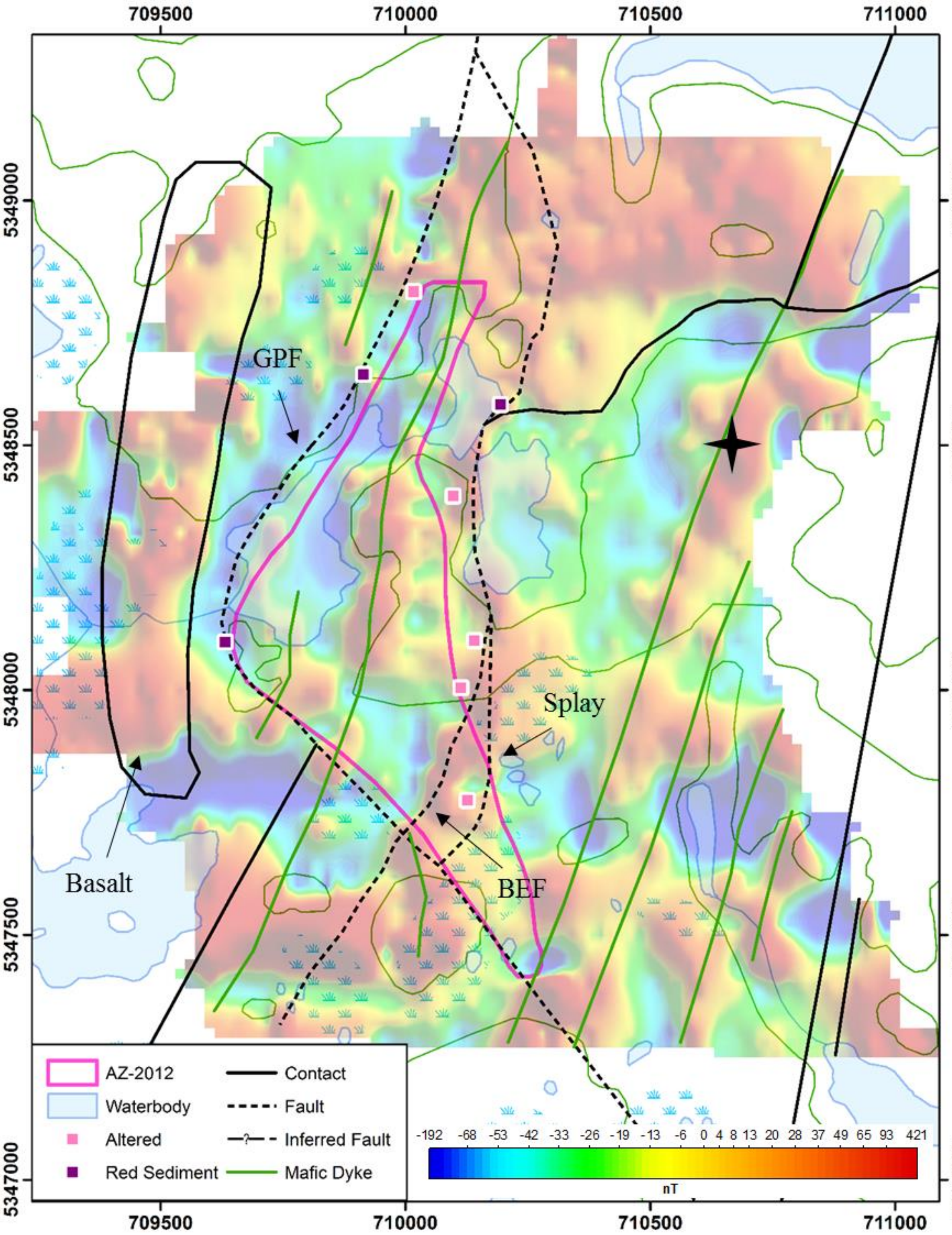

Figure 4.9: Interpretations based on both the minimum curvature gridding and bigrid methods of residual magnetic data. BEF and GPF represent the Big Easy Fault and the Grassy Pond Fault, respectively. Semi-transparent magnetic map was generated from minimum curvature gridding method (Figure 4.7). Squares show constraints were used from bedrock information.

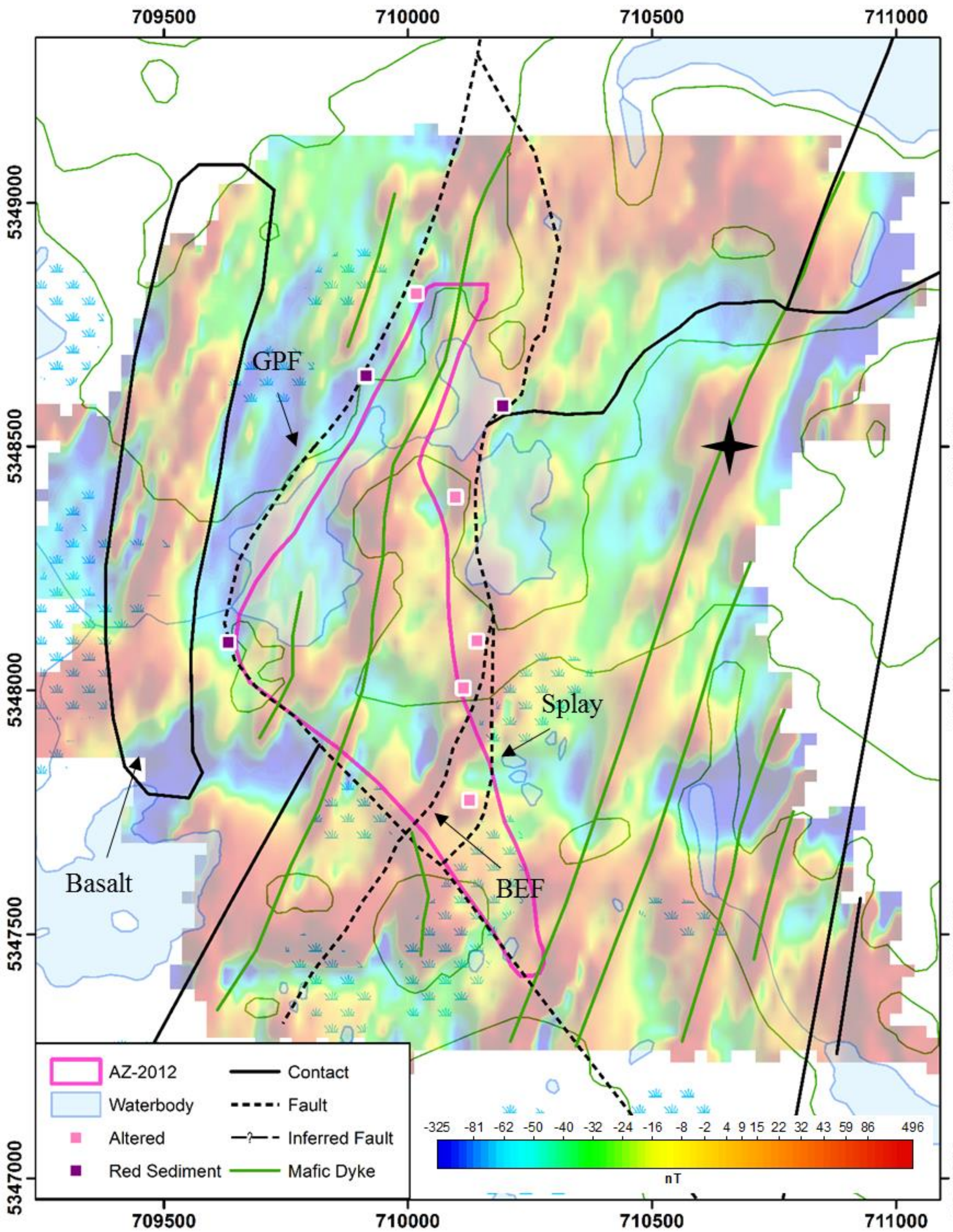

Figure 4.10: Interpretations based on magnetic residual data gridded using both the minimum curvature and bigrid methods. BEF and GPF represent the Big Easy Fault and the Grassy Pond Fault, respectively. Semi-transparent magnetic map was generated from bigrid method (Figure 4.8). Squares show constraints were used from bedrock information.

4.3 Gravity Maps

The gravity results, in the form of a map of the Bouguer anomaly with the Canadian Gravity Grid (CGG) removed, are shown in Figure 4.11. The map includes including both the regional and local scale survey data. Since some of the measurements taken were several hundred metres apart, a grid cell size of 100 m was used for the interpolation. In this map, it is clear that there is a strong, roughly E-W trend in the data. The gravity values range from less than -1.25 mGal from the west to over 2.5 mGal to the east. It is evident that there is a measureable response from the alteration zone near the centre of the survey area. While a large halo is present about AZ-2012, a profound signature is observed along Line 7700 and extends northward with a NE-SW trend. The most intense gravity depression exists between the three ponds along Line 8000. For a closer look at the smaller scale variations in the gravity response, the local scale survey data was plotted with a cell size of 25 m (Figure 4.12).

The southern limit of the alteration south of Line 7700 becomes clearer in the local scale survey results. If altered material existed within AZ-2012, south of Line 7700, one would expect the gravity results to reflect that. Since the large anomaly terminates over such a short distance, there is reason to believe that alteration ceases somewhere between Lines 7400 and 7700. Incidentally, the *BEF* and the *GPF* appear to meet near Line 7500 (Figure 4.9 and Figure 4.10) further supporting the idea that these two faults act as structural boundaries. Additional gravity surveys over Line 7500 and Line 7600 may help in resolving this interpretation. Conversely, as mentioned previously, altered material exists in outcrop at the southern tip of AZ-2012. Since this outcrop lies outside the structurally controlled alteration zone, it could open up the possibility for other localized satellite occurrences. Another possible satellite occurrence is approximately 200 m

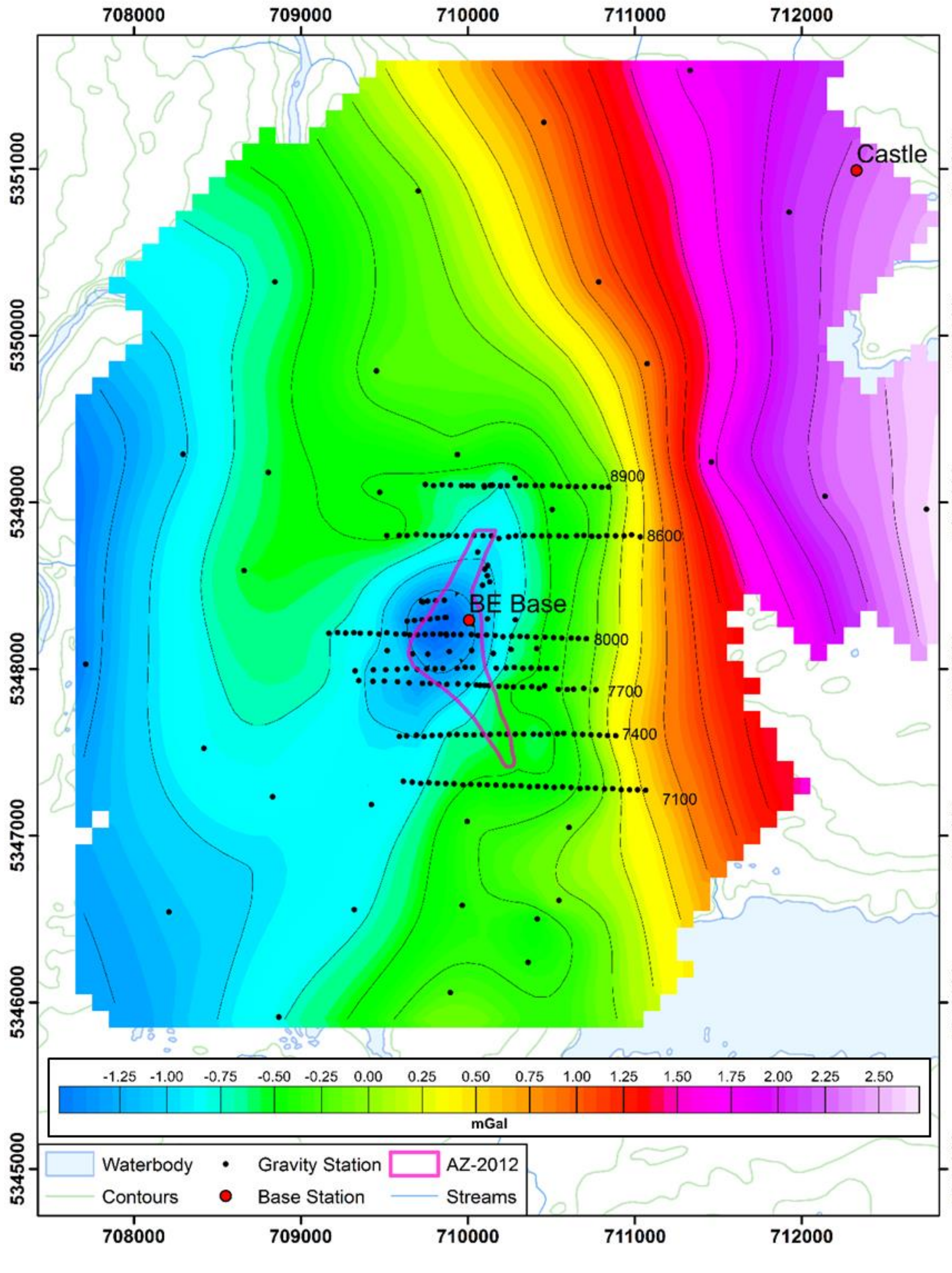

Figure 4.11: Map of complete Bouguer corrected regional scale gravity survey (including local scale) with regional CGG removed. Black dots indicate measurement locations while red dots represent base station locations. Gravity contours (black lines) plotted at 0.25 mGal intervals.

to the northeast (labelled ‘X’ in Figure 4.12). It was in this region that Sample 14907, a strongly silica altered sediment unit, was collected (Section 1.3) proving there is altered material in this area. The gravity response also suggests there is a considerable volume of a low density material here. Further prospecting and drilling would be required over this portion of the property to determine whether gold bearing material is present at this anomaly; a model of this section assuming the gravity low is due to alteration is shown in Section 4.4.

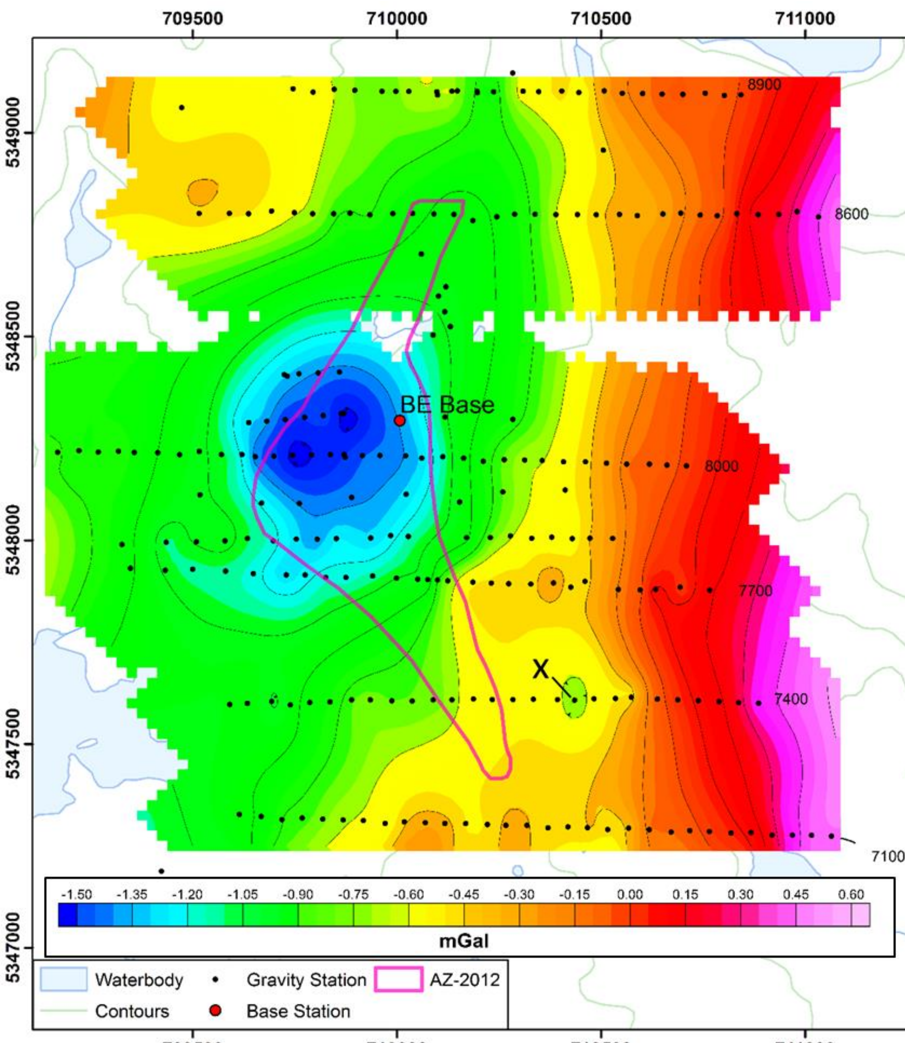

Figure 4.12: Map of complete Bouguer corrected local scale gravity survey with regional CGG removed. Black dots indicate measurement locations while red dots represent base station locations. Gravity contours (black lines) plotted at 0.15 mGal intervals.

4.4 2D Modelling

The following section displays the results of the 2D forward modelling using the software package GM-SYS. The data is displayed in four panels. From top to bottom, these include the magnetic response (observed and calculated), gravity response (observed and calculated), RTK elevation data, and the model itself. Here, the models are represented with no vertical exaggeration so true angles are represented in all features. It should be noted that the depths of the models are presented with respect to sea level and not with respect to the topographic surface. Figure 4.13 describes the color coding for all units used in the modelling. While the physical properties of each unit varies slightly within a given model, all density and susceptibility values used coincide with those measured in Section 3.1. The models are labelled by line number which indicates their respective Northing (in NAD27) and each line is discussed in the order from south to north. As mentioned previously, the measured response is non-unique so a multitude of models could represent the data equally as well. Therefore, the author has made use of several constraints that are currently available. Some of these include drill hole data, physical property measurements, structural measurements, and general notes taken during the field season. Even with these data available, there are still many uncertainties and therefore speculative modelling takes place. Under these circumstances, highly detailed models of the altered zone or surrounding geology would be inappropriate, so the models presented below are simplified representations of the proposed anatomy of the alteration zone and surrounding geology.

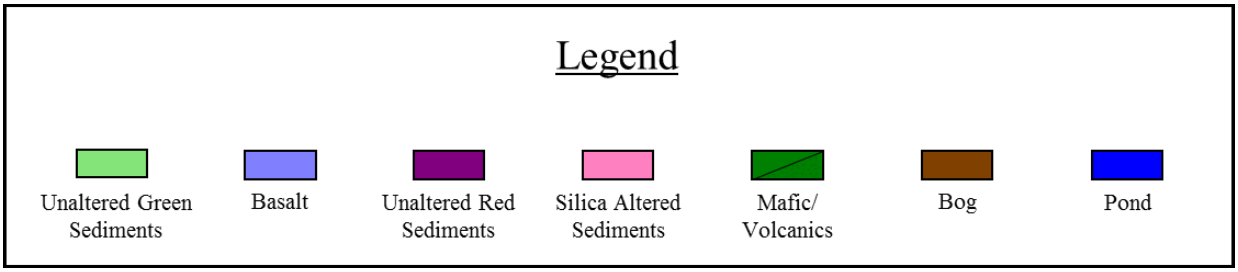

Figure 4.13: Legend of units used in 2D modelling.

4.4.1 Model 7100

The most southerly line, Line 7100, surveys an area believed to lie beyond the southern extent of AZ-2012. There is a noticeable rise of about 0.5 mGal in the gravity profile to the East due to the mafic volcanics. However, the centre of the profile, wear mineralization would be present, is relatively flat. Therefore, the gravity profile suggests that, as modelled in Figure 4.14, little to no alteration is present beneath Line 7100. If alteration is present it is likely to be smaller, deeper and/or less pronounced than most exposed areas near the centre of the property. The magnetic profile is mostly flat, varying only a few 10's of nT with an increase of about 200 nT to the East. There are also a series of localized spikes upwards of about 300 nT. The increase to the East is likely due to the mafic volcanic unit while most of the thin spikes can be modelled with a series of mafic dykes. Most of these dykes are between 5 and 10 m wide and dip 60 to 70 degrees to the East. The smaller, more subtle fluctuations are believed to be created from minor variations of susceptibility properties between different beds within the sedimentary package or smaller scale mafic dykes.

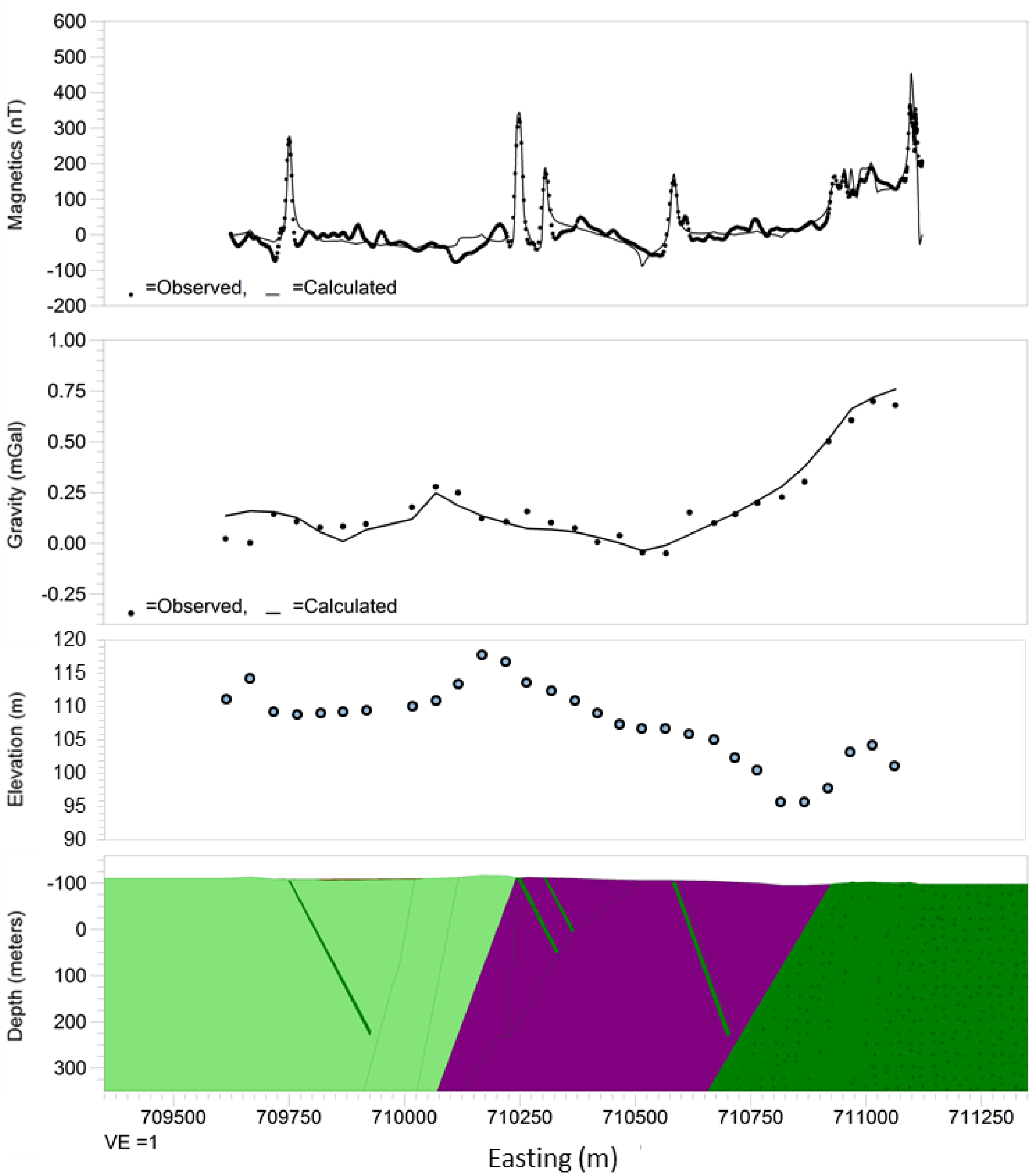

Figure 4.14: 2D modelling of Line 7100. From top to bottom: measured and calculated total magnetic field; measured and calculated Bouguer gravity; RTK elevation profile; and forward model of Line 7100 generated in GM-SYS (elevation in metres with respect to sea level). Dots represent observed data while thin black lines represent the calculated response of the model. Colour legend for units given in Figure 4.13.

4.4.2 Model 7400

As seen for Line 7100, the greatest influence on the gravity response over Line 7400 is from the volcanic unit to the east (Figure 4.15). Originally, this line was believed to encompass a 150 m wide altered zone that lay directly under the bog (labelled A in Figure 3.15 and Figure 4.15). This altered zone is merely speculative since it is coincident with a wetland which has never been drilled or sampled. The profiles do not require such a zone since the observed data can be modelled with the absence of any altered material. A depression of approximately 0.28 mGal is present directly over this region; however, it can be reproduced by modelling a bog with its bathymetry based on the GPR survey and densities based on core sample measurements of 1.025 g/cm^3 (Figure 4.3). Therefore, it is suspected that no mineralization is present below this portion of the bog; or again, like Line 7100, it may exist at a greater depth where it is much more difficult to detect.

A few hundred metres to the east, another bog and pond exist (on either side of label B; Figure 4.15). Neither of these were surveyed by GPR due to inaccessibility but were modelled based on the gravity signatures, using density values of similar bogs, and reasonable depth values. Gravity anomalies from both the pond and bog can be replicated but in order to fit the observed data between the two, a lower density region must exist at B. It is reasonable to assume that a small zone of altered material may account for this since Sample 14907 taken by Cornerstone Resources recorded the presence of illite a few 10's of metres south of the gravity station (Figure 1.3). This region of altered material was modelled conservatively since the true dimensions of the pond and bog are unknown. For this reason, there is potential for this zone to extend laterally beneath either the bog or pond, or both.

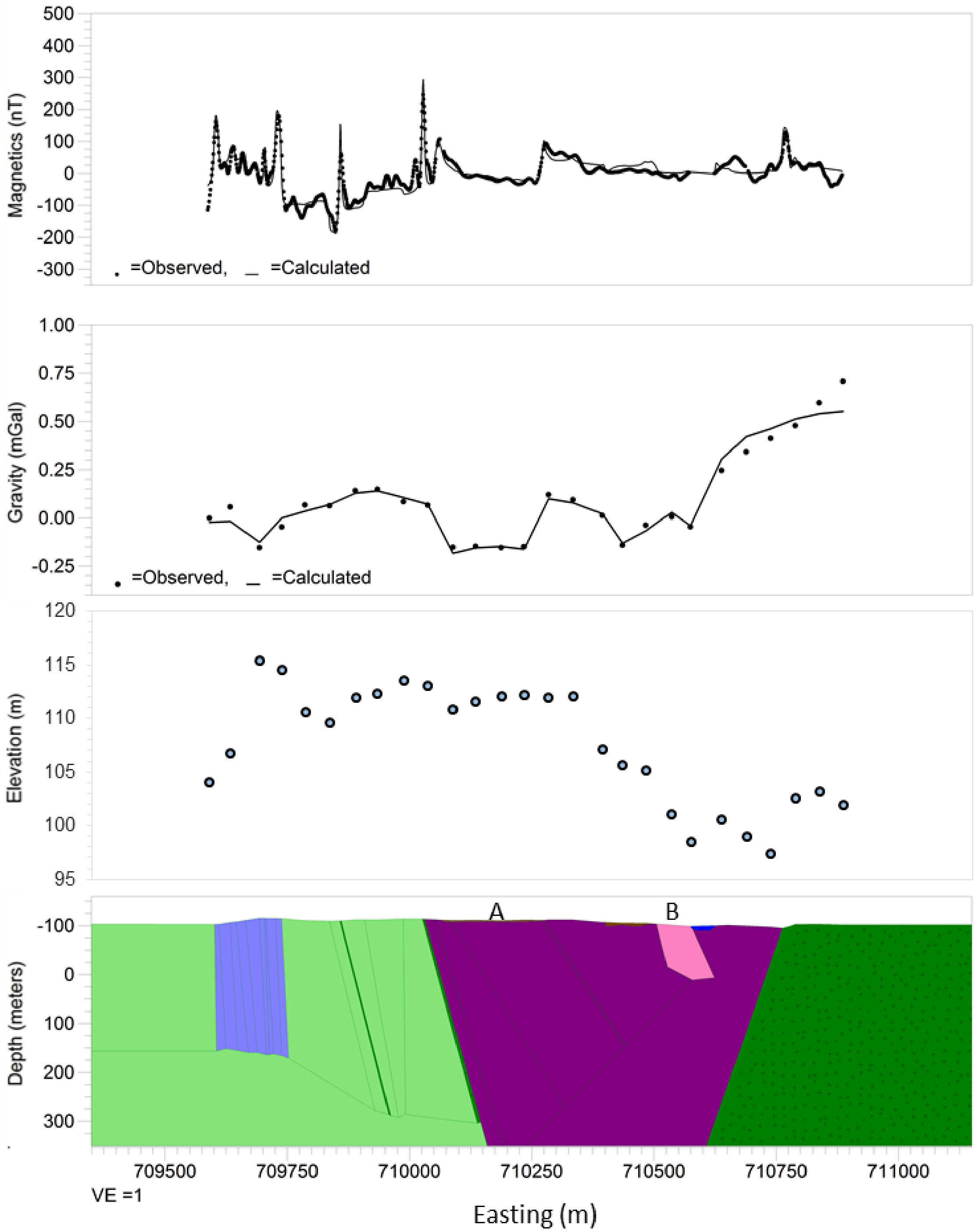

Figure 4.15: 2D modelling of Line 7400. See caption for Figure 4.14 for general description. A represents a bog not visible at this scale, and B represents an alteration zone with a wetland area to the West and small pond to the East.

On the western side of the profile, the presence of the basalt unit (pale purple block) is apparent within the magnetics profile. A notable decrease in the gravity data is coincident with this region. Both gravity measurements making up the depression were taken on a ridge with approximately 10 – 15 metres of topographic relief. So, it is presumed that this depression is the result of an under compensation during the terrain corrections and not from a body with lesser density. Additional spikes in the magnetic data throughout the line are consistent with other profiles and they can be modelled by thin dykes dipping steeply to the east.

4.4.3 Model 7700

The magnetic profile collected along Line 7700 is useful in providing structural information. A very prominent magnetic spike is present near the center of the line (Figure 4.16). Based on its amplitude, it is proposed that this is caused by a mafic dyke. However, its profile is much more distinct than other mafic signatures present throughout the property since it is broader and not masked by higher frequency features. This magnetic signature can be generated from a thin mafic unit dipping moderately to the east. The significance of this observation is two-fold; as the mafic dykes in the area have been noted to be spatially related to faulting, these mafic dykes not only give information about the fault localities, but they also give information about fault orientations. As discussed below, this fault zone may be a structural control for the eastern extent of the alteration. Since many smaller dykes are present throughout the altered zone, the zone may be represented as a series of faulted blocks but the amount of offset between blocks is difficult to model accurately based on the broad gravity signature.

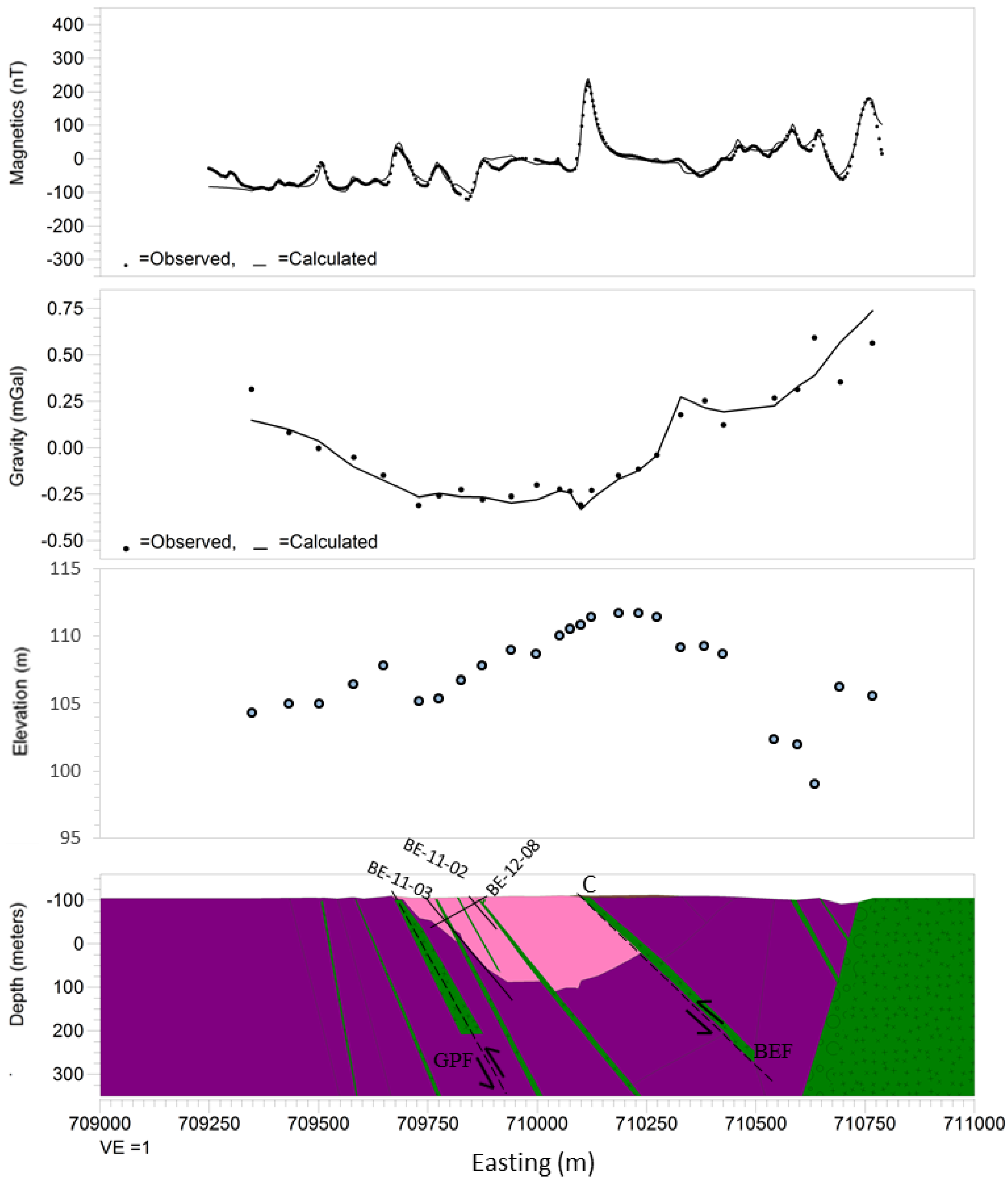

Figure 4.16: 2D modelling of Line 7700. See caption for Figure 4.14 for general description. C is a prominent mafic dyke, GPF and BEF are locations of the Grassy Pond Fault and Big Easy Fault, respectively. Drill holes are plotted and labelled appropriately.

Three drill holes exist on this Line 7700; BE-11-03, BE-11-02, and BE-12-08 (Appendix A). BE-11-03, the western most drill hole on this line commenced in altered sediments. This indicates that the alteration zone extends at least as far west as this drill hole. The gravity data indicates that this region may actually extend an additional 100 metres to the west, as modelled in Figure 4.16. Because it extends into unaltered sediments, BE-11-03 also gives an indication of the vertical extent of the alteration zone as approximately 200 metres, in agreement with the model. The depth further east is not constrained by bore hole data so it was modelled to suit the gravity data which indicated it is also approximately 200 metres below the surface. Both BE-12-08 and BE-11-02 commenced in altered material, so the eastern extent of the alteration is also unknown. However, at surface little alteration is evident east of the large mafic dyke. As mentioned above, this dyke could be used as a fault proxy. Since there is no further evidence in the gravity to suggest more alteration at depth to the east, the fault has been modelled as a thrust fault.

Simple models such as the ones presented in this study represent individual zones as homogeneous bodies which is a gross oversimplification. Commonly, when generating simplified models such as these, smaller-scale features are lost within major units. For example, BE-11-02 ended in unaltered red sediments which raised questions as the sediment package was thought to extend nearly 200 metres further east. One explanation is that there could be a large lateral offset along an east-west fault. It would be difficult to detect an E-W fault along an E-W survey line so understandably, there would be no signature in the magnetic survey (Figure 4.7 and Figure 4.8). However, if an E-W fault did exist any offset would be present within any N-S oriented dykes/faults since they are reportedly the most recent events (Section 1.3). Also, the gravity anomaly continues to the east of this area. Since a larger region of unaltered sediments is undetectable from either of the surveys, it is assumed here that BE-11-02 ends in a localized zone of unaltered material within the larger package of silicified sediments; hence the small region of unaltered sediments has been ignored in this model. This model is backed up by the fact that BE-12-12, located 80 m northeast of BE-11-02, showed that alteration extends further east, and this hole did not encounter any unaltered red sediment package.

4.4.4 Model 8000

Just like Model 7700, Line 8000 can be modelled (Figure 4.17) as a series of faulted blocks using mafic dykes as fault proxies. Here, the major mafic dykes and/or faults consistent amplitude and spacing which further supports the idea of faulting. Between the dyke signatures, the magnetic profile is relatively flat with a slight increase to the east which, again, is assumed to be the contribution of the underlying volcanics.

The depression in gravity due to the alteration zone is very clear over this line: relative to all other survey lines, Line 8000 has the largest gravity anomaly of approximately 1.2 mGal. A portion of this is attributed to Grassy Pond (labelled "D") which has been modelled based on the GPR data (Figure 4.5). The broader depression is due the presence of altered material. The gravity profile suggests the western boundary of the alteration zone is very close to that of region AZ-2012 (Figure 3.15) as drill holes BE-11-05, BE-11-06, and BE-11-07 serve as strong constraints for the outer limit of the north-western limb of the alteration zone. The eastern boundary, which was previously defined loosely by drill hole BE-14-13, is extended an additional 80 metres in order to match the observed data. Data collected over a 250 m wide area centred on feature "E" has been poorly fitted by this model. This feature is believed to be created by an under-correction of the data due to significant topographic relief as observed in the elevation plot.

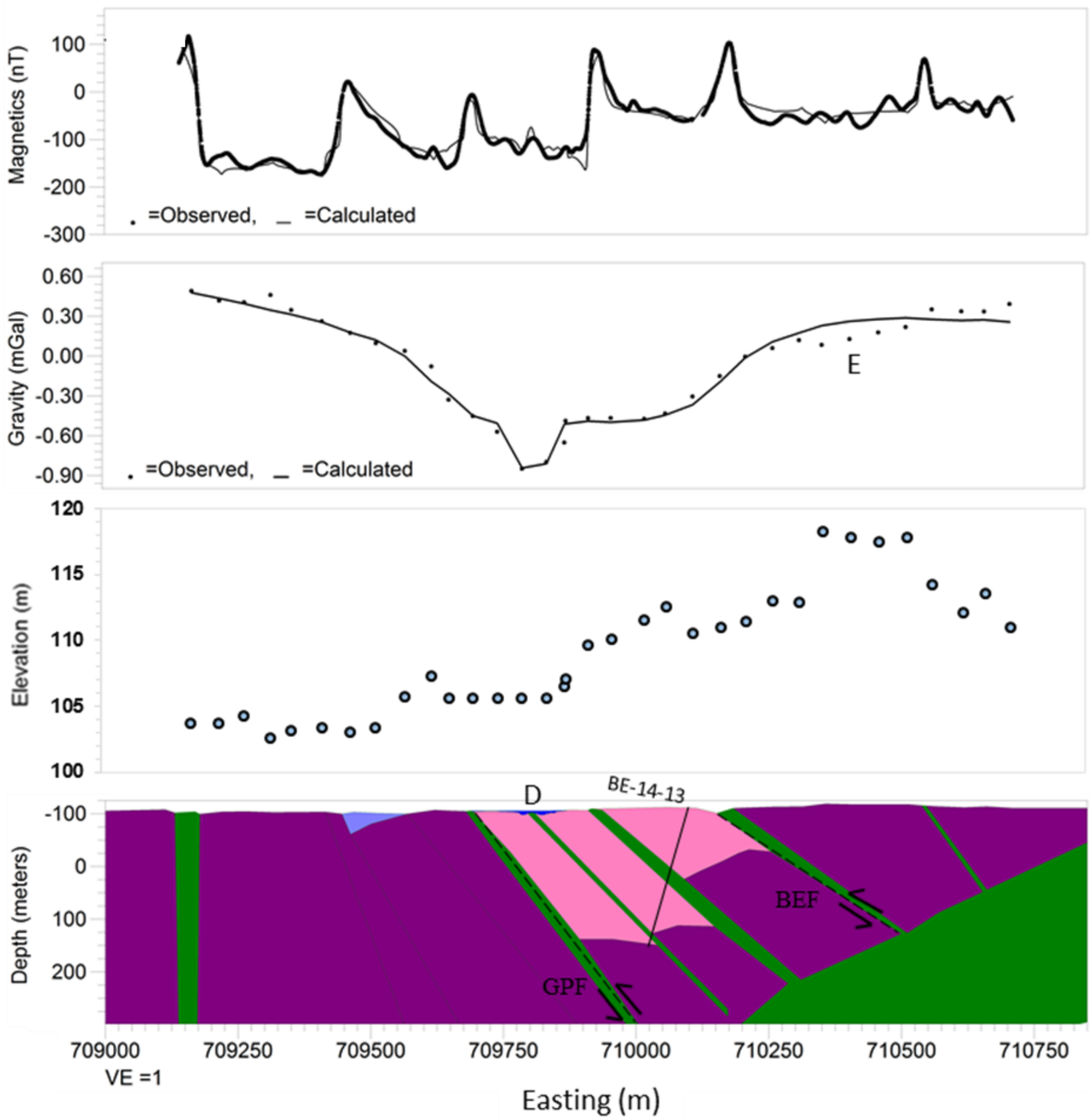

Figure 4.17: 2D modelling of Line 8000. See caption for Figure 4.14 for general description. D is Grassy Pond as seen in Figure 4.5. GPF and BEF refer to the Grassy Pond Fault and the Big Easy Fault, respectively.

4.4.5 Model 8600

There is a prominent, approximate 1 mGal, depression along the gravity profile of Line 8600 (Figure 4.18). Although the lowest portion of this anomaly can be attributed to the alteration zone, the model includes a large zone of unaltered green sediments (pale green unit) situated to the east and contributing to the gravity low. As displayed in Figure 3.2 the density of the unaltered green sediments is greater than the altered sediments but less than the unaltered red sediments. These rocks were noted as subcrop and boulders during the gravity data acquisition. The inflection point in the gravity data (labelled “F”) defines the approximate contact between the unaltered green and silica altered sediments. A slight increase in the magnetic total field is observed over this region as well. Although the general location of the contact can be defined, it is not possible to determine the exact relationship between the two units. Because of this, uncertainty exists in the vertical extent of the alteration zone as well. Since the units are magnetically similar and there are no mafic dyke fault proxies, it is difficult to determine any unit contacts or faults along this line. The magnetic signature to the east suggests the volcanic unit is dipping moderately to the west which is consistent with the bedding of the unaltered red sediments. The western limit of region AZ-2012 is well defined by drill hole BE-11-07 as it is collared into altered material while unaltered red sediments are observed a few metres to the west. Drill hole records state that silica-altered conglomerate is present to a vertical depth, from the surface, of approximately 210 m. The model agrees with the drill hole data along the western margin but suggests that this altered zone may either deepen to the east, exhibit a less silicification to the east, or (as shown in the model panel) be underlain by unaltered green sediments.

Approximately 50 metres to the west of the altered zone exists a small dimple within the gravity profile (labelled “G”). This is present because the survey line falls on the southern edge of

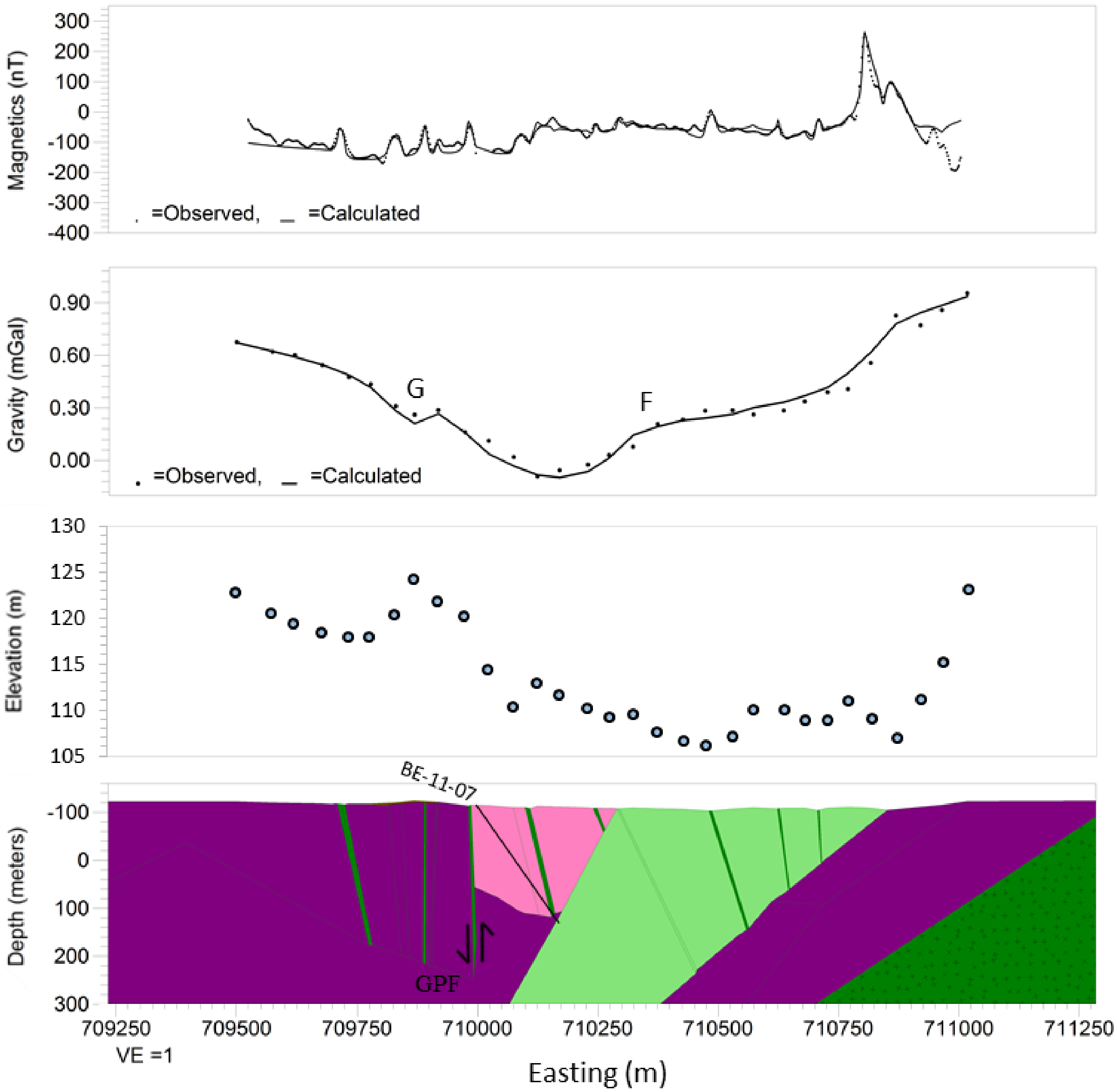

Figure 4.18: 2D modelling of Line 8600. See caption for Figure 4.14 for general description. G and F are anomalies mentioned in the text, GPF refers to the Grassy Pond Fault.

a small wetland area and is modelled as such but is difficult to see at the current scale. The wetland is visible from the aerial photo in Figure 3.15 but again, due to inaccessibility this bog was not surveyed with GPR.

4.4.6 Model 8900

The magnetic profile of Line 8900 (Figure 4.19) indicates a clear contact between two units with contrasting magnetic susceptibilities at point H. These units are inferred to be separated by the Grassy Pond Fault (Figure 4.9 and Figure 4.10). The magnetic field over the unit to the east is about 140 nT higher than it is over the units to the west. Boulders of the green sedimentary unit are dominant in the north-eastern portion of the survey grid and it has been modelled as such. The magnetic properties of the unaltered green sediments do not differ drastically enough from the unaltered red sediments (Figure 3.1) to create such a response. To account for the increased amplitude of the magnetic profile, the underlying mafic unit has been modelled with a shallower dip, compared to more southern lines so that it is closer to the surface. There is a gravity depression centered about “I” that can mainly be accounted for by the presence of an alteration zone. The depression itself is small, approximated 0.3 mGal, which is less than one quarter the largest anomaly present over the property. This suggests that the zone is becoming shallower, narrower, and/or less altered. Here, the alteration zone has been modelled to extend to a maximum depth of approximately 100 metres.

The bowl shaped feature in the gravity profile to the west (labelled “J”) is somewhat of an enigma. Field notes taken during the survey state an abundance of red sediment boulders and ground conditions were dry and firm. Since no other explanation presents itself, a localized zone of altered material has been modelled, but confirmation of its existence would require further investigation.

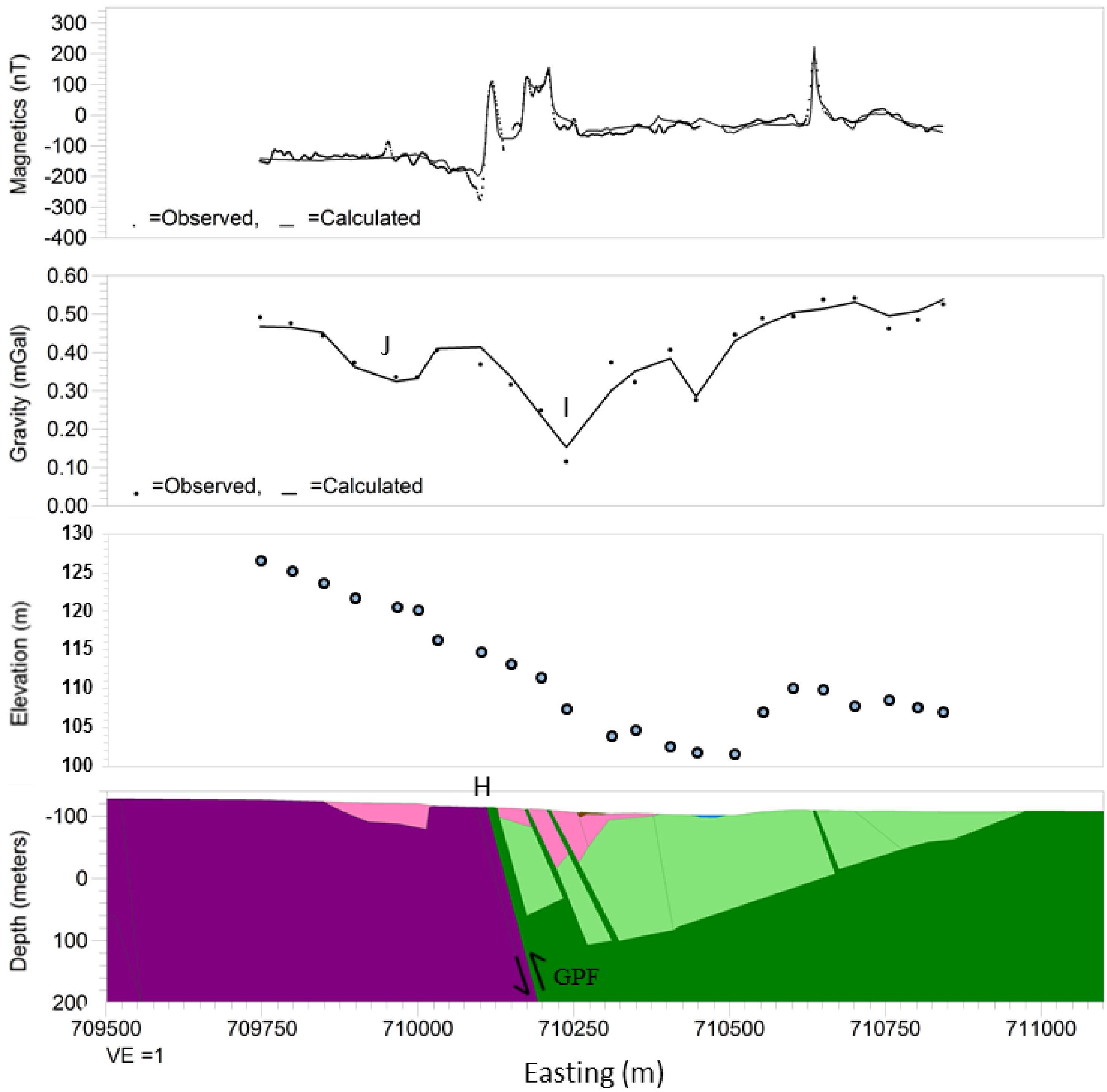

Figure 4.19: 2D modelling of Line 8900. See caption for Figure 4.14 for general description. H is the contact between units with contrasting magnetic properties, I and J are presumed alteration zones, and GPF refers to the Grassy Pond Fault.

4.5 2D Inversion

In this section, results of the 2D inversions are analyzed. These models were discretized by triangular meshes, generated using programs developed by Dr. Lelièvre. The inversion codes attempt to generate geologic models that reproduce the observed data within an acceptable tolerance which is typically based on the data uncertainty. In this case, the inversion becomes an optimization problem where a trade-off exists between data misfit and model parameters. The program makes use of a priori knowledge such as bog bathymetry, known geologic trends, and allows one to assign physical property values, or a range of values, to any region within the model. This does not eliminate the non-uniqueness issue of inversion, as discussed in Section 0, but it greatly reduces the range of results. The models generated below were created using the observed magnetic and gravity data over Line 7700. To account for the effect of the bog on the gravity data, a response due exclusively from the bog was generated in the forward program 'fwd' which is also developed by Dr. Lelièvre. The response of the bog was then removed from the observed data prior to inversion.

4.5.1 Magnetic Inversion

As shown in Section 3.1.1, the magnetic properties of the units investigated, excluding the mafic rocks, are very similar. This makes distinguishing between units very difficult which is evident in the magnetic inversion results (Figure 4.20). Any subtle difference in magnetic susceptibility that may have been present in the inversion model is over shadowed by the broad structures with slightly higher magnetic susceptibilities. Although the calculated data fit the observed data relatively well (Figure 4.21), the physical representation of the subsurface is poor.

The high susceptibility regions are created to match the high magnetic response of the mafic dykes however, they appear much broader and have much lower magnetic susceptibility than any dykes present in drill core. This broadening effect occurs because smallness weights were set for the inversion to generate a smoothly varying model which is typically more geologically reasonable. However, some features to be modelled, such as the dykes, have sharp contacts and are very thin. Increasing the smallness weight (*i.e*. decreasing the smoothness) to the degree where individual dykes would be resolved would add unwanted complexity to the model. For instance, two cells with strong contrasting values could be placed in close proximity to one another. These cells, or combination of cells could be peppered throughout a model. While their contribution to the calculated data would seem reasonable as they average out, such strong gradients do not exist in nature. One method of resolving this is to incorporate the mafic dykes into the model, in a similar manner to how the bog was included. As the exact dimensions and locations of dykes are unknown, this would be extremely time-consuming as it would be on a trial-and-error basis. Therefore, fitting the magnetic data with a geologically reasonable model using forward modelling is more appropriate (Section 4.4).

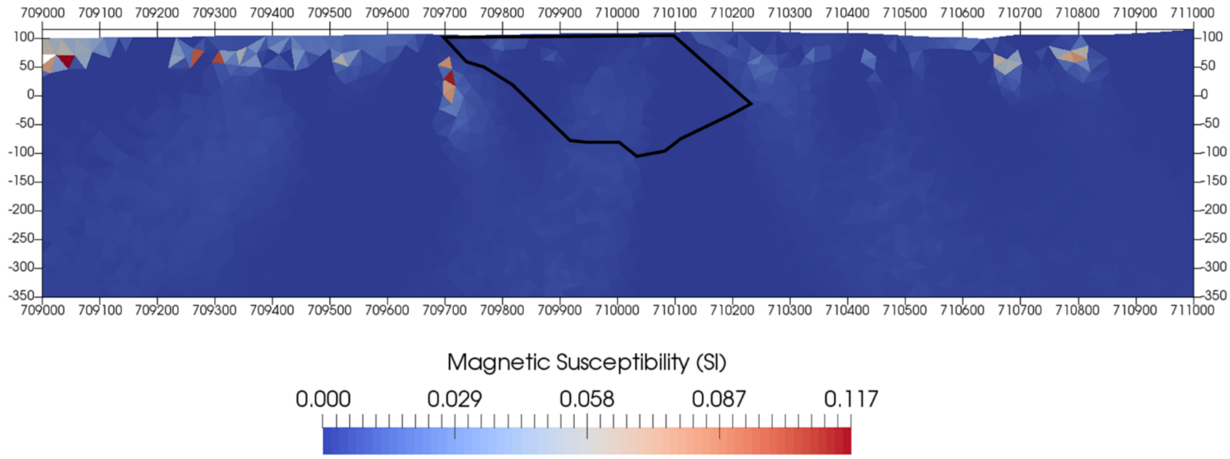

Figure 4.20:Model produced from inverting magnetic data collected over Line 7700. Model is cropped laterally to the extent of the survey and to a depth of 350 m below sea level. Black outline represents alteration zone as produced from forward modelling. Respectively, the x- and z-axis are the easting and elevation in metres.

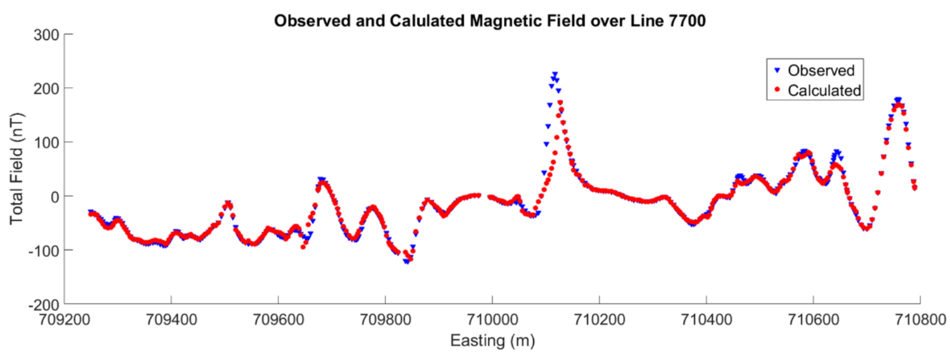

Figure 4.21:Observed magnetic data collected over Line 7700 (blue) and calculated magnetic data generated by the inversion model (red).

4.5.2 Gravity Inversion

The gravity inversion results over Line 7700 are shown in Figure 4.22. Here, the outline of the alteration zone obtained from the forward modelling (Section 4.4.3) is superimposed. The location of the eastern boundary near the surface is in good agreement with that obtained from the forward modelling. However, even with a trend enforced (discussed in Section 3.4.4), the inversion produces an anomalous body that is near-vertical. The vertical extent is also unclear because the sensitivity to the gravity data decays with depth creating a fuzzy lower boundary. The overall density contrast is also lower than measured values and would require a larger area to generate the same anomaly. Additionally, the western boundary extends several hundred metres west of the forward-modelled result, where the boundary is defined by drill holes. Again, there is an acceptable fit to the observed data (Figure 4.23) but even with the constraints implemented, the generated model section was not acceptable. It is likely that with further adjusting of model parameters, an acceptable result could be achieved but the efforts involved would be beyond the scope of this thesis. Therefore, as with the magnetic data, in light of the geological control available at this site, fitting the data with a geologically reasonable model is best done with forward modelling.

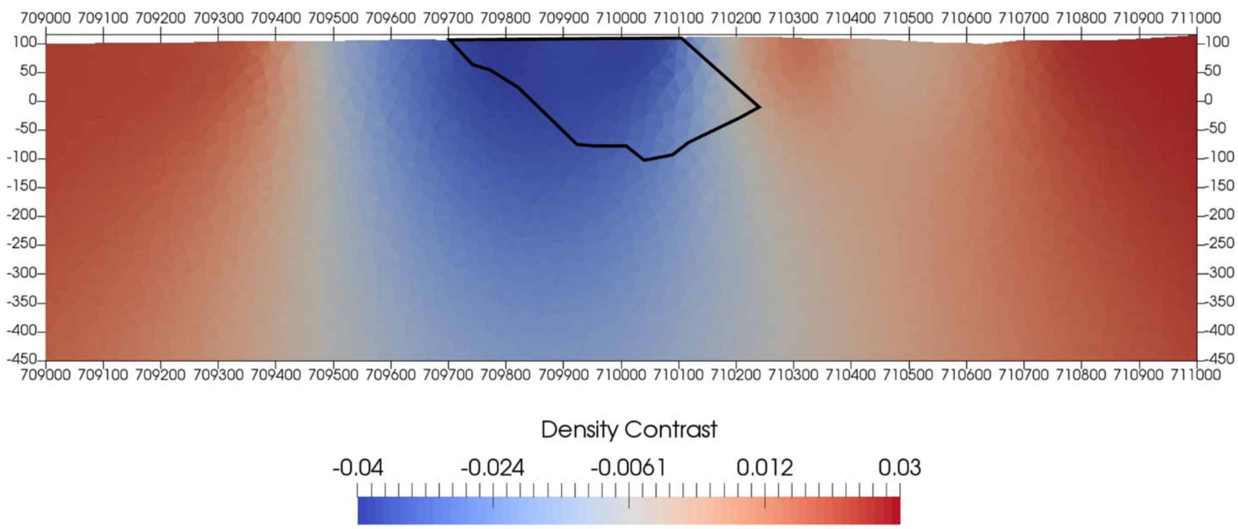

Figure 4.22: Model produced from inverting gravity data collected over Line 7700. Model is cropped laterally to the extent of the survey and to a depth of 450 m below sea level. Black outline represents alteration zone as produced from forward modelling. Respectively, the x- and z-axis are the easting and elevation in metres.

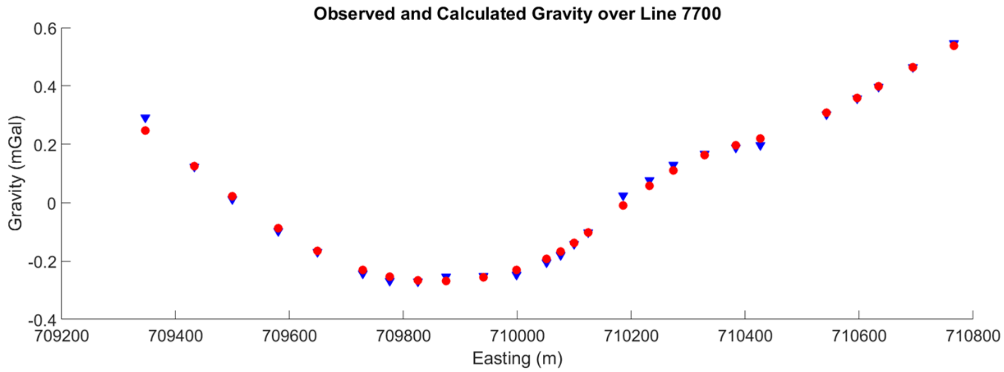

Figure 4.23: Observed gravity data collected over Line 7700 (blue) and calculated gravity data generated by the inversion model (red).

Chapter 5 Summary and Conclusions

Integrating new geophysical data with the existing knowledge of the Big Easy prospect in order to develop a better understanding and a representative model has served as the underpinnings of this research. Surveys presented here included a high-resolution ground magnetic survey, a ground-based gravity survey, as well as an RTK elevation survey and ground-penetrating radar (GPR) surveys. Magnetic susceptibility and density values obtained from a physical property study of the altered material and surrounding units suggested that a measureable response is obtainable.

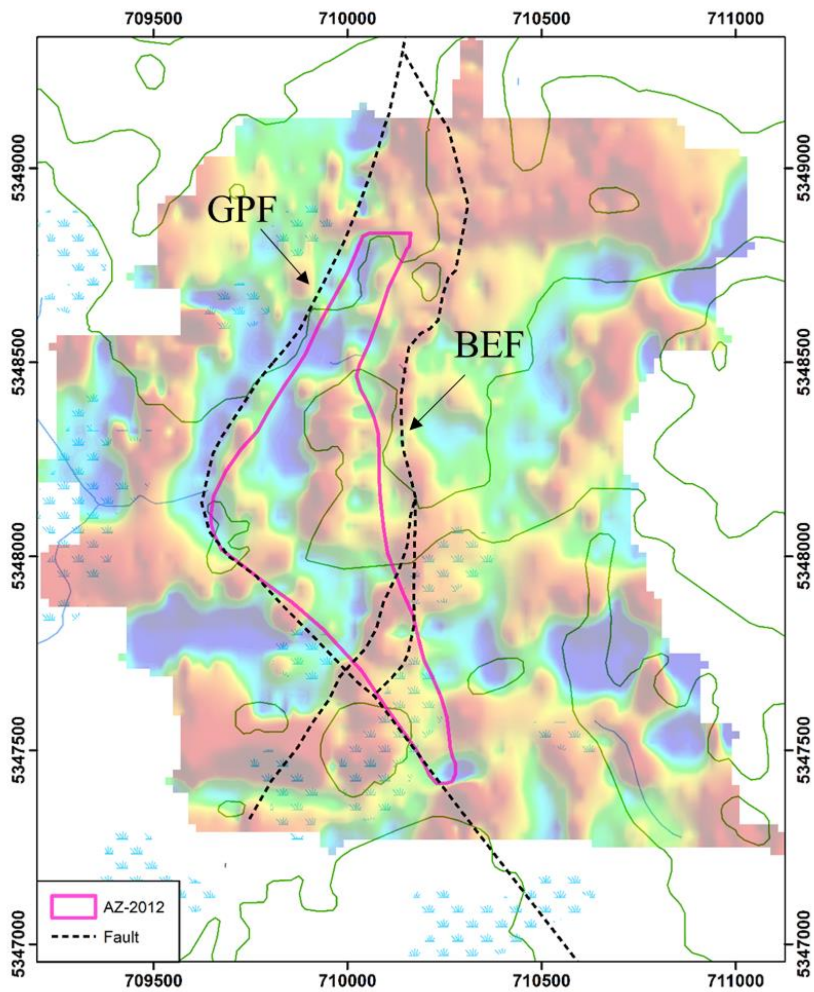

Figure 5.1: Magnetic grid with faults superimposed.

Whereas this was mostly true for the density study, the only distinguishable unit from the magnetic data was the mafic unit. However, the magnetic data gave additional structural information. These property measurements were also utilized to provide reliable values to use during the 2D modelling.

An attempt was made to generate inversion models using the gravity, magnetic and GPR data. However, the results were not favourable. The gravity inversion resulted in a model with poor resolution at depth and the magnetic inversion was unable to resolve the mafic dykes. Therefore, efforts were focused on generating 2D forward models in which realistic geologic constraints were easy to apply.

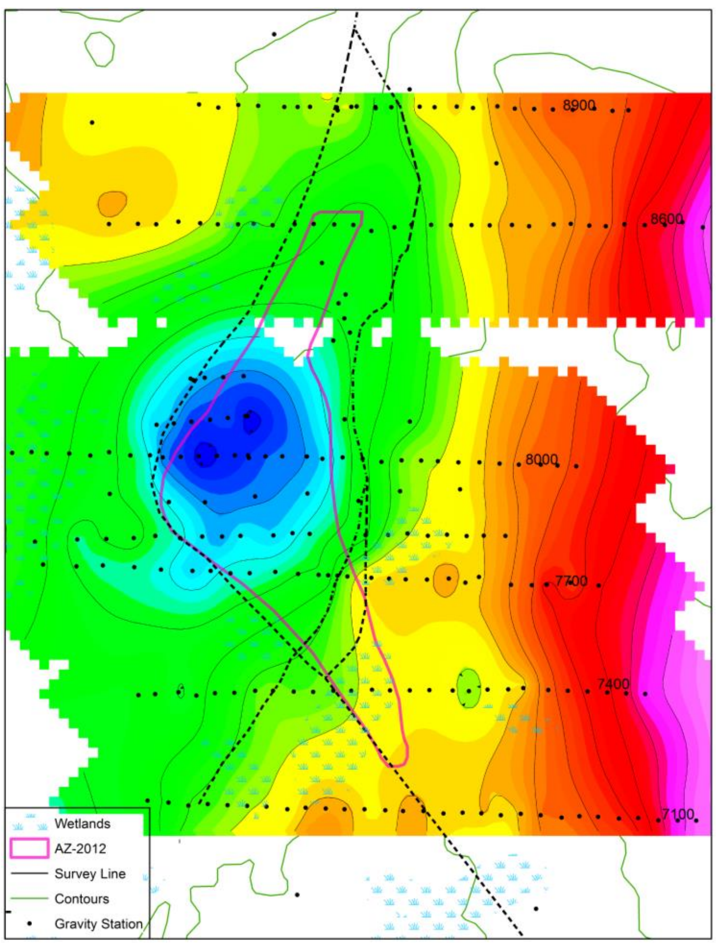

Figure 5.2: Grid of residual gravity Bouguer anomaly data.

Zones of alteration were located based largely on the gravity data through 2D modelling along several survey lines throughout the property (Figure 4.14 to Figure 4.19). As the survey data along Lines 7100 and 7400 (Figure 4.14 and Figure 4.15, respectively) were reproduced with models absent of any altered material, it was determined that the main alteration zone, AZ-2012, does not extend as far south as previously believed. However, based on the model for Line 8900 (Figure 4.19), it is likely to extend further north than previously believed. The greatest gravity anomaly was recorded along Line 8000 (Figure 4.17) where the zone is thought to be at its widest and likely most strongly altered. Along this line, the altered zone is modelled to extend from the surface to a depth of approximately 250 m. In addition to the main alteration zone, two unexplained gravity anomalies along Line 7400 and 8900 present the possibility of localized zones of altered material outside the main alteration zone.

Although it was discovered that the magnetic properties did not vary significantly between the altered and unaltered sediments, prominent magnetic signatures were present from mafic dykes. These signatures proved to be invaluable since dykes are known to be spatially related with faulting in the area. Therefore, correctly modelling the magnetic response gave additional insight to the fault localities (Figure 5.1) as well as structural orientations. The gravity signature from the alteration zone is also very clear in Figure 5.2. With the aid of drill logs and field observations, it was proposed that two main faults, the *Big Easy Fault* (*BEF*) and the *Grassy Pond Fault (GPF)*, likely act as structural constraints on the alteration. Based on the evidence provided in this study, as well as existing information, a new geology map of the region is supplied (Figure 5.3) including a newly proposed alteration zone, AZ-2016. Here, AZ-2016 is presented with AZ-2012 as a reference. In the new map, the main body terminates to the south where the *GPF* and the *BEF* intersect. AZ-2016 extends approximately 500 metres north of AZ-2012, however, the gravity signature diminishes significantly toward the north implying that the alteration zone is shallowing. Also shown in this map are to two anomalous zones to the northwest and southeast of AZ-2016. The northern and southern extents of these two regions are unknown, but given that they are each supported by only single gravity survey lines, they are likely less than a few hundred metres in length.

The only way to determine the true extent, and to gain a full understanding of the deposit, is through additional drilling. However, this study presents a more refined depiction of the alteration zone that also highlights encouraging targets for future exploration.

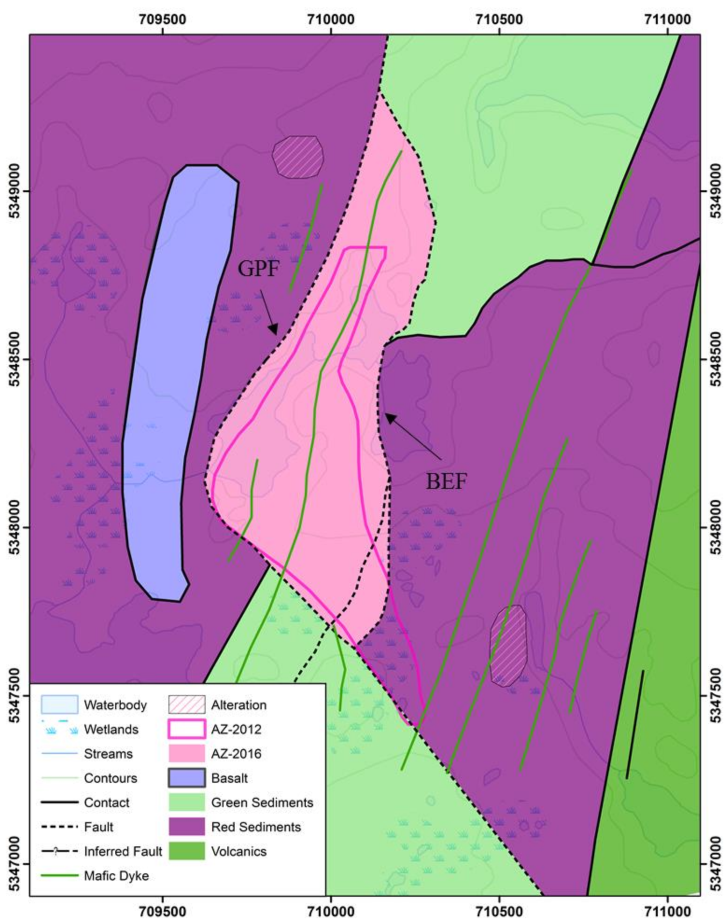

Figure 5.3: Updated geology map with a newly proposed alteration zone, AZ-2016, projected to surface.

References

Akima, H. (1978). A Method of Bivariate Interpolation and Smoth Surface Fitting for irregularly Distributed Data Points. *Transactions on Mathematical Software, Vol 4, No 2*, 148-159.

Annan, A. P. (2004). *Ground Penetrating Radar Principles, Procedures, and Applications.* Mississauga, ON.: Sensors & Software.

Ayuso, R., Wooden, J., Foley, N., Seal, R., & Sinha, A. (2005). U-Pb Zircon Ages and Pb Isotopes Geochemistry of Gold Deposits in the Carolina Slate Belt of South Carolina. *Economic Geology, v. 100*, 225-252.

Blackwood, R. F., Walsh, D. G., & Gibbons, R. V. (1987). *Current Research.* St. John's, NL: Department of Mines and Energy.

Blakely, R. J. (1996). *Potential Theory in Gravity and Magnetic Applications.* New York, NY: Cambridge University Press.

Canada, N. R. (n.d.). *Natural Resources Canada*. Retrieved from Geoscience Data Repository for Geophysical Data: http://gdr.agg.nrcan.gc.ca/

Clarke, M. (2013). *Host lithologies, breccia development, alteration and gold mineralization at the Big Easy Prospect.* St.John's, NL: Memorial University of Newfoundland and Labrador.

Dal Bello, A. (1977). *Stratigraphic Position and Petrochemistry of the Love Cove Group, Glovertown-Traytown Map Area, Bonavista Bay, Newfoundland, Canada.* St.John's: Memorial University of Newfoundland.

Daniels, J. (2000). *Ground Penetrating Radar Fundamentals.* Columbus: Ohio State University.

Davenport, P. (1988). *Gold and associated elements in lake sediment from regional surveys in the Gander Lake map area [NTS 2D]*. St. John's, Newfoundland: Department of Natural Resources, Mineral Lands Division.

Dimmell, P. (2013). *Annual General Meeting* (p. 24). Dartmouth, NS: Silver Spruce Resources Inc.

Dimmell, P. (2012). *Report of 2012 Exploration (Prospecting, Stream Sediment Geochemistry, Airborne Gweophysics, Diamond Drilling, Compilation,) on the Big Easy (BE) Property.* St. John's, NL: Department of Natural Resources.

Dressler, M. M. (2009). Art of Surface Interpolation. Kunstat.

Dyke, B. (2008). *Assessment report of prospecting and terraspec analysis on licence 13446M (first and second year) Thorburn Lake Project.* Mount Pearl: Cornerstone Resources Inc.

GEM Systems, Inc. (2008). *GSM-19 v7.0 Instruction Manual.* Markham, ON: Gem Systems, Inc.

Geosoft. (2014). *Montaj MAGMAP Filtering How-to Guide.* Toronto: Geosoft.

Geosoft. (2016). *Topics in Gridding*. Retrieved from Geosoft: www.geosoft.com/media/uploads/resources/technical-papers/topicsingriddingworkshop.pdf

Geosoft Inc. (2015, 16 11). montaj Gravity and Terrain Correction How-To Guide.

Geosoft Incorporated. (2010). *montaj Gravity & Terrain Correction Tutorial and User Guide.* Toronto, ON: Geosoft Incorporated.

Geotek. (2017, May 08). *Geotek*. Retrieved from Gamma Density: http://www.geotek.co.uk/products/gammadensity

Glatzmaier, G. A. (2016, June 15). Retrieved from The Geodynamo: https://websites.pmc.ucsc.edu/~glatz/geodynamo.html

Government of Canada. (2015, 02 06). *Natural Resources Canada*. Retrieved 03 12, 2015, from Tools and Applications: http://webapp.geod.nrcan.gc.ca/geod/tools-outils/ppp.php?locale=en

Heath, T. L. (1897). *The Work of Archimedes.* London: Cambridge University Press Warehouse.

Hedenquist, J. W. (2013). *Observations on the Big Easy epithermal Au-Ag prospect, eastern Newfoundland, and comments on its potential.* Ottawa, Ontario: Hedenquist Consulting, Inc.

Hedenquist, J. W., Arriba, A. R., & Gonzales-urien, E. (2000). Exploration for epithermal gold deposits. *Reviews in Economic Geology*, pp. 245-247.

Hibbard, J. (2007). Links among Carolinia, Avalonia, Ganderia in the Appalachian peri-Gondwanan realm. *The Geological Society of America Special Paper 433*, 291-311.

Hussey, E. (1979). *The stratigraphic, structure and petrochemistry of teh Clode Sound map area, northwestern Avalon Zone, Newfoundland.* St. John's, Newfoundland: Memorial University of Newfoundland.

Jenness, S. (1963). Terra Nova and Bonavista map areas, Newfoundland (2 D E 1/2 and 2 C). *Geological Survey of Canada, Memoir 327*, 34-65.

Kane, M. (1962). A comprehensive system of terrain corrections using a digital computer. *Geophysics, Vol. 27, No. 4*, 455-462.

Last, B. J., & Kubik, K. (1983). Compact gravity inversion. *Geolphysics Vol. 48, No. 6*, 713-721.

Lelièvre, P. (2012). Joint inversion of seismic traveltimes and gravity data on unstructured grids with application to mineral exploration. *Geophysics Vol. 77 No. 1*, K1-K15.

Lelièvre, P. (2016, November 29). Personal communication.

Lelievre, P., Carter-McAuslan, A., Farquharson, C., & Hurich, C. (2012). Unified geophysical and geological 3D Earth models. *The Leading Edge, Special Section: Mining Geophysics*, 322-328.

Li, Y., & Oldenburg, D. W. (2000). Joint inversion of surface and three-component borehole magnetic data. *Geophysics, Vol. 65, No. 2*, 540-552.

Longman, I. M. (1959). Formulas for Computing the Tidal Accelerations Due to the Moon and the Sun. *Journal of Geophysical Research Volume 64, No. 12*, 2351-2355.

Mac Gillivray, G., Delazzer, A., & Dimmell, P. (2011). *Report on 2010/2011 Exploration Prospecting, Trenching and IP/Resistivity Surveys on the Big Easy Property*. St. John's, NL: Government of Newfoundland and Labrador, Department of Natural Resources.

MetGen. (2014, Oct 22). *The Architect of Your Metrology*. Retrieved from Calculation of the density of water: http://metgen.pagesperso-orange.fr/metrologiefr19.htm

Moritz, H. (1980). The Geodetic Reference System. *Bulletin géodésique Vol. 54(3)* , 395-405.

National Oceanic and Atmospheric Association. (2015, 06 23). *Magnetic Feld Calculators*. Retrieved from National Centers for Environmental Information: http://www.ngdc.noaa.gov/geomag-web/#igrfwmm

Normore, L. (2010). *Geology of the Bonavista Map Area.* St.John's, NL: Newfoundland and Labrador Department of Natural Resources.

NovAtel. (2016, September 23). *An Introduction to GNSS*. Retrieved from http://www.novatel.com/an-introduction-to-gnss/chapter-5-resolving-errors/gnss-measurements

O'Brien, S. (1987). *Geology of Eastport (west half) map area, Bonavista Bay, Newfoundland.* St. John's, Newfoundland: Newfoundland Department of Mines and Energy, Mineral Development Division.

O'Brien, S., & King, A. (2002). Neoproterozoic stratigraphy of the Bonavista Peninsula: preliminary results, regional corrections, and implications for sediment hosted stratiform copper exploration in the Newfoundland Avalon Zone. *Current Research (2002) Newfoundland Department of Mines and Energy*, 229-244.

Reusch, D., & O'Driscoll, C. (1987). *Geological and Metallogenic Investigations in the Western Belt of the Love Cove Group (NTS 2D/1,2,8), Avalon Zone, Newfoundland.* St.John's, NL: Newfoundland Department of Mines and Energy.

Robert, F., Brommecker, R., Bourne, B., Dobak, P., McEwan, C., Rowe, R., & Zhou, X. (2007). Models for Exploration Methods for Major Gold Deposit Types. *Proceedings of Exploration 07: Fifth Decennial International Conference on Mineral Exploration*, 691-771.

Saunders, P. (1996). *First year assessment report on prospecting and geochemical exploration for licence 4554 on claim block 17112 in the Henry's Pond and Thorburn Lake areas, eastern Newfoundland.* St.John's, NL: GT Exploration.

Scintrex Limited. (2009). *CG-5 Scintrex Autograv System Operation Manual.* Concord, ON: Scintrex Limited.

Sensors and Software Inc. (2015). *EKKO_Project with Processing, Bridge Deck Condition and Pavement Structure Modules User's Guide.* Mississauga: Sensors and Software Inc.

Shewchuk, J. R. (1996). Triangle: Engineering a 2D Quality Mesh Generator and Delaunay Triangulator. Pittsburgh, Pennsylvania, United States.

Silver Spruce Resources. (2015). *Silver Spruce Encouraged by High Silver Values in "Classic" Quartz Adularia Veins in Big Easy Diamond Drilling.* Bridgewater, NS: Silver Spruce Resources Inc.

Silver Spruce Resources Inc. . (2012). *Big Easy - Epithermal Gold/Silver Prospect.* Bridgewater, NS: Silver Spruce Resources.

Silver Spruce Resources Inc. (2010). *Silver Spruce Defines Large, Strong, Altered / Mineralized Zone Big Easy Property, NL.* Bridgewater, NS: Silver Spruce Resources.

Silver Spruce Resources Inc. (2013). *Silver Spruce Reports on Independent Assessment of its Big Easy Epitermal Au-Ag Prospect.* Bridgewater, NS: Silver Spruce Resources Inc.

Sparkes, G., & Dunning, G. (2014). *Late Neoproterozoic epithermal alteration and mineralization in the Western Avalon Zone: A summary of mineralogical investigations and new U/Pb geochronological results.* St. John's: Department of Natural Resources Geological Survey.

Telford, W., Geldart, L., & Sheriff, R. (1990). *Applied Geophysics Second Edition.* New York, NY: Cambridge University Press.

Topcon Corporation. (2014, 10 27). *Topcon Dual Frequency GNSS Receiver.* Retrieved from Topcon: http://www.topconpositioning.com/products/gnss/receivers/hiper-v

Tycholiz, C. (2013). *Gravity gradient inversions using unstructured tetrahedral meshes.* St. John's, Newfoundland: Memorial University of Newfoundland and Labrador.

Williams, N. (2008). *Geologically constrained UBS-GIF gravity and magnetic inversions with examples from the Agnew-Wiluna greenstone belt, western Australia.* Vancouver: University of British Columbia.

Wilton, D. (1996). *Petrographic report on a sample from the Henry's Pond gold property, eastern Newfoundland.* St.John's, NL: GT Exploration.

Appendix A Diamond Drill Logs

Silver Spruce Resources Inc.

Project: Big Easy (BE)	Northing: 5347563	NAD 27	AZM: 090	Core Size: NQ / Start: Mar. 25/2011
Drill Hole No.: BE-11-01	Easting: 709951	Elev: 115 m	DIP: -52	Logged by: A. DeLazzer / Finish: Mar. 27/2011
Contractor: Cabo Drilling	Length (m) 107	Samples: 38 (553001-553038)		Report: 201130021
				Survey Tools: Rhino GPS, Pjari (one reading)

From (m.)	To (m)	Rock Type	Colour	alt Degree	alt Type	Texture	Structure	(%) Mineralization	Comments
0.0	8.0	OB							
8.00	10.00	6c, qtz	gy to light rd	2	sil, weak fe	fg	vns CA 70, weak bx	py - 1-3%, stringers	Sil, weak fe (hem) alt congl; wh QV's
10.00	11.30	QV, 6c, bx	gy-dk gy	3	sil, wk hem	bx QV's	bedded CA 45-50	py - 1-3% stringers	Bx w int sil and multi phase QVs Xcutting - clr vns w/ cherty qtz; banded dk gy-gy, beige qtz; fine hem strs along banding CA 40-50
11.30	25.50	3c	dk gy	1	ep	ms	ep+QVs CA 40-50	tr py, pyr	unalt, msv, mafic dike, ep + cb + QVs
25.50	25.70	3c, 6b	drk gy to gn	1	chl, sil	ms, assimilated		tr py, pyr	weakly alt in congl - assimilated w/ dike
25.70	26.30	6c	gy, bn	2	sil	fine gr	vns of py @ 70-80 to CA	py >15%, mass py bnds >3 cm	fg, gy bn; py bands CA 70-80
26.30	26.90	6c	gy, gn	2	sil, chl?	beds	beds @ 40-60 to CA	py - 3-10% in vns	light gn to gy, gn alt (chl?), bedded congl,
26.90	28.90	6c	gy, gn	2	sil	beds	beds @ 40-60 to CA	diss py, f-cg; euhedral, strs - 3-7%	lt gn-gy; bedded congl / sandstone; less dev CA 40-60; v. sil w/ chal. Qtz;
28.90	31.60	6c, qtz vns	drk to pale gy	3	sil, hem	vns	loc bx vns, some bnding	py 1-3%	similar to start of hole, int sil, multiple vns, some clear and poss chal., some gn staining (chl?), some hem in qtz vns, py repl clasts and bnded w/in qtz clasts, loc vuggy
31.60	44.20	6c	gy, bn, gn	1	sil	clasts vis	drk (chl) vns @ 50 to CA	py 1-3%	not highly sil, variable clasts, some alt flds (saucer), py replacing some clasts, some felsic vol clasts, rare wh to cream colour qtz vns
44.20	47.10	6a	red	0	hem	clasts vis	bedded		unalt congl, not sil, hem, beds weakly vis
47.10	55.90	6b	gn, gy	1	chl, cb, sil	clasts vis	bedded @ 70-80 to CA	py tr to 2%	mostly chl rich congl, clasts vis, not very sil, trace py, becoming more py and sil towards L.C., beds @ 70-80 to CA, some cb alt
55.90	61.00	6c	gy, gn	2	sil	, clasts weakly	beds @ 70 to CA	py 1-3%, loc > 3%	Weakly sil conglomerate - some sil rich sections, py as str and diss, beded, loc py more abundant
61.00	64.00	6a, 6c	rd, gy	1	hem, chl, cb, sil	clasts vis	beds @ 70 to CA	py tr to 1%	mostly unalt congl to sandstone, reddish colour, some chl and cb alt, weakly sil sects, beds, clasts vis, py variable but not abund mostly in str.

Silver Spruce Resources Inc.									
Project: Big Easy (BE)				Northing:	5347563	NAD 27	AZM: 090	Core Size: NQ	Start: Mar. 25/2011
Drill Hole No.: BE-11-01				Easting:	709951	Elev: 115 m	DIP: -52	Logged by: A. DeLazzer	Finish: Mar. 27/2011
Contractor: Cabo Drilling				Length (m)	107	Samples: 38 (553001-553038)			Report: 201130021
								Survey Tools: Rhino GPS, Pjari (one reading)	

From (m.)	To (m)	Rock Type	Colour	alt Degree	alt Type	Texture	Structure	(%) Mineralization	Comments
64.00	70.00	6c	gn gy	1	chl, sil	clasts vis	beds @ 70 to CA	py 1-3%	more py rich, chl alt dom., soft not really sil, beds visible. Returning to red unalt congl at L.C.
70.00	83.10	6a	rd, gy	0	hem	clasts vis	beds @80 to CA		unalt red conglom, some cb in vns, some chl alt and shearing.
83.10	83.40	6b, flt	gn, gy	2	cb, ep, chl?		beds @80 to CA		int cb + ep alt, possible flt, slics at U.C., still in unalt congl, beded like above
83.40	89.20	6c	gn, gy	2	chl, cb, sil	qtz vns		py tr - 1%, loc 3-5%	loc sil, some int chl, cb alt sects, py in strs, near L.C qtz vns becoming common, some looking chal
89.20	91.00	6b, 6c	gn, gy to bn	1	chl, sil	qtz vns	beds @ 70-80 to CA	py tr	mostly weak chl or sil in congl, some cln wh qtz vns, clast vis.
91.00	102.40	6a	rd, gy	0	hem	clasts vis			mostly unalt coarse gr congl red beds, one sm sh @ 92 m w int chl alt
102.40	107.00	6a	rd, gy	0	hem	clasts vis			same as above, but finer grained, sandstone.
	107.00	EOH							

Silver Spruce Resources Inc.

Project: Big Easy					Northing	5347700	NAD 27 / AZM: 090	Core Size: NQ	Start: Mar. 29/2011
Drill Hole No: BE-11-02					Easting	709880	Elev: 115 m / DIP: -50	Logged by: A. DeLazzer	Finish: Mar. 29/2011
Contractor: Cabo Drilling					Length (m)	98	Samples: 80 (553039-553118)		Report: 201130024
								Survey Tools: Rhino GPS, Pajari (one reading)	

From (m.)	To (m)	Rock Type	Colour	alt Degree	alt Type	Texture	Structure	(%) Mineralization	Comments
0	4.5	OB	OB						like bedrock, blocky from 3.4 to 4m; chalcedonic vn intersected at 3m.
4.5	6.9	6c, qtz	gy - dk gy	2	sil	vns multiphase	beds CA 40-50, bx bnded QVs	vf diss py, some strs 1-5%	vfg dk gy bn; wh cln QVs <2cm; alt sst ? fuchsite in vns; clasts vis
6.9	10	6c	gy gn	2	sil	cherty qtz vns		py rich 5-10%, loc > 15%	c-mg clasts, cherty qtz vns, gy gn colour (fuchsite)
10	10.3	QV	gy, wh	3	sil		bx cherty QV, contact CA's 40-50	py tr - 2%	bx, no banding, contact CA's 40-50, cream to dark coloured sections
10.3	10.45	6c	gy, pale bn	2	sil	clasts vis		py 1-5%	alt silic congl; beige, spotty alteration, clasts visible
10.45	10.7	QV	drk gy, gy	3	sil	bx qtz vn	contacts @ 40-50 to CA	py tr - 2%	sim to prev vn, contacts at 40-50 to CA, mostly gy to drk gy colour, py in strs
10.7	16.9	6c	gy, gn	2	sil, chl	vis clasts	qtz vns, some bx, fract w sil.	py 1-5%, fuchsite?	gn gy alt congl; qtz vns, parallel to CA; fuchsite; chlorite alt assoc w/ shearing
16.9	17.4	6c, QV	light gy, wh	3	sil	multiphase qtz vns	some bx qtz vns	py 1-2%	gy to wh v sil; bx; multiphase qtz vns; yellow alt; py mainly stringers
17.4	20.5	6c	pale gy	3	sil	fg; vuggy	bnds @ 70-80 to CA	py (1-2%)	intense sil. alt; chaotic, multiple vns / variable alt; pale beige to gy; vfg w/ bands CA 70-80; qtz vns parallel to CA.
20.5	21	6b	gn gy	2	chl? Ser?			py 3-10%	strong sericite alt with py rich stringers
21	26.1	6c	wh, gy	2	sil	vis clasts, f dk gy to bk vns/stringers	wh qtz vns @ low angles to CA	py repl clasts, weakly diss	lt gy; bleached; dk gy and bk, cream qtz vns; chlorite in wh qtz vns, no sig py
26.1	38.1	6c	bn, gy	2	sil, chl?	vis clasts, graded beds	beds grade up; CA - 40; blue qtz eyes, joints @ low angles to CA	py - 1-3%, strs; graphite on joints; speck cpy	m-fg alt congl; variable grain size; graded - fining up; blue qtz eyes; fuchsite in gy to dk gy qtz vn; strong slickensides w/ graphite on joints; py strs CA 70-80
38.1	40.9	6c	drk gy	3	sil	alt congl	minor blue qtz eyes	py - 3-5%, loc > 5%, diss / strs	m-fg alt congl; variable grain size; graded; qtz vns; speckled appearance (alt flds?), matrix pyritic (diss); minor blue qtz eyes; fine cherty qtz vns
40.9	41.4	QV, 6c	drk gy, gy	3	sil	chery qtz vn	bnded / mottled cherty vn CA 70-80	graphite on joints; gn alt (chl?) at UC; py > 10% in vns CA - 60	cherty qtz vn, gy to dk gy, banded; mottled appearance; fuchsite; sericite alt.
41.4	42.8	6c	drk gy, bn	2	sil	mg, vis clasts	blue qtz eyes; minor qtz vns/strs	py 5-10%, diss and vns; graphite on joints	dk gy to bn mg; vis clasts; py rich - rims clasts; blue qtz eyes; some qtz vns (mostly wh)
42.8	45.9	6c	drk gy	3	sil	cherty; clasts not very vis.	weakly bx; chalcedonic qtz clasts; fine multiphase qtz vns	py rims clasts; fine diss 1-3%	dk gy; fg; cherty, qtz rich, clasts not visible; weakly bx, large chalcedonic qtz clasts; multiphase qtz vns, argillic alt,
45.9	50.1	6c	light gy to	2	sil	clasts vis, graded beds	qtz vns @ 60 - 70 to CA one w lime gn alt/min, most drk	py 1-3%, higher at contacts w vns	lt gy - wh bn; m-cg congl; large qtz vn, mod argillic alt CA 70; fuchsite
50.1	51.2	6c, ?	pale pk, gy	1	sil	looks like a felsic vn?	one sm qtz vn @ 70 to CA	py tr	some sil congl w poss felsic vn or alt contacts, w pale pk, gy colour

Silver Spruce Resources Inc.

Project: Big Easy | Northing 5347700 | NAD 27 | AZM: 090 | Core Size: NQ | Start: Mar. 29/2011

Drill Hole No: BE-11-02 | Easting 709880 | Elev: 115 m | DIP: -50 | Logged by: A. DeLazzer | Finish: Mar. 29/2011

Contractor: Cabo Drilling | Length (m) 98 | Samples: 80 (553039-553118) | Report: 201130024

Survey Tools: Rhino GPS, Pajari (one reading)

From (m.)	To (m)	Rock Type	Colour	alt Degree	alt Type	Texture	Structure	(%) Mineralization	Comments
51.2	54.1	6c	drk gy, gy	2	sil	qtz vns (cherty to chal) bnding @ 80 to CA	vn contacts @ 30-40 to CA	py 3-7%, loc 10-20%, decr abund towards L.C.	drk gy to gy v fine grained bned by py, some cln qtz vns @ low angles to CA, some coarser grained sections with less py
54.1	60.3	6c, QV	light gy, wh to pk beige	2	sil	variable gr size, cherty qtz vns	vn contacts CA 60-70	py rich >15-20% in bnds / vns 1-2%; 3-7% total	var grain size, sections of mostly fine gr, v py rich to coarser gr and less py rich, some lrg qtz vns or cherty alt sects > 0.5m wide, at L.C fuchsite, broken fractured.
60.3	62.7	6c, QV	rd, gy, gn	2	sil	clasts vis, qtz vns	vns @ 20-30 to CA, others @ 60 to Ca	jasperoid(?) in vn w int py in vns at contact	clasts are vis, possible jasperiods in qtz vns w int py, some vns chal looking
62.7	63	QV	gy, beige, pale pk	3	sil	cherty qtz vn	bnding @ 10-20 to CA	py tr , poss fuchsite?	cherty qtz vn, gy to beige w pale pk bnding, chl or fuchsite?
63	65.4	6c	gy beige	2	sil	clasts vis, qtz vns	fine grained, vuggy, fractured vns	py tr -1%, one vn of ms py @ contact w qtz vn	sim to prev, sil unit, vuggy, fractured, sm vns throughout from <1 to 5cm, @ 30-60 to CA, poss jasperiod(?) in qtz vn parallel to CA near L.C., some beige, yellow alt clasts.
65.4	66.2	6c	pale, gy, gr	2	sil	med to coarse grained, clasts vis.	graded	diss py tr - 1%	m-cg, vis clasts, cg graded beds; weakly py
66.2	69.9	6c	drk gy, gn	2	sil	v. fine grained, bned w py	py in strs/bnds, CA 45	py 10-15%, loc 15 - 20%	py strs / bnds CA 45; gy qtz, mottled appearance; some weak py sections
69.9	71.4	6b	drk gn	2	chl	fine gr, bedded	beds CA 40-60	py int @ contact w qtz vn, overall fine diss 2-3%	int chl alt in sandst, fine gr bedded, py in strs, one qtz vn, bnded beige to wh.
71.4	72.9	6b	light gn	2	chl, ser?	fine gr, loc bedded	beds CA 40-60	weak py tr - 1%	chl and poss ser alt, and loc rare qtz, bedded, minor py, loc alt is int (chl)
72.9	73.7	6b, 6c	gn, wh	1	chl	med to coarse grained		py tr - 2%	m-cg congl, vis clasts; white alt; mod alt; minor py
73.7	80.2	6c	pale gn, gy	1	chl, sil	beds, clasts vis	beds CA 40-60; steeper near LC - CA 70-80	py tr - 2%	bedded mod alt congl, py in strs follow beds, some more ms sects esp near L.C., bedding becomes steaper near L.C 70-80 to CA
80.2	85	6b, 6c	beige, drk	1	chl, sil	clasts vis.	beds CA 60-70; loc fract w/ slickensides	py tr - 2%, to 3-7%	weak to mod alt congl, weak sil; chl/ser(?) alt; beds prom loc, one sect w/ slickensides ll to CA
85	87.8	6b, 6c	rd, bn, gn	2	chl, sil	clasts vis.	beds CA 60-80	py tr - 2%	var alt in congl., clasts vis., bedded, mostly chl and sil alt, rare qtz vns
87.8	91.8	6a	rd, gy, gn	0	hem	clasts vis.	graded beds	rare py	red beds; unaltered; f-mg, graded beds
91.8	92.2	6b	gn	1	chl	clasts vis.	graded beds	rare py	chl alt congl., cg, graded
92.2	92.6	5a	gn	2	chl	v fine gr	sheared CA 80	py tr - 1%	py smeared on shear, vfg; mudstone w/ chlorite alt?
92.6	98	6a	rd	0	hem	fine to coarse gr	graded beds	rare py	red beds - unalt., f-mg; graded
	98	EOH							

Silver Spruce Resources Inc.

Project: Big Easy (BE)	Northing	5347701	NAD 27	AZM: 090	Core Size: NQ		Start: Mar. 30/11	
Drill Hole No.: BE-11-03	Easting	709743	Elev: 110 m	DIP: -50	Logged by: Adree DeLazzer		Finish: Apr. 5/11	
Contractor: Cabo Drilling	Length (m)	302	Samples: 249(553119-150; 553251-350, 553451-500, 619651-715)				Reports: 201130028, 29, 32	
					Survey Tools: Rhino GPS, Pajari (one reading)			

From (m.)	To (m)	Rock Type	Colour	alt Degree	alt Type	Texture	Structure	(%) Mineralization	Comments
94.8	104.2	6c	beige-pale	2	sil, cb	cb infilling, vuggy	int fract	vf diss py, 1-2%	cherty, fract, strong cb infill, blocky, cb infilling decr towards LC, rubble zone, LC @ 98m; 101m - mottled gn gy,
104.2	107	6c	beige-gy w	2	sil	int vns,	fract, LC	py 3-5%, diss and strs	chaotic, multi vns, some banded,
107	109	6c	beige	2	sil	bx, vuggy	poss flt/sh CA 20 @ UC	py tr to 2%	alt congl, bx, poss flt/sh @ UC, vuggy,
109	109.2	6c, flt	gn, bn	2	chl	gouge	shp contact @ 30-40 to Ca,	py tr	sharp contact on shear w/ gouge;
109.2	117.2	6c	pale gn, gy	2	sil, cb	vis clasts	LC	py to 5-10%, strs/vns to 2cm	patchy alt, loc int cb, yellow alt?, some
117.2	135.5	6c	pale beige-	1	sil, cb	vis clasts, bedded	bedding CA 70, QV's random	py vns/strs/weak diss, 3-5%	bedded, vis clasts, var grain size, cb vns, QV's, bands w/random
135.5	136.4	6c	beige	2	sil	bx, clasts vis	dk bk hrd, QV's CA 70-80	py w bk infill 1-3%	bx sil congl, beige to gy, dk bk hrd
136.4	141	6c	gy-pale blu	3	sil	beds/bnds, qtz	beds @ 70-80	py 2-7&, loc high w strs	int sil congl, pale blue fine clasts, qtz
141	145	6c	beige	1	sil	clast vis	QV's	py in vns/strs, 1-2%	weaker alt, lrg bn clasts in congl, qtz
145	151.2	6c	beige-gn	1	sil, clay?	clasts vis, alt contacts	bx-2, variable, alt cont @ 30	py 1-5, loc in strs, repl clasts	sil congl, clasts vis, alt contacts and bx dev, cherty sections vs alt congl w lrg
151.2	160	6c	beige to gy	1	sil	clasts vis	beds @ 60-70, var alt	py 3-5%, incr towards LC	var alt in congl, clasts vis, beds @ 60-
160	161	6b	gy gn	2	chl, sil	clasts vis, alt contacts	beds @ 50-60	py in strs w bnds 1-5%, loc >5%	become chl alt congl, still weak sil, grad contact, beds, py in strs w beds
161	170.5	6c	gy wh	3	sil	v hrd, qtz vns		py 3-7%	v sil, clay alt in some vns?, alt flds,
170.5	173.5	6b, 6c	gn gy	2	chl, sil	var alt, clasts vis	alt contacts @ 40-50 to 10	py 3-5%	var alt, soft, gn chl alt w/ pyrop clasts? to sil, hard; alt contacts CA 40-50; QV's
173.5	186	6c	gy, gn	3	sil	clasts not vis	QV's, wh or clr	py strs/bnds, 1-5% to>5%	clast not vis, QV's wh/clear, some pale
186	187.8	6c	gn gy-lt pu	3	sil	cherty, clasts		py vns, to ms, 3-7% along CA	v sil, dk gn/gy, w/ purple tinge, loc >
187.8	189.3	6b	dk gn	3	chl	prev alt, alt flds		py in vns/strs, semi msv, 1-4%, loc >5-10%	prev chl alt, poss pyrop alt, alt flds, speckled app, py semi msv in vns loc
189.3	192.3	6c	beige-lt pk	2	sil	lrg wh qtz vns some drk	chl sh @ 40-50 to CA, clasts become vis @ LC	py in vns nr QV's, repl clasts,	mostly sil alt, var, chl sh CA 40-50, clasts vis near LC, some gn alt xtals
192.3	194	6b	dk gn	2	chl	loc clasts vis, soft	bedding CA 70	weak py diss, tr - 2%	int chl alt, soft, clasts vis in places, bedding CA 70
194	196	6c	gy	1	sil	clasts vis	graded beds, CA nr 90	weak diss py, tr - 2%	weakly sil congl, vis clasts, graded beds
196	198.5	6c	gy	2	sil	fg, clasts weakly vis	bedded @ 50-60 to CA	py strs along beds, 1-5%, CA 40-50	v sil alt, sst?, fg, clasts weakly vis
198.5	206	6c	gy	2	sil	c clasts, bnded QV's	cg, graded beds oblique to 30-40, QV's CA 70	py in str, 3-5%	as above, cg, graded beds, bnded QV's w dk bnds CA 70
206	209.8	6c	pale-dk gy	2	sil	vis clasts, bedding	beds CA 50, QV's CA 30	py loc str, 3-5 to 5-10%	pale-dk gy, sil congl, var grain size, graded beds, int ch alt in 1 area
209.8	213.8	6c	gy-dk bn	3	sil	grain size var, QV's, bx	vns @ 50	py vns/strs, msv > 5%, gen 1-5%	sil, var grain size, QV's gen CA 50, alt flds, bn wh bnds in qtz, bx w/ dk bk
213.8	218.7	6c	gy-dk bn	2	sil	vis clasts, QV's		py vns/strs CA 40-70, 3-7%, pos cpy	sim to prev, not as bx; dk, hrd
218.7	219.3	6c	lt gy	2	sil	clasts weakly vis		py vns, diss 3-5%	looks bleached,, sil, vuggy, py in dis, vns/strs
219.3	224.8	6c, 6b	gn, beige	1	sil, chl	vis clasts,	weak bedding, CA 70-80	py repl clasts/strs, 1-5%	congl, var sil alt, minor QV's, weak
224.8	232.7	6c	beige-pale gy	2	sil	vis clasts, QV's, bx	some bx QV's CA 30	py in vns/strs > 2cm, 1-5%	sil congl, QV's bnded, bx, CA 30, graphite on joints, chaotic loc, var vns
232.7	236.1	6c	variable	3	sil	bx QV's, banding	qtz bx w/ py, dk infilling	py diss/strs, 1-5%	mostly all qtz, var colours, py infill fact, [illegible]
236.1	245	6c	beige, variable	3	sil	bx qtz vns,	shear @ 242m, bx contact CA 30, overall bx 1-2	py 1-5%, ff/strs/diss, graph jts	beige; QV's; bx, var colour bands, contacts sharp CA 30, graphite on [illegible]

Silver Spruce Resources Inc.

Project: Big Easy (BE) | Northing 5347701 | NAD 27 | AZM: 090 | Core Size: NQ | Start: Mar. 30/11

Drill Hole No.: BE-11-03 | Easting 709743 | Elev: 110 m | DIP: -50 | Logged by: Adree DeLazzer | Finish: Apr. 5/11

Contractor: Cabo Drilling | Length (m) 302 | Samples: 249(553119-150; 553251-350, 553451-500, 619651-715) | Reports: 201130028, 29, 32

Survey Tools: Rhino GPS, Pajari (one reading)

From (m.)	To (m)	Rock Type	Colour	alt Degree	alt Type	Texture	Structure	(%) Mineralization	Comments
0	8	OB							
8	14.3	3c	dk gn/gy	0		ms		py, pyr tr - 1%	homogeneous; unalt; <1cm to 10 cm
14.3	15.1	3c, 6a	rd, gn	0		bedded, assim	beds @ 70 to CA	rare py	mafic dike assimilated w/ rd seds, rare
15.1	18.4	6b	gn	2	chl	Texture	sheared @ 50-70 to CA	trace py	soft; mod to int chl alt in congl; joints
18.4	19.2	6c	dk gy	1	sil?, cb			trace diss py to 1 %	alt flds, fg, hard
19.2	19.5	6c	gy	3	sil			py 5-10%, loc >15%	v py rich, int sil. congl
19.5	19.9	6c	gy	2	sil, chl	var alt	heterogeneous	diss sms py, vns to 10 cm	Variable alt / comp, qtz rich / chl rich sections
19.9	21.1	6c	gy	2	sil, chl	var alt	heterogeneous	py var, tr to 1%, to 5-7%	qtz vns, var alt, chl rich and sil sections, poss fuchsite.
21.1	21.3	6b	lt gy - gn	2	chl	schist?	slicks on joints	fuchsite in QV's, py tr to 1%	qtz clasts, schist w/ int chl, ser?
21.3	21.8	6c	cream to g	2	sil		U + LC CA - 20-30	py rich - m to sms	cream QV and clasts
21.8	22.4	6b	yellow-pale	2	chl	bedded	beds CA - 70	tr - 2% py	bedded; v int chl ser? altered, some
22.4	24	6c	dk gy to br	2	sil	beds, bnded qtz	LC CA - 80, QV's CA 70-80	py vns ms-sms, 1-2 cm	poss fuchsite, banded wh QV w/ py strs, blue qtz eyes
24	28.2	6c	dk bn, gy	2	sil		LC CA - 80, alt ll to contacts	py 5-15%, in vns/ bnds	v. sil, hard, wh QV's, alt flds clasts, weak chl, some pk alt?
28.2	38.4	6c	lt gy to bn	3	sil		LC sheared w int chl CA 60	py 5-15%, in vns/ bnds CA 60-80	sim to above, more sil, QV's, wh QV's CA - 10-20
38.4	44.5	6c	beige to dk	3	sil	qtz vns, chal	some bx, bnded QV's	py in stringers - tr to 3%	v int wh QV's, pale yell-gn alt overprint, chalced QV's, chaotic
44.5	44.9	6b	dk bn - brig	3	chl, ser?	schistose?	fol/sheared CA - 80	tr py	sharp sheared/alt contacts CA - 80,
44.9	53.2	6c	gy to beige	3	sil	clast vis, chal vn		py str/diss/repl clasts, 1-5%	vis clast in congl, 1 chalced QV 15-40 cm, low angles to CA
53.2	53.5	3c	dk gy	0		fine grained	UC CA 60-70, LC CA 30; bx	chl in cb vn, tr py, pyr	looks like a weakly chl
53.5	56.3	6c	beige to gy	3	sil	clast vis, fine beige alt flds		py to 3-7%, gen 1-5%, repl. clasts in clusters	sil congl, vis clasts, lime gn alt in QV, pk in QV
56.3	56.9	3c? 6b?	dk gy, gn	0		fol?, fract?	contacts @ 30-40 to CA	py UC, tr throughout	dike or mudstone; mixed w/ congl?, fg,
56.9	62.3	6c	beige to gy	2	sil	qtz vns, clasts vis	qtz vns, some w chal app, one looks bx	py 1-5%, strs to 7%	alt congl, QV's, some chalced , fuchsite?
62.3	65	6b	dk gn, yellow	2	chl	clasts vis, qtz vns and clasts		py mostly in strs near QV's, in qtz clasts, 2-5%	chl rich alt congl, vis clasts, some qtz, QV's,
65	68.8	6c	light beige	2	sil	clasts vis	qtz vns @ low angles to CA	py 1-4%	sil congl, vis clasts, some chalced QV's
68.8	68.9	6b	gn, lime	2	chl, ser?	schist?	nr vert. contacts (alt or fol)?	py in str, 1-5%	int alt, fol or alt contacts nr vert CA's
68.9	71.9	6b	dk gn	2	chl	alt congl	clasts barely vis, some QV's	weak py 1-2%	int chl alt? soft, clasts weakly vis, some QV's, more sil near LC, bnded, lt gn to
71.9	73.8	6c	lt beige to gy	2	sil?	grad contact	chl to sil, cherty, beds CA-70-80	tr py	grad contact between prev unit and cherty unit
73.8	75.2	6c	lt beige-pale gn	2	sil, chl	cherty, no vis clasts	shearing @ 74.5 CA 50	vf weak diss py	chl alt/shearing, mostly strong sil, cherty, clasts not vis.
75.2	80.7	6c	lt beige	2	sil	fract	bx-2 to 3	py ff, graphite ?	same as above, but bx, fract/alt
80.7	83.5	6c	lt beige	2	sil	less fract	bnded QV's CA 20-30; bnds CA 70	f bnds py in qtz	same as above, less fract, bnded fine QV's
83.5	84	6c, flt	bn, gn	3	chl, cb, sil	gouge	flt CA 20-30?; bx-2, 3	tr py	same as above but gouged, highly
84	88.6	6c	beige	2	sil, chl	rubble	v broken, fract	py ff	same as prev, but rubble zone,
88.6	94.8	6c	beige	2	sil	mod broken	QV's, some chalced	py in dk bands in QV's	sim to above, weaker bx near UC, no vis clasts, QV's, banded, some Xcutting

Silver Spruce Resources Inc.

Project: Big Easy (BE)					**Northing**	**5347701**	**NAD 27** / **AZM: 090**	**Core Size: NQ**	**Start: Mar. 30/11**
Drill Hole No.: BE-11-03					**Easting**	**709743**	**Elev: 110 m** / **DIP: -50**	**Logged by: Adree DeLazzer**	**Finish: Apr. 5/11**
Contractor: Cabo Drilling					**Length (m)**	**302**	**Samples: 249(553119-150; 553251-350, 553451-500, 619651-715)**		**Reports: 201130028, 29, 32**
								Survey Tools: Rhino GPS, Pajari (one reading)	
From (m.)	To (m)	Rock Type	Colour	alt Degree	alt Type	Texture	Structure	(%) Mineralization	Comments
245	272.2	6c	wh, gy-dk gy	3	sil	mottled	bx-2, var colours in qtz clasts	py diss/ff/strs, 3-7%	v qtz rich, flt breccia?, bx-2, var colours/bands, mottled, gouge @ 248,
272.2	272.4	flt, 6c	bk, gn, gy	3	sil, chl	flt bx	chl mudst gouge?, w qtz frags	py tr to 2%	flt contact @ 30, some graphite, qtz
272.4	273.6	6b	bk-dk gn	2	chl	fol, beds	beds @ 30 to CA	py, smeared tr to 1%	mudstone; chl, fol, bedded, some pale
273.6	274.2	6b	lt-dk gn	1	chl,	fol, beds	bedding CA 30	py, f diss, tr-3%	weakly alt congl, chl, fol/beds, some
274.2	276.3	6b	pale gn,	2	chl,	qtz vns, fol	bedding CA 30-40, QV's	py tr to 2%	mudstone, chl, fol, bedded sim to
276.3	276.9	6b	bk	2	chl	flt bx	bx w qtz clasts	py in vns 2-3%, some lrg clasts	flt breccia like 272.2 to 272.4
276.9	283.9	6b	drk gn, gy	2	chl	mudstone	beds/fol CA 30, shears? @ 30	py diss/ff - tr to 2%	mst, sst, chl alt, shs, w qtz clasts as bx,
283.9	292	6b	drk to pale	2	sil, cb	vn bx w cb,	int cb alt, some vns	py diss, tr to 1%	v chaotic, bedded, foliated, grain size
292	294.4	6b	gn, drk gn	2	chl	bed, fol, pale	bedded @ 70, smeared py	py, 1-2%, diss, euhed	fg, sheared/bedded, mylonitic ? hard,
294.4	297.2	6b	gn, yellow	2	chl	beds, clasts	beds @ 70 to CA	py, tr-1%, loc alb+cb vn	cg, bedded, yellow to lime gn clasts,
297.2	302	6b	gn	2	chl	mudstone	beds @ 70 to CA	py, tr-rare	vfg, gn (chl) alt, mudstone, beds near
	302	**EOH**							

Silver Spruce Resources Inc.

Project: Big Easy	Northing	5347880	NAD 27	AZM: 095	Core Size: NQ		Start: Apr. 7/11
Drill Hole No.: BE-11-04	Easting	709682	Elev: 115 m	DIP: -48	Logged by: Adree DeLazzer		Finish: Apr. 10/11
Contractor: Cabo Drilling	Length (m)	167	Samples: 121 (619716-836)		Reports: 201130034,36,39		
					Survey Tools: Rhino GPS, Multishot @ 30m intervals		

From (m.)	To (m)	Rock Type	Colour	alt Degree	alt Type	Texture	Structure	(%) Mineralization	Comments
87.5	89.1	6c	gy, wh	2	sil	clasts vis, v hrd	oured clasts (purple, pk, org) look	py dis, repl clasts, 1-3%	sil congl, lrg clasts vis, var colours, alt, some qtz vns, poss chal @ low angles to CA
89.1	90.5	6b	gn, gy	2	chl	soft, loc clasts vis	beds CA 70-80, shear CA 40-50	py - 1-3%, diss/rep clasts	pale gn, soft, chl alt congl, sndstone, at LC sect of mudstone, no clasts vis
93	95.5	6b, 6c	gn gy	1	sil, chl	vis clasts	bedding CA 70-80	py, tr to 1%,	var alt congl, clasts gone in places, soft, chl rich section
95.5	97.2	6b, 6c	gn gy	2	sil, chl	less vis clasts	QV's, chalced ll to CA	py in vns, dis, 1-5	sim to prev, but more qtz vns, some chal, py increases, clasts less vis, var alt
97.2	98.2	qtzvn	gy	2	sil	bx	look chal, vuggy	py infilling fract, 3-7	bx chal qtz vn w py, vuggy
98.2	104	6c	gy gn	2	sil, chl	clast vis, QVs	vns @ 30, beds @ 70	py 1-5, loc >3	sil congl; vis clasts; beds CA 60-70; QVs chalcedonic, CA 90, banded; others 10-30; w/ py nr vns
104	106.6	6c, 6b	gy gn	1	sil, chl	var alt, clasts vis	ns, some w blue, var colours, poss	py in strs, 2-5	coarse greained, clasts vis, var alt, chal clasts and vns, var colours, loc vuggy, bx
106.6	107.8	6c	bn, blue, gy	2	sil	fg, w/ blue qtz	sheared - low CA	py more abund 3-7%, loc > 7	fg, distinct blue, sheared qtz, CA 10-30
107.8	113.5	6c	gy	1	sil	cg, chalced clasts	patchy alt	py 3-7, mostly diss	coarse gr, gy pebble congl, sm chl alt sects, some fine chal vns, py in strs, diss, str near LC
113.5	115.4	6c	gy, blue	2	sil	v hrd, chal vn	hal vn near vert to CA, beds @ 7(	py 5-15%, repl clasts, in strs	vfg, dk gy-blue, bedded, py rich, chalced vns @ low angles
115.4	116.5	qtz vn	wh, gy, gn	3	sil	chal vn	bx sects	py diss, tr to 1%	chl vn, bx, fractured, some banding
116.5	117	6c	gn gy	2	sil	cherty?	bnded, alt clasts	py 7-10%, blebs, strs	v sil, alt clasts, bands 90 CA, var colours
117	121	6c	gy, gn	2	sil	clasts gone	bedded, chalced QV's CA 60-70	py diss, loc euh, 1-5%	bleached, wh-pale gy, banded, sil, clasts not vis
121	124.6	6b, 6c	pale gn, gy	1	sil, chl	var alt, clasts vis	QV's - wh, ll to CA	py repl clasts, vns/str, diss 1-5%	gy gn, f-mg pebble congl, vis clasts, wh-gy QV's, var alt
124.6	131	6c	gn gy	1	sil	var alt, clasts vis	var alt, Xcutting QV's	py 1-5%, in strs follow beds, some flourite in vn	bx app to rock, var alt, clasts vis, py 1-5
131	134	6b	dk gy - lt bn	2	chl	soft		v f diss py, 1-3%	alt contacts, prev chl alt, vis clasts; almost a mudstone
135	137	flt	gy	3	chl, cb	soft, broken	blocky fract/rubble, LC	py diss 1-3	mostly rubble, some qtz, bx
137	139	flt, gouge	gy	3	chl, cb	soft, broken	gouge, rubble, LC	py diss 1-3	bx
139	145.5	6b	gn gy	2	chl	mudstone	blocky, shs parallel to Ca	py, tr to 1%	mudstone, blocky, sh par to CA
145.5	145.7	gouge	gn	3	chl		contact @ 40-50	tr py	
145.7	148.2	6b	gn gy	2	chl	blocky	sh @ 40	fine dis py tr to 1%	mudstone, alt sediments, beds/sheared
148.2	148.4	gouge	gn	2	chl	sm bx zone		tr py	
148.4	150.2	6b	gn	2	chl	mudstone	sheared py	py tr to 5%	mudstone sim to 145.7-148.2
150.2	151	gouge	gn	2	chl	rubble zone	contact CA 70	tr py	
151	160	6b	gn	2	chl, cb	rubble, broken	sheared/beds @ 70	py 1-4%	foliated, mix dk gn-lt gn seds
160	165.9	6b	gn	2	chl	mudstone	beds60-70	py 1-4%	soft gn fol seds, smeared py?
165.9	167	gouge	gn	2	chl, cb	mudstone	contact CA 30-40, gouge	py 3-5%	gouge in mudstone unit

Silver Spruce Resources Inc.

Project: Big Easy					**Northing**	**5347880**	**NAD 27** **AZM: 095**	**Core Size: NQ**	**Start: Apr. 7/11**
Drill Hole No.: BE-11-04					**Easting**	**709682**	**Elev: 115 m** **DIP: -48**	**Logged by: Adree DeLazzer**	**Finish: Apr. 10/11**
Contractor: Cabo Drilling					**Length (m)**	**167**	**Samples: 121 (619716-836)**	**Reports: 201130034,36,39**	
								Survey Tools: Rhino GPS, Multishot @ 30m intervals	

From (m.)	To (m)	Rock Type	Colour	alt Degree	alt Type	Texture	Structure	(%) Mineralization	Comments
0	9	OB							
9	12	6c	gy, gn	2	sil, hem	vis clasts	QV's CA 10	py - 3-5%, to 3-7% - f diss, stgs	sil congl; clasts visible; wh-gy QV's, w/ gn (chl?), f. orange red clasts; LC - 1 m soft chl alt congl
12	15	6c	gn gy	2	sil	clasts not vis	bedding CA 70-80	py - 1-5%, to 3-5%, strs/diss,	intense sil alt congl, vis clasts, loc chl. Alt; jasper in QV - vns oblique to CA, soft @ LC
15	24.4	6b	gn	2	chl	vis clasts	chl alt, soft, beds CA 70-80	py - tr to 1%, diss	int chl alt, gn, soft w/ graded beds CA 70, coarsening up beds, some patchy sil sects
24.4	25.6	3c	gy, dk gn	1	chl, cb	cb vns	msv	py - tr diss	cb vns in fresh mafic dike, broken
25.6	27	6b, 6c	gn, dk gy	2	chl	bedded, vis clasts	beds CA 70-80	py - weak diss, euhedral	intense chl w/ hem rich sect. in soft, alt congl; beds? CA 70-90; hem - mass over 0.1m
27	29.5	6b	dk-pale gn	2	chl	beds,vis clasts	beds CA 70	py - tr-1%, vns/strs to 1cm	sim to prev, very strong chl - wh powder clay alt zone but no hem, dis py, some euh
29.5	32.5	6c, 6b	gn, gy	2	sil, chl	var alt, clasts	beds CA 70-80	py - 3-5%, diss / strs	patchy alt, sil to chl, clasts part visible; chaotic QVs, banded; contacts CA 70; clear sil mtx?
32.5	40.5	6c	pale-dk gy	2	sil	haotic, multi qtz vn	var alt, vns, py strs CA 70	py - strs, in vns from 39-40.5	chaotic; sil w/ abund QVs banded/strs w/ py; soft chl alt sects; f pk strs in soft zone
40.5	42.6	6c	pale blue-gy	3	sil	v. fine gr, sil	beds CA 70, QV's Xcutting	py - 1-5%, strs/repl, ms >10%	sil congl; beds CA 70; QV's, clasts gone - some sect, some blue, alt flds,
42.6	43.5	6c	variable	3	sil	QV's, beds	beds CA 70, QV's, chalcedonic	py - tr-2%, repl clasts	sil congl; bedding CA 70;
43.5	56.3	6c	gy-dk gy	3	v sil	beds, vis clasts	beds CA 70, QV's CA 10-30	py - 1-5%, strs; fluorite (purple)	QV's chalcedonic, bnded w/ var colours, CA low angles; alt contact?, wh hrd, orange-red clasts
56.3	59.5	6c	gy-dk gy	3	sil	cherty, broken	fract set, fine chalcedonic vns	py - 1-5%, diss/strs	bx, blocky, cherty, clasts not vis
59.5	64.7	6c	dk gy - lt bn	2	sil	bedded, vuggy	ds CA 70-80, var QV's, blue, cher	py - 3-5, to >5%, str/mtx/repl clasts,	sil congl; vis clasts, beds, vuggy sect, cherty, ded qtz vns, str py
64.7	65.3	qtzvn	var colours	3	sil	bnded, poss chal	vn near vertical	py 1-3% in str/vns	bnded chal looking qtz vn near vert, py in strs
65.3	68.4	6c	gn, pk	1	sil	QVs, soft chl sec	h-gy QV's, purple fluorite, bx-2 l	py - 1-3%, diss/strs	v f diss sulph, ff in sil congl - clasts visible, buff-gy chert w/ vugs, bx QV's
68.4	75	6c	gy gn	2	1	vis clasts	beds CA 70	py, strs/vns, repl clasts, 1-3%	sil congl, lrg clasts, bedded, gy blue qtz, blocky, vuggy,
75	76	6c	gy	2	sil	cherty, no clasts	some bx, blocky sect	py - 1-3%, rare vns	cherty unit, loc bx-2, py in vns rare, some blue gy qtz
76	79	6c	gn gy	1	sil	lrg clasts, rd bn	chal vns @ 10-30	py - 1-5%, to > 3%, rep clasts/strs	sil congl, clasts vis, slics on joints, cb in strs, lrg bn rd clasts
79	79.5	qtz vn	gn gy	3	sil	bx	bx, contacts parallel to CA	py - tr-2%, strs	bnded qtz vn, bx, vuggy
79.5	85.1	6c	gy gn	1	sil, chl	clast vis	blue gy qtz, alt clasts, var alt	py -1-5%, diss/strs	sil congl; vis clasts, beds CA 60-70; clasts alt; gy blue, patchy alt; chl rich sects
85.1	87.5	6b	light gn gy	2	chl	soft, clasts vis	beds CA 80	py - 3-7%, vns/strs/diss	sericite and chlorite alteration - soft light gn to gy conglomerate - clast visible graded beds

Silver Spruce Resources Inc.

Project: Big Easy					**Northing**	**5347880**	**NAD 27** **AZM: 090**	**Core Size: NQ**	**Start: Apr. 11/2011**
Drill Hole: BE-11-05					**Easting**	**709560**	**Elev: 115 m** **DIP: -50**	**Logged by: Adree DeLazzer**	**Finish: Apr. 17/2011**
Contractor: Cabo Drilling					**Length (m)**	**239.0**	**Samples: 108 (619837-944)**	**Reports: 201130040, 41**	
								Survey Tools: Rhino GPS, mutlishot @ 30m intervals	
From (m.)	To (m)	Rock Type	Colour	alt Degree	alt Type	Texture	Structure	(%) Mineralization	Comments
0	12	OB							
12	44	6a	rd	0	hem, sil, cb	clast vis	beds CA 80		red sandstone, fine cb str and on joints, beds near vert., var weak sil, mostly all sndst.
44	45.7	6c	pale gy, y	2	sil, cb	rare QVs, bnded			bleached, rare bnded qtz vns (light pk, wh to rd), cb on joints and in strs.
45.7	53.5	6a	rd	0	hem, cb, sil	clast vis	beds @80		red unaltered conglomerate and sandstone, beds, cbstrs, minor qtz
53.5	554.7	6b	gn gy	1	chl, cb	clast vis	beds @80		chl alt congl and sndst, bedded, poss shearing?, cb mod to str, not sil
54	65	3c	drk gn	1	chb, chl	gr, hom., minor qtz+cb	UC @ 40 to CA, vns @ 20 to 40	tr py, mg	mafic dike, calcite vns, looks to be @ 20 to 40 CA, from 62.7 to 65 mafic ass w congl
65	65.9	6c	gn, y, gy	1	sil?, cb	rare qtz+cb vn	LC @ 20	tr py	seems to be silicified, gn chl? and yellow strs
65.9	67.3	6a	rd	0	hem, cb, sil	cb str, beds	sheared @ 45 to Ca		red hem sndst, sheared or beds @ 45, cb in str
67.3	69.8	6c	gn, gy	1	sil	clast vis		tr py	sil congl, clasts vis, no beds
69.8	72.7	6a	rd	1	hem, sil	clast vis, beds	beds @80		red bed, starting to be silicified, bedded
72.7	76.4	6a, 3c	gn, rd	1	cb, sil	assim, beds	beds @80	tr py to 2% in beds of congl, tr dis in dike	mix of rd bed and mafic dike, loc sil, py becoming more abund dis,
76.4	79.2	6a, 6c	rd, gy	1	sil	sheared?	beds/shs @ 70-80	py tr to 3%, tr cpy loc	mostly rd unalt sndst, beds, becoming sil near LC, clasts look sheared, py becoming more abund.
79.2	80.2	6b	wh, gn	2	chl	bx?		py - 3-7%, f diss/ repl clasts	pervasive chl, poss ser, kao alt; clasts gone; some mudstone
80.2	84.1	6c	gy, gn	2	sil/chl	vis clasts;	chaotic, var alt	py in strs, loc 3-7%, dis 1-5%	mg; vis clasts; 1m sects of chal qtz - pk-bge-wh mottled app; chaotic vns, no orient; soft (chl) alt
84.1	85.2	6c	blue, gy	2	sil	bnds in qtz vns	chaotic, var alt	py - 5-10%, QVs/diss, strs CA 70	blue gy, fg; clasts barely vis., sil rich; bnds in qtz follow py, vns abund and chaotic
85.2	86.2	6b	gn	1	chl, sil	clast vis	slics common, sh @ 45 to CA	py - 3-5%, strong @ UC, f diss	gn gy chl alt cong, str py, alt flds, bed/sh @ 40-50
86.2	90	6c, 6b	6c, 6b	2	sil, chl	chaotic, veined	sheared in chl rich sects CA 70	py - tr-3%, more near QVs, chl alt	var alt, patchy chl in sil congl QVs, multiphase?, shearing in chl alt sects
90	93.2	6b	gn	1	chl	vns, clasts vis		py - 2-5%, diss/strs	chl alt, clasts vis, alt flds, some QVs CA 40-70
93.2	100.7	6c	drk bn, gy	2	sil	clasts vis, chaotic vns	slics on joints	py - 1-5%, 3-7%, vns/diss, graphite	sil congl, dk bn, clasts vis, QVs CA 20-40; blue clasts
100.7	105.1	6c	var colours	3	sil	QVs common		py - tr-2%, poss graphite, bk met	v qtz rich, chal looking vns, var colours, peach to blue gy colours in QVs
105.1	110.1	6c	bn, gy	2	sil	loc chaotic QVs	loc int vn bx, bx QVs	jasper 107 to 108.6m, rd bn rhins, py - 3-5%, 1-5%	similar to qtz bx in Hole 3, in sects 10cm-0.5 m, mostly gy fg; v sil; clasts part vis w/ bk-blue met

Silver Spruce Resources Inc.

Project: Big Easy	Northing	5347880	NAD 27	AZM: 090	Core Size: NQ	Start: Apr. 11/2011
Drill Hole: BE-11-05	Easting	709560	Elev: 115 m	DIP: -50	Logged by: Adree DeLazzer	Finish: Apr. 17/2011
Contractor: Cabo Drilling	Length (m)	239.0	Samples: 108 (619837-944)		Reports: 201130040, 41	
					Survey Tools: Rhino GPS, mutlishot @ 30m intervals	

From (m.)	To (m)	Rock Type	Colour	alt Degree	alt Type	Texture	Structure	(%) Mineralization	Comments
110	130.5	6b	gn, gy	1	chl	fol	sheared, fol @ 60-70, UC @ 45 to CA, LC destroyed	py smeared follow fol, tr to1%	sheared mudstone, poss mylonitic, loc weakly sil, smeared py, rare qtz vns, rare cb
130.5	134.5	flt bx, 6b	bt gn-gy	3	chl?, ser?	sheared?, bx	int shearing @ 40-45 and a second @ 20, bx 2 to 3	tr py	int bright gn (ser, pyrop) qtz bx, sheared @ 45 and 20, bx2 to 3
134.5	137.6	flt bx, 6b	gn, gy	3	chl, sil	chl schist w qtz bx	flt contacts @ 20	v fine diss py	qtz flt bx, chal looking qtz frags in chl schist matrix, flt contacts vis @ 20 to CA, tr py
137.6	140.7	6b	gn, gy	2	chl	schist, fol	fol @ 70	smeared py, tr to 1%	chl schist to mudstone, int chl, fol @ 70 to CA, smeared py, near LC v int alt?, friable
140.7	143.3	6c	drk bn, gy	2	sil	clast not vis	loc chal vns, var oreint	py tr to 2%	drk bn, sil, clasts not vis., loc chal looking vns, poss strs of bk metallic
143.3	165.7	6c	buff beige	3	sil	cherty, clasts not vis, loc vuggy	fractured, blocky, chal vns rand oreint	py infilling fract w blk metallic?, tr to1%	cherty, clasts not vis, loc vuggy, v poor RQ, better after 158m, veining @ 163-166m; dk strs, fract, vn bx text CA 30-40; slickensides; graphite; clasts become vis nr LC
165.7	170.8	6b?, sh	drk gn, lime	3	chl, ser?, sil	var alt, loc perv.	fol CA 70; lt pk, bge, gn clasts; blue qtz eyes; mylonitic	py - tr-1%, some euh	gn alt (pyrop)? In a qtz bx?, pk adularia?, mica fish?, mylonitic, acicular pk xtals, more sil to LC; fol @ 70 where vis, but var; alt is pervasive
170.8	174	6b, 6c	gy to lime gn	3	sil, chl, ser?	chaotic, var alt, sh	fol @ 70 where vis but it's wavy	py - tr, pk, acicular xtals	v chaotic, var alt, sil and chl/ser?, pk to beige; clasts part vis; fol well dev in sects
174	175	6b	gn, lime gn	3	chl, ser	per alt, sh, mylonitic	mylonitic, clasts w tails - two directions - 70-80 and 50-60	py - tr-1%, repl clasts/diss	perv chl, poss ser alt, two dir of movement, mylonitic, py dis and repl clasts
175	178	6c	beige to gy b	3	v sil	cherty, bx-1 to 2	vn bx textures, fol to mylonitic @ 40-70	py - 3-7%, f diss	cherty; bx-1 to 2; mylonitic, sheared qtz clasts, fol CA 70, shallows to LC
178	192.5	6c	beige to pale	3	sil	cherty	loc bx text like above	py abundant 3-7%, poss bk met	cherty; chal vns, no clasts vis, loc bx w/ f diss py; vuggy; weird bx text, gradational LC; blk coating on fract, rare vns
192.5	195	6c	org, bn, gy	3	sil	qtz vns, mottled	fract, bx loc	py in str, loc coarse and dis 1-5%	chaotic looking w minor chal vns in v sil multi vn unit, weakly bx, poss adularia?, bk met strs
195	197.2	6c	org, bn, gy	3	sil	recryst?, bx	v bx, fract, vuggy and sugary qtz	v fine py diss throughout, 1-3%	sim to above but more int bx and fract, in vuggy sect, sugary qtz, hard to see textures
197.2	199.2	6b	bright gn, y,	2	chl	bx, sheared	shearing @ 50-60 to CA	poss opal?, adularia w bk rims, tourmaline	gn alt chl and yellow gn (pyrop)? In a qtz bx?, fol?, xtals look like opal and adularia have bk rims
199.2	202.6	6c	drk bn, beige	3	sil	chaotic vn bx	alt contacts @ 60, vn bx @ 30	py - 1-3%, euh	alt contacts; bn to bge; v sil; chaotic, sheared; xtals - opal / adularia?, w/ rims
202.6	213.9	3c	drk gn, gy	1	cb, chl	hom, cb vns, strs	fg @ UC, flt @ 203.5 CA 20-30	py, pyr - tr-2%; on LC, coarse euh	mafic dike, calcite vns, CA 20 to 40

Silver Spruce Resources Inc.

Project: Big Easy	Northing	5347880	NAD 27	AZM: 090	Core Size: NQ	Start: Apr. 11/2011
Drill Hole: BE-11-05	Easting	709560	Elev: 115 m	DIP: -50	Logged by: Adree DeLazzer	Finish: Apr. 17/2011
Contractor: Cabo Drilling	Length (m)	239.0	Samples: 108 (619837-944)		Reports: 201130040, 41	
					Survey Tools: Rhino GPS, mutlishot @ 30m intervals	

From (m.)	To (m)	Rock Type	Colour	alt Degree	alt Type	Texture	Structure	(%) Mineralization	Comments
213.9	216.7	6c	org, gn, beig	3	sil	fol, chaotic vns, bladed qtz	fol @ 40-50, some QVs follow	py - tr-3%, some in QVs, diss	chaotic; minor chalcedonic vns in v sil multi vn unit - sheared?, sim to 192-197, 199-202.6; peach bladed qtz
216.7	217.8	6c	gy, wh, bk	3	sil	cherty w qtz vns	fract @ 10-30, vns @ 30-50	py dis throughout 1-3%	cherty w/ QVs; wh-bk bands; some chalcedony frags; fractured; vn bx contacts CA 40-50
217	221.9	6b	gy gn	1	chl	bedded, fol	beds/fol @ 60-70, UC @ 40-50	smeared py tr-1%	mudstone well fol/bedded, smeared py, loc weakly sil, cb in vn @ low angles
221.9	223.5	6c	gy	1	sil	clasts vis, beds	cb vns @ 40-50, beds @ 60	py tr	weakly sil congl - gy w clast vis, no notable qtz vns
223.5	226	6b	gy, gn	1	chl	fol/beds	beds @ 60	smeared py tr	mudstone, cb vns @30-40, finely laminated
226	234.6	6b, 6c	gy, gn	1	chl, sil	fol/beds	beds @ 60	py v rare	weakly sil congl, clasts vis, beds, no py, pale gn alt loc
234	239	6b	gy, gn	1	chl	fol/beds	beds @ 60	smeared py	mudstone, like prev

Silver Spruce Resources Inc.

Project: Big Easy	Northing	5348419	NAD 27	Azimuth: 090	Core Size: NQ	Start: Apr. 19/11
Drill Hole: BE-11-06	Easting	709858	Elev: 131 m	Dip: -50	Logged by: Adree Delazzer	Finish: April 24/11
Contractor: Cabo Drilling, Springdale	Length (m)	359	Samples: 266 (619838-620000, 721001-210)			Reports: 201130043 (2); 201130044; 201130045
					Survey Tools: Rhino GPS; multishot @ 30m intervals	

From (m.)	To (m)	Rock Type	Colour	alt Degree	alt Type	Texture	Structure	(%) Mineralization	Comments
0	12	OB							
12	16.5	6a	red	0		bedded	beds 45 CA, graded		sst: loc sil
16.5	17.6	3c	gn gy	1	chl, cb, hem	homogeneous	poss flt/sh str; gouge @ 20	py - tr to 1%	alt dike ? - chl alt? cb vns/strs, sheared CA 20
17.6	25.75	6a	red	0		bedded	bedding CA 40-50		sst / cgt; loc alt; becomes silicified
25.75	27.4	6c	red, gn, gy	1	hem, cb, sil	some clasts visible	shearing/fol @ LC	py - rare in stringers	alt congl;
27.4	28	flt	gn, red	2	hem, cb, sil	slickensides, gouge	shear CA 80 10-20	py - tr to none	shear / fault; mod alt; weak bx
28	32	6c	gy-dk gy	3	sil, minor cb	clasts not vis, bx	bx - less to LC	py - tr to 1% - ff/strs; bk-gy met	LC > 2m; bx v sil - gy cherty;
32	35.2	6c	beige-gy	3	sil	clasts vis locally		py - tr to 1% ff/strs	as above; LC > 1m; locally - congl w/ vis clasts
35.2	37.7	3c	gn	1	cb, chl veins/ff	homogeneous		py - tr	poss dike; not sil;
37.7	49	6c	gy-dk gy; wh	3	sil	no clasts vis; broken	RQ - poor; low angle fractures	py - tr	cherty; not bedded; LC > 1m @39 and 41m; v blocky, loc bx-2, prom. slickensides
49	52.7	6c	gy-buff	2	sil	clasts vis, RQ better	as above w/ better RQ, < alt; fract @ 10-30	py - 1-5% - strs	chert; broken, not bx; some bl gy qtz; alt flds, minor slicks, lg QV's near LC - gn mottled app
52.7	63.1	6c	gy, dk bn	2	sil	clasts visible	QV's; some chal, some lg up to 1m, loc banded, some @ low	py - strs, 3-7%	sil congl; clasts vis; chal QV's, some banded, pale gn, pk, wh to gy; fractured locally, up to 1m
63.1	64.2	3c	gy, gn	1	chl, cb, hem	broken, rubbly	weak slicks, poor RQ	py - rare diss	mafic dike; blocky
64.2	65	6c	gy, wh, bl	2	sil	clasts vis	var colours of qtz in vns	v py rich, 5-15%, in vns, and repl clasts	var colours of qtz, v py rich, some clasts vis, py in vns and repl clasts
65	95.6	6c	bn, gy	2	v. sil	fg, clasts vis	68-71 > 1m LC, rubble zone	py - 3-5 to 10%, strs/ff; graphite / bk met ff	most clasts not vis; chalced QVs, CA 30; minor cb ff; alt contact / beds CA 30-40; LC / rubble 68-71m, chl more abund nr LC
95.6	105.4	6c	gy	3	sil	cherty to chal QVs	QVs CA 40	py - 1-5, to 3-7%, vns/strs to 5cm; jasper	cherty to chalced QVs, w/ py, distinct clasts, jasper / felsic vol clasts; jasper in QVs w/ py; banded, fract QVs
105.4	116	6c	beige,gy, gn, pk	3	sil	clasts vis, fg	chaotic, beds CA 40-60, alt contacts CA 30-40	py - 3-10%, strs/vns, beds CA 20	sim to above; chalced QVs; clasts rarely vis - sects > 0.5m: chl rich sect; chaotic sect; some bl pk qtz / purple tinge /alt; Xcutting, QVs common, multi phase vns?
116	118.2	6c	purple, gy, gn	2	sil, ch	clasts vis		py - 1-3%, f diss	sil alt congl, clasts vis, purple tinge/alt?, gn chl alt, v sil; some vns, Xcutting, var colours; QVs var colours
118.2	118.8	3c	gn, gy	0	chl	hom, fine, soft	UC CA 30	py rare	mafic dike?, soft, chl alt, rare py
118.8	120	6c	beige, gy	3	sil	most fg,	Xcutting QVs, some purple, alt	py - 3-5% between vns	sim to 105.4 to 116m, QVs common
120	131	6c	beige to gy	2	sil	clasts vis incl rip ups	sm cherty QVs CA 30-80	py - 1-3%, strs/repl clasts	sil congl, clasts vis, some rip up clasts; bn clasts; rare QVs; beds CA 40, grains look aligned?
131	132.5	6b	y, gn, gy	2	chl	clasts vis	grad contact into more chl alt congl, clasts looks sheared @ 40	distinct rd gn to bl gn clasts, py in vns/strs and dis, tr to 2%	chl alt congl, grad contact, chl on joints, some distinct clasts, looks sh @ 40
132.5	135.9	6b	gn, gy	2	chl	clasts vis, fg clasts	sh/bedding @ 40-50 to CA	py tr to 1%	sim to above but fg, bedded/sh, alt flds prom, sil increasing to LC
135.9	138.7	6c	gy, beige	2	sil	clasts vis	no beds	py 1-5%, loc 3-7%, dis/strs	sil congl, clasts vis, some dist bn clasts, few QVs
138.7	140.8	6b	gn, gy	1	chl	clasts vis	loc sh @ 70-80	py 3-7%, euh/vns/strs	alt pebble congl, chl, soft same as 131 to 132.5m
140.8	151.3	6b	gn, gy	2	chl	fg		py - to 2%, diss	fine gr chl rich mudstone, cb vn/str, becoming more prom near LC

Silver Spruce Resources Inc.

Project: Big Easy	Northing	5348419	NAD 27	Azimuth: 090	Core Size: NQ	Start: Apr. 19/11
Drill Hole: BE-11-06	Easting	709858	Elev: 131 m	Dip: -50	Logged by: Adree Delazzer	Finish: April 24/11
Contractor: Cabo Drilling, Springdale	Length (m)	359	Samples: 266 (619838-620000, 721001-210)		Reports: 201130043 (2); 201130044; 201130045	
					Survey Tools: Rhino GPS; multishot @ 30m intervals	

From (m.)	To (m)	Rock Type	Colour	alt Degree	alt Type	Texture	Structure	(%) Mineralization	Comments
151.3	158.2	6b	gn, bright gn	3	chl, ser	schist, friable	sh CA 40-50, CA 10-20 nr LC	py - 5-15%, vns/strs/euh, ms >1cm	int chl, ser?, alt, sheared, clasts stretched CA 40-50; friable, loc qtz rich sects; 153-154.6, < alt / sheared, mdst sects
158.2	160.3	6b, bx	bright gn, gn	3	chl, ser	qtz bx	shearing CA 10, gouge near LC	py - tr	chl, ser, qtz bx; intense shearing w/ gouge; increase in qtz to LC, var colours
160.3	162.6	6b, gouge	gn	3	chl, ser	gouge w/ qtz	shearing along CA, some CA 40	py - tr	wavy bed, int shearing parallel to CA, some @ 40, qtz clasts look rotated, unconsolidated clay in gouge
162.6	163.1	flt	gn	3	chl	chl mud w qtz bx	one @ 30, second @ 10	py - tr	flt zone, two @ different angles, qtz bx w mud
163.1	166.4	6c	buff/bge-pch-gy	3	sil, chl	qtz bx	bx 1 to 2	py - 3-5%, ff w/ bk met/graph	qtz bx; similar to DD3, chl ff more than py;
166.4	167.9	6c	pch to bn	3	sil, chl	f-mg qtz	fract w chl ff	py - 1-3%, graph ffs?	similar to above; less bx
167.9	171	6c	lt pch-buff bge	3	sil, chl	cg qtz	qtz bx-2	py - 1-5%, gy met ff	sim to above but more bx
171	172	6c	lt pch-buff bge	3	sil, chl	finer gr, qtz bx	loc bx-1, minor fract	py 1-5% infill fract	sim to above; fg, less bx; weak fract; mudst seams
172	177.1	6b	gn, gy	2	chl, cb	weak bx	contacts CA 40; fract CA 10-20	py-tr-1%, gy met/py in QV CA 90	mdst; chl alt, cb vn, f, bge, alt flds xtals; speckled app, fract/minor bx;
177.1	178.8	6c	wh, gy	3	sil	qtz bx, gouge	bx-3, fract CA 30-40	py - 1-5%, strs; gy met?	qtz rich bx, loc well dev, gouge, fract CA 30-40
178.8	180	6c	beige to pk	3	sil	bx	bx-2, chl infill	py - 1-5%, ff	qtz bx w chl infill; lt pk;
180	181.5	6c	wh to beige	3	sil	bx	bx-2 to 1	py - tr, gy met ff	qtz bx; sim to hole 3; few fract jasper xtals on fract?, fg in bx-3 sect
181.5	189.4	6c	beige	3	sil	weak bx	var angles - vns / fract CA 30-50	py - 1-5%, diss, 3-7%, ff	beige qtz clasts; weak bx; wh QVs w/ chl - var angles, most oblique; fract CA 30-50; bladed qtz;
189.4	190.6	6c	beige	3	sil	wht qtz vns	fract @ 10-20, slics w chl	jasper from 189.4 to 189.8, @ 45 to CA, v py rich 3-7%, overall py	sim to above unit but sect w jasper and int py, not bx, but fract and slics common w chl
190.6	196.5	6c	gy, wh	3	sil	clasts not vis, fract	fract, loc bx-1 to 2, @ 40 to CA	py - 1-5%, mainly in bx	intense qtz (silica), loc bx w/ chl ff; gy-wh qtz; clasts mostly not vis, fract CA 40
196.5	200	6b	gn	2	chl	schist, friable	sh @ 30-40, some @ 10	py - tr-2%	schist, int alt by chl, shearing, clasts look stretched.
200	202.5	6b, 6c	gy, gn, bl, pk	2	chl, sil	var, qtz w chl	sh @ 20-30	py - tr-2%	more qtz rich, chl zones, chaotic, qtz bx sheared, some bl, pk qtz
202.5	203.5	6b, 6c	gn gy	2	chl, sil	sheared, var	sh mudstone w sil congl	py - tr	sheared mudstone, w sil congl, lrg clasts, smaller org bn, clasts, also occurs clasts
203.5	207.1	6c	gy, pk	3	sil, cb	QVs / clasts	var coloured qtz clasts	py - tr-1%, diss	gy-pk; v sil; clasts vis in places, alt; gy sect - f bl-gy qtz, rare dk opaque; chl; f clear QVs, gy-bl w/ cb alt, gn xtals, wh QVs CA 20-30; bn rd xtals, shearing parallel to CA
207.1	208.1	6c	y, gn, gy	2	sil, cb	bx	fract common	py - 1-3%, gy met?	sil congl, clasts vis, py diss, poss pyrop?, adularia, gy met, cb alt
208.1	209.7	6c	gy	2	sil	mg, clasts vis		py tr dis, spec hem	qy sil, most mg, lrg > 10cm, jasper?, spec hem, gy blue qtz, sim to 203.5-207.1
209.7	213.1	6c	gy, light bn	3	sil	fg, clasts vis	beds CA 40	py-tr, weak diss/strs, spec hem	gy congl; clasts most not vis; beds CA 40; cb on joints, f wh QVs CA low
213.1	214.9	6c	gy	2	sil	mg, sh	shear CA 50-60	tr py	med gr congl, clasts vis, sil, org bn clasts, sheared, fine wh str/fract w cb alt
214.9	215.3	6b	gn	1	chl	fg, mudstone	LC @ 45, no bed	rare tr py	mudstone no beds, tr py
215.3	216	6c	pk, beige	3	sil, cb	clasts not vis	weakly bedded @ 50, LC @ 40-50	weak tr py	pk to beige, v sil, clasts not vis, some bk clasts (soft chl), cb vns/strs, weak bedding, shp LC
216	216.6	6b	gn	1	chl				mudstone; not bedded, same as before
216.6	217.9	flt	gn, gy	2	chl	gouge w qtz	bx-2, 3, flt @ 10-20 and 30	tr py	gouge w flt, one at 10-20, another @ 30, some qtz clasts in gouge.
217.9	219.5	6c	gy, wh	3	sil	qtz bx	bx-2, 3, flt 10-20 and 45	py 1-5%	qy wh qtz bx w flts @ 10-20, 45 to CA, shp LC

Silver Spruce Resources Inc.

Project: Big Easy					Northing	5348419	NAD 27	Azimuth: 090	Core Size: NQ	Start: Apr. 19/11
Drill Hole: BE-11-06					Easting	709858	Elev: 131 m	Dip: -50	Logged by: Adree Delazzer	Finish: April 24/11
Contractor: Cabo Drilling, Springdale					Length (m)	359	Samples: 266 (619838-620000, 721001-210)			Reports: 201130043 (2); 201130044; 201130045
									Survey Tools: Rhino GPS; multishot @ 30m intervals	

From (m.)	To (m)	Rock Type	Colour	alt Degree	alt Type	Texture	Structure	(%) Mineralization	Comments
219.5	222.7	6c	pk, gy	3	sil	qtz bx	bx 1	py 1-3% infilling frac	qtz bx but w more pk, adularia, loc v int bx, py, chl infilling fract
222.7	223.6	flt gouge	gn gy	2	chl, sil	gouge w qtz	flt @ 40-50, 10-20	py tr to 1%	fault gouge, chl rich w qtz clasts, shs
223.6	226.3	6c	gy	2	sil, chl, cb	clasts vis	loc bx, shp LC @ 30	dis tr py, some spec hem	sil congl, clasts vis, cb strs, some chl loc, weak bx
226.3	229.6	6b	gn	1	chl	clasts vis	fract @ 40-50, clasts look sh	py tr	friable, chl alt congl, clasts vis, sh
229.6	232	6b, 6c	gn, gy	2	chl, sil	qtz bx, gouge	fract @ 40-50, some @ 10	py in fract 1-3%	qtz bx w/ int chl gouge; broken, fract CA 40-50, some CA 10, cb alt strs
232	241	6b, 6c	gn, gy	1	chl, sil	clasts vis, ksp		py - tr-3-5%, diss	pebble congl; var clasts, ksp, mdst - sm secs < 20cm
241	246.6	6c, 6b	gy, wh, pk beige	3	v. sil, chl	loc bx, vugs	bx, fract	py - 3-5%, gy met?	bx, var colours, ksp?, mudst up to 0.5m
246.6	271.9	6c	gy, wh, dk gy	3	sil, chl - patchy		incr vns towards LC,	py - 3-5%, vns/diss	pebble congl; clasts vis, QVs cherty/chalcedonic, banded; bx w/ gy-bk qtz; chal vns to LC; bn clasts fel vol?, fractured, vuggy;
271.9	279.1	6c	var colours	3	sil	qtz bx, var colours		py - 1-2%, diss, tr cpy?	qtz bx, vuggy, bladed qtz, poss adularia, yellow xtals
279.1	284.3	6c	var colours	3	sil	qtz bx, vuggy	bx more dev compared to above	py - tr	sim to above but more bx; poss adularia
284.3	285.2	6c, 6b	var colours	3	sil, chl	qtz clasts in chl mtx	int flt bx	py - tr	
285.2	286	gouge	gn	3	chl	gouge w qtz		py - tr	chl gouge w rare qtz frags
286	289.2	6c, 6b	gy, gn	3	sil, chl	qtz bx w chl	qtz bx well dev	py - 3-5%	qtz bx w chl infill, well dev, v py, loc >5%
289.2	289.7	gouge	gn	3	chl, sil	gouge w qtz	mostly all gouge, UC @ 10-20	py - tr, f diss	mostly all gouge w rare qtz, dis py
289.7	299.5	6b	gn	2	chl, cb	mudstone	sh @ 30, fol 50-70	py to >3%, smeared	mudstone, fol/sh @ 30 w smeared py, cb strs
299.5	300.7	6b	gn	3	chl	almost gouge	sh plane @ 20, unconsolidated	py - tr, smeared	almost a gouge, unconsolidated, sh @ 20
300.7	312.2	6b	gn	2	chl, cb	bedded after 306 m	smeared py, bed/fol @ 70	py - 1-2%, diss, tr cpy?	mdst; abund cb str/vns; f bk phenos; some beige sil sects
312.2	312.7	6b,gouge	gn	3	chl, cb	gouge w mudst	flt @ 10-20; LC 0.5m @ 331	py -tr-1%	mudstone w gouge, unconsolidated, 10-20 to CA, weak py
312.7	334	6c	wh, gy, pk	3	sil	qtz bx	gouge @ st CA 20; shears @ 323 CA 30 to 40, @ 325 CA 60; alt/bx	py - 1-3%, ff, cpy? graph	qtz rich bx; pk adularia?, gouge < 10cm, sheared contacts CA 30-50; vuggy
334	334.2	6b	gn	2	chl, ser		contact @ 30-50	py - tr-1%	strong chl, ser alt, shp contact
334.2	337	6b	gn	2	chl, sil, cb	mudstone w qtz frag	gouge to mudstone w bx qtz	py - tr-1%	mudstone to gouge w qtz frags, cb al, minor hem
337	343	6c	gy, gy	1	weak-mod sil	clasts vis, bedded	beds CA 60-70	py - 1-3%, strs along beds	congl, bedded; bn clasts sheared?, strong cb alt
343	359.5	6b	drk gn, gn	1	chl, rare sil		beds CA 60-70	py - 3-5% in mdst, gen tr-1%	mudstone/congl; bedded, faulted / displaced?, cb alt common
359.5	262.5	6b	gn gy	2	chl, sil	clasts vis	shear CA 20	py - tr	congl; weak alt - most chl, sect sil; rd bn clasts, poss hem alt, sm sh CA 20
262.5	365	6b	gn gy	1	chl	mudstone	beds CA 60-70	py - tr	mudstone - sim to previous
	365	EOH							

Silver Spruce Resources Inc.

Project: Big Easy	Northing: 5348591	NAD 27	AZM: 090	Core Size: NQ	Start: Apr. 25/11
DDH: BE-11-07	Easting: 709950	Elev: 116 m	DIP: -50	Logged by: Adree DeLazzer	Finish: Apr. 30/11
Contractor: Cabo Drilling	Length (m) 305	Samples: 204 (721211-721414)		Survey Tools: Rhino GPS, multishot @ 30m intervals	Reports: 201130047 (2); 201130051; 201130052

From (m.)	To (m)	Rock Type	Colour	alt Degree	alt Type	Texture	Structure	(%) Mineralization	Comments
0	3	OB							
3	4.5	6c	lt gy	3	sil, oxidized	sugary, vuggy	broken	py - 1-2%, diss, strs	oxidized, v sil; sugary qtz; minor vugs; v blocky
4.5	7	6c	gy	2	sil	clasts vis	broken	py - tr to 1%, diss	fg sil congl; clasts vis; no prom vns
7	8.5	6c	dk gy	3	sil	cherty	broken	py - tr diss	
8.5	11	6c	bge-dk gy	2	sil	clasts partly vis	broken, bedding CA 50	py - strs 1-3%	
11	11.5	6c	drk gy, bn	2	sil	clasts vis	blocky	py in strs 3-7%	some blue xtals ?
11.5	13.9	6c	bge-dk gy	2	sil	clasts partly vis	blocky, beds @ 50	py in str 1-3%	same as 8.5-11
13.9	14.4	6c	lt gy-wh	2	sil	clasts vis, bedded	beds CA 50-60, broken	py - 1-2%, diss, strs	lt blue, fg qtz; cheryy vn - bnded, dk beds in unit
14.4	21	6c	bge-gn	2	sil, chl	clasts vis, bedded	beds CA 50-60, broken	py - 1-3%	bedded; banded to bx QVs, w/ chl; fg to LC; alt flds
21	33	6c	gy	3	sil	cherty QVs	some vns bx, banded	py - 3-5%, to 3-7%, vns, strs	bx cherty; v sil; chal QVs w/ py strs; wh-gy, gn; cb strs; more vns after 26m
33	35	6c	dk-lt gy	2	sil	vns, dk bk rims		py- sts, ff - 1-3%	fg; sil; massive
35	44.5	6c	dk-lt gy	3	v. sil	QVs	bx near LC	bk-gy met ff ?, py - 3-5%	qtz rich; some orginal clasts, ang / alt w/ py; vns lt-dk gn gy; bx esp to LC
44.5	46.5	6c	dk bn, gy	3	sil	QVs, clasts not vis		py - 5-15%, f diss, vns	QV w/ blue, var. colours
46.5	50.7	6c	blue, gy	2	sil, cb	bedded		py - strs, repl clasts, 1-5%, to 3-7%; increases to LC	blue gy; bedded, congl; clasts vis; cg wh/gy equant xtals w/ f blue-gn xtals; minor cb strs;
50.7	63	6c	gn gy	2	sil, chl	clsts vis, alt; QVs		py - near vns 3-7%, 3-5%	alt congl; clasts vis; yellow strs, alt flds, some chal QVs; clasts alt - chl; matrix v sil esp nr LC
63	64	6b	gn gy	2	chl	sheared	shear parallel to CA	py - vns CA 60, 5-15%	sheared chl, alt
64	79.5	6b,6c	gn, gy, bl	2	chl, sil	patchy alt, beds?	beds CA 60-70, 10-30?, shear CA 10-20	py 3-7%, loc 5-15%, replaces clasts, more in chl sect.	bl qtz, f-mg; poss bedding contact?; distinct orginal bn clasts esp in sil sect; vn @ 74m w jasper, poss hem?, most wh gy w/ py bnds
79.5	87.1	6b	gn, gy	2	chl	clasts vis, bedded	beds CA 40-50	py - diss 3-5%, loc > 10%	alt (chl) congl to mudstone
87.1	89.6	6c	pale gy-gn	2	sil, chl	clasts vis, bedded	beds CA 40-50	py - 1-3%	sil alt, w/ chl; bedded w/ frag QVs, weakly bx, bl qtz @ 88-88.8
89.6	98	6b	gn-gy	2	chl	clasts vis, bedded	beds CA 40-50	py - diss 3-5%, loc > 10%	same as 79.5-87.1
98	106.4	6c	gy	3	sil	loc qtz bx	loc bx-2	bk met, py ff, py - 3-5%	v sil, Q bx w/ bk met / py ff; cb strs, 103m jasper; calcite on joints
106.4	108.5	6c	bn	2	sil	QVs		py - 5-15%, to > 20% w/ jasper vn	sil; jasper in QVs
108.5	118.2	6c	gy	3	sil	rare QVs, loc bx	loc bx-2	bk met / py ff; py - 3-5%	sim to 98-106.4m, not as bx; sil but clasts vis
108.5	119	6c	blue, gy	3	v. sil	matrix sil		py - 3-10%, loc > 15%, str/repl clasts	blue xtals dom; hard; matrix clear silica
119	125	6c	bge-gy	3	sil	bx qtz rich	broken esp 121-125	py - 3-10 to > 10%, in vns	more bx; silica rich; cb alt, esp @ 121, blocky 121-125
125	130	6c	bge-gy	3	sil	int bx, vuggy	gouge - 128 - 10 cm, broken, LC	py - 1-3%	int bx; vuggy; poor RQ - LC 125-128 > 2m, 128-133 > 1m, gouge; some clasts vis;
130	135	6c	gy-gn	2	sil, chl	clasts vis, bx	broken to 132m, LC @ 130	py - 1-3%	less bx, v blocky; cb alt in strs; clasts vis
135	136.2	6b	dk gn	1	chl	chl schist	sheared parallel to CA	py - tr	chl schist; friable; sheared paralllel to CA; cb vns
136.2	137	6b	gn-gy-bl	2	chl, sil	clasts vis	vn parallel to CA	py - tr	alt congl; one blue QV parallel to CA
137	137.4	6b	gn-gy-bn	1	chl	chl schist		py > 15-20%, mass vn	
137.4	138.2	6c	gn, gy	3	sil	crystalline, v hrd		py - 1-5% in vns/lenses/diss	v hrd; fg; cb vns;

Silver Spruce Resources Inc.

Project: Big Easy	Northing:	5348591	NAD 27	AZM: 090	Core Size: NQ		Start: Apr. 25/11
DDH: BE-11-07	Easting:	709950	Elev: 116 m	DIP: -50	Logged by: Adree DeLazzer		Finish: Apr. 30/11
Contractor: Cabo Drilling	Length (m)	305	Samples: 204 (721211-721414)				Reports: 201130047 (2); 201130051; 201130052
					Survey Tools: Rhino GPS, multishot @ 30m intervals		

From (m.)	To (m)	Rock Type	Colour	alt Degree	alt Type	Texture	Structure	(%) Mineralization	Comments
138.2	155.3	3c	dk gy-gn	1	cb, hem		LC @ 50-60	py - 1-3%, diss / strs	dike w cb alt; hem on joints
155.3	158.6	6c	blue, gy	3	sil	bedded	sharp contact, bedded	py - 3-5%	v hrd; sil congl to sndst; graded beds, chalcedony vns, banded CA 30; bk equant soft clasts
158.6	160	6b,6c	blue, gy	2	sil, chl	bedded, poor RQ		py - 1-3%	sim to above but chl alt more abundant; v poor RQ, rubbly
160	160.6	6c	gy	3	sil	cherty vn	v broken, rubble, poor RQ	py - tr	recrystallized? cherty vn, crystalline
160.6	161.7	6c	gy	3	sil, cb	bx, qtz rich	bx-3 to 1	py - tr	bx sect, less intense near LC; cb, calcite ff
161.7	164	6c	gn, purple	3	sil	clasts vis, bedded		py - 5-7%, in vns 10-15%	v sil, hrd; clasts vis near top; bedded; vn w/ purple nr LC
164	165.4	6b, 3c	dk gn	2	chl, cb	chill margin		py - tr	poss chill margin; strong chl w/ bk chl+cb vn along CA
165.4	179.5	3c	dk gn	1	chl, cb				mafic dike - sim to previous
179.5	180.1	6c	pk-gn	2	sil	vns var colours	contacts - U @ 70, L @ 20	py - tr	sil congl? or sil vn; variable colour - peach, pk, gn, and gy xtals?
180.1	194.2	3c	drk gn	1	chl, cb				mafic dike - sim to previous
194.2	195	6c, QV	blue-pu-gy	3	sil	QV	fractures common	py - tr-1%, repl clasts	most QV; var colours -blue-pu-gy; sect of alt sndst w/ alt flds
195	214.4	3c	dk gn	1	chl, cb				mafic dike - sim to previous
214.4	215.1	6c	rd-bn	2	sil	QV	UC CA 45, LC masked	py to 2%, strs	sil congl; wh-gy-transl QV to rd bn alt congl w distinct clasts; alt flds
215.1	217.8	3c	dk gn	1	chl		LC CA 30 to 40	py - weak diss, str @ LC	mafic dike; fg chill margin; sharp LC
217.8	222	6c	wh-gy-gn	2	v. sil, chl	clasts vis; bnded vns	vns CA 30-40, UC CA 30	py - 3-7%, in str/bnds along QVs; graphite on joints	alt congl; wh-gy-gn-transl QVs, some bnded; frag/bx; loc chl alt; clasts vis in places
222	227.5	6c	beige to bn	2	sil	clasts vis, QVs	bedding CA 50-60	py - 1-5%, repl clasts, strs	sil congl; bk opaque; sm cherty vns w/ jasper @ 223.9, 226.5; wh-gn gy QV w/ py/jasper - 40 cm; chl alt; clasts visible in places, some blue; bedded in places
227.5	228	6c, 3c	bge-gn	2	sil, chl	congl / dike	contact along CA	py - tr	mafic dike; contact along CA
228	231.3	3c	gn	1	chl, cb		UC follows CA	py - tr-2%, repl lge clasts	mafic dike; minor cb vns
231.3	231.6	qtz vn	wh-gn	3	sil	clasts in vn; frag	LC CA 30 to 40	py - rich at LC; gy met; graphite in vn	
231.6	232	6c, qtz vn	bn, rd	3	sil	QV w/ congl, frag	bx/frag QV	py - 5-10%, to > 15%; jasper	sil congl; frag QV w/ jasper
232	232.2	QV w/ jasper	rd, wh	3	sil		LC CA 30-60	py - 3-5%, ms w/ jasper in vn; strs, diss	QV w/ jasper
232.2	232.6	QV	wh	3	sil	banded		jasper in vn	
232.6	233.3	6c	blue, gy	3	sil	clasts vis, QVs	vns CA 20	py - rich w/ bk-gy sulphide; jasper	alt congl; pale blue qtz xtals; QV w/ jasper
233.3	233.7	QV	gy-dk gy	3	sil	cherty QVs	fract		vuggy, cherty w/ jasper
233.7	238.1	6c, QV	wh-gy	3	sil	chalcedonic	vuggy; bx 237-238.1	py - vns/strs, framboidal; graphite; gal/spal; fuchsite in vugs	sim to above; wh-gy chalcedonic vns w/ py, graph, galena, spalerite, v vuggy; fuchsite, bladed qtz
238.1	238.9	QV	wh-gn	3	sil	chal bladed qtz	vns CA 40	py - 1-3%, vns	strong fuchsite; bladed qtz
238.9	240.7	6c	beige	2	sil	QVs; clasts not vis	QVs @ low angles	py - tr-2%, graphite	sil congl to sndst; wh-gy QVs; fuchsite, py, graphite in vns @ low angles
240.7	242	6c	gy	2	sil	QVs common	bx; clasts mostly vis	py - tr	bx w/ QVs, rounded alt textures?, clasts to 242m; less alt beige material
242	245	6c	gy	3	sil	cherty frag vns	vns CA 20-30	py - 1-3%, strs/vns	clasts not vis; cherty vns, loc frag, w/ jasper approx 1cm

Silver Spruce Resources Inc.

Project: Big Easy | **Northing:** 5348591 | NAD 27 | AZM: 090 | Core Size: NQ | **Start: Apr. 25/11**

DDH: BE-11-07 | **Easting:** 709950 | Elev: 116 m | DIP: -50 | Logged by: Adree DeLazzer | **Finish: Apr. 30/11**

Contractor: Cabo Drilling | **Length (m)** 305 | Samples: 204 (721211-721414) | **Reports: 201130047 (2); 201130051; 201130052**

Survey Tools: Rhino GPS, multishot @ 30m intervals

From (m.)	To (m)	Rock Type	Colour	alt Degree	alt Type	Texture	Structure	(%) Mineralization	Comments
245	247.5	6c	gy	2	sil	clasts vis, cherty/chal vns		py - tr-2%, in vns; graphite	sil congl; weakly vuggy, clasts vis; cherty to chalcedonic vns, blue gn (no fuchsite), distinct gn blue clasts w original ? rims
247.5	249	6c	beige	3	sil	fg, clasts vis	minor fractures	py - tr-3%	
249	249.9	qtz vn	gy-pale pu,pk	3	sil	clasts vis?	fractured	py - tr	
249.9	256.9	6c	bn-beige, gn	2	sil	bedded, clasts vis	beds CA 60-70	py - tr-3%	clasts; bedded; cherty to chalcedonic vns, some large esp @ 252 CA 20; beige alt flds
256.9	260	6b	gn, beige	1	chl	clasts vis, cg	beds CA 60-70	py - tr	chl alt congl, cg
260	264	3c, 6b	gn	2	chl	mafic dike / congl		py - 1-3%	mafic dike / chl alt congl; assimilated; v chl rich sects w/ chalcedonic clasts; frag vn
264	266	6c	gy	2	sil	mylonitic?	bx	py - repl clasts, 1-3%; gy met	flow bx?; angular clasts; mylonitic,
266	268.2	3c	gn	1	chl		UC CA 50	py - tr	weakly alt dike
268.2	269	6c	gy	2	sil	bx, vuggy		py - 1-3%; grey met in vugs	well bx, qtz rich; vuggy, fractured
269	271	6c	gy-bge-pk	3	sil	cherty, clasts vis	bnded vns CA 60-70	py - tr-1%, diss, inc to LC	v sil, cherty, vuggy, banded vn; clear-gy f QVs;
271	212.6	6b	gn	2	chl	clasts vis		py - 2-7%, strs	chl alt congl;
271.6	276.3	6c	bge-gn, gy	2	sil	clasts vis	loc bx, frag, bedded?		sil congl; pale lime-gn, rose-beige cherty vns; chaotic, bx, frag; bedded ?; pale yellow-gn xtals, lime gn clasts; trans? QVs / xtals common
276.3	277.4	6c	gy-beige	2	sil	clasts vis		py - tr-3%, strs	cherty-fract/bx; minor lime gn clasts; f beige alt flds
277.4	279	6b	gn, gy	1	chl	bedded	beds CA 70-80	py - 3-7%, 278.4 w/ mafic dike	mudst; bedded; weakly sil,
279	281	6b	pale gn, gy	2	chl, sil			py 3-10%	mudstone w/ pale gn alt; weakly sil
281	285.5	6b	dk gn, gy	1	chl	bedded	beds CA 70-80; fol CA 10-20	py - 1-5%	v fg; not sil; loc pale gn alt; bedding better to LC
285	285.5	6c	gn, gy	2	sil, ep?	clasts vis		py - 1-3%, diss	strange ep alt?; sil w/ mint gn xtals, ep clusters, ang bk opaque common
285.5	288.1	6b	gn , gy	1	chl	bedded	beds nr vertical	py - tr-1%	mudstone
288.1	288.2	gouge	gn	3	chl	sheared	gouge CA 40-50		
288.2	288.8	6b	gn, gy	1	chl	bedded	beds CA 50-60		mudstone
288.8	289	gouge	gn	2	chl		gouge CA 10-20		
289	293	6b	bk, by	2	chl	bedded	beds CA 50-60, near 90 @ LC	py - 1-2%, in beds	mudstone; bedded, not from 291.5-293 - sect of chl alt congl
293	294	6b	gn, gy	2	chl, sil	clasts vis	LC CA 70	py - tr	weakly sil chl congl
294	295.2	6b	gn	1	chl, sil	bedded	beds almost parallel to CA @ LC	py - tr	mudstone, loc weakly sil; bedded
295.2	295.3	gouge	gn	2	chl	sheared			
295.3	297	6b	gn	1	chl, sil		bedded near vertical	py - 1-2%	mudstone; small sect weakly sil congl
297	305	6b	gn	1	chl		beds CA 50-60	py - 1-2%	mudsone w sm lenses of congl, bedded, var angles
	305	EOH							

Silver Spruce Resources Inc.

Project: Big Easy	Easting:	709907	NAD 27	Az:	270	Core Size: BQTK	Start: June 14/12
DDH BE-12-8	Norhitng	5347701		Dip:	-59.0	Logged by: Peter Dimmell	End: June 16/12
Location:	Elevation:	117 m		Length:	146 m	Sample #'s: 553501-553609	Flexit Tests: 146 m - Dip -57.1 / Az 283.5

Hole #	From (m.)	To (m)	Rock Type	Colour	Alteration	Grain Size	Structure	(%) Mineralization	Contractor: Cabo Drilling Comments
	0.0	6.5	OB						silicified / oxidized boulders
	6.5	9.2	6c	m-dk grn	Si5/Chl0-4	cg	bedding - 20 deg.	fg diss py - 2-5%	**Sandstone**, m-dk grn, silicified, some chlor, soft sections w/ slickensides; vns - 6.55-6.65 - gy chal 30 CA, 7.1-7.3- mgy chal, CA's 30/10; FZ's - gouge - 6.6m - 1cm CA 40, 6.8m - CA 40;
	9.2	27.6	6c	lt-m grn	Si3-5	sst cg, cgt-f	bedding - 40-65 deg	fg diss py - 2-5%	**Sandstone/Conglomerate**, alt, sil; some broken core; QV's - 11.9m - 3cm wh CA 10, 15.5m - 1 cm wh CA 10, 17.1m - 2cm wh-blk chal CA 35-45,19.5m - 3-4mm wispy CA 20, 20.4-22.8m -var banded w/ py, gy sulph? selvages, 20.45 - 3cm CA 50, 21 - strong Si, 21.25 - 2 cm CA 30, 21.45 - 1cm broken, 21.7 - 3-4cm, broken, 22 - 3-4cm CA 60, 22.1 - 5mm, 22.2 - 1cm gy wh chal CA - 15 irreg, 22.7 - 2 cm gy wh CA 60, 22.8 - 1-2cm, gy-blk centre, banding CA-50
	27.6	31.8	6c	lt-m grn-gy	Si3/minor 5	fg	broken core	py - fg, diss, 2-5%	**Siltstone, silicified** - grn-yell sericite as ff; 28-28.2 - py bands to 0.5 cm; 30.5-30.9 - wh alt w/ py bnds;30.9-31.8 - vuggy w/ grn-yell sermore common, shears w/ gouge - CA 70;
	31.8	34.5	6c	lt-m grn gy	Si5	cg		py - fg, diss / clots 2-5%	**Sandstone, silicified** - strong silicification; 33.6 - ser on ff w/ gy met (C?); 34.1 - 2 cm vn, CA 80-90;
	34.5	36.7	QV	lt crm-gy - y grn	Si5	vfg	Contacts - 70/60	py/gy met - vfg - 2-5%	**Quartz Vein, chalcedonic** - banded / brecciated; fspar - adularia ??? 35.7-36.1 - sil sst, py - diss 5%;
	36.7	40.5	6c			m-cg			**Sandstone, silicified** - very strong silicification, finer grained on UC
	40.5	41.0	QV						**Quartz vein** -
	41.0	54.3	6c	lt-m grn gy	Si5	silst/cgt fg, sst - cg	bedding 65	py - diss / ff - 3-5%	**Sandstone/Siltstone, silicified**, some cgt - mainly m-cg sst at top, 46.8-54.3 - more siltst w/ sst sects; narrow QV's - chal w/ minor py, blk met - 41.4,42.1,43.4,44.1,45.3-45.4,45.6,46.4 -CA's 20-50,42.4-.7 - CA - 50 (bottom), top irreg; 2-3 QV phases w/ grn fuchsite ? mineral; 51.6-.85, 52.45,52.6,53.05,54.1; 51.15 py vn; yellow ser slickensides prevalent on fracts.
	54.3	55.2	1c	dk grn	Chl4	fg	contacts 80/60	nvs	**Mafic Dike** - highly chloritized, slickensides on contacts; massive wh QV on bottom contact
	55.2	67.2	2c				63.5-.7 - shear - CA 60		**Mafic Tuff** ? some sst/silst - silicified; amygdaloidal, amygdules filled w/ chlor; QV's - 55.35 2cm, 55.4 1cm,56.4 1cm cut by later 5mmgn banded, 57.1-1cm,57.25 3 cm,57.4 1cm w/ grn fuchsite ?,58.8 1 cm,59-59.3 - 3/4 vns,59.7 1cm,60.5-60.7 - 1 cm gy-grn irreg,60.9 1cm, broken, 61.5 1.5cm, bk selvage CA 40, 62.3 wh 10cm nvs,62.5-62.7 - 2mm w/bleaching, py;57.4-grn fuchsite? on fol var alt w/ py; 63.5-63.7 - shear/FZ
	67.2	69.1	2a	lt gy-crm	Si5	fg groundmass	Contact 30		**Felsic Lapilli Tuff, orbicular** - silicified; orbs are banded w/ centre of chlor? Narrow QV/vnlets - chalcedonic,1-2mm - 1 cm; grn fuchsitic alt assoc w/ wh vnlets, CA gen 75;
	69.1	72.6	2a/2c	lt-m gy-grn -crm	Si5 (FLT) Si2-3 (MT)	fg groundmass		py - diss - 1-2%	**Felsic Lapilli Tuff/Mafic Tuff, mixed, silicified** - FLT - orbicular, chlorite in amygdules in MT; 69.7 - banding over 2-3cm - CA 15; 70.7 - 1 cm QV CA's 70/irreg
	72.6	78.9	5b	dk gy - lt m grn	Si2/3-0 ser2-5	f-mg	contact 70 / bedding 55-60	py - fg diss, semi-mass 5-15% in mst 1-2% in banded silst, gy met in ser zone	**Mudstone/Siltstone, pyritic** - sericitic, well bedded, v. minor vns parallel to beds, 71.6-74.3 - strong ser alt, poss vfg gy met; 74.3 - shear - gouge CA 90; bleached - 74.3-75.6,

	78.9	110.0	6a	m-dk gy-grn	ser3/chl3-4	f-mg	bedding 25-55	py - minor, diss/blebs <1%	**Sandstone/Siltstone, chlor/ser** - unsilicified, no vns noted; 80.4 - grn fuchsitic mineral on fractures; 81.7-85.8 - mixed silst/sst, highly ser/chlor, more chlor in sst; 85.8-90 - mainly cg sst, narrow silst beds; 90-94.2 - heavy chlor on top sect, 91-6-92.6 - red colour;
	110.0	136.9	6c	lt gy-grn	Si5, minor chlor/Ser	f-mg	bedding 35-40 nr top, more massive to bottom	py - diss -1-3% py - diss 3-5%	**Siltstone/Sandstone/Cgt mixed, silicified** - chlor/ser alt assoc w/ shears; QV's - chalcedonic t..out CA's 35-80, gen 45-60; 111.6-bedding cut off by cg sst - CA-70; 118.5-120.1 - alt crm-gy, w/ py vns; 120.6-120.9 - band crm-gy vn; 124-128.3 - cg sst, ser alt of fract, CA's 45-80, 5 vns - 1 cm wide; 128.3-132.5 - mix silsst/cg sst - cgt; vns 131-131.2 - 3 CA's 40-50, 131.6-131.8 - CA's 70-85, py bands top contact; 132.4-135.1 - broken core, mainly cg sst/cgt; 132.8-5 cm crm-gy banded vn; 134.9 - grn fuchsitic mica ?; 134.6-gouge; 134.3 - 5 cm crm vn, CA-70; 136.4-.5 - mafic dike CA's 55/40
	136.9	143.3	1c	m-dk grn	Chl2/3	fg	contacts 60/70	py - ff, minor <1%	**Mafic Dike, chloritized** - chilled margins; amygdules; non mag to v. weak mag in places
	143.3	146.0	6c	lt-m gy-grn -crm	Si5	fg cgt / cg sst	bedding not apparent	py - diss 1-3%, some vfg	**Sandstone/Cgt, silicified** - narrow (2-3mm) gy chal QV's throughout, some wh vns all CA's 70-75, mafic dike assimilated at topr of section
		146.0	EOH						

Silver Spruce Resources Inc.

Project: Big Easy	Easting:	709950	NAD 27	Az: 270	Core Size: BQTK	Start: June 18/12
DDH BE-12-9	Northng:	5347799		Dip: -60	Logged by: Peter Dimmell	End: June 22/12
Location: 78+00N, 0+23E	Elevation:	119.5 m		Length: 230 m	Sample #'s: 553610-553786 (177)	Flexit Tests: none

Hole #	From (m.)	To (m)	Rock Type	Colour	Alt Type	Grain Size	Structure	(%) Mineralization	Contractor: Cabo Drilling Comments
	0.0	5.0	OB						**Overburden** - sand, silt, silicified sedimentary boulders
	5.0	21.5	6c	m gy-grn	Si5	fg	most massive, 6.8 - 70	diss py 1-4%, variable	**Siltstone** - silicified; oxidized on fracts to 11.5m;
	21.5	89.7	6c	m-dk gy-grn	Si5	cg	bedding - 60	diss/ff py 1-5%, gen 1-3%	**Sandstone**, some silst; silicified;
	89.7	91.2	1c	med grn	Cl2	fg	Contacts 50-60	nss	**Mafic Dike** -
	91.2	115.3	6c	lt bg	Si5	mg	massive	diss py 1-3%, euhedral	**Siltstone** - silicified;
	115.3	116.1	FZ	lt grn bg	Si4	cg qtz	contacts - 60	nvs	**FZ/Breccia** - QV?
	116.1	128.3	6c	lt gy grn	Si5	cg sst	no bedding apparent		**Sandstone / Conglomerate - silicified;**
	128.3	137.0	1c	m gy grn	Cl2/3		contacts - 30		**Mafic Dike** - chloritic, amyg in places, chilling on contacts
	137.0	141.0	6b	lt-med grn crm	Si3/Cl2	f-mg	138-138.4 - 60-70		**Conglomerate** - sst interbeds;
	141.0	151.7	6b	gy-bg	Si4/Cl2/3	mg	1 cm gouge TC - 70		**Siltstone** - var alt - sil/ser/chlor;
	151.7	159.8	6c	m grn gy	Si5	f-cg	massive	py - diss - 1-2%	**Mixed Sandstone / Cgt** -
	159.8	164.2	1c	m grn gy	Cl2/3	fg	massive, contacts 55/35	nss	**Mafic Dike** - chloritized, chilled margins, wh QV's - irreg 45-70
	164.2	192.1	6c	lt gy grn	CL5 TC / Si5	f-cg	60-85 at 171m	py - diss - 1-3%, to 5% locally	**Mixed Sandstone / Cgt** -
	192.1	200.0	1c		Cl2	fg	Qcarb vns - 60-80		**Mafic Dike - chloritized**, chilled margins;
	200.0	208.9	6b	lt-m gy grn	Cl2	fg	bedding - 60	nss	**Siltstone** - chloritized, well bedded - fine laminations, some chert / brecc, more chlor nr TC;
	208.9	212.6	1c	med grn	Cl4	fg	contacts 55/irreg	nss	**Mafic Dike** - as above
	212.6	228.3	6b	m-dk grn	Cl2	fg	bedding - 60	nss	**Siltstone**, chloritized; finely bedded;
	228.3	230.0	1c	med grn	Cl4	fg		nss	**Mafic Dike** - as above
		230.0	EOH						

Silver Spruce Resources Inc.

Project: Big Easy	Easting	710003	NAD 27	Az: 270	Core Size: BQTK	Start: June 23/12
DDH BE-12-10	Northing	5347800		Dip: -64.0	Logged by: Peter Dimmell	End: June 28/12
Location: L 78+00N, 0+77E	Elev (m)	121		Length (m) 236	Sample #'s: 553787-553963 (177)	Flexit Test: 230 m - dip -60.6 / Az 290.2
						Contractor: Cabo Drilling

Hole #	From (m.)	To (m)	Rock Type	Colour	Alteration	Grain Size	Structure		Comments
	0.0	4.5	OB						**Overburden** - sand, gravel, till, extensive silicified sedimentary boulders
	4.5	42.1	6c	lt-med gy grn	Si5	f-mg	massive-bedded	py - diss/ff, euhed, 1-3%	**Siltstone, conglomerate/sandstone interbeds, silicified** -
	42.1	45.0	6c		"	mg			**Conglomerate, silicified** -
	45.0	56.4	6c		"	fg - cg			**Siltstone/Sandstone, mixed, silicified** -
	56.4	67.2	6c		"	fg	massive		**Siltstone, silicified** - minor sst/cgt interbeds;
	67.2	76.7	6c						**Conglomerate, silicified** -
	76.7	93.0	6c						**Conglomerate, silicified** - sericitic on fractures
	93.0	94.5	FZ				CA's 40-45	py - fg diss, 1-2%	**Fault Zone** - breccia,
	94.5	100.0	6c						**Conglomerate, silicified** - sericitic on fractures;
	100.0	106.0	6c						**Siltstone, silicified** - pyritic - 5-10%; 104-105 - alt bg cherty; slickensides throughout
	106.0	138.5	6c						**Siltstone/Sandstone, minor Conglomerate, silicified** -
	138.5	158.0	6b/c	lt-m gy-grn	Si5	variable	bedding 65-75, vns 10-80	py diss 1-3%	**Siltstone/Sandstone, minor Conglomerate, silicified, sericitic to chloritic in part** - vns throughout, scattered <1cm except 143 -3-4cm, 147.8-3cm,148.4-2cm;
	158.0	178.8	6c				bedding 65-70	py - diss/ff, 1-3%	**Siltstone/Sandstone, silicified** - variably bedded, chlor/py assoc w/ late shears,
	178.8	184.1	6c						**Siltstone** - w/ Sst/Cgt interbeds;
	184.1	185.0	1c	m-dk grn		fg	contacts 80/60	nvs	**Mafic Dike** - highly chloritized; chilled margins; frags sil cgt nr top contact
	185.0	188.3	6c						**Sandstone, silicified** -
	188.3	190.8	6b				bedding 60-70		**Sandstone, chloritized** - chlor assoc w/ shrs at 188.3-188.6, 189.3-189.6; chal vns scattered throughout, best 190.2-190.5
	190.8	191.4	FZ				CA 70		**Fault Zone** - chloritized,
	191.4	208.0	6c						**Sandstone/Conglomerate, mixed, silicified** -
	208.0	220.7	6b/c	m grn					**Sandstone/Conglomerate, mixed, sericitized/chloritized** - rhy frags (flesh colour) in cgt;
	220.7	228.9	6c	grn flesh-wh			vns 50-85 to irreg contacts 60/70	py - diss, euhedral 1-3%	**Sandstone, silicified** - extensive QA vns - 220.7-222, 225.4-226.4, 227.35-227.85, brecciated, gy-bk chal qyz, sst frags; mafic dike - 226.9-227 - chlor w/ shrd contacts
	228.9	236.0	5b	lt-med grn	Cl3	fg	Contact 80; bedding variable 35-80	py - minor diss in places	**Mudstones** - variably altered, chloritic, poss some mixed mafic dike
		236.0	EOH						

Silver Spruce Resources Inc.

Project: Big Easy				Easting	709953	NAD 27	Az	270	Core Size: BQTK	Start: June 28/12
DDH BE-12-11				Northing	5347000		Dip	-60	Logged by: Peter Dimmell	End: July 3/12
Location: L 79+00N, 0+23E				Elev. (m)	121	Length (m)		209	Sample #'s: 948501-948650 (150)	Flexit Test: 200m - dip -55.9 / Az 283.5

Hole #	From (m.)	To (m)	Rock Type	Colour	Alteration	Grain Size	Structure	(%) Mineralization	Contractor: Cabo Drilling Comments
	0.0	6.0	OB						Overburden - silicified sed boulders, rusty till
	6.0	9.8	6c	lt-m gy-grn	Si4	fg	bedding 60-70	py - diss 1-5%	Siltstone, silicified - well bedded, oxidized fract to 11 m; minor narrow sst sects
	9.8	109.1	6c	"	Si4/5	m-cg	bedding 75	py - diss 1-3%	Sandstone, silicified -
	109.1	114.1	1c	m-dk grn	Chl3	fg	contacts 45/55	py - minor, fg blebs	Mafic Dike - chloritized, chilled margin, QF vning on top contact;
	114.1	129.2	6c	bg-lt brn	Si5	f-cg		py - fg diss 1-3%	Conglomerate/Sandstone, silicified - f-cg;
	129.2	135.2	1c	m-dk grn	Chl2	f-mg	contacts 25/35		Mafic Dike - chloritized, finer grained on margins, weakly mag in places; qtz -ep vning throughout - variable; hem slickensides on fracts
	135.2	168.4	6c	lt gy-grn - m gy	Si5	f-cg	minor bedding - 60	py - diss - 1-2%	Siltstone/Sandstone/Conglomerate - mixed, silicified - chalcedonic in places; some ser on fracts (137.5-138.5); breccia 1-3 cm CA 20 - 135.5-135.8;
	168.4	177.3	1c	m-dk grn	Chl3	f-mg	contacts 25/40		Mafic Dike - chloritized,
	177.3	194.0	6b	lt gy-grn - purple	Si3/Chl2	m-cg	massive		Sandstone, chloritized - silicified; spots / frags;
	194.0	196.7	1c	m-dk grn	Chl3	mg	massive, contacts 60/45	py - v. minor blebs	Mafic Dike - chloritized; weak to mod mag; cut by irreg, discont calcite vns, hem on slickensided fracts
	196.7	209.0	6b	lt-m gy-grn	Chl2	f-mg	well bedded 30-45	py - diss, minor <1%	Siltstone, chloritized - unsilicified; well bedded, some brecciation 203-204.7, assoc. calcite vning
		209.0	EOH						

Silver Spruce Resources Inc.								
Project: Big Easy	Easting	709974	NAD 27	Az	270	Core Size: BQTK	Start: July 3/12
DDH BE-12-12	Northing	5347750		Dip	-60	Logged by: Peter Dimmell	End: July 11/12
Location: L 77+50N, 0+57E	Elev. (m)	121	Length (m)	209	209 m	Sample #'s: 948651-948858 (208)	Flexit Test: 230 m, -55.6 dip / 288 Az

Hole #	From (m.)	To (m)	Rock Type	Colour	Alteration	Grain Size	Structure	(%) Mineralization	Contractor: Cabo Drilling Comments
	0.0	5.0	OB						**Overburden** - extensive silicified sedimentray boulders, hard; till, sand, gravel
	5.0	122.5	6c	lt gy crm - m grn	Si5	m-cg	massive, no bedding	py - diss, 1-3%	**Sandstone, silicified** - variably lt gy-crm to m grn;
	122.5	124.9	FZ				gouge		**Fault Zone** - gouge, comminuted qtz/rock frags, some vns 122.5-.7 fl/wh,
	124.9	144.3	6c	m gy	Si5		massive		**Sandstone, silicified** - m gy; minor qtz-carb vns;
	144.3	145.5	6b	m-dk y-grn	Chl3		massive	py - diss, 1-2%	**Sandstone, chloritized** - pyritic
	145.5	161.2	6c	lt-m gy bg	Si5				**Sandstone, silicified** -
	161.2	163.2	1c	m gy-grn	Chl3	fg	contacts 80/35		**Mafic Dike** - chloritized, non mag; carb vns/vnlets; epidote esp 161.9-162
	163.2	170.4	6c	lt bg crm-brn	Si5	f-mg	massive		**Sandstone, silicified** -
	170.4	171.3	FZ				CA 80	py - diss 1-3%	**Fault Zone** - chlor gouge to ext. chlor/ser alt; narrow broken qtz vnlets; Note zone shorter than m indicate - probs with marking by driller:
	171.3	185.6	6c	m gy	Si5	m-cg	massive	py - minor diss	**Sandstone, silicified** -
	185.6	190.0	6b	m-dk grn	Chl4		well bedded - 45		**Sandstone, chloritized** - some cgt interbeds, poss tuffaceous in part, gradational contacts alteration sil/chlor
	190.0	196.5	6c	gy bg - lt - m gy	Si5		massive		**Sandstone/Conglomerate, silicified** - brecciated in places, esp to bottom, yellow/grn (fuchsitic?) micas/clays prev;
	196.5	198.6	6b	med-dk y grn	Chl4		bedding 45		**Sandstone, chloritized** - well bedded
	198.6	215.4	6c	lt-m gy grn	Si5		massive		**Sandstone, silicified** - highly silicified on top contact,
	215.4	218.6	1c	m-dk grn	Chl3	fg	contacts 70 / grad		**Mafic Dike** - chloritized, non mag; carb vns
	218.6	219.2	6c		Si5		brecciated		**Sandstone, silicified** - brecciated, mixed w/ mafic dike top contact w/ qtz-carb vns minor gy-wh vns through rest of section, broken on bottom contact
	219.2	238.0	6b	m-dk gy grn	Si2/3, Chl3		bedding 45-70, some 10 - ss defm ?		**Siltstone/sandstone, unsilicified, chloritized** - gen well bedded esp in siltst sects, siliceous groundmass, carn vns 10-60 to CA, variable, scatterec
		238.0	EOH						

Silver Spruce Resources Inc.

Project: Big Easy	**Easting**	710115	**NAD 83**	**Az**	**270**	**Core Size: NQ**	**Start: Oct 24/14**
DDH BE-14-13	**Northing**	5248203		**Dip**	-74	**Logged by: Peter Dimmell**	**End: Nov. 3/14**
Location: L 80 N, 1+00E	**Elev (m)**	118	**Length (m)**	**279.6**		**Samples: 948901-9000; 159001-138 (238)**	**Reflex Tests:** 77.7 - 273.1, -74, 52004, 68.4, 13; **196.6** - 272.8, -72.9, 51829, 68.4, 8; **279** - 272.1, -71.2, 51478, ?, 9;

Hole #	From (m.)	To (m)	Rock Type	Colour	Alteration	Grain Size	Structure	(%) Mineralization	Contractor: Whitewulf Drilling Comments
13	0.0	4.6	**OB**						boulders, mainly granite, minor silicified sedimentary rocks
	4.6	32.8	**Cgt/Sst**	gy - bg	strong Sil	f-cg	bedding variable - 30-80, generally 75-80	diss euhedral py - 3-5%	strongly silicified, mixed cgt/sst; fg sst, mg cgt; red hem on fractures nr surface;some yellow ser/chlor in upper part; 17 m - rock becomes vuggy; 17.5-17.9 strong fuchsite (grn mica) on fractures; 19.4-19.8 - bg/brn sil w/ 2-3 mm banded QV's; 23.3-23.5 - bg/brn broken QV's; 23.5-24.1 - FZ - brecc w/ gouge, slickensides, Low C - CA 30; 24.4-25 ext slicks - high angle CA's 20-45; **LC - 25-28.3 (2m), 30.8-32.6 (1m);**
	32.8	38.4	**FZ**	lt gy grn	ser/chlor	f-cg	bedding generally 80	diss euhedral py - 3-5%	mainly strongly ser/chlor cgt; gouge zones/ narrow sil cgt zones interspersed; variable orientations on gouge zones - 32.5-32.6,33.9-34,36.9-37,37.4-37.7,37.95-38.4; sil cgt - 32.8-33.5,34.4-34.6,37.1-37.4,37.7-37.95,38.4-38.7;
	38.4	72.1	**Cgt/Sst**	lt gy- bg	strong Sil	f-cg	minor beds upper part of section then beds 75-90; 59.1 - 75; 67.8 - 60, 76.8 - beds - 70; 81 - beds 70/65; 81-83 - beds 40-70;84.5 beds 70-80;	diss euhedral py - 3%; 60.8-61 - py bands (2-3 mm) at CA 75; 63.8-63.9 - py bands to 2 cm at 75; ff's - 64.3, 66.2 (80),	mixed cgt/sst; 38.7-40 - becomes brecciated/silicified; 61 - mainly mg sst; 69.5-.6 - 6 cm bed silst; 69.6 - cgt, sil, fg - bg w/ diss / ff flesh colour mineral throughout; 45.6-46 - bg QV w/ gy selvages (ginguro?) along CA; 47.85-47.95 - 1-2 cm wh/bg QV CA 40, black selvages; 51.7 - white Q gash vns CA 15; 54-56 sil cgt - brecciated; 56.4-56.8 - mafic dike - gouge/bleached, contacts CA's - 15; 56.8-58 - sst - gy/bgw/ flesh coloured blebs/xls (like leucoxene); 58.5-59 - contact of 2 cgts (f/mg) along core; 69.4 - 2-3 mm gy wh QV - irreg w/ brecc sil cgt; **LC - 40-41.7 - 1m, 47.9, 50.9, 53.9;**
	72.1	157.8	**Silst**				93.4 - bedd CA 70; 111.7 beds CA 70	diss /ff/bands py 3%+	siltstone, fg; scattered irreg, QV's to CA 10; cgt beds - 73.3-73.9 (65), 75.3-75.6 (40/20), ext py, diss and ff, around clasts to 10%, gen 3-5%; 75.6 - mixed silst/cgt f-cg; 77.7-81 - mainly silst, some sst; 81-81.35 - mainly silst, some sst - cgt sections; **83.35-84.5 - breccia zone - broken/brecc vn/cgt, contact CA 75**; 84.5 - mixed silst/sst - silicified, bleaching (alteration) along bedding cutt by QV's; Cgt - 91.1-91.5, 92.2-92.4; 93.4 - silst/sst/cgt - spheroidal in part ? - silicified, mixed/interbedded; cgt brecc/spheroidal - 93.7-.8, 95.1 - 3 cm, 96.1-.2, 96.4-.8, 99-100, 100.5-101; 101.9 - mixed silst/sst to 108 m then mg cgt mixed w/ sst/silst; cgt - 108-108.5, 108.8-109, 109.3-110; 111.7 - mainly sst, f-mg, sil; 119.4 - sst, sil; 119.7-124.8 - cgt, f-mg, some silst/sst, sil, py bands gen along bedding; 125.2-131 - sst/silst, mixed, sil; 126.3-.5 - breccia - gy metallic infilling silst;py banding ext through sections (CA 35-80); 131-131.2 - Coll Si (CS) banding? - CA 60, v fine; 132.4-137.5 - mainly cgt, minor interbeds silst/sst; 133.5-.8, 137.5 - broken/brecc w/ moly /py ff's Vns - 76.8-77.7 - broken/brecc vn, strongly sil, bands/ff py; 81.3 - 2-3 mm QV w. gy selvages; 88.5-88.9 - 2-4 mm banded wh QV w/ assoc bleaching, some gy qtz, CA 0-15; 89.8-90 - wh-bg QV w/ gy selvages 1-3 cm, CA 35; 93.4 - vns sometimes along bedding w/ assoc. alt (bleaching) and py; QV - 95.1; 95.8 - 2-3mm w/ 4 cm alt (cm above, 3 below); 96.05; 96.3; 99.55; 99.75; 99.9 (25); 101.3 (10); 101.9 - vns - qtz/py, gy -blk; 102.9 -
	157.8	161.3	**Colloidal Silica (CS)**	lt brn-crm	sil	vfg	nvb; Contacts Top - 75, bottom 30; 160.6-161.3 - contacts 25/55	minor diss py <1%;	massive silica - CS or chert, no fol or bedding; massive but fractured; some alt sst w/ chl; ext py diss/ff to 10%; 157.5-160.4, 160.6-161.3 - mixed zone (both);
	161.3	170.0	**Cgt**	lt-m gy grn	sil	m-cg	nsb; 164.3 - sst beds - 70		167.9-168 - wh alt bands (80-90); Si zones - 162.1-162.3, frags 164.3-.5; 166,2-.6 (40/50); Vns - 157.8-158.2 <0.5 cm; 168-168.3 - 3 QV's gy/crm (55), wh gy, 1.5 cm (45), wh, banded, 3-4mm (30); ,
	170.0	188.0	**Sst/Cgt**	m gy grn	sil	m-cg		170-171 - mm scale py bands, CA 80-85; 181-183.4 - 1-3% py, diss/ff/bands	181-183.4, 184.3-185.3 - strongly silic cgt; 183.4-184.3 - FZ in cgt - brecc/gouged esp nr bottom; 185.3-188 - sst, sil, more chloritic, core is broken/faulted; 172.25 - 1 cm QV gy/wh; 172.4 QV, vfg, gy; **175.2-.5 - banded ging vn, 6 cm, CA 35**; 175.8-176.1 - QV - irreg/discont - ging banding; 178.8-180 - QA vn - contact 45 then along CA, grn wh to gy, w/ ging banding;gy selvages, brecc? 180.3-181 - QA vn along CA, gy wh, ging bands;
	188.0	199.6	**Colloidal Silica (CS)**	lt-m gy to gy grn			nvb; 200.7 - beds 75-85;	v minor diss py;	192 - siltstone, cherty, sil; 192.7-194.7 - cgt, sil w/ tuff, below, some bleaching; 194.7-195.2 - gy Si, massive, vfg; 195.2-199.6 - cgt, sil; 195.2-195.6 - brecc w/ QV's, broken to 195.6; 190.2-192 - soft sed features ??? 199.4 - becomes fg w/ chl; 200.7-200.9 - grn Si band (85); 201.4 - end of silicification; 188.4-.6 - QV's 2-7 mmcrude banding (25); 188.9 - same, irreg.; 188.9-190.2 - Xcutting vns/fracts w/ assoc bleaching; 197.9-198.3 - wh/grn/crm QV's - 2-3 mm, CA gen 40, irreg; 198.8 - 1 cm QV, banded, gy wh (35); 199 - 0.5 cm QV, minor banding (45);

Hole #	From	To	Rock	Colour	Alteration	Grain	Structure	(%) Mineralization	Contractor: Whitewulf Drilling
	(m.)	(m)	Type			Size			Comments
	199.6	201.6	**Sandstone**	m-dk grn	chl	mg	beds 75-85; contacts T-80, B-45 to irreg	diss py, 1% or <	200.7-.9 - grn Si bands, CA 85; 201.4 - end silicified;
	201.6	209.0	**CS**	m gy grn	sil	vfg	gen massive; beds? 70-80		205 - alteration (bleaching) along irreg fractures - extensive; Vns - 201.6-.9 - 3 mm wh QV along core; 202.6 - 4 mm wh QV, banded CA 80); 203 - 0.3-1 cm banded QV (CA 25); 203-204.4 - 1 cm brecc vn along core, wh QV along one side, brecc vn cuts off QV at 203.5; 205.9-206.2 - wh QV cutting bleached / alt units;
	209.0	210.2	**Mafic Dike**	m-dk grn	chl	fg	contacts T 60, B - 50	scattered blebs py	
	210.2	215.7	**CS**	m gy grn	sil	vfg	contacts CA 60; beds 60-70	py - ff's, bands - 1%	212.2-.5 - py as ff's - poss gy metallic; 213.1-.4 - sst, sil/chl, bleaching on contact; 214.3-.7 - broken/gouged core - FZ, LC ?;
	215.7	217.0	**Cgt**	m gy gen	chl/sil	f-cg	nvb	minor py, diss, <1%	coarser to bottom, large rhy clasts to 4-5 cm;
	217.0	219.2	**Mafic Dike**	dk gy grn	chl/ep	f-mg	contact B-30	scattered blebs py	more chl/ep on bottome contact;
	219.2	226.7	**Sst**	gy-bg	sil	f-mg	nvb	diss <1%; bands to 1cm -15% py, CA 75-80	conglomeratic in places - 224.3-.8,225.2; some sericite - yellow; 222.3 - QA vns more prev - narrow - < 0.5cm, along and 25-30 to CA; 226.5-.7 - QA vns; some brecc on bottom contact
	226.7	230.9	**CS**	m gy grn	sil	vfg	beds 60-85	py as ff's along beds	bleaching prev along fracts; 230.5-.9 - brecc/bleached contact zone w/ black ging?; QV's - occasional, wh variable CA 35-45; 224.7 - QV w/ red stain - adularia?, 1 cm, irreg, CA 65, py ff's assoc;
	230.9	232.85	**Sst/Silst**	lt gy bg	sil	fg	nvb		brecc/veined, wh/g-blk QV's, variable orientations (to 75), blk ging bands prev;
	232.85	243.3	**Breccia Zone** sst/silst	m brn-m gy	sil	fg	nvb	py diss/ff, variable 1-2%, w/ gy metallic - moly	intensely brecc/QV'd zone w/ wh/gy ging bandedvns, vns broken; upper part section 1 cm-mm scale QA vns at CA 60-75; 235.4-235.5 - QA vn at CA 30/40; 236.4 - yellow ser on fractures, , less gy ging bands; 241.7 - more finely brecciated, gy brn w/ blk frags;
	243.3	248.3	**mixed MV/silst**	my gy grn - dk gy	chl		beds 65	minor py - ff/blebs; 247.2 - fg diss py - 3%+	non silicified / chloritized; 243.3-.6 - grn seds/tuff; 243.6-.7 - dike w/ chilled margins CA's 55/60; 243.7-.9 - mv; 243.9-244 - grn seds, CA 70; 244-244.2 - dk gy sed - massive; 244.6-247 - mv, lighter colour 0.5 m from contact; 247-247.2 - banded sed, f diss py - 10%; 247.2-248.3 - silst, f diss py; alt of dk gy sed by bleaching along fractures;
	248.3	252.9	**Mafic Volc ?**	dk gy grn	chl/ep	fg	contact CA 65 (bottom)		amygdaloidal - calcite amygdules; scattered qtz calcite vns, chl as clots;
	252.9	256.8	**Silst**	m gy grn - m gy	chl	f-vfg	finely bedded, mainly 55-65, some to 45		chloritized, non silicified
	256.8	260.4	**Mafic Volc ?**	m-dk grn	chl/ep	f-mg	contacts T30, B50	nss	lighter on top contact - chilled ? finer grained to contacts; scattered qtz-carb vning, variable orientations, some reddish colour
	260.4	275.2	**Silst**	m gy grn - gy	chl	f-vfg	beds 50-65; 260.7 - beds 55-80	261.2 - minor py bands at CA 70	chloritized / non silicified; finely bedded to massive, rhythmic banding; 262.2 - bleaching/alt - minor; 266.2 - mixed silst/sst/cgt, top contact at CA 60 crosscuts bedding at CA 60; 275-275.2 - cgt, fg, w/ flesh colour rhy? Clasts;
	275.2	279.6	**Mafic Volc ?**	m-dk grn	chl/ep	f-mg	contact - 65	nss	amygdaloidal - chl/calcite; non magnetic; chilled on contact; calcite vns 277-EOH, variable orientations - 20-50 CA;
		279.6	**EOH**						

Silver Spruce Resources Inc.

Project: Big Easy | Easting 710121 | NAD 83 | Az 270 | Core Size: NQ | Start: Nov. 8/14

BE-14-14 | Northing 5348401 | Dip -75 | Logged by: Peter Dimmell | End: Nov. 10/14

L 82 N, 1+00 E | Elev (m) 117 | Length (m) 131.1 | Samples: 159139-253 (115) | Reflex Test: 108.8 m - Az 298.2 (275), Dip -73.6, MF 51910, MD 68.3

Contractor: White Wulf Drilling

Hole #	From (m.)	To (m)	Rock Type	Colour	Alteration	Grain Size	Structure	(%) Mineralization	Comments
	0.0	8.2	**Overburden**						mixed float boulders - unalt red seds, granite, some alt seds
	8.2	11.5	Silst/Sst/Cgt	m gy grn	Sil	f-cg	bedding - 55-80	diss py 1-2%	8.2-11.1 - silst/sst interbedded cm-mm scale; 11 m - FZ - gouge - LC - 2.6 m? 11.1-11.5 - cgt - mg, clasts to 2-3 cm; polymictic
	11.5	12.4	**FZ in Cgt**	lt gy grn	Sil/chl	m-cg	nvb	diss py 1-2%	gouge, broken/brecc cgt; LC - 0.5m
	12.4	24.0	**Sst/Cgt mixed**	m-dk gy grn	Sil/chl	mg	bed var - 60-80, gen 70-75	diss/bands py - 1-2%	variably altered mixed sst/cgt,, some silicified sections, some more chloritic/softer, cgt sections more silicified, unknown bg mineral (UM) (adularia?) diss and bands
	24.0	34.5	**Cgt/sst mixed**	m gy grn	Sil	mg	beds 60-65	diss/ff py 1-3%	more chloritic/softer on top contact; UM bg, diss/bands; 25-25.6 - py/QV along core axis - 0.5 cm wide, 20-30% py;, poss gy met; becoming more chlor to bottom, grad contact; 28.6 - scattered narrow QA vns, <0.5 cm, some banding; 30.1-31.6 - QA vns, CA 20-30, parallel bedded vns/alt - CA 55-65; minor vns/alt to 32.2, 34.1-.2 - 2 wh QV's 0.5cm/2mm;
	34.5	46.4	**Cgt/sst mixed**	m gy grn	Sil/chl	m-cg	beds less 55-75	diss/ff py 1-3%	units softer; chl more prevalent; 36.4-37.2 - py/QV along CA, 1-3mm,; 38.4-39 - QA vns, some gy selvages; along CA, broken/brecc; 39.5-39.8 - py as ff/diss - 10%+; 39.8-40.1 - FZ - gouge, in sst; 41.1 unit becomes more arkosic - fspars? As wh(alt?) frags/phenos; 42.8 - some QV's - gy/wh, wk banding, 43.3-43.6 - py as ff/bands to 15%, poss gy met; 45 m - 5 cm silst; 45.1 - py bands CA 70; 45.5-45.6 - same;
	46.4	59.9	**Sst/silst mixed**	m gy - m gy grn	Sil	mg	beds 60-80, some xbeds	fine diss py 1-2%; 59.4 - py pu diss 3-4%	5/6 QV's - narrow ((<3mm) in top 1 m; some Xcutting (bedding)QV's w/ gy met at top section (<2mm); 48.6-48.7 - 2 wh QV's 0.5/0.2 cm; 50.2-50.3 - QV at CA 30 <1 cm; 50.8 - band of alt - flesh-bg, fspar?; 54.1 - wh QV CA 40, 3mm, cuts bedding at 55; 54.8 - 1 cm chert band CA 70; 54.9-55.4 - wh QV's - some banding, gy selvages along CA; 55.8-56.6 - narrow (mm scale) QV's w/ py along CA; 57.2-.4 - narrow (<3mm) Qtz/py vns, minor grn QV; 57.8 - 2 cm chert band, CA 60; offset 2 cm along CAat CA 40 xcutting fracture; 59.4 - becomes more finely bedded silst - CA 60, chloritic but silicified;
	59.9	70.8	**Cgt**	m gy grn	Sil	m-cg	beds fairly massive, 60	py - diss/ff - 2-4%	60.7-61.2 - colloidal Si beds? 0.5-1.5 cm wide, conformable, some Xcutting narrow QV's; 61.2 - cgt gets coarser w/ clasts to 3-4 cm+; rhy clasts prevalent; 66.5- 3 mm wh QV CA 40; 2/3 in next m; 69 - fg colloid. Si;
	70.8	71.25	**Silst**	m-dk gy grn	Sil/chl	fg	beds 65-70	fine py 1-2%	mixed zone - Si (QV?) - broken; finely bedded, chl (softer), grn silst; at bottom section 3 cm py band 20-30% py;
	71.25	73.5	**Silst**	m gy bg	Sil	fg	beds 65	fine diss py 1-2%	lt gy Si bands; 72 - 5 cm brecc vn CA 65; 71.9-72.2 - fine, narrow py/Ad vns 2-3 mm max; 72.2 - becomes bg w/ minor wh QV's w/ chlor; 72.5 - 1 cm QA vn at 30 Xcutting bedding, CA 65;
	73.5	85.2	**Sst**	m gy-bg	Sil	m-cg	beds 75-80; 82.6-85.2 CA 65-75	fg diss py 1-2%	76.2-78 - bg, minor mm scale QA vns along CA; 79-79.6 - 2 QA vns - 1, 3 mm along CA; 2- 1 cm at 20 CA; 80.7-81 - 3-4 cm QA vn at CA 30; 81 m - 2 mm QA vn at CA 15; 82-82.6 - sst w/ chl on fract, brecc at bottom; 82.6-85.2 - sst/silst - sil
	85.2	85.9	**Chert**	lt brn bg		vfg	massive/brecc; contact 75	minor diss py - 1%	minor wh QV's
	85.9	88.0	**Sst/silst**	lt-m gy grn	Sil	f-mg	bedd 70	diss/ff py 1-3%	87-87.5 - QA vns along CA, 0.5 cm or <; some "ging" banding; 87.5-87.8 - alt (bleached) along fracts, minor QV's.
	88.0	100.4	**Tuff**	lt gy - gy grn	chl/sil	m-cg	finely bedded in places	diss py 1-2%	gradational contact w/ sst above; variable colour, grain size; chl as frags/clasts; 88-88.8 - QV - mainly wh, generally banded,broken/discont along CA; 89.6-90 - wh/massive; 90.3-91.1 - narrow <0.5 cm banded QV's along CA, vn offset 2 cm at CA 80; 91.5 - 3 mm vn along CA; 91.9-92.3 - 3-4 mm banded wh QV, wavy along CA; 92.6-.7 - orange/wh QV / brecc along CA; 93-93.2 - qtz/py vn, 1-2 mm along CA; 93.4-93.8 - QV's - upper - orange/wh, lower 2-3 mm, CA 20; 94.2-.3 - 8 mm banded wh/orange vn CA 15; 94.6 - intersecting QV's - gy/wh banded at CA 30 / grn/wh w/ fuchsite? (emerald grn mineral) along fract/margin vnsCA 35; 95 - 0.5-1 cm wh/or vn CA 35; 95.3-95.8 - 2-3 cm gy/wh QV, banded w/ ging bands, some orangeqtz; some grn - chl? 99.7-.8 - cgt bed, grad. contact; 96.8 - 97 - 1-1.5 cm QA vnw/ orange red jasper, CA 20,80, poss ging bands
	100.4	109.9	Cgt/silst/sst	m gy grn	chl/sil	m-cg	contact 70, var beds	fine diss py 1-2%; 107-107.3 py diss 2-3%	100.7-.9 - bleached bg, contact CA 70; 102.2 - py bands, 1-2 mm CA 75; 104.3 - 1mm CA 75, 104.4 - py vn 25; 105 - becomes cg, clasts to 4/5 cm; rhy clasts prev; some alt/clasts - chl; 107.5-108 - 3-4 mm irreg QA vn w/ gy selvages along CA, minor late QV's at CA 40 cut QA vns and clasts; 107-107.3 - sst/dk grn/chl?/sil
	109.9	114.8	Silst/sst	lt-m gy grn	sil	f-mg	well bedded 70-80	py - diss/bands - 1-3%	conformable contact;chloritic, dk grn diss clots; 112-112.5 - QA vns along CA; 113.5 - end - becomes bg w/ scattered irreg /wh QV's, some at CA 45, some bleaching assoc.
	114.8	117.2	Sst	m-dk grn	sil/chl	mg	well bedded 65-75	py - diss/bands - 1-3%	chl in groundmass; frags /clasts bg flesh coloured alt mineral; 116.5-117 - bleached

Hole #	From	To	Rock	Colour	Alteration	Grain	Structure	(%) Mineralization	Contractor: White Wulf Drilling
	(m.)	(m)	Type			Size			Comments
	117.2	131.1	Cgt/sst	lt bg - gy grn	sil	f-cg	massive, minor beds 55-65	as above	mainly fg cgt, massive, minor silst; 117.2-.8 - wh QV along CA, minor gy selvage; 119.9-120.5 - silst, fg; 120.5-121.1 - banded wh QV along CA; 123.4-123.7 - silst/sst - 2 cm colloid Si/chert at top CA 90; 124.2-124.9 - QV's - wh, var orient, QA vn 0.5 cm CA 15; 126.2 - FZ - brecc/broken 0.1 m; 126.9-128.3 - QV's - wh/grn, minor QA vns var/irreg; 127.4 - qtz brecc vn, 3-4 cm, cuts grn/wh QV's w. gy selvages; 130.2-.8 - 0.5 cm QA vn along CA, cut off by later vn w/ banding/gy selvages.
	131.1		EOH						hole abandoned due to caving; appears related to casing at surface - not seated properly ???

Silver Spruce Resources Inc.

Project: Big Easy	Easting	5348404	NAD 83	Az	270	Core Size: NQ	Start: Nov. 11/14
Drill Hole # BE-14-15	Northing	710082		Dip	-80	Logged by: Peter Dimmell	End: Nov. 18/14
Grid L 82 N, 0+60 E	Elev (m)	122	Length (m)	248.7		Samples: 159254-470 (216)	Flexit Test:
							Contractor: White Wulf Drilling

Hole #	From (m.)	To (m)	Rock Type	Colour	Alteration	Grain Size	Structure	(%) Mineralization	Comments
BE-14-15	0.0	4.9	**Overburden**						mixed red stt, grn unaltered, sil sediments, some granite
	4.9	7.2	**Sandstone**	m-dk grn	sil/chl	f-mg	beds - 75	v. minor diss py	minor cgt in part;
	7.2	14.5	**Conglomerate**	lt-dk, gy-grn	sil/chl	f-mg	beds - 75-85	diss py 1-2%, sil sections	mainly cgt w/ minor sst, variably silicified/chloritized; oxidized to 7.5 m; soft/chl rich to 7.9 m, variably sil to 9.5 m, softer/chl to 10.5 m, sil to 12.6 m, sofeter/chl to 14.5 m; chl in matrix and clasts; 7.3-.4 - FZ/gouge; 9-9.4 - patchy xcutting gy QV's, irreg/discont, vf sulphides;
	14.5	21.0	**Sandstone**	lt-m gy grn	sil/min chl			diss py 1-2%, some py bands xcutting beds	minor fg cgt sections; minor wh QV's w/chl - high angle to core (20); 21.4-.7 - irreg/discont QA vn w/ blk "ging" bands, wispy; silic w/ vn, orange / flesh colour along margins;
	21.0	25.9	**Conglomerate**	m gy-grn	sil, mod chl	f-mg	beds 70-80	f diss/bands py 1-2%; 24m - 2 cm 30% py	mainly cgt w. sst interbeds; chl mainly interstitial, some frags/clasts
	25.9	32.3	**Sandstone**	m-dk gy grn	sil/chl	mg	beds 80-85; 31.7 - 85		cgt in places; 28-28.2 gouge/FZ (lost water return); 27.3 - orange QA vn - 4/5 mm at 45; 28.6-.8 - 5-7 mm QA vn at 20; 31.5 - wh QV at 15, no banding; 31.7-.9 - fg sil beds in sst - coll sil?; 32.1-.3 - silst beds - 75;
	32.3	34.1	**Conglomerate**	lt-m gy-grn	sil, mod chl	m-cg	massive	fg diss py - 1%; 30-30.2 - 1-2 mm py	
	34.1	34.9	**Siltstone**	m gy grn	mod chl	fg	contacts 80-90; beds 80-85	35.6-.8 - 10-20% py	35.6-.8 - arkosic cgt
	34.9	36.0	**Conglomerate**	lt gy grn	mod chl	mg	massive	diss py - 3%; poss gy metallic	arkosic; becomes chloritic to bottom section;
	36.0	54.3	**Congl/Sst**	lt - m gy grn	sil	m-cg	beds 65-80, gen 80; contact 65	diss py 1-3%	variable clast size/shape - rounded to sub ang; becomes more chloritic to bottom section; QA vns 37.8-38.3 - 0.5-1 cm, along CA, qtz centre, ad on margins, v minor "ging" bands; 42.5 - gy wh vn at 25, 3 mm; 46-46.1 - 3mm vn at 25; 38.7 - Si clast, w/ sst clast in it; 51.5-52 - 1 cm banded QA vn - disrupted but continuous, cut off to bottom - 20-30; 53.5-.6 - 1-2 cm QA vn w/ wk beanding, some offsest, minor gy met;
	54.3	62.5	**Sst/Silst**	m-dk grn	sil/chl	f-mg	beds 65-80, gen 75-80; 59.5 - beds 80-85	diss py 1-3%, some bands 20%+; euhedral to blebs;	57.8-58.2 - gouge/FZ; 58.4-59 - more chloritic, chl clasts / interstitial; 59.5 - more silicified silst/sst, minor cgt
	62.5	68.0	**Conglomerate**	lt-m gy grn	sil	f-c	gen massive, contact 80	diss py 1-2%	sharp contact fg sst-m-cg cgt; polymictic w/any orange rhy clasts; 66.4 - more chloritic, interstitial and clasts; 67.2 - 0.5 cm gy QV, irreg, wispy banding;
	68.0	71.1	**Colloidal Silica**	crm-m gy brn	sil	vfg	bedding?75-85, well developed 68-68.5, 69.1-69.8; rest more massive	minor diss py	finely bedded/banded Si - colloidal ??, wispy bands noted; banded QA vns xcutting, narrow, <2mm; 70.9-71 - cgt bed, silicified
	71.1	84.60	**Silst/Sst**	m-dk brn	sil	f-vfg	gen massive, 70-80; 79.2 - Si band at 65; 83.2- Si band - at 80;	minor diss py; 83.2-84.2 - diss py 1-2%	mixed silst/sst, mainly fg but m-cg in places, intensely silicified; 71.1-.6 - QA vn along CA, irreg discont. To 1 cm, minor banding, flesh colour, gy selvages; 73.1-.5 - irreg/discont QA vn 3-4 mm along CA, minor banding; 78-78.9 - QA vn 2-3 mm, banded, along CA; 79.2-.3 - Si band, gy, CA 65; 798.-80.6 - bleached/alt zones - fspar/ad? 80.6-82.6 - scattered, narrow, QV's - irreg/discont, gy brn; 82.6-.8 - wh/gy QA vn, discont, 15: 83 m - 1 cm QA vn at 70; 83.2-84.2 - Si, banded;
	84.6	99.0	**Tuff**	lt bg brn	sil	f-mg	beds 80-85	fg diss py - 1-2%	some interbeds silst/sst; 84.9-85.5 - 3-4 mm QA vn along CA, gy selvages; 85.9-87 - QA vn along CA, wh-gy w/ ext chl, 2-6cm wide, some emerald grn mineral nr bottom; 87.6 - m gy vn, 1 cm at 80; 88.8/88.9 - 2 QV, brn red, 3-4 mm at 80; 4-5 mm at 75, conformable w/ bedding; 89.9-90 - 2-3 cm Si vn along CA, orange selvages; 90.6-91 - 1 cm QA v, gy w. wh/orange selvages, irreg along CAbut stops to bottom; 92.2-.9 - 2 parallel QA vns, 15-20 to CA, upper 2-3 cm, gy to wh, brecc, lower - 2-4 cm, gy/wh w/ fuchsite ?(emerald grn), along fractures, gy selvages on both vns, vfg gy Si vns between the QA vns; 93.1-.2 - mg tuff w/ alt frags/chl frags, narrow qtz/py vn, offset; 93.5-.7 - orange qtz interstitial to frags - alt? 94.4-.7 - QA vn, 3 cm, irreg 20 CA, wh-gy, banded, grn fuch? assoc; 95.9 - 3 mm vn, gy brn at 60; 96.2-.3 - 2 vns at 80, < 4mm; 97.1 - wh QV at 40, 0.5 cm w/ py/flesh col alt assoc; 97.55 - 1 cm wh/brn vn, irreg at 70-80; 97.8 - gy vn, 1 cm at 85; 98.5 - 1-1.5 cm vn, red brn at 60; 98.8- - 1 cm wh gy vn at CA 35;
	99.0	102.8	**Sst/Silst**	lt-m brn	mod chl/ strong sil	f-mg	massive	fg diss py - 1% + py in clasts,	100.2-.7 - more chloritic; more cgt, minor tuff to bottom section, fg; QA vns throughout; 99-100.2 - QA vns along CA, 1 cm w/ 1 2-3 cm (2nd); wh/banded, w gy selvages, disrupted/discont in part; 100.3-.5 - 0.5-1 cm grn/wh disrupted vn; 101.1-.6 - QA vn, 0.5-3 cm at 10 CA, gy-wh w/ orange,, gy selvages, disrupted at end; 102.2-.6 - QA vn along CA, 1-2 cm; gy/wh, chl brecc in centre vn;
	102.8	106.9	**Conglomerate**	m gy grn	strong sil	mg	massive	fg diss py - 1%	minor silst; minor vns - not banded, many orange rhy frags/clasts

Hole #	From (m.)	To (m)	Rock Type	Colour	Alteration	Grain Size	Structure	(%) Mineralization	Contractor: White Wulf Drilling Comments
	106.9	118.0	**Tuff / Silst**	m gy grn	mod chl/ strong sil	f-mg	massive, contact CA 80	fg diss py 1-2%	unit lt gy/grn to 112.8 then m bg/gy to 114.6 then m gy grn to dk gy to 116 then m-lt bg to end; core is badly broken/blocky 112.8 - end section; 107.3-108 - 0.5 cm QA vn along CA, irreg, discont, gy/wh/orange; 109.15-109.25 - 4 mm QA vn at 30, wh/brn; 109.3 - 5-6 mm gy QV at 35; 109.9-110 - gy grn Si bed at 60; 111.7-.8 - 1-1.5 cm gy Qtz breccia vn at 55, wh selvages; 112.8-113.1 - gy fg vns in vfg silst, wh-grn selvages; 116.4 - 3-4 mm QA vn at 20; 116.6-.7 - mafic dike at 40; 116.7 - fine breccia along core and in dike; 116.7-117.3 - 5% vns, wh/gy, broken/discont; 117.5-118 - mixed bg sst, chl prevalernt;
	118.0	134.7	**Cgt / Sst**	m bg/brn-red	strong sil	fg	brecciated, top to 121 m; 129-end silst/sst CA 80	py, diss/ff - 1-2%	rhy frags 20%+, orange red; v. minor vns, gen along CA; 129-end - silst/sst prev to bottom section; some tuff sections, all silicified; chl prevalent in tuff sections / more prevalent to bottom section; 119.75 - 2-3 cm Si band at 75, chl ff's; 118-120.7 - brecciated, chl ff's;
	134.7	150.6	**Tuff**	dk gy red	mod chl strong sil	f-mg	silst interbeds, 70-85	py, diss 1-2%	minor silst/sst interbeds; Chl prevalentas spots/frags throughout; some areas of QA vning - 135.4-.9 - 7 vns, 3-4 mm, CA 30-85, mainly 80-85; 138.2-.9 - 3 vns at low angles(15-25), 0.5,0.3,0.5 cm, banded; 140.7-.9 - minor vns along core; 143.5-144.4 - 3/4 mm QA vns along CA, irrge/discont; 145.2-.4 - 3 - 4 mm vns along CA; minor vns to bottom contact;
	150.6	155.3	**Sandstone**	reddish gy	mod chl / strong sil	m-fg	mainly massive, beds 75-80; grad contact	py, diss 1-2%	some sst above, tuff below; coarser grained nr top; reddish due to rhy frags; 155.1-155.3 - well bedded sst, chloritic, soft; minor QA vns 152.4-.6 - 2 vns <0.5 cm at 70/60;
	155.3	156.1	**Conglomerate**	reddish grn	strong chl / mod sil	m-cg	massive	minor diss py < 1%, also in clasts	red hematite in groundmass;
	156.1	160.7	**Mafic Dike**	m-dk grn	weak chl	fg	contact 60	occasional, scattered py bleb	chilled/silicified margin; 157.5-.8 - QVw/ epidoteat 10 CA, no banding; qtz ep vning throughout; lower contact - Qtz ep vn at 50;
	160.7	164.9	**Sandstone**	lt brn-orange brn	weak chl / strong sil	mg	massive	diss py - 1%	minor cgt; variably vn'd w/ mainly qtz chl vns; 160.9-161.4 - brecciated w/ QV's; 161.7 - calcite vn w/ hex xls on fracture, some blk metallic; chl on fractures; other areas of xline calcite
	164.9	174.1	**Conglomerate**	orange grn	strong chl / sil	cg	massive	diss py 1-3%, some areas 5%+	unsorted, silicified; minor variable QV's, not banded, gen qtz/chl; 166.4-.165.3 - some poss QA vns, crm wh w/ Ad? 166.4-.9 - QA vn, banded, crm/clr along CA; 168.1-168.8 - crm wh QA vn along CA; 168.8 - chl clast? w/ pink fspar xls? 169.6-.9 - brecc QA vn, irreg, discont; 171.5-173.5 - QA vns more prev, gen irreg/discont; gy wh, some along CA, main areas - 171.8-172, 172.5-172.7, 173.3-174, gen narrow to 0.5 - 3-4 cm, some brecc;
	174.1	191.6	**Mafic Dike**	m-dk grn	mod chl	f-mg	Up contact CA 45;	minor blebs py	fg on contact, chilled?; scattered qtz/ep, qtz/calcite vns throughout; chl ff's w/ py as blebs, ff's; 185.1-.3 - qtz/ep vn, 3 cm at 25; qtz calcite vns 185.3-186.2 at 10-35 CA;
	191.6	204.4	**Sst/Silst/Cgt**	m gy; 203.5-204 - lt gy grn fspar ?	mod chl / strong sil	f-cg	mainly massive, beds 80-85	minor diss py <1%	mixed, sst/cgt, minor silst/tuff; scattered QV's and other vns; 192.5-.7 - irrge QA vn, banded, to 1-2 cm, gen <0.5 cm; 193.7 - 3 cm qtz/ep vn at 20-25; 195.8-197.1 - scattered vns along CA <0.3 cm; 198.6 - 2 cm qtz/chl vnat 45; 200.2-.6 - 3 QA vns, <0.5 cm at 55-70 w/ minor "ging" bands; 201.5 - 1 cm vn along CA; 202.6-203.5 - many, max 3 mm QA vns along bedding, CA's 75, w/ chl;
	204.4	213.0	**Quartz Breccia**	grn-wh	strong sil	vfg	brecciated	minor dis py, black "ging" vns	highly silicified throughout, cherty; wh QV's, some banded w/ "ging" banding, Xcutting/brecciated; groundmass is cherty; chl prevalent as ff's, multiple vns/types; 209.9-210.3 - more gy metallic (ging?) / chl
	213.0	213.5	**Siltstone**	lt gy bg	wk chl / strong sil	fg	beds 55-60, disrupted / brecciated	fg diss py <1%	healed breccia, silicified; some wh QV's, minor banding
	213.5	215.6	**Tuff**	m gy grn	strong chl/sil	mg	gen massive, 214.5 - silst beds at 85	v minor diss py as blebs	chl prevalent as clasts / frags/ff's although unit is silicified; 214.5-.8 - silst, finely bedded; wh QV's sometimes var. banded throughout; some patches dk gy grn - chl?
	215.6	216.7	**Siltstone**	lt-m bg	wk chl / strong sil	fg	beds 70-75	minor diss py <1%	216-216.7 - brecciated w/ grn chl as ff's; wh QV's prev - irreg/discont throughout, some banding - wh/crm;
	216.7	218.7	**Conglomerate**	crm/gy patchy	mod chl / strong sil	m-cg	massive	py - diss/ff 1-2%; 217.2 - 3 qtz/p vns, 1 cm each at 40	chl interstitial throughout section; wh QV's assoc. w/ brecc;
	218.7	220.0	**Breccia/Silst**	m gy-brn bg	wk chl / strong sil	f-mg	beds - 55, brecciated	py - diss, bands 1-2%	218.7-219.4 - strongly brecciated w/ broken/discont wh/gy QV's; brecc vns - qtz w/ silst frags esp to bottom section, some chl assoc.
	220.0	221.3	**Sandstone**	m bg brn	strong sil	fg	massive, brecc in places	py - f diss / ff 1-2%	more brecciated at top section; breccia vns, wh qtz to bottom
	221.3	222.5	**Breccia**	lt-m crm gy	strong sil	vfg-fg	brecciated	py f diss/ff 1-2%; 222 m - 1 cm band py	intensely brecciated w/ gy/wh QV's to 222 m then similar but less brecciation; host - gy silst ? 222m - 1 cm wh QV at 65;
	222.5	224.9	**Siltstone**	lt-m gy	strong sil	vfg	gen 65-70, some finely bedded to 30	finely diss <1%	cherty, cryptocrystalline silica, concoidal fractures; wh QV's - some banded, variable but gen CA 60; some more highly fractured areas;
	224.9	225.9	**Conglomerate**	lt-m gy	mod chl / strong sil	m-cg	massive; contact 50	py as bands, 225.6 - 10% over 4 cm at 70 CA	to 225 - sig chl as ff's/clasts cut bt wh QV's, var to 40; 225.7-.9 - completely silicified
	225.9	226.9	**Sandstone**	m gy grn	strong sil	fg	brecciated		fine vns - qtz/Ad? ff's;
	226.9	227.1	**Fault Zone**	m-dk gy grn	mod chl/sil	f-mg	banded gouge, contacts 50-60	py as blebs w/ brn qtz - 2%	soft, chl at top; silicified at bottom, sharp contacts;
	227.1	229.7	**Siltstone**	lt bg gy	strong sil	vfg	massive w/ remnant bedding at 75; contact 60	f-vfg diss py <1%	massive w/ remnant bedding; cherty w/ concoidal fractures; var wh QV's throughout, irreg/discont; 227.2, 228.5-229.7 - some poss "ging" bands

Hole #	From	To	Rock	Colour	Alteration	Grain	Structure	(%) Mineralization	Contractor: White Wulf Drilling
	(m.)	(m)	Type			Size			Comments
	229.7	231.3	**Conglomerate**	lt-m gy	strong chl/sil	f-cg	massive	diss py - 1%; some py vns - 231m 2 mm vn at 30	some tuff sections; 230.3 - end - orange red rhy clasts prevalent; minor wh QV's, discont/irreg;
	231.3	233.3	**Siltstone**	lt-m gy	strong sil	f-mg	well bedded 70-80	py - finely diss/vns/bands 1-2%	upper contact irreg, bottom contact gradational; fspar vns (Ad?) Xcutting bedding, irreg/discont;
	233.3	236.2	**Sst/Silst/Cgt**	lt gy	strong sil	f-mg	brecciated	diss py <1%	brecciated / broken section, variable qtz infilling; 235.4-.8 - massive QV/Si alt - crm bg w/ broken bands/ff py
	236.2	237.0	**FZ - silst**	m-dk gy grn	mod chl	f-mg	sheared CA 55-65	diss/ff py 2-3%+	sheared / boudinaged FZ contact; interbedded dk gy/grn beds/bends; dk bands carry extensive py;
	237.0	248.7	**Siltstone**	m-dk gy grn	mod chl	fg	beds gen 65-75, some to 45	v. minor fg diss py <1%	finely bedded throughout, beds mm scale; gen consistent bedding; v minor qtz vns, no alt or mineralization assoc.; non magnetic; 245.7-.9 - qtz calcite vns as ff's; no assoc sulphides, CA 25-45.
	248.7		**EOH**						

Silver Spruce Resources Inc.

Project: Big Easy	Easting	710202	NAD 83	Az	270	Core Size: NQ	Start: Nov. 19/14
DDH BE-14-16	Northing	5348594		Dip	-75	Logged by: Peter Dimmell	End: Nov. 22/14
L 84 N, 1+38.5 E	Elev (m)	115	Length (m)	130.2		Samples: 159471 (1)	Reflex Test: 100.6 m - 282.2 (301.2), - 79.7, 51189, , , (questionable)

Hole #	From (m)	To (m)	Rock Type	Colour	Alteration	Grain Size	Structure	(%) Mineralization	Contractor: White Wulf Drilling Comments
BE-14-16	0.0	8.2	**Overburden**						boulders - red unaltered sedimentary; minor granite; grn, alt (sil) sed units;
	8.2	20.6	**Cgt/Sst**	bright red	none	m-cg	beds 55-75, mainly 65-70	nvs	interbedded cgt/sst - red, hematitic, polymictic; siliceous; 11 m - 2-4 mm, qtz fspar vns at CA 25, scattered calcite vns, 1-3 mm, irregular; 27.5-27.7 - qtz calcite vns, 3-4 mm at CA 20;
	20.6	35.1	**Sandstone**	brick red	weak sil	m-cg	beds 65-80,	nvs	34.6-35.6 - 1-3 cm qtz/calcite vn along CA; QV's like epithermal; rest - scattered qtz calcite vns
	35.1	48.2	**Conglomerate**	brick red	none	m-cg	massive	nvs	ploymictic, mainly coarse grained; 44.8-45.5 - bleached/silicified - light colour/finer grained;
	48.2	50.9	**Sandstone**	brick red	none	f-mg	beds 65-75	nvs	siltstone beds to bottom section;
	50.9	60.0	**Sst/Silst - mix**	brick red	none	m-fg	beds 55-60	nvs	interbedded sst/silst w/ minor cgt
	60.0	65.5	**Tuff / Sst**	brick red	chl	m-cg	beds - not well defined - 60	nvs	dk grn-blk chl clasts in red groundmass, less tuff last m; calcite vns 35-85;
	65.5	69.2	**Conglomerate**	brick red	none	m-cg	massive	nvs	gradational contacts top and bottom;
	69.2	82.6	**Sandstone**	brick red	none	f-cg	beds 35-65 variable	nvs	mainly sst, f-mg, some interbeds cgt/siltst; 80.4-81.4 - calcite vns to 1 cm wide (CA 20-50);
	82.6	93.9	**Conglomerate**	brick red	none	mg	massive, minor beds 50/55	nvs	indurated; polymictic, minor calcite vns 30-70 CA;
	93.9	104.3	**Sandstone**	brick red	none	f-mg	variable 50-65	nvs	minor cgt/silst;
	104.3	110.0	**Cgt/Sst**	brick red	none		beds 60	nvs	mixed cgt/sst, some silst; scattered calcite vns, variable angles; 99.4-103.4 - siltstone beds up to 1 cm wide;
	110.0	126.4	**Sandstone**	brick red	weak sil	f-cg	beds variable 50-70	nvs	gradational contact; mainly sst with narrow cgt beds, minor silst; scattered calcite vns along CA to 75-80; lower contact "baked" to m grn 0.1 m from contact;
	126.4	130.2	**Mafic Dike**	m-dk gy grn	chl	f-mg	contact 40	nvs	chilled contact; reddish colour for 1st m then dies out; qtz/calcite/ep vns to 0.5 cm max at CA's 25-35; red hematite on fractures.
		130.2	**EOH**						

Silver Spruce Resources Inc.

Project: Big Easy	**Easting**	710128	**NAD 83**	**Az** 270	**Core Size: NQ**	**Start: Nov. 23/14**
DDH BE-14-17	**Northing**	5348008		**Dip** -75	**Logged by: Peter Dimmell**	**End: Nov. 28/14**
L 78 N, 1+25 E	**Elev (m)**	110	**Length (m)**	267.3	**Samples: 159472-159645 (174)**	**Flexit Test:**

Hole #	From (m.)	To (m)	Rock Type	Colour	Alteration	Grain Size	Structure	(%) Mineralization	Contractor: White Wulf Drilling Comments
BE-14-18	0.0	4.6	**Overburden**						boulders of silicified / mineralized sst/cgt - cherty
	4.6	9.2	**Sandstone**	lt gy	strong sil	f-mg	mainly massive, beds - 70	diss py 1-2%, blebs, euhedral	mainly sst, some silst, strongly silicified; minor vns - 6.7 - 0.5 cm QV wh/brn selvages w/ blebs py; 8.5-.6 - 3-4 cm QV, grnwh w/ dk grn selvages - chl?
	9.2	10.1	**Conglomerate**	lt-m gy	strong sil	m-cg	mainly massive, 10.1 beds at 45	diss py 1-2%, as above	minor sst; 9.4-.5 - irreg QV, 3-4 mm at 15;
	10.1	11.9	**Sst/Silst**	m gy grn	mod chl	f-mg	beds var to 60	diss py 2-4%, some bands	soft/chloritic; some silicified sections up to 0.1 m; minor cgt
	11.9	21.4	**Sst/Silst**	lt-m gy	strong sil	f-mg	beds 65	diss py 1-2%, also ff's w/ moly	some fine cgt sections; scattered wh QV's, 13.8 - 1.5 cm at 40 Xcutting 3 mm QV at 65; moly/py ff's, slickensided, 13.1-.5, 14.4-.7, 16.5-17.1, along CA w/ wh/grn QV, 17.1-.6, 18.8-19.2 vns/ff's irreg, 19.6-21 - chert assoc.
	21.4	25.3	**Silst/Sst/Chert**	lt-m gy	strong sil	f-mg	irreg to 60	minor diss py <1%	interbedded sst/silst/chert (coll Si), chert 30% of section; 22.6-.8 - 2 cm wh QV w/ grn blk bands at 30;
	25.3	27.4	**Sst/Cgt**	lt-m gy	strong sil	mg	gen massive	diss py 1-2%+	unit cut by qtz/py vns, variablemto 35-40, gen narrow <3-4 mm; 27-28 more cgt; 26 - 2 cm wh QV at 35; 26.5-27.4 - qtz/py vns, narrow, <4 mm, irreg;
	27.4	31.5	**Conglomerate**	lt-m crm	strong sil	f-mg	mainly massive, some beds sst to 70	diss py 1-3%	mainly cgt, minor interbeds sst/silst; 30.7 - becomes m gy grn, contact 90 but stepped, crm up hole to gy grn below; some wh QV's 50-65;
	31.5	36.0	**Sst/Cgt**	m gy	strong sil	f-mg	beds 60	fine diss py 1-2%	mainly sst, some cgt interbeds; 32-32.5 - wh QV's (4/5) at 50; 35.8 - 1 cm vn at 30 + along core, dk gy, banded;
	36.0	41.4	**Sst/Silst**	m-dk gy	strong sil	f-mg	gen massive	diss py 1-2%	interbedded sst/silst, minor fg cgt; 38.5 - 3 cm banddk py/Ad - flesh colour; 36-37 - broken/disrupt vns, sig alt (some sericite) w/ assoc. py; scattered QV's through section; 39.5-39.8, 40-41.4 - bleached, assoc. w/ narrow QV's??
	41.4	57.8	**Cgt/Sst**	lt-m gy grn	strong sil	f-mg	mainly massive, beds at 70	diss py 1-2%	interbedded cgt/sst, minor silst; some Ad ??\ bands at 43.1, at 70; 44.8-45 - 0.5 cm wh QV along core; 47.3-.85 - silst CA 75; 48-48.3 - QA vn, 1 cm or <, gy/wh at 20; 48.9-49.1 - similar vn along core; 51.6 QV, gy wh w/ fg diss py, 2 cm at 75; wh QV's scattered throughout at 45; 53.3-54.4 - crm sst/cgt w/ dk gy vn frags throughout, sericite, some moly ff's; 54.4-.5 - QA vn, brecciated, top contact sheared, gouge at 20, bottom - 30; 57.5 - 7 cm bed bg sst, beds/contacts 75/60;
	57.8	79.1	**Sst to Silst**	m gy grn	strong sil	m-fg	mainly massive, beds at 60; 75.2 - beds at 65-70	62-62.1 - 2 cm py vn, semi massive, along core	interbedded sst/silst w/ silst increasing to bottom of section; scattered vns, mainly gy qtz w/ fg py, narrow 1-2 mm, along core; 58.4 - 3 cm qtz breccia; 59-59.3 - ser/chl ff's; 60 m - 1-2 mm qtz/py vn along core; 60.1-.3 - 1 cm wh QV along core; 60.8 - 2 cm wh qtz brecc vn at 70; 60.9-71.2 - 1 cm wh QV w/ yellow ser at 20; 61.5-65.5 - var bleaching assoc. w/ QV's, 62-63 strongest, contacts 65/40/55; 67.7-68 - QA vn along CA, selvages Ad? (flesh colour mineral); 65.5 - scattered vns, irreg to CA 60, 66.5 - < 1 cm vn at 20 w/ Ad/py; 67.7-68 - QA vn along CA, Ad? on margins, some Coll Si ?? 69.1 - 1 cm QA vnat 60, Ad alt (diss flesh colour), 70.5, 71.7-.8, 74-74.2, 74.6-.8; 72.9-73.4 - QA vn + gy-crm coll Si, core is broken; 75.2 - more silst interbedded w/sst, cgt interbeds to bottom section
	79.1	82.8	**Conglomerate**	m-dk gy	strong sil	m-cg	contact 70; massive; 79.9-80 beds chert at 70;	diss py 1-2%	79.9-80 - gy coll Si; 81.8-92.8 - more coll Si, frags vns/beds, banded
	82.8	84.9	**Colloidal Silica**	m-dk gy	strong sil	vfg	beds 65-70	diss py, patchy	mixed vns / coll Si ?? 84.5-.9 - banding/bedding 75-90, gy-crm beds/vns
	84.9	94.2	**Silst/Sst**	m-dk gy to m gy grn	strong sil	fg	beds 70-80; 87.4 - 75; 87.8 - along core to 25;	fine diss py 1%	87.4-88 - silst, well bedded; 87.8-88.3 - QA vn, brecciated, 88.15-88.3 - main vn, 7 cm wide; 88 m - gouge, 3-4 mm CA 50; 87.4-90 - siltst; 89-89.4 - irrge / discont QV's, wh/gy; 90-94.2 - sst, becomes broken 93-94.4, some LC?
	94.2	96.6	**Breccia**	m gy grn crm ly gy	strong sil	f-cg	brecciated	94.4-95.2 - vfg py ff 2-5%; 95.2-96.6 - py didd/ff 3-4%	94.4-95.2 - crm-wh frags in a gy pyritic groundmass w/ vfg Si; 95.2-96.6 - m gy massive breccia w/ ghost breccia textures (rehealed).
	96.6	106.4	**Silst/Tuff/Sst**	lt-m gy	strong sil	f-cg	gen. well bedded, 75-80	py - diss/ff 1-2%	minor cgt beds; tuff sections become more prevalent; QA vns cutting unit, gen low angles; 98.8-100.2 - gen along core; 100.8-101.1 - 10-15% - 1cm gy blk; 103.2-.3 - 4/5 mm gy wh w/ blk selvages at 40; 104.8 - 3cm at 45, bleached margin (wallrock),; narrow vns continue to 105.3; 105.8-106.4 - lt gy crm vn w/ dk gy blk selvages, vfg, w/ breccia; some flesh colour alt to bottom
	106.4	109.8	**Tuff**	m gy grn	mod chl / strong sil	m-cg	massive		chl as clasts/diss; 107.75-108.7 - vns along CA, m-dkgy, 3-5 cm to narrow <3mm;
	109.8	115.8	**Sst/Silst**	m gy grn	strong sil	f-mg	beds 75-80		interbedded silst/sst, some cherty sections, some tuff sections w/ chl to bottom; 110.8-111.2 - wh/gy QV w/ gy selvages w/ py; 112.9-113.4 - gy wh QV at 15, 6/7 cm, broken frags to bottom
	115.8	116.6	**Colloidal Silica**	lt-m gy	strong sil	vfg	well bedded 60-75	fg diss py/bands 1-2%	interbedded w/ clastic seds to bottom
	116.6	121.0	**Sst/Silst/CS**	lt-m gy	strong sil	mg	beds 75-80	fg diss py 1-2%	becomes coarser, more cgt to bottom; 119.6-120.5 - brecciated CS w/ patchy alt (bleaching), strong py banding at bottom; scattered vns throughout - 116.6-.7 - gy/wh, irreg121.9-122.2 - 2, 4-5 mm banded QA vns along core, irreg, discont; 120.8 - vn w. gy selvages, irreg to 3-4mm; 123.1-.5 - gy QV along CA; 124.5 - gy QV, 5 mm at 90;
	121.0	127.5	**Conglomerate**	m gy	strong sil	mg	silst/sst interbeds 70-85	fg diss/ff py 1-2%	polymictic; minor interbeds sst/silst up to 4-5 cm, mainly 1-2 cm;

Hole #	From	To	Rock	Colour	Alteration	Grain	Structure	(%) Mineralization	Contractor: **White Wulf Drilling**
	(m.)	(m)	Type			Size			**Comments**
	127.5	137.5	**Siltstone**	m gy	strong sil	f-mg	contact CA 75; beds (top) 55	minor diss py, bands/vns scattered mm scale	top section well bedded, becomes more massive, mg; 132.5 - unit becomes patchy w/ med crm coloured spots, irreg/discont; scattered vn sections / bleached areas - 127.5 - crm; 128.1-.2 - crm vn frag; 128.5-129.7 - vns prev gy, vfg - narrow ff style; 129.2-.7 - lt crm section cut by irreg/discontgy qtz/py vns, some banding; 130.4-131.4 - py as bands/vns/ff's 5%+; 132-132.7 - same;
	137.5	144.5	**Silst/CS**	m gy grn	strong sil	vfg	massive	minor diss py - 1%	patchy/blotchy, lt-m gy - dk gy w/ crm colour blotches; 139.9 - qtz chl vn, 1.5 cm at 15;
	144.5	147.1	**Silst/Sst/Cgt**	m-dk gy	strong sil	mg	massive	py - diss/ff 1-2%	contact irreg, frags cherty silst nr top, aslo 145-145.2; 146.2-.8, 148.8 - QA vn, frags/ discont, 3-5 mm, along core;
	147.1	150.6	**Conglomerate**	lt-m gy	strong sil	mg	gen massive, interbeds sst 55-60	py - diss 1-2%; 147-147.8 - moly/py ff along core;	gradational contact; 147.3 - scattered QA vns, gy/wh, 3-4 mm at 30;
	150.6	174.0	**Sst/Cgt**	lt gy crm	mod chl / strong sil	sst f-mg,, cgt - m-cg	gen massive, beds - 65-75	py - diss/ff 1-2%; 171.4 -.5 - py ff network to 20-30%	interbedded sst/cgt; 152.3 - becomes more chloritic; v minor vns, mainly as frags; 150.6-.7 - QA vn frags; 152.3-.6 - chl ff'sm dk grn-blk, at 25/75; 153.1-.7 -, 153.9-154, 158.7 - 2 cm chl/py at 40; 161.4-.5 - QA vn, w/ wh/gy selvages at 20; 166.7-167.6 - silst, fg, dk gy; 167.55-168.5 - QA vn to 3 cm wide, some fg gy qtz; 169.6-171.2 - QA vn along core, some assoc. brecciation; 172-173.1 - QA vn along core, irreg/discont, some breccia;
	174.0	185.0	**Sandstone**	m gy grn	strong sil	mg	massive, nvb	diss py 1-2%	182.1 - c; hl as ff's, dk grn w/ heavy py; 177.1-.8 - QA vn, 3-4 mm, gy/wh selvages, irreg along core w/ assoc py;
	185.0	186.9	**Conglomerate**	m crm grn	strong sil	mg	massive; 231.8 silst bed - 70	diss py 1-2%	chl ff's as above;
	186.9	193.9	**Sandstone**	m-dk gy grn	mod chl / strong sil	m-cg	beds 60-70; 186.9 contact at 75	diss py 1-3%, chl zones up to 10-20% py	variably chl along fractures; sst silicified; chl zones w/ v strong py to 20%; chl "shears" along core to 70; 186.9-187.2 - fg silst/coll Si w/ chl/py; 192.45 - 3 mm QA vn at 45;
	193.9	213.8	**Sandstone / Shear Zone**	dk grn	strong chl / weak sil	mg	py bands at 35;	diss/ff py 10-30%, heavy diss to ff to semi-massive blebs/bands; 200-200.2 - moly ff, slickensided, at low angles to CA	mainly chloritic (dk grn) sst, heavy py throughout chl sections, chl alt irreg/discont, along core to 25 and 40-50 CA; minor sil sst sections; some brecciation; shear zone ?? areas of silst/chert - 207.1, 207.2, 210.3-.4, 210.7-211;
	213.8	214.9	**Mudstone**	m-dk grn	strong chl / weak sil	vfg	irreg/discont	fine diss py - 10%+; 214.1, 214.5-.6, 214.7, 214.8 - areas of semi-massive py,	pyritic mudstone, chloritized, very soft
	214.9	224.7	**Colloidal Silica**	lt gy grn	strong sil	f-vfg	contact 40; beds 45-65	v minor diss/ff py	colloidal Si/silst; some bedding; cut by wh QV's at 25-40CA; scattered poss QA vns, narrow <0.5 cm; 220.8-221.3 - breccia zone, coll Si/cgt/sst w/ gy vns
	224.7	230.0	**Sst/Cgt**	lt-m gy bg	strong sil	f-mg	massive	diss py 1-2%; ff moly	massive sst unit cut by irreg/discont hairline (mm scale) fractures w/ gy met (moly?) and chl; 226.2-228.1 - QA vns, gy/wh w/ gy bands along core; 229-230.8 - as above QV's + py/chl vns along core;
	230.0	231.4	**Siltstone**	m brn bg	strong sil	vfg	massive, nvb	diss/ff py 1-2%	230.9-231.4 - brecciated fg bg silst; more brecciated w/ chl to bottom
	231.4	233.1	**Conglomerate**	m gy	strong sil	mg	231.8 - silst bed at 70	diss/ff py 1-2%	minor chl as vns/clasts
	233.1	239.0	**Sst/Silst/Coll Si**	m gy-dk grn blk	strong chl	f-mg	silst beds 60-80	moly ff at top of section	mixed sst/coll Si/black mudstone; brecciated or soft sed deformation; frags of each mixed in the other; some pyritic mudst sections to bottom; 236.5-.8 - FZ, qtz chl, 3 cm gouge at 65;
	239.0	247.8	**Mudstone (pyritic)**	m-dk grn	mod chl	fg	beds 45-55	heavy py, f-vfg in mudst 5-10%+; heavy py throughout, moly ff's in section	pyritic mudstone w/ some silst sections; some brecciation; 241.9-242.75 - silst breccia; 243.1-.9 - silst, sil, some vns; 242.8 - FZ in mudst, gouge 3 cm at 85/60, chloritic; 239 - mudst becomes brecciated/ s sed deformed; 247.25-.35 - well bedded section sst/mudst at 65; 247.7-.8 - as above CA 80;
	247.8	255.5	**Mafic Dike? / Volc.**	m-dk grn	mod chl /epidote	f-mg	massive, contacts - 55	nss	cut by extensive qtz epidote vns, irreg, discont; contacts finer grained - chilled ?
	255.5	256.6	**Siltstone**	lt-m gy grn	mod sil	fg	contacts 85/65, beds - 65	nss	cut by QV's - irreg, discont; 256-256.2 - mafic dike - as above
	256.6	267.3	**Mafic Dike / Volc?**	m-dk grn	mod chl/epidote	f-mg		nss	as above, QV's throughout, irreg, discont., no associated mineralization
		267.3	EOH						

Silver Spruce Resources Inc.

Project: Big Easy	Easting	710099	NAD 83	Az	270	Core Size: NQ	Start: Nov. 29/14
DDH BE-14-18	Northing	5348105		Dip	-45	Logged by: Peter Dimmell	End: Dec. 6/14
L79 N, 0+90 E	Elev (m)	113	Length (m)	157.9		Samples: 159646-720 (75)	Reflex Test: 100.6 m - 270.5 (mag 289.5), -46.1, 50718, 68, 3

Hole #	From (m.)	To (m)	Rock Type	Colour	Alteration	Grain Size	Structure	(%) Mineralization	Contractor: White Wulf Drilling Comments
BE-14-18	0.0	11.0	Overburden					minor QA vns, py diss in boulders	mainly altered / silicified sedimentary units - boulders, minor granite cobbles
	11.0	15.4	Cgt/Sst	lt gy grn	sil	sst - cg, cgt - fg	massive, QV CA - 20	diss py 1-2%	oxidized (surface weathering); broken core; mainly cgt f-mg; some cg sst; 13.5-13.6 - 1.5 cm wh/cl QV w/ gy selvages - irreg.
	15.4	70.0	Sst/Silst, minor Cgt	lt-m gy grn	sil	f-mg	beds 30-40, contacts 45/35	diss py 1-2%	oxidized to 17.5 m; interbedded gradational sst/silst, minor brecciated top section to 16.1m - sharp contacts;cgt 18.8-19.3; 27.4 - unit becomes m gy; 37 m - bedding 40; 44.2-46.3 - cgt - m-cg w/ flesh coloured alteration Adularia?, silst beds (35-65); 53.2 - 65+ - interbedded sst/cgt/silst - silst - well bedded (40-65) - diss py 1-2%; vns - 18.2-18.4 - 0.7 cm gy wh (35); 16.8-16.9 - 0.5 cm red brn (30); 20.3-20.45 - 2/3 vns - red brn to wh w/ gy selvages - 1.5 - 0.5 cm (45);**21.9-22 - 10 cm vn, brn bg to wh-dk gy(70)**; 22.1 - 3 vns wh-gy 0.5, 1, 0.3 cm (60); 25.2-25.5 - dk gy 2/3, 3-4 mmvns/ff's - py?; 35-35.1 - 1 cm wh grn (50); 35.2-35.3 - 1 cm gy QV at 35; 47.1 - 1 cm gy wh; 47.2 - 5 cm banded QA - bg crm , gy selvages (45), 1 cm gy wh (35); 50.4 - 51.4 - Qtz chl vns along core to 15 CA, grn wh, no banding, nss: **53.9-54.2 - banded QA vn - 25 cm (60)**; 61.5-61.6 - banded 2 cm vn, gy wh (40); 67.3-68.8 - 7/8 wh QV's - mm scale; 70.2-70.3 - 1 cm QA, banded w/ silicification associated (40); other narrow vns noted / not sampled;
	70.0	71.6	Colloidal Silica (CS)	m - dk gy	sil	vfg	massive	vfg diss py - 1%	top contact - gradational, bottom - mixed w/ silst - dk gy;
	71.6	77.8	Silst/Sst	m gy grn	sil	f-mg	silst beds - 25-45	diss py 2-3%, some ff CA 75	silst grading to mainly sst; silst gen well bedded (25-45); 72-4-72.7 - 2/3 QA vns - mainly wh, disrupted; 77.55-77.75 - 15 cm QA vn w/ CS, black "ging" bands (75).
	77.8	100.0	Cgt/Sst	m gy grn	sil	mg	mainly massive, silst beds - 50	diss / ff py 2-3%	mainly cgt w/ silst interbeds, 86 m - more sst; Vns - 80.2-80.5 - 3 wh QA vns - no banding, gy/wh selvages, irreg/discont; **84.8-85.3 - QA vn - banded - wh/crm/gy/bg/blk w/ emerald grn ff on one band (35/30)**; minor vns - 86 - blk-wh; 87.45-87.6 wh/grn - 1-3 cm, banded (60); 89.5-89.9 - blk-gy w/ sulphides - along CA to 20; 90.5 - grn wh, minor banding, 1-2 cm (55); **89.9-90.25 - QA vn - banded, wh/brn/grn, ging bands (45/40)**; 91.6-92 - 3/4 wh Qv's - minor banding (35); 92-92.15 - QA vn - gy - dk gy, banded (50); 94.3-94.8 - 4 QA vns, 3 - 1cm, other 3 mm (50-60).
	100.0	102.6	Breccia / FZ	lt-m gy grn	sil	f-mg	brecciated / LC - 40	py diss in frags - 1-2%	brecciated silst; 101.9 - 102.6 - strongest breccia; nss in breccia
	102.6	157.9	Sandstone	m-dk gy	sil	m-cg	beds - 55; 109.2 - 60; 120 m - 5-25	diss py - 1%; 154.5-.9 py ff's along core; Mo ff's 130.3-130.6, 154.9-155.4	generally massive sst - silicified; 107.5 - interbedded, irreg. dk gy silst (45-70) w/ scattered broken vns; 108.3-108.8 - sst brecciated, finely vn'd w/ fg py - variable; 114.9 - 1 m? LC; 140.5-141.5 - core is broken / brecciated w/ pyritic slickensides, yellow grn sericite prev. on fractures; 144.2-144.8 - unit becomes bg w/ irreg/discont vns; 146.5 - cherty/broken/brecc - minor vns; 149 - bg contact (70); 150.6 - 151.5 - core is broken / brecciated; 154.9-155.4 - Mo ff's throughout, some brecciation, becomes more cgt below 150 m; QA vns - 103.05-103.25 - 3 @ 1 cm (40); 104.2 - 3 cm - gy crm, well banded (50); 105.1 - 3 vns, 1 - 1 cm, wh/crm/grn, minor banding (40); 107.2 -107.3 - 4 cm QA vn, gy to wh (60); 110.3-111.3 - 10/11 banded wh QV's < 1 cm, some QA (along CA to 50); 112 (45); 113.2 (70); 112.75-.85 - 5 cm QA crm/gy, wh selvages (55); **115.15-115.5 - 20 cm QA vn, well banded, crm/brn/gy/orange**; 116.2 - 2, 4mm wh vns (50); 117.4 - 0.5 cm, wh irreg, QV (70); 120.3-.5 - 4 cm banded QA, crm-orange w/ black bands / silver metallic? (45/40), 2 cm ly gy QV 2 cm below(35); 120.6 - vns < 5 mm (50/55); 125.5-.7 - 3 vns, 1/0.5/0.3 cm (70); 126.2-.4 - banded QA vns, 1 4cm others narrow (35-40); 126.85-.95 - 3 cm QA vn wh/blk, banded; 130.3-.6 - 3/4 mm scale QV's / FF's along CA w/ Moly; 132.2-.4 - gy / blk qtz/py vn + 1 cm gy/wh qtz vn (40); 135.2 - 2 QA vns - gy/wh (60-70); 135.8-136.1 - 3 QA vns, 1, 0.5, 0.4 cm, gy/wh, some banding (55-65); 137.3 - 2 cm QA vn, gy/wh (45); 138 - 1 cm/ gy vn (50); 138.5 - 1 cm QA vn, gy/wh (50), some py ff's below w/ associated bleached areas a;long vns to 139.3 m; 142.4 - 2.5 cm gy vn ((55); 142.9-143.3 - 3 vns 0.5/4/2 cm, gy wh - dk gy (60,70,50); 143.95 - 1 cm gy/crm vn (65); 148.1 - 2 vns 0.5/1-2 cm, - gy/wh (70); 148.4 - broken vns; 148.5 - 3 mm vn; 149.5 - broken vns; 150.3-.4 - 6 cm vn, 3 bands - crm/m gy/crm (45); 152.4-.5 - 4 QA vns , 0.5 cm (65); 154.5-.9 - 4 vns, QA/QV's, max 1 cm (45-80), py ff's along core;
		157.9	EOH						

Silver Spruce Resources Inc.

Project: Big Easy	Easting	710157	NAD 83	Az	270	Core Size: NQ	Start: Dec 15/14
BE-14-19	Northing	5348105		Dip	-43	Logged by: Jim Harris	End: Dec 22/14
L79 N; 1+46E	Elev (m)	110	Length (m)	176.5		Samples: 159728-776 (49)	Reflex Test: 16.8 m -43.2, Az 269.3; 117 m -42.2, Az 271.2
							Contractor: White Wulf Drilling

Hole #	From m	To m	Rock Type	Colour	Alteration	Grain Size	Structure	(%) Mineralization	Comments
BE-14-19	0.0	6.7	**OB**						
	6.7	15.55	**conglomerate/ sandstone**	red/grey	silica/ sericite	med/sst pebble cong	beds 50 to 60 deg CA	<1% disseminated py	Reddish and locally grey-green pebble conglomerate with fine to med grained sandstone interbeds; assorted sediment, chert and k-spar? Pebbles. Alteration and pyrite content increases down hole; 10.05-10.1 is a sparry qtz vein 75 deg tca; Minor, very thin, barren qtz veinlets elsewhere.
	15.55	15.9	**mafic dyke**	green	chl				fine grained dyke, irregular lower contact, upper contact broken
	15.9	30.6	**sandstone/ conglomerate**	grey - green	silica- ser-chl	med/sst pebble cong	bedding/foliation 45 to 60 deg tca	1 to 5% disseminated py, variable	Grey and green, variablly altered sst with a few pebble cong beds. Commonly green, chloritic, may be tuffaceous locally; pyrite is locally concentrated along layering; 17.9-17.97 - mafic dyke vein; local blk chl and/or arg clasts in cong; no qtz veining.
	30.6	50.8	**sandstone/ conglomerate**	grey - green	strong silica - sericite	fine to med	bedding/layering at 60 to 70 deg tca	2 to 5% disseminated pyrite	Interlayered fine to med grained sst and pebble cong. Mostly strong alteration but variable and not as silica rich as usual. From 31.1 to 31.4 2 to 3 thin, (4 to 10mm), qtz veins with fine py and black zones/bands at 20 to 30 deg tca. Some cross-cutting veins at 60 deg. and an occasional thin veinlet down to 32.0m. Minor fault gouge at 33.5m. From 37.56 to 38.05 is a 6 cm banded qtz vein at 60 deg tca followed by a 2 to 3cm vein at about 30 deg. Veins are banded with some green and grey banding. From 41.0 to 42.0 m is pink coloured, less altered. From 41.15 to 41.4 is a <1cm qtz vein at 20 to 30 deg tca with py and chl. From 42.7 to 43.05 there is a 1cm black chl-py vein and two 1 to 3mm, barren qtz veins all at 30 deg tca. From 47.2 to 50.8 is well layered to foliated at at 50 to 70 deg tca and has more common chloritic layers/beds.
	50.8	60.5	**sandstone/ conglomerate**	grey	mod-strong silica - seriocite	fine to med	bedding at 40 to 50 deg tca	2 to 10% dissem. Py	Interbedded sst and cong as above. Very strongly altered and sheared from 50.8 to 52.5 with about 10% py. Strong shear to breccia from 51.4 to 51.6, shearing at 50 to 60 deg and brecciation at 30 deg. Moderate alt'n below 52.5. From 53.85 to 54.6, minor thin, low angle qv.From 54.6 to 55.1m qv at 30 to 40 deg, grey-white with black and green bands and some sst inclusions. At 60.5m a 2 to 3cm banded qv at 40 to 45 deg tca with some pale green sericite.
	60.5	129.3	**sandstone/ alteration**	dark grey	strong silica	fine	massive at 111.5 bedding 40 deg tca	2 to 5% disseminated and stringer pyrite Local pyritic breccia vein/network with 20%+ py	Dark grey, very strongly silicified/altered sst, occasional recognizable cong. Rare, thin, barren qtz veinlets, mainly at low core angles. From 72.0 to 72.3 15 to 20% fine py as a network of py-sil flooding/vein breccia. Local similar zones below 72.3m. From 78.2 to 80.8 10%+ py. Local vuggy silicification, ie 84.0 to 84.7 and 87.0 to 89.0m. Alteration is often flecked with an off-white 'clay' mineral. From 93.6 to 94.0 30% py as semi-massive brecciation of sst. At 100.1m -a 3 to 4cm fault gouge, apparently at approx 60 deg tca but core is broken. Some fracturing to brecciation from 98.7 to 100.1m. No apparent bedding, likely destroyed by alt'n. Below 101.0m there are local zones of lighter grey alt'n apparently cutting the darker grey. The only apparent difference is less fine py in the light coloured zones. at 112.9 small inclusion of colloidal silica or vein edge. 115.37 to 115.5 large col. sil. or vein qtz inclusion, some banding. 116.9 to 117.4 colloidal sil and semi-massive py. **117.4 to 117.54 banded qv, white, green and thin wavy black bands.** 119.0 to 120.4 mostly creamy white, colloidal? silica, localy vuggy and some irregular silica-py veining. 10cm white qtz vein breccia at 120.4. From 120.4 to 126m minor thin qv and 5%+ py. From 129.65 to 129.3 is broken & rubblly core, possible fault near 127m.
	129.3	176.5	**sandstone / conglomerate**	grey	mod. Sil'n	coarse	at 130m bedding at 45 to 50 deg tca at 143m bedding 45 deg tca at 147.7 bedding at 35 deg tca.	2 to 3% dissem py. *129.3 to 135.6 is broken & rubbly core. 129.5 to 132.6 about 90% recovery. 132.6 to 135.6 only 70cm recovered, (No gouge or evidence of grinding) 135.6 to 138.7 2.8m recovered. From 166.1 to 169.2 about 75% recovery. From 169.2 to 172.2 about 85% recovery.*	Not as altered as above. Mostly a coarse sandstone to pebble conglomerate with an occasional siltstone bed and/or clast. From 135.6 to 135.75 is a **QA vein at 34 deg tca,** white, pink, grey & black bands. The upper vein contact is lost and maybe some of the vein. From 137.1 to 137.15 lighter coloured alt'n or col. silica for about 3/4 of core. At 141.35 2 to 3cm qv at 60 to 70 deg tca. From 142.2 to 143.4 6 to 7 thin, white and dark grey qv, mainly at approx 30 deg tca but largest is at 50 deg. From 143.4 to 143.6 a 2 to 3cm white, black and grey banded qv at 30 deg tca. **From 148.7 to 148.74 QA vein at 60 deg tca,** creamy white, grey and black. From 150.5 to 154.1 common broken, rubblly core, some lost core, (~30 cm). Short broken zones continue down to 163m. From 153.8 to 153.83 QV at 50 deg tca, mainly creamy white qtz. At 159.35, 1-2cm 'inclusion' of white vein qtz or col. silica. A 1cm, broken white qv at 162.9m. At 163.6 a 2 to 3cm banded, irregular qv. From 163.7 to 163.85 banded QV, banding at 60 deg tca, partially rubble, may be some lost core. From 165.3 to 175.3 common rubble zones, minor gouge/breccia recovered locally, ie at 165.4 & between 169.2 and 169.5m. From 169.9 to 169.75 a 2 to 3cm qv to breccia at 35 deg tca. At 171.9 a 1cm broken qv at about 50 deg tca. From 173.0 to 176.5 is mostly fault gouge and breccia with about 60% recovery.
		176.5	**EOH**						

Appendix B Regional Gravity

A map of the regional residual gravity, obtained from Natural Resources Canada, centered about the Big Easy is shown in Figure B.1 and the regional geology is shown in Figure B.2. In Figure B.1 the Musgravetown Group is outlined in black. It is clear from this map that the Musgravetown Group has a gravity high associated with it while the Big Easy prospect sits in a local gravity low. This grid of gravity data is used in Section 3.2.4 as the regional trend to be removed.

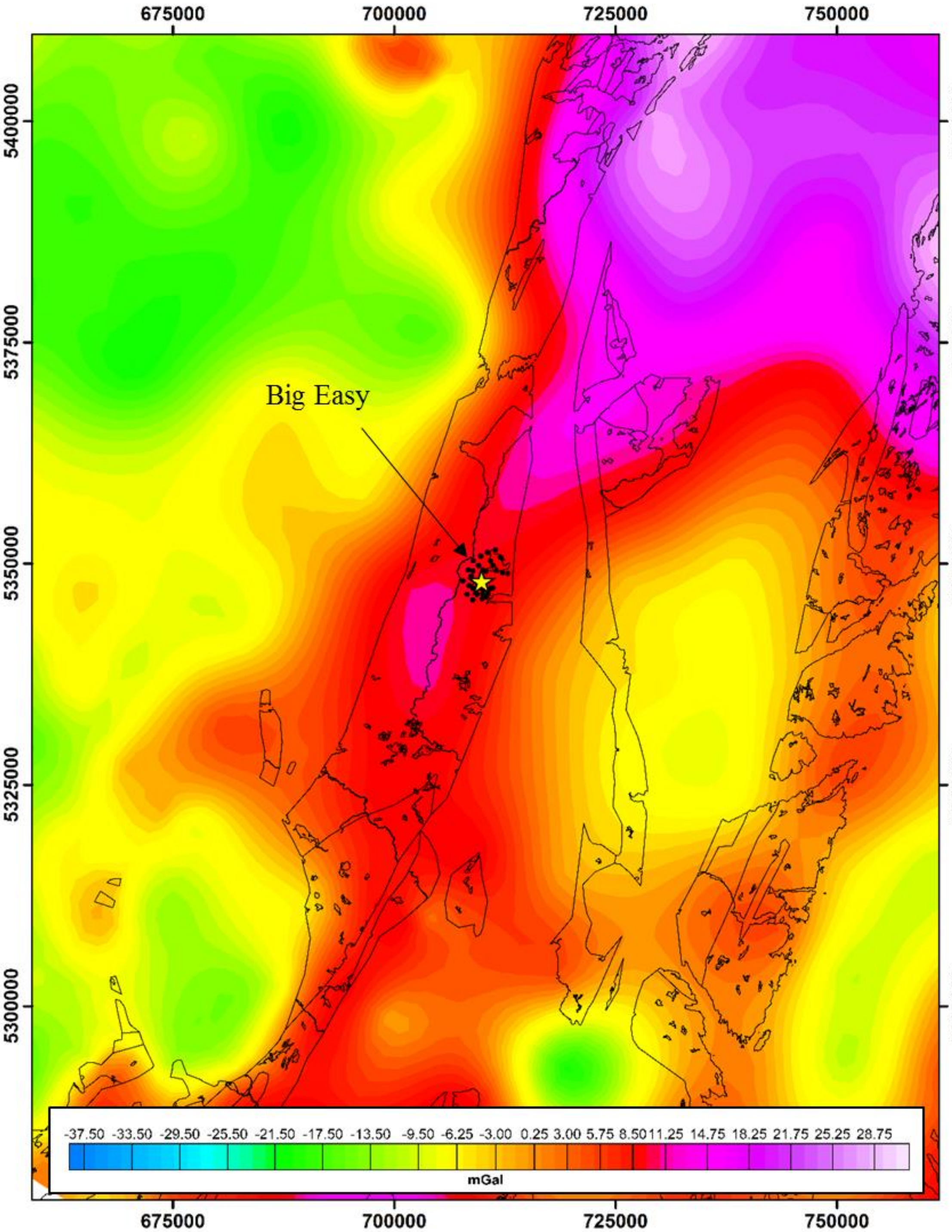

Figure B.1: Regional residual Bouguer anomaly gravity map centered about the Big Easy Prospect. Data was obtained from the Geoscience Data Repository for Geophysical Data (NRCan, 2016) via Oasis Montaj. Outlined in black is the Musgravetown Group.

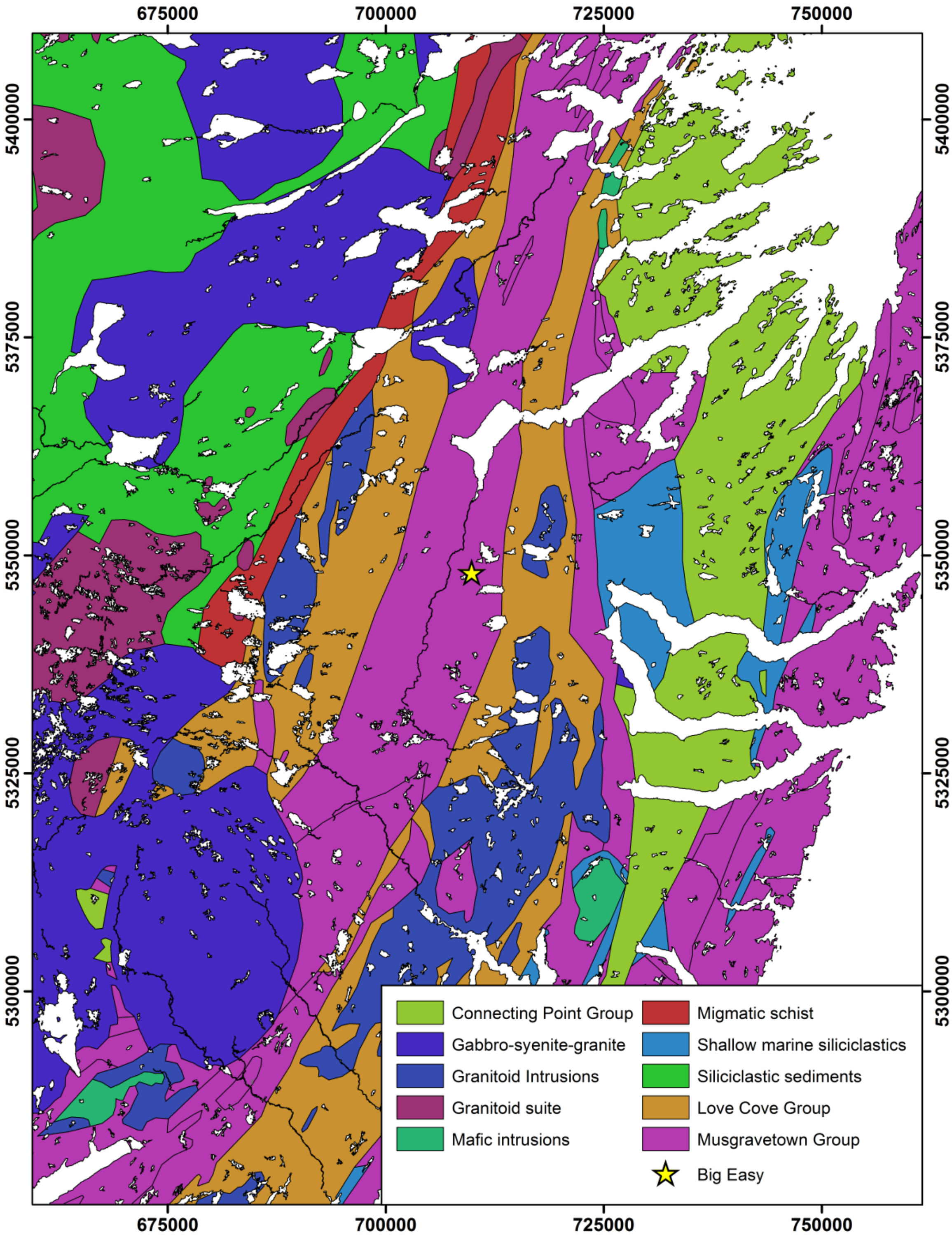

Figure B.2: Regional geology map centered about the Big Easy Property. Map was generated in ArcMap with shape files obtained from the Geologic Survey Division of the Department of Natural Resources of Newfoundland.

Appendix C Terrain Correction

The terrain correction can be calculated a number of ways, however the method used in this study is derived from a combination of Nagy (1966) and Kane (1962) and implemented through the Oasis Montaj Gravity and Terrain Correction extension. The corrections are calculated by dividing the survey area into near, intermediate, and far zones. A different algorithm is used to calculate the contribution of each zone on the terrain correction for a given station. The near zone (Zone 0) is divided into 4 tetrahedral sections (Figure) and the effect of the triangular slopes are calculated from Equation C-1 where each parameter is illustrated in Figure C.2.

$$g_{Z0} = \gamma\rho\theta\left(-\sqrt{R^2+H^2}+\frac{H^2}{\sqrt{R^2+H^2}}\right) \tag{C-1}$$

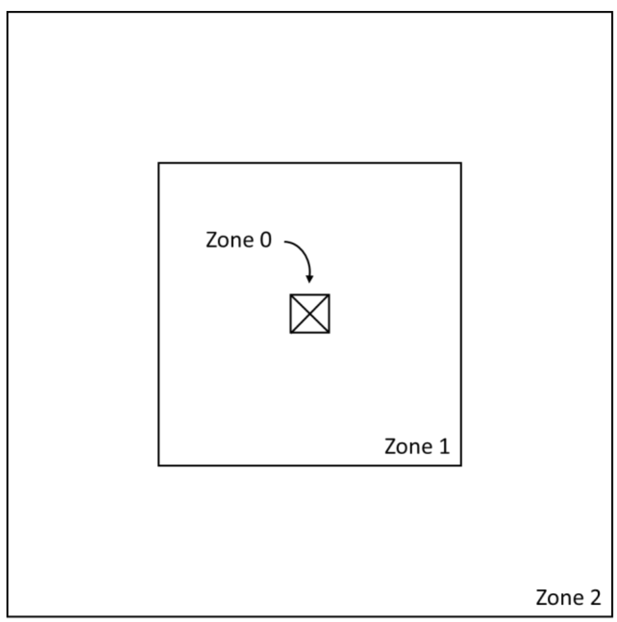

Figure C.1: Plan view of zones used in calculating the terrain corrections (modified from Geosoft, 2015).

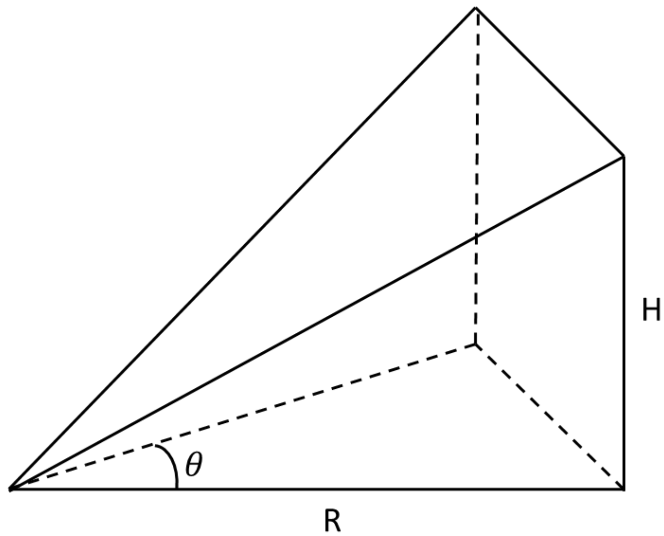

Figure C.2: Illustration of Zone 0 portion used to calculate terrain correction (Geosoft Inc., 2015).

The terrain correction within the intermediate zone is calculated using the cube approach by Nagy (1966). The gravitational effect on an observation point is determined by integrating over the volume within Zone 1 by

$$g_{Z1} = -\gamma\rho \left| \Big|_{z_1}^{z_2} \Big|_{y_1}^{y_2} \Big|_{x_1}^{x_2} x \cdot \ln(y + r) + y \cdot \ln(x + r) + Z\, arctan\, \frac{Z \cdot r}{x \cdot y} \right| \Big| \Big|$$

where each variable is depicted in Figure C..

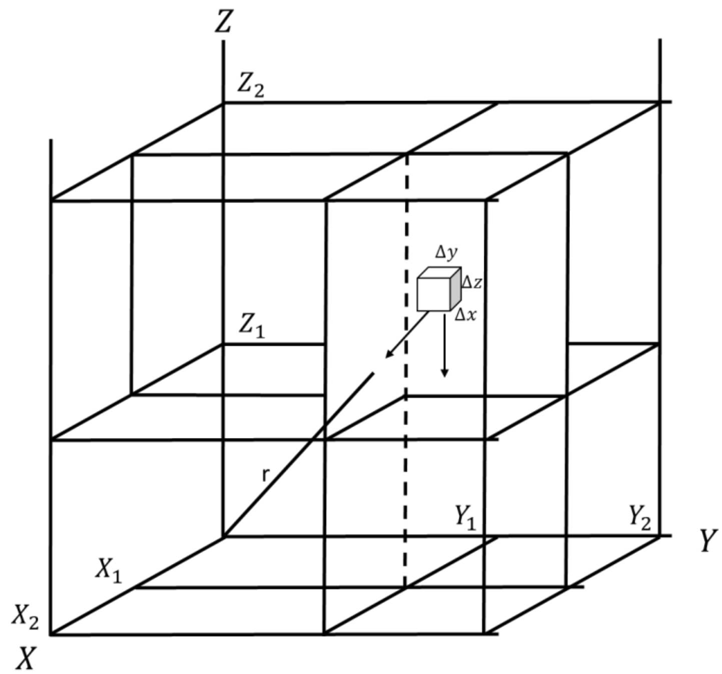

Figure C.3: The gravitational attraction of a right rectangular prism used to calculate the terrain correction from Zone 1 (Modified from Nagy, 1966).

In Zone 2, the method for calculating the terrain correction is derived from Kane (1962) where a square prism is approximated by segment of a ring (Figure C.4). Integration of a ring improves computation time since integrating over a square prism has been proven to be more computationally intense (Kane, 1962). The effect of each segment on a gravity measurement is calculated by

$$g_{Z2} = 2\gamma\rho A^2\left(\frac{R_2 - R_1\sqrt{R_1^2 + H^2} - \sqrt{R_2^2 + H^2}}{(R_2^2 - R_1^2)}\right)$$

where each variable is illustrated in Figure C..

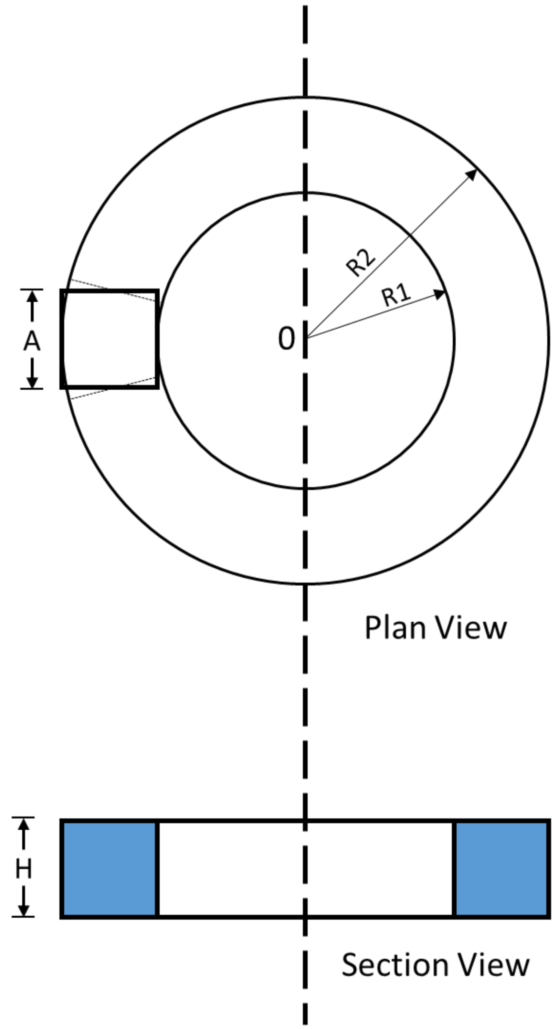

Figure C.4: Schematic diagram showing the relationship of a square to a segment of a ring of the same area (modified from Kane, 1962).

Appendix D Inversion Program

Inversion Program: Voxel Inversion (VINV)

An example of *vinv.inp* is shown in Table D-1. The boundsfile is used for constrained inversion where the upper and lower physical property bounds are set for any given cell. Typically, these are set over regions or over the entire model and are based on geologic knowledge. The bounds file is an .ele file that contains a list of nodes that make up each triangle and it also contains two attribute columns. The lower and upper index indicate which attribute column to use for the bounds.

Table D-1: Input file for inversion

! Mesh Information		
gridtype	"unstructured"	! type of mesh used
meshfile	"meshfile.1.node"	! file containing mesh information
modelfile	"modelfile.1.ele"	! file containing model information
neighfile	"neighfile.1.neigh"	! another file containing mesh information
proptype	"den"	! specifies property to obtain from inversion
boundsfile	"boundsfile.ele"	! file containing model bounds
lowerindex	1	! attribute index to use for lower bounds in bounds file
upperindex	2	! attribute index to use for lower bounds in bounds file
initvalue	0	! initial model value
wmode	"sensitivity"	! defines what type of weighting is used
wbeta	1	! distance/sensitivity weighting strengths
wnorm	2	! distance sensitivity weighting power
datatype	"gz"	! specifies the data type
datafile	datafile.node	! specifies the datafile to use
chifact	0.1	! normalized target misfit
engine	"local"	! defines the type of optimization used
usebounds	"t"	! specifies whether bound-constrained inversion is used
! Regularization Options		
wmfile	"model_weights.txt"	! file containing across face smoothness weights
maxbetasteps	100	! maximum number of steps in a beta-search
betainit	1.0E-4	! initial beta value
! Parameters specific to magnetic data		
form	"sus"	! magnetic formulation
igeo	"82.42"	! geomagnetic field inclination in degrees
dgeo	"-19.5"	! geomagnetic declination in degrees
sgeo	"51530"	! geomagnetic field strength in nT

Appendix E Data Files

An attached disk contains a series of folders that correspond to the GPR, magnetic, and gravity data collected during this project.

The *GPR* folder has a subset of folders dividing the data into three main areas; GrassyPond, BottlePonds, and BigBog. These folders contain the raw data files for each individual line which includes a HD, DT1, and GPS file. The HD file is text file that contains the survey parameter information. Any post-possessing steps that have been applied within EkkoProject is contained in the file as well. The DT1 files contain the bulk of the information collected during the survey and is stored in a 25 element array. The array number and corresponding unit description is shown in Table E-1. The GPS file contains the location information of every n^{th} trace set by the user. It is important to note that the locations in the attached files are those of the GPS and not the location of the measurement location. There is an offset equal to the separation between the GPS unit and the centre of the transmitter-receiver set-up. These values are also those collected directly from the RTK rover and have not undergone the PPP.

The *magnetic* folder contains all of the magnetic data collected and is saved as a geosoft database file (.gdb). In this file, the magnetic data is sorted by the last four digits of the line number and the base line has been designated as a tie line. All lines have been leveled to the base line and all (known) anthropogenic features have been manually cropped.

The *gravity* folder contains two folders: *Raw* and *Oasis.* The raw folder contains the individual text files from each survey, labelled in the format of YYMMDD, as they were exported from the CG-5 gravimeter. The *Oasis* folder contains the same individual surveys except written in a specific format that allows them to be read in the *Oasis Montaj Gravity and Terrain Correction*

Extension. Only the essential information required for the gravity calculations and reductions remain in these files and the reading value has the E.T.C removed from it so it could be more accurately obtained during processing. Additional files in this folder are the *Bases* and *Locations* which contain the location information of the base stations and survey stations, respectively. The high resolution DEM is also included in this folder and is labeled *ThorburnLake_DEM_NAD83*. Finally, the database file containing the all of the survey data as well as the reduced data is labelled *Master*.

Table E-1: List of arrays along with corresponding GPR information contained in a DT1 file.

Array	Description
1	Trace number
2	Position
3	Number of points per trace
4	Topographic data (if available)
5	Not used
6	# bytes/point (always 2 for Rev3 firmware)
7	Time window
8	# stacks
9	Time window
9-10	GPS X position
10-12	GPS Y position
12-14	GPS Z position
15	Receiver X position
16	Receiver Y position
17	Receiver Z position
18	Transmitter X position
19	Transmitter Y position
20	Transmitter Z position
21	Timezero adjustment
22	Zero flag
23	Multi-channel channel numbers
24	Time of day (seconds past midnight)
25	Comment flag